

WESTINGHOUSE NON-PROPRIETARY CLASS 3

WCAP-14047
Revision 1

SG-94-08-017

BRAIDWOOD UNIT 1
TECHNICAL SUPPORT FOR CYCLE 5
STEAM GENERATOR
INTERIM PLUGGING CRITERIA

AUGUST 1994

WESTINGHOUSE ELECTRIC CORPORATION
NUCLEAR SERVICES DIVISION
P. O. BOX 158
MADISON, PENNSYLVANIA 15663-0158

© 1994 Westinghouse Electric Corporation
All Rights Reserved

9409120129 940831
PDR ADDCK 05000456
P PDR

BRAIDWOOD UNIT 1: TECHNICAL SUPPORT FOR CYCLE 5
STEAM GENERATOR INTERIM PLUGGING CRITERIA

TABLE OF CONTENTS

<u>SECTION</u>	<u>PAGE</u>
1.0 Introduction	1-1
2.0 Summary and Conclusions	2-1
2.1 Overall Conclusions	2-1
2.2 Summary	2-3
3.0 Braidwood-1 SG Pulled Tube Examinations	3-1
3.1 Introduction	3-1
3.2 NDE Results	3-1
3.3 Leak Testing	3-2
3.4 Burst Testing	3-2
3.5 Destructive Examination Results	3-3
3.6 Conclusions	3-4
3.7 Evaluation of Pulled Tube Data for ARC Applications	3-4
4.0 Accident Considerations	4-1
4.1 General Considerations	4-1
4.2 Thermal Hydraulic Loads on TSP in a SLB Event	4-2
4.3 Structural Modeling for SLB TSP Displacement Analyses	4-5
4.4 Results of SLB TSP Displacement Analyses	4-10
4.5 SLB TSP Displacements by Tube Location	4-13
4.6 SLB Frequency at Hot Standby and Full Power Conditions	4-15
4.7 Tubes Subject to Deformation in a SSE + LOCA Event	4-16
4.8 Allowable SLB Leakage Limit	4-18
4.9 Acceptability of the Use of TRANFLO Code	4-20
4.10 Updated Model D4 SG SLB Thermal Hydraulic Loads on TSPs	4-24
4.11 Updated Model D4 SG SLB TSP Displacement Analyses	4-26
4.12 References	4-30
5.0 Database Supporting Alternate Repair Criteria	5-1
5.1 Data Outlier Evaluation	5-1
5.2 Database for ARC Correlations	5-6
5.3 NDE Uncertainties	5-6
5.4 References	5-7
6.0 Burst and SLB Leak Rate Correlations	6-1
6.1 EPRI ARC Correlations	6-1
6.2 Burst Pressure vs. Bobbin Voltage Corelation	6-2

BRAIDWOOD UNIT 1: TECHNICAL SUPPORT FOR CYCLE 5
STEAM GENERATOR INTEPIM PLUGGING CRITERIA

TABLE OF CONTENTS (Continued)

<u>SECTION</u>	<u>PAGE</u>
6.0 Burst and SLB Leak Rate Correlations (continued)	
6.3 Burst Pressure vs. Throughwall Crack Length Correlation	6-3
6.4 NRC Draft NUREG-1477 SLB Leak Rate POD and Uncertainty Methodology	6-5
6.5 Probability of Leakage Correlations	6-6
6.6 SLB Leak Rate vs. Voltage Correlation for 3/4" Tubes	6-9
6.7 SLB Leak Rate Analysis Methodology	6-11
6.8 Simulation of Equation Parameter Uncertainties	6-13
6.9 Influence of Braidwood-1 Pulled Tube Results on Burst and Leak Rate Correlations	6-20
7.0 Braidwood-1 Eddy Current Inspection Results	7-1
7.1 General	7-1
7.2 Inspection Results	7-2
7.3 Voltage Growth Rates	7-3
7.4 Historical Operating Chemistry	7-5
7.5 Relation Between Operating Chemistry and ODS-CC Growth	7-6
7.6 Pulled Tube Eddy Current Data	7-7
8.0 Braidwood-1 IPC Criteria and Evaluation	8-1
8.1 General Approach to IPC Assessment	8-1
8.2 IPC Repair Criteria Implemented at Braidwood-1	8-2
8.3 Operating Leakage Limit	8-4
8.4 Projected EOC-5 Voltage Distributions	8-5
8.5 SLB Leakage Analyses	8-6
8.5.1 Reference SLB Leakage Analyses (Log logistic POL)	8-7
8.5.2 SLB Leak Rate Sensitivity to POL Correlations	8-7
8.6 Assessment of SLB Burst Margins and Probability of Burst	8-8
8.6.1 Deterministic Burst Margin Assessment	8-8
8.6.2 Method of Analysis for SLB Tube Burst Probability	8-9
8.6.3 Demonstration of Method for SG-D at EOC-4	8-11
8.6.4 Conservative Burst Probability for SLB at Normal Operating Conditions	8-11
8.6.5 Burst Probability for SLB at Hot Standby Conditions	8-12
8.6.6 Braidwood-1 Frequency of SLB Event with a Tube Rupture	8-13
8.7 Updated SLB TSP Loads, Displacements, and Burst Probability Assessment	8-13
8.8 Tube Integrity Assessment Based on Braidwood-1 Pulled Tube Results	8-16
8.9 Summary of Results	8-17

BRAIDWOOD UNIT 1: TECHNICAL SUPPORT FOR CYCLE 5 STEAM GENERATOR INTERIM PLUGGING CRITERIA

1.0 INTRODUCTION

Revision 1 of this report revises the initial March 1994 report to include results of destructive examinations of the Braidwood-1 pulled tubes and updated SLB TSP hydraulic loads, displacement analyses and associated tube burst probability analyses. The updated hydraulic load analyses were performed for the expected operating conditions, such as water level, at the time of the SLB event and thereby eliminate unnecessarily conservative assumptions in the prior analyses. Revision 1 is provided as a complete report although most sections of the report are not changed from the initial release. To facilitate identification of the Revision 1 changes to the report, all revisions are marked with solid lines in the right margins of the pages.

Following the completion of Cycle 4 operation, eddy current inspections of the tube support plate (TSP) intersections of the steam generator (S/G) tubes have identified 2733 bobbin coil indications of which 1566 were confirmed as being axial crack-like ODSCC indications using RPC inspection techniques. The size and number of indications could result in significant tube repairs with current plugging criteria and repairs that are not required to meet NRC Regulatory Guide 1.121 guidelines for tube repair. Braidwood Station has therefore requested a Technical Specification change to implement an interim plugging criteria (IPC) for ODSCC at TSP intersections. The requested IPC repair limits and inspection requirements have been based on the Catawba-1 NRC SER which approved a 1.0 volt repair limit. The methodology to support the Braidwood-1 IPC differs from previously approved IPCs in that it applies the EPRI data outlier evaluation methodology and SLB leak rate versus voltage correlation based on the NRC guidance of the February 8, 1993 NRC/industry meeting on resolution of comments on draft NUREG-1477. In addition, Braidwood-1 IPC analyses demonstrate limited TSP displacement relative to the tube in a SLB event, and show structural integrity with respect to tube burst considerations.

The evaluations supporting the Braidwood-1 IPC are based upon bobbin coil voltage amplitude which is correlated with tube burst capability and leakage potential. Detailed analyses provided in this report (Section 4) have demonstrated limited relative tube support plate to tube movement which minimizes the potential for significant leakage or tube burst during both normal and accident conditions. For SLB leakage analyses, the tube support plate crevices are assumed to be free span or open crevices, which lead to more conservative leak rates compared to the expected packed crevices under normal and accident conditions. The analyses for demonstrating limited TSP displacement utilize thermal-hydraulic loads for a postulated SLB at normal operating conditions and for a SLB at hot standby conditions. The

Revision 0 report loads utilized existing analyses and the hot standby loads are very conservative as the initial conditions include low water level combined with an excess feedwater transient, both of which tend to increase the loads. The updated analyses of Revision 1 eliminate these very conservative assumptions and updated results are provided for a SLB at both hot standby and full power conditions. The dynamic structural analyses yield TSP displacements as a function of tube location. Tube burst analyses performed for the crack length exposed by the TSP displacements have been conservatively performed by assuming that the exposed crack length is throughwall. Even with these conservative assumptions, it is demonstrated that Braidwood-1 has adequate tube burst margin.

In accordance with draft NUREG-1477, SLB leak rates were calculated for a total of six probability of leak (POL) correlations including the EPRI reference log logistic correlation. The six correlations (Section 6) evaluated included linear and log voltage formulations for logistic, normal and Cauchy cumulative distribution functions. The reference leak rate with the log logistic correlation and five additional leak rates for assessing the sensitivity to the POL correlation are given in this report (Section 8). The SLB leak rate analyses utilize voltage distributions consistent with the draft NUREG-1477 guidance including adjustments for probability of detection.

The plugging criteria were developed from testing of tube specimens with laboratory-induced ODSCC, extensive examination of pulled tubes from operating S/Gs and field experience for leakage due to indications at TSPs. The recommended criteria represent conservative criteria, based upon Electric Power Research Institute (EPRI) and industry-supported development programs that are continuing to further refine the plugging criteria. At the end of Cycle 4, four tubes with 13 intersections and 6 RPC confirmed indications were pulled at Braidwood-1 for future enhancement of the EPRI database and to validate the industry developed EPRI leak and burst correlations applied in this report. Results of the destructive examinations for these pulled tubes, including burst and leak test results, are given in Revision 1 of this report.

Implementation of the tube plugging criteria was supplemented by 100% bobbin coil inspection requirements at TSP elevations having ODSCC indications, reduced operating leakage requirements, inspection guidelines to provide consistency in the voltage normalization, and rotating pancake coil (RPC) inspection requirements to establish repair requirements for indications above the 1.0 volt repair limit and to characterize the principal degradation mechanism as ODSCC. In addition, potential SLB leakage was calculated for tubes with indications left in service at TSPs to demonstrate that the cumulative EOC-5 leakage is less than the allowable limits.

2.0 SUMMARY AND CONCLUSIONS

This report documents the technical support for a Braidwood Unit 1, Cycle 5 Interim Plugging Criteria (IPC) of 1.0 volt for ODSCC indications at TSPs. Revision 1 of this report updates the May 1994 initial release to include: currently available results of the Braidwood-1 pulled tube examinations including NDE data, leak tests, burst tests and available destructive examination data; an assessment of the impact (found to be negligible) of the Braidwood-1 pulled tube data on the EPRI burst pressure, probability of leakage and leak rate correlations; updated SLB hydraulic loads on the TSPs to reflect the actual operating conditions rather than the bounding loads used in the prior analyses; and updated SLB TSP displacements and associated tube burst probabilities based on the revised hydraulic loads.

2.1 Overall Conclusions

An IPC with a 1.0 bobbin voltage repair limit has been developed for Braidwood-1, Cycle 5 operation. Inspection requirements typical of IPC practice, such as the guidelines of the Catawba-1 NRC SER, were applied at the Cycle 4 refueling outage to support implementation of the IPC. These requirements include eddy current analysis guidelines, training of analysts, cross calibration of ASME standards to a reference standard, use of probe wear standards, 100% bobbin probe inspection and RPC inspection of bobbin indications above 1.0 volt together with a sample of dented TSP intersections.

The Braidwood-1 pulled tube examination results show burst pressures and SLB leak rates in very good agreement with the EPRI correlations used in the initial release of this report. There is no need to update the EPRI correlations based on the Braidwood-1 results and the prior analyses for SLB leak rates and free span burst probabilities remain applicable. All burst test results exceeded R.G. 1.121 burst requirements with the lowest measured burst pressure of 4,730 psi obtained for the 10.3 volt indication, which was the largest indication found in the 1994 inspection. Eleven indications were burst tested and all indications burst, as expected, in the axial direction. The crack morphology of dominantly axial indications is consistent with the EPRI database and the EPRI correlations are applicable to Braidwood-1. SLB leak rates measured for the Braidwood-1 pulled tubes are slightly below the regression fit to the EPRI database. Bobbin indications at 2.05, 5.00 and 10.3 volts had measured SLB leakage while indications at 0.21, 0.28, 0.91, 3.35 and 3.73 volts had no SLB leakage. The results indicate that all tube integrity requirements were satisfied at EOC-4 in that burst pressures for the largest indications met R.G. 1.121 requirements and SLB leak rates would have been well below 10CFR100 limits. Since tube integrity requirements were satisfied at EOC-4 and the limiting indications at EOC-5 are expected to be smaller than or no worse than found for Cycle 4, it can be expected that all tube integrity requirements will be satisfied at EOC-5. Thus, the Braidwood-1 pulled tube results strongly support full cycle operation for Cycle 5.

R G 1.121 guidelines for tube integrity are conservatively satisfied at end-of-cycle five (EOC-5) conditions for the 1.0 volt IPC. The results of the Braidwood-1 assessment can be summarized as follows:

- The projected EOC-5 SLB leakage is 3.1 gpm (3.2 gpm by Monte Carlo analyses) for the limiting SG, which is less than the allowable limit of 9.1 gpm for Braidwood-1. The SLB leak rate was evaluated for the six alternate formulations of the probability of leak versus voltage correlation identified in draft NUREG-1477 and found to be essentially (within 0.1 gpm) independent of the correlation applied in the analysis. The SLB leak rates were obtained by applying the leak rate versus voltage correlation based on the EPRI database and outlier evaluation consistent with the NRC guidance of the February 8, 1994, NRC/industry meeting on resolution of draft NUREG-1477 comments. The Braidwood-1 NRC SER of August 18, 1994 applies changes to two datapoints in the EPRI database and an estimated SLB leak rate of 6.8 gpm is obtained at EOC-5. This leak rate remains below the limit of 9.1 gpm without coolant activity reductions. The Braidwood-1 reactor coolant dose equivalent I-131 concentration has been reduced from 1.0 to 0.35 microcuries per gram of coolant for Cycle 5, which further increases the margin between predicted and allowable SLB leakage.
- Based on the updated hydraulic loads, the EOC-5 conditional tube burst probability is conservatively estimated at 5.4×10^{-6} for an SLB at full power conditions which envelopes an SLB at hot standby conditions. The updated analyses reflect the expected operating conditions at the time of the postulated SLB event. The principal difference between the updated and prior bounding analyses for an SLB at hot standby conditions is that the updated analyses are based on the controlled water level of 487 inches above the tubesheet while the prior bounding analyses conservatively assumed a water level of 280 inches at the uppermost TSP elevation. The prior conditional tube burst probabilities were estimated at EOC-5 as 5×10^{-5} for a SLB at normal operating conditions and 8×10^{-4} for a SLB at hot standby conditions. Weighting these probabilities by the relative operating times led to a combined burst probability of 3.1×10^{-5} . Thus the updated analyses lead to a further reduction in the burst probability by about a factor of 6 for the combined probability and about a factor of 70 for an SLB at hot standby conditions. All burst probabilities are significantly lower than the IPC acceptance guideline of 2.5×10^{-2} shown to be acceptable in NUREG-0844. When the conditional burst probabilities are combined with the corresponding SLB event frequencies, the frequency of a postulated SLB event with a subsequent tube rupture is very low at 5.5×10^{-8} per year for the prior bounding analyses and 9.7×10^{-9} per year for the updated analyses. The tube burst probabilities are developed based on limited TSP displacements calculated during a SLB event for the Braidwood-1 S/Gs, even when applying very conservative load conditions for the hot standby SLB. Deterministic tube burst analyses show that the projected

EOC-5 voltage obtained with voltage growth rates up to 99% cumulative probability on the Cycle 4 measured growth distribution, is less than the R.G. 1.121 structural limit of 4.54 volts for a $1.43 \times \Delta P_{SLB}$ accident condition burst margin. The R.G. 1.121 structural limit guideline of three times normal operating pressure differential is inherently satisfied by the tube constraint provided by the tube support plates at normal operating conditions.

The modest SLB leakage, acceptable tube burst margins and low tube burst probabilities presented in this report support full cycle operation for Cycle 5 at Braidwood-1 following implementation of the 1.0 volt IPC.

2.2 Summary

Braidwood-1 Interim Plugging Criteria

The implementation of the IPC at Braidwood-1 for ODSCC at TSPs can be summarized as follows:

- Tube Plugging Criteria
Tubes with bobbin flaw indications exceeding the 1.0 volt IPC voltage repair limit and ≤ 2.7 volts are plugged or repaired if confirmed as flaw indications by RPC inspection. Bobbin flaw indications > 2.7 volts attributable to ODSCC are repaired independent of RPC confirmation.
- Inspection Requirements
A 100% bobbin coil inspection was performed for all TSP intersections. All bobbin flaw indications greater than the 1.0 volt repair limit were RPC inspected and the RPC inspection included a sample of dented TSP intersections.
- Operating Leakage Limits
Plant shutdown will be implemented if normal operating leakage exceeds 150 gpd per SG.
- SLB Leakage Criterion
Predicted end of cycle SLB leak rates from tubes left in service, including a $POD = 0.6$ adjustment and allowances for NDE uncertainties and ODSCC growth rates, must be less than 9.1 gpm for the S/G in the faulted loop.

- Exclusions from Tube Plugging Criteria

Certain tube locations, as identified in Section 4 of this report, are excluded from application of the IPC repair limits. The analyses indicate that these tubes may potentially deform or collapse following a postulated LOCA + SSE event.

EOC-4 Inspection Results

Eddy current inspection at EOC-4 resulted in the identification of 2733 bobbin indications at the TSP intersections and 1566 or 57% of the bobbin indications were confirmed by RPC inspection. The indications ranged from 272 in S/G B to 1061 in S/G C. To evaluate Cycle 4 voltage growth, all indications of ODSCC at TSP intersections at EOC-4 had the EOC-3 bobbin data reevaluated to obtain Cycle 4 growth rates. In addition, Braidwood-1 had a 100% inspection of S/G C during October, 1993 as the result of a primary to secondary tube leak unrelated to ODSCC at the TSPs. This allowed a growth evaluation for S/G C from October 1992 to October 1993, a S/G C evaluation from November 1993 to March 1994 and a growth evaluation on S/Gs A, B and D for the entire Cycle 4. The results of this growth rate analysis were conservatively applied to the BOC-5 indications left in service to project the EOC-5 voltage distributions for tube integrity analyses. The average growth for all 4 S/Gs over Cycle 4 was 0.23 volts per EFPY or 48% of the BOC-4 average voltage amplitudes. The average growth for S/G C over the first part of Cycle 4 was 0.19 volts per EFPY (48%) and was 0.11 volts per EFPY (16%) over the second part of Cycle 4. A few indications (~1%) showed larger than typical growth with the largest growth rate being 9.76 volts.

The Braidwood-1, RPC confirmed TSP bobbin indications show axially oriented indications that are typical of those of other plants which have been confirmed as having ODSCC; i.e., the Braidwood-1 results are consistent with axial ODSCC as the degradation mechanism and the associated EPRI database is applicable for the Braidwood-1 IPC. Four tubes including 13 TSP intersections and six RPC confirmed bobbin indications ranging from 1.0 to 10.4 volts were pulled during the outage for subsequent laboratory testing and destructive examination. The results from these pulled tube examinations will be used to enhance the EPRI database and leakage/burst correlations. The Braidwood-1 pulled tube leak and burst test results are consistent with the EPRI database correlations and there is no need to update the correlations to include the Braidwood-1 data.

Correlations of bobbin voltage to burst pressure and to SLB leakage and a correlation for the probability of SLB leakage are provided which are consistent with NUREG-1477 and the Catawba-1 SER. These correlations form the basis for determining repair limits and the corresponding margins for burst and leakage as summarized below.

Structural Integrity Assessment

To support the Cycle 5 tube integrity assessment under the conservative assumptions of the larger Cycle 4 growth rates reoccurring in Cycle 5 and a probability of detection of 0.6 (draft NUREG-1477 guidance), additional analyses were performed to demonstrate limited TSP displacement in a postulated SLB event. With limited displacement, the part of the overall ODSCC crack length covered by the TSP is constrained against burst and the burst capability of the indication is that associated with the exposed crack length. Thus, limited relative displacement of the tubes and TSPs results in increased tube burst margins and an associated low probability of tube burst.

The two sets of Model D4 S/G thermal-hydraulic loads available for the initial release of this report were (a) those for a SLB at normal full power operating conditions and (b) those for a very conservative SLB at hot standby conditions with low water level combined with an excess feedwater transient. The initial conditions for the latter hot standby SLB event are excessively conservative as shown by comparison with a Model D3 S/G, hot standby SLB event with normal water levels and no feedwater transient. For Revision 1 of this report, updated hydraulic analyses using the TRANFLO code were performed for an SLB at hot standby and normal operating conditions. The updated analyses are based on water levels at the controlled setpoint of 487 inches above the tubesheet (prior hot standby analysis at 280 inch water level corresponding to the elevation of the uppermost TSP) and eliminate the unnecessary conservatism associated with the water level and excess feedwater transient. Two cases were run for the SLB at normal operating conditions. The first updated full power case (Case 5 in this report) establishes low TSP pressure drops at the steady state, initial conditions (time = 0) for the SLB event. Case 6 establishes the expected steady state TSP pressure drops based on performance analyses for the Braidwood-1 S/Gs. It is found that Case 5 results in the largest maximum TSP displacements for the updated analyses. TSP displacements for each TSP and each tube location were obtained by dynamic, finite element analyses for each of the aforementioned SLB loading conditions.

The results of the updated Model D4 S/G SLB analyses at both normal operating and hot standby conditions, the prior analyses at normal operating conditions and the Model D3 S/G loads at hot standby conditions show maximum TSP displacements at tube locations of <0.48 inch. These displacements expose a crack length less than the 0.51 inch throughwall crack length that satisfies R.G. 1.121 criteria for the structural limit of $1.43 \times \Delta P_{SLB}$. The estimated burst probability at the limiting tube location for the updated SLB analyses, very conservatively assuming a throughwall crack equal to the 0.48 inch maximum exposed crack length, is 7×10^{-7} per indication which is negligible for tube integrity considerations. Thus structural integrity based on R.G. 1.121 guidelines is maintained throughout Cycle 5 for the updated SLB analyses for a SLB event at either full power or hot standby conditions.

Even for the very conservative, bounding Model D4 hot standby loads of the prior analyses, TSP displacements are limited to less than 0.35 inch for all TSPs having bobbin indications at Braidwood-1 except for plates 3 and 7. At plate 3, the maximum TSP displacement at a tube location is 0.57 inch which is well less than the 0.75 inch length for burst at the SLB pressure differential of 2560 psi for tubes with LTL material properties. The probability of tube burst for an assumed 0.57 inch throughwall crack is about 6×10^{-4} which is negligible compared to allowables since only 12 (0.26% of TSP intersections) tube locations on plate 3 have TSP displacements greater than the 0.51 inch structural limit. At the EOC-4 inspection, only 1 indication was found on plate 3 at a location with displacements >0.5 inch. This indication had a small 0.59 volt amplitude at a tube location with 0.51 inch TSP displacement. Thus the number and voltage amplitudes of indications found at plate 3 locations with significant TSP displacements is negligible for tube integrity considerations. Since maximum TSP displacements maintain adequate tube burst margins even if throughwall cracks are assumed and since the larger tube displacements involve only a few tubes, it is concluded that adequate structural margins are maintained for Cycle 5 operation for all potential indications at plate 3 even for the bounding loads of the prior hot standby SLB analysis.

For the prior, bounding SLB analysis at hot standby conditions, only plate 7 had significant tube-to-TSP displacements which provide potential concerns for exceeding EOC-5 structural integrity considerations. At plate 7, 124 tubes (2.6% of TSP intersections) have TSP displacements exceeding 0.5 inch corresponding to the R.G. 1.121 structural margin for throughwall cracks and the maximum TSP displacement at any tube location is 0.87 inch. Based on the EOC-4 inspection results of plate 7 locations, only 8 indications in any one S/G, and a total of 20 indications in all 4 S/Gs (0.7% of all indications) have SLB displacements exceeding 0.5 inch. The maximum bobbin voltage at any tube location with SLB displacements exceeding 0.35 inch was 1.24 volts and the maximum voltage indication found in any S/G at plate 7 was 2.74 volts. This is well below the 4.54 volts corresponding to R.G. 1.121 margins against burst for free span indications. Thus it is concluded that only a few, relatively low voltage indications are likely to occur at the plate 7 locations with significant SLB displacements at hot standby conditions. A statistical assessment is necessary to assess the potential for a structurally significant indication to occur at a plate 7 location with relatively large TSP displacements. A tube burst probability assessment was performed for SLB hot standby conditions (prior, bounding Model D4 loads) and the resulting probability of a tube burst at EOC-5 conditions was only 8×10^{-4} ; this is negligible compared to IPC acceptance guidelines of 2.5×10^{-2} . The burst probability for an SLB during power operation at EOC-5 for the prior analysis was 5×10^{-5} . Since only about 3.8% of the Braidwood-1 operating time is at hot standby (Mode 3) conditions, the combined burst probability is only about 3×10^{-5} for the prior analyses. The updated load analyses, which eliminate the prior hot standby analysis assumptions of a low water level and a excess feedwater transient, result in a conservatively (all hot leg TSP locations assumed to have throughwall cracks equal to the

TSP displacement) estimated tube burst probability of 5.4×10^{-6} which envelopes both a SLB at either full power or hot standby conditions. Thus, the updated analyses support the prior analyses as a bounding estimate and further demonstrate large burst margins against the acceptance guideline of 2.5×10^{-2} based on NUREG-0844 evaluations.

The Braidwood-1 SLB event frequencies and conditional tube rupture probabilities described above have been combined to obtain a frequency of 9.7×10^{-9} per year for the updated analyses and 5.5×10^{-8} per year from the prior analyses for a SLB event with a subsequent tube rupture. This very low frequency has negligible influence on the core damage frequency and supports full cycle operation at Braidwood-1 for Cycle 5.

Leakage Integrity

Based on sensitivity analyses for SLB leakage, it was concluded that S/G D is the most limiting S/G and was analyzed for potential SLB leak rates at EOC-5. The analysis utilized the EPRI IPC database, probability of leakage correlation and SLB leak rate versus voltage correlation following the NRC guidance at the February 8, 1994, meeting on resolution of draft NUREG-1477 comments. Projected EOC-5 bobbin voltage distributions were obtained including a POD adjustment of 0.6, an allowance for NDE uncertainties, and an allowance for voltage growth based on the S/G D voltage growth distribution obtained for Cycle 4. The resulting SLB leak rate for the limiting SG at EOC-5 was 3.1 gpm, which is significantly less than the allowable leak rate of 9.1 gpm obtained for Braidwood-1.

Based on draft NUREG-1477 guidance, the SLB leak rate was assessed for six alternate formulations of the probability of leakage correlation including linear and log voltage forms for logistic, normal and Cauchy distributions. A negligible leak rate dependence on the probability of leakage form was found, with a variation of only 0.1 gpm between the six distributions.

3.0 BRAIDWOOD-1 SG PULLED TUBE EXAMINATIONS

3.1 Introduction

Four hot leg steam generator tube segments from Braidwood Unit 1 (tubes R16-C42 and R37-C34 from SG D and tubes R27-C43 and R42-C44 from SG A) were examined at the Westinghouse Science and Technology Center. The examination was conducted to characterize corrosion at steam generator hot leg support plate crevice locations. The tubes were selected to obtain a sampling of the indications observed in the 1994 field eddy current inspection. The first (Flow Distribution Baffle), third and fifth support plate crevice regions (SP1, SP3 and SP5) of tubes R16-C42, R27-C43, R37-C34 and R42-C44 and the SP7 region of tube R42-C44 were removed for examination. Six of these locations had original field eddy current calls of OD origin indications.

After nondestructive laboratory examination by eddy current, ultrasonic testing, radiography, dimensional characterization and visual examination, eight support plate regions were leak tested at elevated temperature. Subsequently, room temperature burst testing was conducted on these eight SP regions, as well as three non-leak tested SP regions and two free span regions. Five of the burst tested specimens are currently undergoing destructive examination using metallographic and SEM fractography techniques to characterize the corrosion. The following presents a summary of the more significant observations available to date.

3.2 NDE Results

Table 3-1 presents a summary of the more important field and laboratory NDE results. Field and laboratory eddy current inspections (bobbin and MRPC probes) produced similar data for most regions examined. All four SP1 regions (flow distribution baffle) had no detectable degradation (NDD) in the field and laboratory eddy current examinations. The six support plate crevice regions with original RPC field calls of either single axial indications (SAI) or multiple axial indications (MAI) had similar calls in the laboratory. Some increase in signal strength (voltage) was observed in the laboratory eddy current inspections due to the tube pulling operation. Field bobbin probe signal strengths ranged from 1.0 to 10.4 volts. The largest increase was for tube R42-C44, SP3, where the bobbin probe signal strength increased from 3.7 volts to 6.7 volts. This is considered a moderate increase. In addition to the six original field calls, a review of the field bobbin probe eddy current data resulted in the call of a 0.6 volt indication for the case of tube R16-C42, SP5. No MRPC probe indication was observed. A further review of the eddy current data for the field NDD indications is given in Section 3.7. However, the laboratory eddy current data interpretation for this specimen was complicated by a 12 volt dent signal that was not present in the field data. Smaller laboratory-only dent signals were present at two other support plate regions. These three dents were probably caused by the tube pulling operation.

All SP region NDE indications were confined to their crevice regions. UT inspections confirmed the eddy current observations and further suggested the presence of even more extensive corrosion at some SP crevice locations. Furthermore, UT inspections showed the presence of possible corrosion at two other SP crevice regions (tube R16-C42, SP1 and tube R27-C43, SP5) not called by eddy current inspections as having corrosion. Radiographic indications were observed for the four support plate regions with the largest bobbin probe signal strengths. Three of these four radiographic indications were axial indications, but the fourth (SP3 of tube R42-C44) was predominantly circumferential in nature with some axial components. The latter can be an indication of ICC and/or IGA in addition to axial corrosion.

3.3 Leak Testing

Eight SP crevice regions, including the seven SP regions with eddy current indications, were leak tested at elevated temperature and pressure at conditions that ranged from a simulated normal operating condition to that of a simulated steam line break condition. Three of the specimens developed leaks: tube R27-C43, SP3 (4.9 volt field bobbin indication), tube R37-C34, SP5 (10.4 volt field bobbin indication) and tube R42-C44, SP 5 (2.1 volt field bobbin indication). The leak rates ranged from 0.005 liters/hour to 0.114 liters/hour for normal operating conditions and from 0.040 liters/hour to 10.86 liters/hour for steam line break conditions. Table 3-2 presents leak rate data for the eight tested specimens.

As shown in Table 3-2, some of the leak tests were repeated with minor variations in the temperature and pressure conditions for the tests. No significant differences were found in the leak rates between repeat tests.

3.4 Burst Testing

Thirteen specimens (eleven SP crevice regions and two free span regions) were burst tested at room temperature at a pressurization rate of approximately 1000 psi per second. The burst tests were performed simulating free span conditions with no SP enveloping the indications. The field indications were tested using a bladder and a foil for the burst test with a "semi-constraint" condition which simulates the lateral constraint provided by the TSPs located below and above the crack indications at prototypical spacing between TSPs. Results of the burst tests are presented in Table 3-3. All burst specimens developed axial burst openings. The openings for the SP crevice region specimens were centered within the crevice regions, except for the SP1 region of tube R27C43 which burst outside of the crevice region, as expected for a specimen without corrosion. The circumferential positions of the support plate crevice region specimens' burst openings were the same as the location of the deepest UT indications for the specimens that had corrosion indications. The eddy current RPC data does not provide an absolute circumferential position. The lowest burst pressure for the SP crevice regions (tube R37C34, SP5, the 10.4 volt indication) was 4,730 psi, 44% of the burst pressure

of its free span equivalent and typical of a 3/4" diameter tube specimen with a 10.4 volt indication.

Table 3-3 also provides room temperature tensile properties obtained from free span sections of the tubes. The tensile and burst strengths for the free span sections, while typical for Westinghouse tubing of this vintage, show that two of the tubes (tubes R27C43 and R42C44) were relatively high in strength. Generally, pulled steam generator tubes tend to exhibit slightly higher tensile properties than do pre-operational steam generator tubes.

3.5 Destructive Examination Results

A summary of the visual examination information is presented in Table 3-4. Corrosion cracks were observed on eight of the burst tested specimens, including all seven of the specimens with field eddy current indications. All eight specimens with corrosion cracks had UT indications. (The ninth UT specimen with corrosion indications was not burst tested, but was set aside as an archive specimen). The bobbin NDD indications R27C43 TSP 1 and R37C34 TSP 1 (FDB locations) had no visible indications on the burst crack fracture face or in the crevice region following diametral expansion from the burst test, which tends to open crack indications, and these indications are not candidates for destructive examination. The free span sections of R16C42 and R42C44, selected for a reference burst pressure and tensile property tests, also had no degradation as would be expected. The five indications shown in Table 3-4, which include all three indications with measured SLB leakage, were selected for destructive examination.

Table 3-5 summarizes the results from fractography of the burst crack fracture faces. For each indication examined, the crack length versus depth, crack length and number/location/width of ductile or uncorroded ligaments found on the fracture face are provided in the table. Four of the five indications examined had throughwall cracks. R42C44, TSP 3, which had a throughwall crack with a 2 mil ID shear lip of mixed intergranular and dimple rupture (uncorroded) features, did not leak even at SLB conditions. The indication at R42C44 TSP 7 was found to have a maximum crack depth of 42%. This indication was initially called bobbin NDD in the field, was found by reevaluation of the field data to have a small indication prior to the tube exam and was found to have a post pull bobbin indication of about 0.9 volts.

Following the burst tests, the OD surface of the tubes were visually examined to characterize the degradation on the surface of the tube. The resulting OD surface crack distributions for the five intersections destructively examined are shown in Figures 3-1 to 3-5. These figures shown that the four largest voltage indications are dominated by a single crack with some branching adjacent to the main crack. The low voltage, R42C44, TSP 7 has shallow indications around the circumference of the tube. Figure 3-1 shows the OD sketch for the

largest 10.4 volt indication. The small patch of corrosion adjacent to the burst opening was further examined by radial metallography. This section was radially ground and the crack morphology at 21% depth is shown in Figure 3-6. This result shows a small patch of intergranular cellular corrosion. Further destructive examinations are in process at the time of this report. The destructive exams completed show crack morphologies typical of prior pulled tubes in the EPRI database for ODSCC at TSPs.

3.6 Conclusions

The visually inspected burst specimens from the TSP crevice regions of tubes R16C42, R27C43, R37C34 and R42-44 had corrosion present at the locations that had eddy current and/or UT indications. Eight of the nine SP crevice regions found to have corrosion were from true support plate crevice regions (i.e., from TSP 3, TSP 5 or TSP 7 where only a 0.008 mil nominal crevice gap existed). The ninth burst specimen (tube R16C42, TSP 1) with corrosion was from a flow distribution baffle region where the nominal crevice gap was 0.039 inch. Of the three TSP 1 regions that were burst tested, this was the only one with observed corrosion. While the exact morphology of the corrosion was not determined, initial visual examination data suggest that axially oriented OD origin IGSCC was the dominant form of corrosion.

Leak rate testing performed at elevated temperatures and pressures produced leak rates that ranged from 0.005 liters/hour to 0.114 liters/hour for normal operating conditions and from 0.040 liters/hour to 10.86 liters/hour for steam line break conditions for the three specimens which had leakage. The lowest field bobbin probe signal strength specimen which had leakage was 2.1 volts and the highest field bobbin probe signal strength specimen which did not have leakage was 3.7 volts. The SP crevice region burst pressures ranged from 4,730 to 12,640. All burst pressures were above margins required by R.G. 1.121 including the 10 volt indication at R37C34 TSP 5. The burst tests were performed simulating free span conditions with no SP enveloping the indications. The leak and burst pressure data were consistent with expectations and near mean predictions for the APC burst pressure versus bobbin voltage correlation as shown in Section 6.9. The crack morphology for the Braidwood-1 pulled tubes is dominantly axial ODSCC with a few occurrences of small patches of cellular corrosion. This morphology is typical of pulled tubes in the EPRI database.

3.7 Evaluation of Pulled Tube Data for ARC Applications

This section evaluates the pulled tube examination results described above for application to the EPRI database for ARC applications. The eddy current data is reviewed, including reevaluation of the field data, to finalize the voltages assigned to the indications and to assess

the field NDD calls for detectability under laboratory analysis conditions. The data for incorporation into the EPRI database is then defined and reviewed against the EPRI outlier criteria to assure acceptability for the database.

3.7.1 Eddy Current Data Review

Table 3-5 provides a summary of the eddy current data evaluations for the Braidwood-1 pulled tubes. For the field indications, there is little difference in the bobbin voltage calls between the field and the laboratory results. This supports the field analyst training on voltage measurements while recognizing that the larger voltage indications typical of the field calls are typically less difficult to size than the lower voltage indications such as below 1.0 volt. For inclusion of the data in the EPRI database, it is desirable to minimize analyst variability in the voltage calls since this variable is separately accounted for in ARC applications as an NDE uncertainty. Most of the pulled tube EPRI database has been analyzed by the same analyst that performed the field reevaluation of Table 3-5. Thus the reevaluated field bobbin voltages are applied for application to the ARC correlations.

The field bobbin data for the field NDD calls were reevaluated to derive the most appropriate amplitude measurements, where possible, for these very small signals. This review indicated that two field NDD indications, R42C44-7H and R16C42-5H, could be assigned a bobbin flaw voltage. For R42C44-7H, called NDD in the field due to significant noise, potentially due to probe wobble, selection of the flaw segment from the 300 kHz data, with due allowance to avoid the probe wobble segment, results in a mix signal with a 0.17 volt amplitude (0.21 volt after adjustment for ASME standard cross calibration). The reevaluated bobbin and RPC data for this indication are shown in Figure 3-7 while the field evaluations are given in Section 7. The reevaluated RPC call for this indication is a 0.11 volt indication. For R16C42-5H, the 300 kHz is again utilized to permit discrimination of the flaw segment; in this case, using the vertical signal segment, as opposed to the field choice of a signal portion consisting of two segments (see Figure 7-41, 0.61 volt), produces a mix signal of 0.23 volt (0.28 volt after adjustment for ASME standard cross calibration) for the flaw amplitude. The reevaluated bobbin and RPC data for this indication are shown in Figure 3-8. The RPC continues to be NDD with no discernible flaw separable from the background level. With these low voltage levels and difficult signal to noise circumstances, the field reanalysis of 0.61 volt was appropriately conservative. However, for the tube burst correlation, it is more appropriate to provide amplitudes less compromised by noise and more technically reliable. However, for both of these indications, the measurement uncertainties are expected to be large. The reevaluated bobbin voltages for these two indications are used for application to the ARC database and correlations.

As previously noted, the increases of 1 to 3 volts for the post pull bobbin voltages are typical of many pulled tubes in the EPRI database. Some tearing of ligaments between microcracks

may have occurred, but significant tearing of ligaments to strongly affect accident condition leakage or burst capability is not expected for these levels of post pull voltage increases. Thus, the pre-pull voltage measurements are acceptable for ARC applications subject to further review if unexpected results are obtained by destructive examination.

3.7.2 Braidwood-1 Data for ARC Application

The Braidwood-1 pulled tube results, as developed above, are summarized in Table 3-6. The measured leak rate data of Table 3-2 are adjusted in the table to the reference normal operating and SLB conditions by applying the leak rate adjustment procedure of the EPRI database report (Reference 5-1). The reference SLB conditions are a pressure differential of 2560 psid at a primary pressure of 2575 psi and a secondary pressure of 15 psi at a temperature of 616° F. The measured burst pressures are adjusted to the reference 150 ksi for the sum of the yield plus ultimate tensile strengths. The data of Table 3-6 are used in Section 6.9 to assess their influence on the EPRI ARC burst pressure, SLB probability of leakage and SLB leak rate versus voltage correlations.

The 10.4 volt response for R37C34, TSP 5 versus the 5.0 volt response for R27C43, TSP 3 indicate the strong influence of throughwall crack length on the bobbin voltage amplitude. Neither burst crack has remaining uncorroded ligaments influencing the voltage response, both have comparable average depths (74% versus 71%) and R27C34, TSP 3 has a longer crack length (0.59" versus 0.46"). The higher voltage for R37C34, TSP 5 is expected to be primarily due to the longer throughwall crack length (0.20 versus 0.10) for this indication.

The indications at R42C44, TSPs 3 and 5 have throughwall lengths of 0.05 inch with 1 and 2 mil bands of corroded/uncorroded material at the ID of the burst crack faces. The indication at TSP 5 had a low (0.041 l/hr) SLB leak rate while TSP 3 with a higher voltage (3.73 versus 2.05) did not leak. These two indications showed the highest percentage increase in the post pull voltages compared to the field amplitudes. While it is possible that both ID ligaments tore during the pulling operations, TSP 3 had the largest voltage increase (Table 3-6) but did not leak even at SLB conditions. TSP 5 had only a one mil ligament which may have torn prior to the tube pull, during the tube pull or during the normal operating condition leak test. The larger voltage for TSP 3 is likely attributable to the greater average depth and the lack of uncorroded ligaments between microcracks.

The Braidwood-1 pulled tube results were evaluated for potential exclusions from the database against the EPRI outlier criteria as given in Section 5 of this report. Criteria 1a to 1c and 1e of Table 5-1 apply primarily to unacceptable voltage, burst or leak rate measurements and indications without leak test measurements. These criteria do not apply to the indications of Table 3-7 and would not lead to any exclusions from the database. Criterion 1d applies to potential tube pull damage but requires analyses to demonstrate that

uncorroded ligaments would not have torn at accident conditions. For the 50 mil long, 1 and 2 mil wall thickness ligaments on R44C24 TSPs 3 and 5, it is unlikely that analyses could demonstrate that the ligaments would not have torn at accident conditions. The 1 mil ligament at TSP 5 had leakage at normal operating and SLB conditions while the 2 mil ligament did not leak even at accident conditions. Test data show that 50 mil throughwall cracks, even without ligaments, may not leak at SLB conditions. In either case, Criterion 1d does not provide a basis for excluding the Braidwood-1 leakage data from the database. Criterion 2b applies only to indications > 20 volts which is not applicable to the Braidwood-1 indications. Criterion 2a applies to atypical ligament morphology and states that cracks having ≤ 2 uncorroded ligaments in shallow cracks < 60% deep shall be excluded from the database. The indication at R42C44, TSP 7 has a maximum depth of 42% and three uncorroded ligaments which does not satisfy the ≤ 2 ligament criterion and the indication is retained in the database.

Criterion 3 of Table 5-3 relates to potential test errors in the leakage measurement and would exclude indications that have less than a 10% increase in leakage between normal operating and SLB conditions or that the measured leak rate for throughwall cracks without ligaments is more than a factor of 50 below the mean leak rate expected for the associated throughwall crack length. All three of the indications that leaked had more than a 10% increase in leakage between normal operating and SLB conditions so that this criterion for exclusion does not apply to the Braidwood-1 tubes. Indications R27C43 TSP 3 and R37C34 TSP 5 have throughwall crack lengths with no ligaments and are evaluated for low leak rates against the factor of 50 criterion. The third indication with leakage, R42C44 TSP 5 has a few mil band of corroded and uncorroded material at the ID of the burst crack, which is equivalent to a ligament, and Criterion 3 would not permit exclusion even if leakage was much less than expected for the associated throughwall length. Figure 3-9 shows the addition of the Braidwood-1 data to Figure 5-1 and shows the EPRI 3/4 inch diameter database, SLB leak rate as a function of throughwall crack length. It is seen that the Braidwood-1 indications, including R42C44 TSP 5, are not significantly below the mean leak rate for their respective crack lengths and the indications should not be excluded from the database.

The bobbin indications at R37C34 TSP 3, R16C42 TSP 3 and R16C42 TSP 5 were not destructively examined and thus cannot be directly assessed against outlier criteria 2a. As shown in Section 4.9, the indication at R16C42 TSP 3 lies below the mean of the burst correlation which excludes application of the outlier criterion 2a (applicable only to conservative high burst pressure indications). The indications at R37C34 TSP 3 and R16C42 TSP 5 lie toward the upper end of the database for the burst correlation (Figure 6-7). However, based on the destructive exam results for the five indications destructively examined, it is reasonable to expect that these indications would satisfy criterion 2a. The indications did not leak and Criteria 1d and 3 do not apply. Therefore, these indications are included in the database for the EPRI IPC/APC correlations.

All the Braidwood-1 TSP intersections of Table 3-7 with bobbin indications were leak and burst tested and should be included in the EPRI database for IPC/APC correlations. The indications with no leakage are appropriate for the probability of leakage and burst pressure correlations and those with SLB leakage would be included in all three correlations including the leak rate correlation. The bobbin NDD indications, while not needed for the EPRI correlations, are applicable for probability of detection assessments. The field bobbin calls for the Braidwood-1 indications were defined prior to considerations for pulling tubes and are not influenced by tube pull considerations. The field calls for R42C44 TSP 7 and R16C42 TSP 5 were NDD and the bobbin calls for these two indications were made subsequent to the tube pull and are more typical of laboratory review than typical field experience.

Table 3-1

Comparison of NDE Indications Observed on Braidwood Unit 1
Hot Leg SG Tube Support Plate Crevice Regions

Tube/ Location	Field EC	Lab EC (Analyst #1)	Lab EC (Analyst #2)	Lab EC (Analyst #3)	Lab UT	Lab X-Ray
R16-C42 SP1 (FDB)	<u>Bobbin</u> : NDD <u>RPC</u> : NDD	<u>Bobbin</u> : NDD <u>RPC</u> : NDD	<u>Bobbin</u> : NDD <u>RPC</u> : NDD	<u>Bobbin</u> : NDD <u>RPC</u> : NDD	SAI, <20% deep at 135°	No Ind
R16-C42 SP3	<u>Bobbin</u> : 3.1 V OD Ind, 70% deep <u>RPC</u> : MAI (>1C), 1.7 V max.	<u>Bobbin</u> : 4.1 V OD Ind, 55% deep <u>RPC</u> : MAI (2C), 3.9 V & 0.28" long & 0.9 V & 0.25" long	<u>Bobbin</u> : 4.1 V OD Ind, 57% deep <u>RPC</u> : MAI (2C), largest 4.2 V & 0.36" long	<u>Bobbin</u> : 4.2 V OD Ind <u>RPC</u> : MAI (2C), largest 4.6 V & 0.36" long; minor crack has volumetric components	SAI (0.4" long overall) at 300°, 85% deep, has several branches 0.1 to 0.25" long	Probable axial Ind, 0.5" long, diffuse in nature
R16-C42 SP5	<u>Bobbin</u> : NDD (0.6 V Ind in review of field data) <u>RPC</u> : NDD	<u>Bobbin</u> : 11.4 V dent <u>RPC</u> : NDD	<u>Bobbin</u> : 11.5 V dent <u>RPC</u> : NDD	<u>Bobbin</u> : 12 V dent <u>RPC</u> : NDD	Possible MAI, all short and <20% deep	No Ind
R27-C43 SP1 (FDB)	<u>Bobbin</u> : NDD <u>RPC</u> : NDD	<u>Bobbin</u> : NDD <u>RPC</u> : NDD	<u>Bobbin</u> : NDD <u>RPC</u> : NDD	<u>Bobbin</u> : NDD <u>RPC</u> : NDD	NDD	No Ind

Legend of Abbreviations:

NDD = No Detectable Degradation
RPC = Rotating Pancake Coil
DI = Disoriented Indication
ICC = intergranular cellular corrosion

SP = Support Plate
Ind = Indication
SAI = Single Axial Ind

V = Voltage
MAI = Multiple Axial
Inds
#C = number of cracks

Circ = circumferential
Max = maximum
FDB = flow distribution baffle

Table 3-1 (continued)

Comparison of NDE Indications Observed on Braidwood Unit 1
Hot Leg SG Tube Support Plate Crevice Regions

Tube/ Location	Field EC	Lab EC (Analyst #1)	Lab EC (Analyst #2)	Lab EC (Analyst #3)	Lab UT	Lab X-Ray
R27-C43 SP3	<u>Bobbin</u> : 4.9 V OD Ind, 85% deep <u>RPC</u> : SAI, 5.3 V	<u>Bobbin</u> : 5.9 V OD Ind, 87% deep <u>RPC</u> : MAI (2C), 4.6 V & 0.45" long & 0.2 V & 0.25" long	<u>Bobbin</u> : 6.0 V OD Ind, 83% deep <u>RPC</u> : SAI, 4.5 V & 0.5" long	<u>Bobbin</u> : 6.1 V OD Ind <u>RPC</u> : SAI, 4.8 V & 0.5" long	MAI: three largest are 0.25" long at 340° (near throughwall), 0.2" long at 120° (27% deep) and 0.2" long at 107° (20% deep) Deposits and possible Circ. Inds at SP bottom	Clear axial Ind, 0.45" long
R27-C43 SP5	<u>Bobbin</u> : NDD <u>RPC</u> : NDD	<u>Bobbin</u> : 3.8 V dent <u>RPC</u> : NDD	<u>Bobbin</u> : 3.9 V dent <u>RPC</u> : NDD	<u>Bobbin</u> : dent <u>RPC</u> : NDD	SAI <20% deep at 330°	No Ind
R37-C34 SP1 (FDB)	<u>Bobbin</u> : NDD <u>RPC</u> : NDD	<u>Bobbin</u> : NDD <u>RPC</u> : NDD	<u>Bobbin</u> : NDD <u>RPC</u> : NDD	<u>Bobbin</u> : NDD <u>RPC</u> : NDD	NDD	No Ind
R37-C34 SP3	<u>Bobbin</u> : 1.0 V OD Ind, 92% deep <u>RPC</u> : SAI, 0.3 V	<u>Bobbin</u> : 1.5 V OD Ind, 64% deep <u>RPC</u> : SAI, 0.7 V & 0.3" long	<u>Bobbin</u> : 1.7 V OD Ind, 71% deep <u>RPC</u> : SAI (possible MAI), 0.6 V & 0.45" long on clear Ind	<u>Bobbin</u> : 1.4 V OD Ind <u>RPC</u> : MAI (2C), 0.7 V & 0.45" long, 0.25" long on minor Ind	MAI: all short and <20% deep	No Ind

Table 3-1 (continued)

Comparison of NDE Indications Observed on Braidwood Unit 1
Hot Leg SG Tube Support Plate Crevice Regions

Tube/ Location	Field EC	Lab EC (Analyst #1)	Lab EC (Analyst #2)	Lab EC (Analyst #3)	Lab UT	Lab X-Ray
R37-C34 SP5	<u>Bobbin</u> : 10.4 V OD Ind, 82% deep <u>RPC</u> : SAI, 8.8 V	<u>Bobbin</u> : 11.9 V OD Ind, 76% deep <u>RPC</u> : SAI, 8.2 V & 0.4" long	<u>Bobbin</u> : 12.0 V OD Ind, 77% deep <u>RPC</u> : SAI, 7.7 V & 0.5" long	<u>Bobbin</u> : 12.3 V OD Ind <u>RPC</u> : SAI, 8.4 V & 0.5" long	Large axial Ind near 210°, 0.32" long and 55% deep; plus several short, shallow axial Inds.	Clear axial Ind (0.6"), composed of 3C with ligaments
R42-C44 SP1 (FDB)	<u>Bobbin</u> : NDD <u>RPC</u> : NDD	<u>Bobbin</u> : NDD <u>RPC</u> : NDD	<u>Bobbin</u> : NDD <u>RPC</u> : NDD	<u>Bobbin</u> : NDD <u>RPC</u> : NDD	NDD	No Ind
R42-C44 SP3	<u>Bobbin</u> : 3.7 V OD Ind, 68% deep <u>RPC</u> : MAI (2C), 3.2 V max.	<u>Bobbin</u> : 6.6 V OD Ind, 67% deep <u>RPC</u> : MAI, 3.6 V & 0.5" long & 0.5 V & 0.4" long	<u>Bobbin</u> : 6.7 V OD Ind, 70% deep <u>RPC</u> : MAI (>3C), 3.6 V & 0.5" long & 0.5 V & 0.4" long	<u>Bobbin</u> : 6.8 V OD Ind <u>RPC</u> : MAI (4C), 4.6 V & 0.6" long & 3 minor ones	MAI in two clusters: one near 60° (45% deep) and other near 230° (20% deep) Possible Circ. Inds in SP center near 35° and 295° (both 35° long)	Clear Circ Ind with axial components (0.25")
R42-C44 SP5	<u>Bobbin</u> : 2.1 V OD Ind, 49% deep <u>RPC</u> : SAI, 1.6 V	<u>Bobbin</u> : 3.0 V OD Ind, 47% deep <u>RPC</u> : SAI, 2.5 V & 0.3" long	<u>Bobbin</u> : 3.1 V OD Ind, 50% deep <u>RPC</u> : SAI, 1.3 V & 0.4" long	<u>Bobbin</u> : 3.2 V OD Ind <u>RPC</u> : SAI, 2.7 V & 0.4" long with volumetric components	MAI: deepest are 27% to 38% deep and 0.2" long at 130°, 110°, 50°, 30° & 345°	No Ind
R42-C44 SP7	<u>Bobbin</u> : NDD <u>RPC</u> : NDD	<u>Bobbin</u> : 2.2 V dent with 0.9 V OD Ind, 27% deep <u>RPC</u> : NDD	<u>Bobbin</u> : dent with 0.9 V OD Ind, 31% deep <u>RPC</u> : MAI, largest 0.5 V & 0.6" long	<u>Bobbin</u> : 2 V dent with 1.0 V OD Ind, 25% deep <u>RPC</u> : MAI (multiple short ones), largest 0.4 V & 0.3" long	MAI, all short & <20% deep	No Ind

Table 3-2
Braidwood Unit 1 Leak Test Results for Steam Generator Tubing

Tube No., Location	Test Type: Differential Pressure (psi)	Leak Rate (liters/hour)	Test Conditions (Pressure in psi, Temperature in °F)
R16-C42, SP3	NOC: 1265	zero	P _p = 2230, P _s = 965, T _p = 610, T _s = 613
	ITC1: 1885	zero	P _p = 2410, P _s = 525, T _p = 618, T _s = 621
	ITC2: 2330	zero	P _p = 2710, P _s = 380, T _p = 621, T _s = 622
	SLB: 2540	zero	P _p = 2740, P _s = 200, T _p = 621, T _s = 622
R16-C42, SP5	NOC: 1325	zero	P _p = 2255, P _s = 930, T _p = 608, T _s = 610
	SLB: 2575	zero	P _p = 2825, P _s = 250, T _p = 610, T _s = 611
R27-C43, SP3	NOC: 1260	0.034	P _p = 2230, P _s = 970, T _p = 609, T _s = 617
	NOC: 1275	0.034	P _p = 2250, P _s = 975, T _p = 609, T _s = 617
	ITC1: 1860	0.290	P _p = 2360, P _s = 500, T _p = 603, T _s = 602
	ITC2: 2315	0.835	P _p = 2690, P _s = 375, T _p = 565, T _s = 563
	ITC2: 2315	0.735	P _p = 2690, P _s = 375, T _p = 563, T _s = 562
	SLB: 2515	1.060	P _p = 2780, P _s = 265, T _p = 568, T _s = 537
	SLB: 2505	0.972	P _p = 2765, P _s = 260, T _p = 614, T _s = 580
	SLB: 2560	1.040	P _p = 2755, P _s = 195, T _p = 564, T _s = 562
R37-C34, SP3	NOC: 1280	zero	P _p = 2220, P _s = 940, T _p = 616, T _s = 619
	ITC: 2350	zero	P _p = 2690, P _s = 340, T _p = 622, T _s = 628
	SLB: 2530	zero	P _p = 2755, P _s = 225, T _p = 625, T _s = 625
R37-C34, SP5	NOC: 1280	0.100	P _p = 2230, P _s = 950, T _p = 579, T _s = 596
	NOC: 1275	0.114	P _p = 2230, P _s = 955, T _p = 592, T _s = 605
	ITC1: 1890	0.794	P _p = 2370, P _s = 480, T _p = 558, T _s = 576
	ITC2: 2255	6.390	P _p = 2680, P _s = 425, T _p = 567, T _s = 490
	SLB: 2500	9.440	P _p = 2730, P _s = 230, T _p = 559, T _s = 480
	SLB: 2495	10.86	P _p = 2920, P _s = 425, T _p = 560, T _s = 490
	SLB: 2500	10.69	P _p = 2930, P _s = 430, T _p = 575, T _s = 473
R42-C44, SP3	NOC: 1275	zero	P _p = 2250, P _s = 975, T _p = 626, T _s = 629
	ITC1: 1895	zero	P _p = 2410, P _s = 515, T _p = 630, T _s = 631
	ITC2: 2310	zero	P _p = 2700, P _s = 390, T _p = 629, T _s = 629
	SLB: 2545	zero	P _p = 2760, P _s = 215, T _p = 626, T _s = 625
R42-C44, SP5	NOC: 1345	0.005	P _p = 2250, P _s = 905, T _p = 623, T _s = 626
	ITC1: 1905	0.013	P _p = 2370, P _s = 465, T _p = 624, T _s = 609
	ITC2: 2330	0.034	P _p = 2700, P _s = 370, T _p = 613, T _s = 618
	SLB: 2555	0.040	P _p = 2770, P _s = 210, T _p = 606, T _s = 613
R42-C44, SP7	NOC: 1320	zero	P _p = 2240, P _s = 920, T _p = 615, T _s = 617
	SLB: 2485	zero	P _p = 2700, P _s = 215, T _p = 620, T _s = 618

Legend: All data within a table block is presented in the order of testing, NOC= normal operating conditions, ITC= intermediate test conditions, SLB= steam line break conditions, P_p= primary side pressure (psi), P_s= secondary side pressure (psi), T_p= primary side temperature (°F), T_s= secondary side temperature (°F)

Table 3-3
Room Temperature Burst and Tensile Test Results for Braidwood Unit 1 Hot Leg SG Tubing

Location	Burst Pressure (psig)	Ductility (% Dia.)	Burst Length (inches)	Burst Width (inches)	0.2% Offset Tensile YS (psi)	Tensile UTS (psi)	Tensile Elong. (%)
R16-C42, FS	10,900	30.8	1.592	0.301	49,700	97,960	34.0
R16-C42, SP1	10,720	31.8	1.499	0.357			
R16-C42, SP3	6,400*	10.9	0.983	0.283			
R16-C42, SP5	10,640	26.0	1.351	0.353			
R27-C43, FS	see below	see below	see below	see below	62,280	113,630	27.2*
R27-C43, SP1 (FS equivalent)	12,640	20.3	1.228	0.267			
R27-C43, SP3	6,140*	9.6	1.002	0.256			
R37-C34, FS	see below	see below	see below	see below	49,170	95,130	30.0*
R37-C34, SP1 (FS equivalent)	10,660	38.4	1.427	0.319			
R37-C34, SP3	8,660*	16.5	1.156	0.350			
R37-C34, SP5	4,730*	10.1	0.688	0.206			
R42-C44, FS	11,630	29.3	1.491	0.274	60,990	104,790	30.5
R42-C44, SP3	5,380*	10.5	0.942	0.251			
R42-C44, SP5	7,100*	11.3	1.015	0.251			
R42-C44, SP7	10,120	19.0	1.155	0.275			
Control (NX7368)	11,760	25.7	1.448	0.370	56,850 56,830	111,350 112,380	20.9* 26.2*

Legend: SP = support plate crevice region location; FS = free span location

* = Tensile specimen broke outside of gage length, possibly reducing elongation value.

+ = Burst specimen used a bladder and foil over largest defect area and was burst in a semi-restraint condition. In addition, after burst testing, the foil was observed to be centered under the burst opening. All other burst specimens were burst without bladders and foils and without a restraint conditions.

Table 3-4
Braidwood APC Destructive Examination Planning Data

Specimen	EC Data (field bobbin probe)	Burst Ratio (specimen/FS)	FF Corrosion (visually observed)	Crevice Region Corrosion (visually observed)	DE Performed
R16-C42, FS	NDD	1.00	no	no	
R16-C42, SP1	NDD	0.98	yes	yes	
R16-C42, SP3	Ind (3.1V)	0.59	yes	yes	
R16-C42, SP5	NDD	0.98	yes	yes (360° around circumference)	
R27-C43, SP1	NDD	1.00*	no	no*	
R27-C43, SP3	Ind (4.9V)	0.48	yes	no	yes
R37-C34, SP1	NDD	1.00**	no**	no**	
R37-C34, SP3	Ind (1.0V)	0.81	yes	yes (360° around circumference)	
R37-C34, SP5	Ind (10.4V)	0.44	yes	yes	yes
R42-C44, FS	NDD	1.00	no	no	
R42-C44, SP3	Ind (3.7V)	0.46	yes	yes	yes
R42-C44, SP5	Ind (2.1V)	0.61	yes	yes	yes
R42-C44, SP7	NDD/Ind (0.9V)	0.87	yes	yes (360° around circumference)	yes

EC = eddy current; FS = free span; FF = fracture face; DE = destructive examination

* = Burst occurred outside of crevice region, therefore the specimen truly was a FS equivalent.

** = Burst ductility was so large that all deposit and oxide films spalled, making crack observations easy. No cracks were observed and the specimen is regarded as a FS equivalent.

Table 3-5
Braidwood Unit 1 S/G Tube Macrocrack Profiles

Tube, Location	Length vs. Depth (inches/% throughwall)	Ductile Ligament Location/ Width (inches)	Comments
R27-C43, SP3	0.00/00 0.05/54 0.10/77 0.20/86 0.25/82 0.30/88 0.32/100 0.35/100 0.40/100 0.42/100 0.45/91 0.50/75 0.55/50 (0.59)/00 (Max. depth = 100% over 0.10 inch) (Ave. depth = 71%, Macrocrack Length = 0.59 inch)	<--crack top no ductile ligaments <--crack bottom	No ligaments found with intergranular features occurring over more than 50% of their length.
R37-C34, SP5	0.00/00 0.05/88 0.10/100 0.15/100 0.20/100 0.25/100 0.30/100 0.35/88 0.40/58 0.45/09 (0.46)/00 (Max. depth = 100% over 0.20 inch) (Ave. depth = 74%, Macrocrack Length = 0.46 inch)	<--crack top no ductile ligaments <--crack bottom	No ligaments found with intergranular features occurring over more than 50% of their length.

Table 3-5 (Continued)
Braidwood Unit 1 S/G Tube Macrocrack Profiles

[illegible]

A 0.002 inch wide shear lip exists at the ID lip of the fracture face over a 0.05 inch length. This shear lip has intergranular features mixed with dimple rupture features in approximately equal proportions in area.

** A 0.001 inch wide shear band exists on the fracture face, starting approximately 0.001 inch below the ID surface of the fracture face. The shear band occurs over 0.07 inch length of the fracture. The region between the ID surface and the shear band had only intergranular features.

Table 3-5 (Continued)
Braidwood Unit 1 S/G Tube Macrocrack Profiles

Tube, Location	Length vs. Depth (inches/% throughwall)	Ductile Ligament Location/ Width (inches)	Comments
R42-C44, SP7	0.00/00 0.05/28 0.10/30 0.15/21 0.20/21 0.25/28 0.30/32 0.35/35 0.40/42 (Max. depth = 42%) 0.45/37 0.50/23 <---Ligament 1 0.55/28 0.60/09 <---Ligament 2 0.65/14 <---Ligament 3 (0.68/00) (Ave. depth = 25%, Macrocrack Length = 0.68 inch)	<--crack top <--Ligament 1 /0.006" wide <--Ligament 2 /0.007" wide <--Ligament 3 /0.005" wide <--crack bottom	Three ductile ligaments observed with dimple rupture features occurring over more than 50% of their length.

Table 3-6 Summary of Braidwood-1 Pulled Tube Eddy Current Results

Tube	T S P	Field Call		Lab. Reevaluation of Field Data					Post Pull Data	
		Bobbin Volts ⁽¹⁾	RPC Volts	Bobbin Volts	ASME Cal. ⁽²⁾	Bobbin Volts ⁽²⁾	Depth	RPC Volts	Bobbin Volts	RPC Volts
Steam Generator A										
R27C43	1	NDD	NDD	NDD				NDD	NDD	NDD
	3	4.99	4.82	4.10	1.22	5.00	90%	4.8	6.1	4.8
	5	NDD	NDD	NDD				NDD	NDD	NDD
R42C44	1	NDD	NDD	NDD				NDD	NDD	NDD
	3	3.73	3.11	3.06	1.22	3.73	69%	2.9	6.8	4.6
	5	2.09	1.51	1.68	1.22	2.05	61%	1.5	3.2	2.7
	7	NDD	NDD	0.17	1.22	0.21	DI	0.11	1.0	0.4
Steam Generator D										
R37C34	1	NDD	NDD	NDD				NDD	NDD	NDD
	3	1.04	0.33	0.76	1.20	0.91	89%	0.4	1.4	0.7
	5	10.4	8.62	8.60	1.20	10.3	84%	7.4	12.3	8.4
R16C42	1	NDD	NDD	NDD				NDD	NDD	NDD
	3	3.12	3.43	2.79	1.20	3.35	79%	2.9	4.2	4.6
	5	NDD	NDD	0.23	1.20	0.28	DI	NDD	Dent	NDD

Notes:

1. Field data include cross calibration of ASME standard to the reference laboratory standard
2. ASME calibration represents the cross calibration factor for the field ASME standard to the reference laboratory standard and is applied to the laboratory reevaluation to obtain the corrected APC volts

Table 3-7 Braidwood-1 Pulled Tube Data for ARC Applications

Tube	T S P	Bobbin Data		RPC Volts	Destructive Exam Results					Leak Rate-l/hr		Burst Pressure Data - ksi			
		Volts	Depth		Max. Depth	Avg. Depth	Crack Length	TW Length	No. Lig. ⁽²⁾	N. O. 1300 psid ⁽¹⁾	SLB 2560 psid ⁽¹⁾	Meas. Burst Press.	σ _y	σ _u	Adj. Burst Press.
Steam Generator A															
R27C43	1	NDD		NDD	-0%					(4)	(4)	12.640	62.280	113.63	10.778
	3	5.0	90%	4.8	100%	71%	0.59"	0.10"	0	0.035	0.84	6.140			5.236
	5	NDD		NDD	(3)					(3)		(3)			
R42C44	1	NDD		NDD	(3)					(3)		(3)	60.990	104.79	
	3	3.73	69%	2.9	100% ⁽⁵⁾	71%	0.52"	0.05"	0	0.0	0.0	5.380			4.868
	5	2.05	61%	1.5	100% ⁽⁵⁾	54%	0.53"	0.05"	3	0.005	0.041	7.100			6.424
	7	0.21	DI	0.11	42%	25%	0.68"	-	3	0.0	0.0	10.120			9.157
Steam Generator D															
R37C34	1	NDD		NDD	-0%					(4)	(4)	10.660	49.170	95.130	11.081
	3	0.9	89%	0.4	(3)			-		0.0	0.0	8.660			9.002
	5	10.3	84%	7.4	100%	74%	0.46"	0.20"	0	0.12	12.8	4.730			4.917
R16C42	1	NDD		NDD	(3)					(4)	(4)	10.720	49.700	97.960	10.890
	3	3.35	79%	2.9	(3)			-		0.0	0.0	6.400			6.501
	5	0.28	DI	NDD	(3)			-		0.0	0.0	10.640			10.809

Notes:

1. Measured leak rates adjusted to reference conditions by applying methods of EPRI data report, Reference 5-1.
2. Number of uncorroded ligaments with > 50% of ligament length remaining in burst crack face.
3. Archive specimen and/or no destructive examinations performed.
4. Leak test not performed. No significant corrosion found by examination following burst test and no leakage would have occurred.
5. A 1 to 2 mil shear band of intergranular corrosion and uncorroded material found at ID of burst crack face.

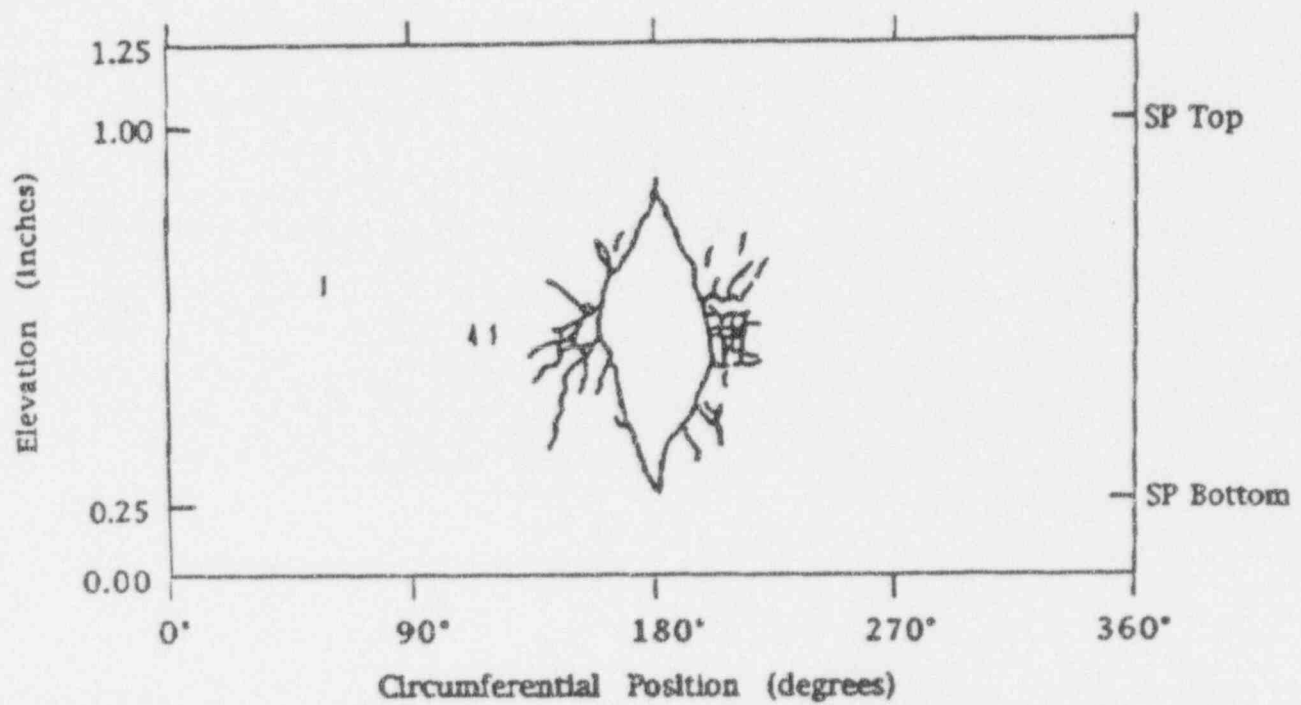


Figure 3-1. Sketch of the OD surface crack distribution found at the fifth support plate (SP5) crevice region of tube R37-C34. Also shown is the location of the burst fracture opening. The corrosion cracking was confined to the crevice region.

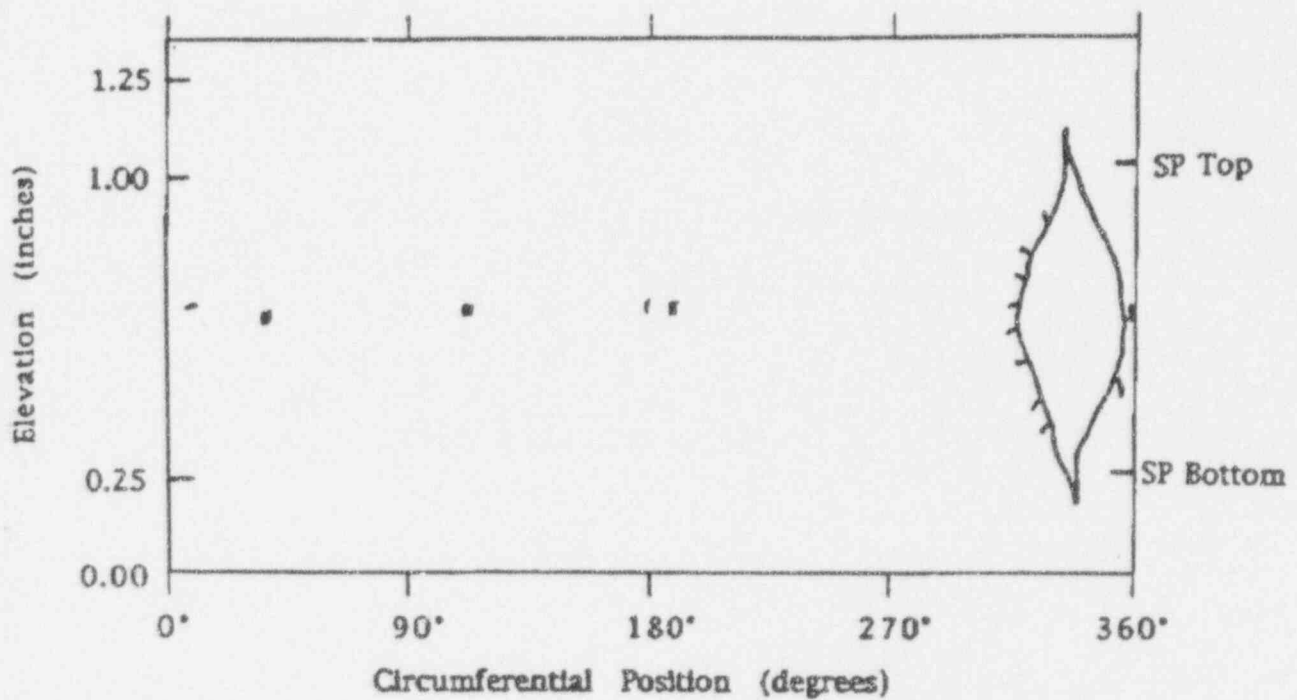


Figure 3-2. Sketch of the OD surface crack distribution found at the third support plate (SP3) crevice region of tube R27-C43. Also shown is the location of the burst fracture opening. (The burst opening extended beyond the SP crevice region, but the corrosion cracking on the burst fracture was confined to the crevice region.)

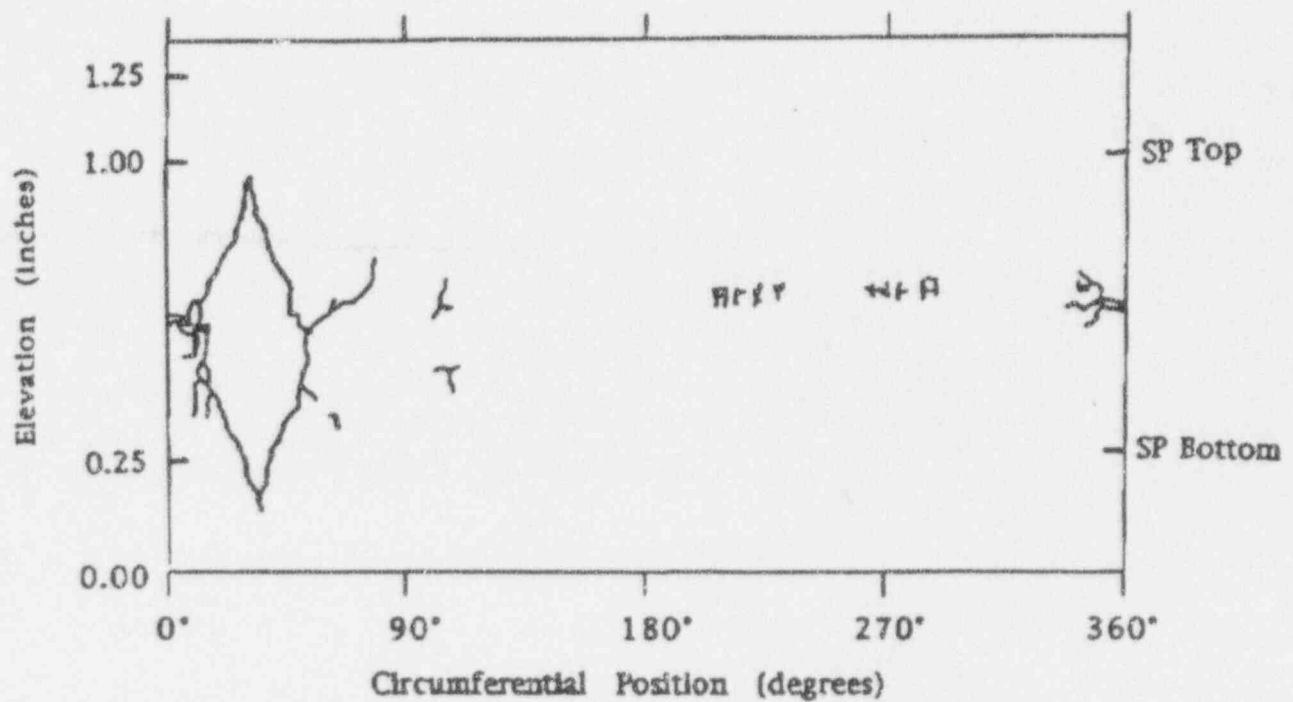


Figure 3-3. Sketch of the OD surface crack distribution found at the third support plate (SP3) crevice region of tube R42-C44. Also shown is the location of the burst fracture opening. (The burst opening extended beyond the SP crevice region, but the corrosion cracking on the burst fracture was confined to the crevice region.)

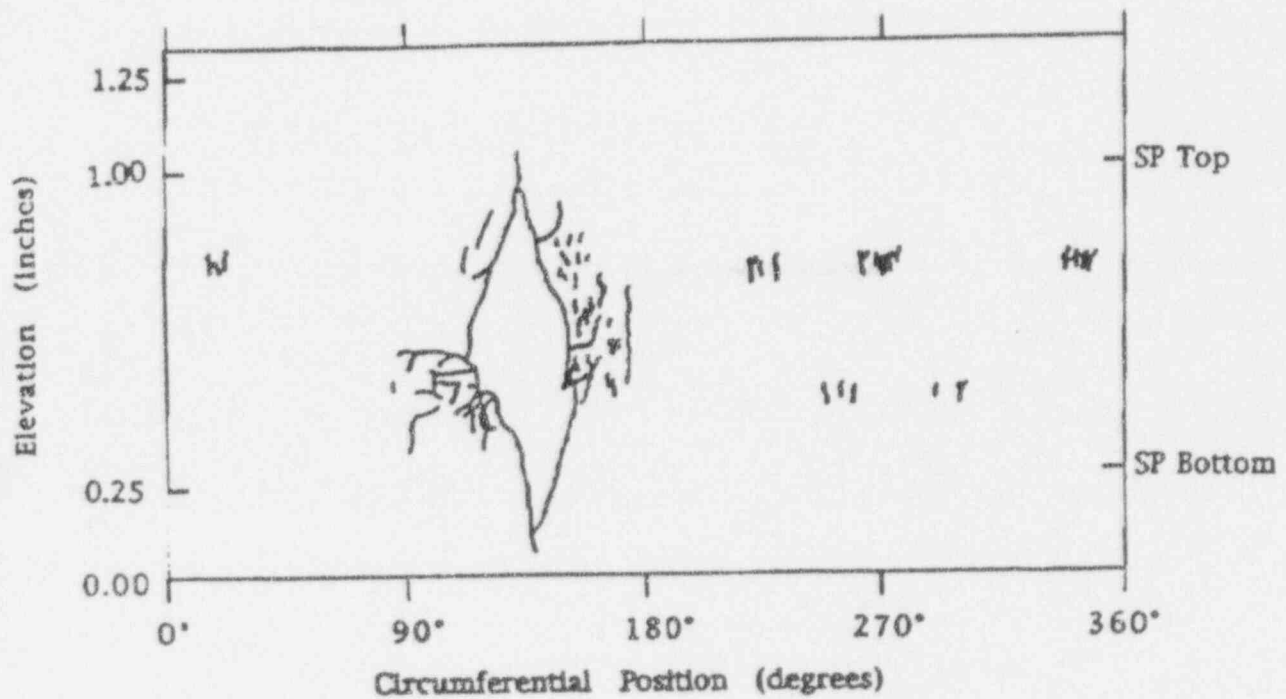


Figure 3-4. Sketch of the OD surface crack distribution found at the fifth support plate (SP5) crevice region of tube R42-C44. Also shown is the location of the burst fracture opening. (The burst opening extended beyond the SP crevice region, but the corrosion cracking on the burst fracture was confined to the crevice region.)

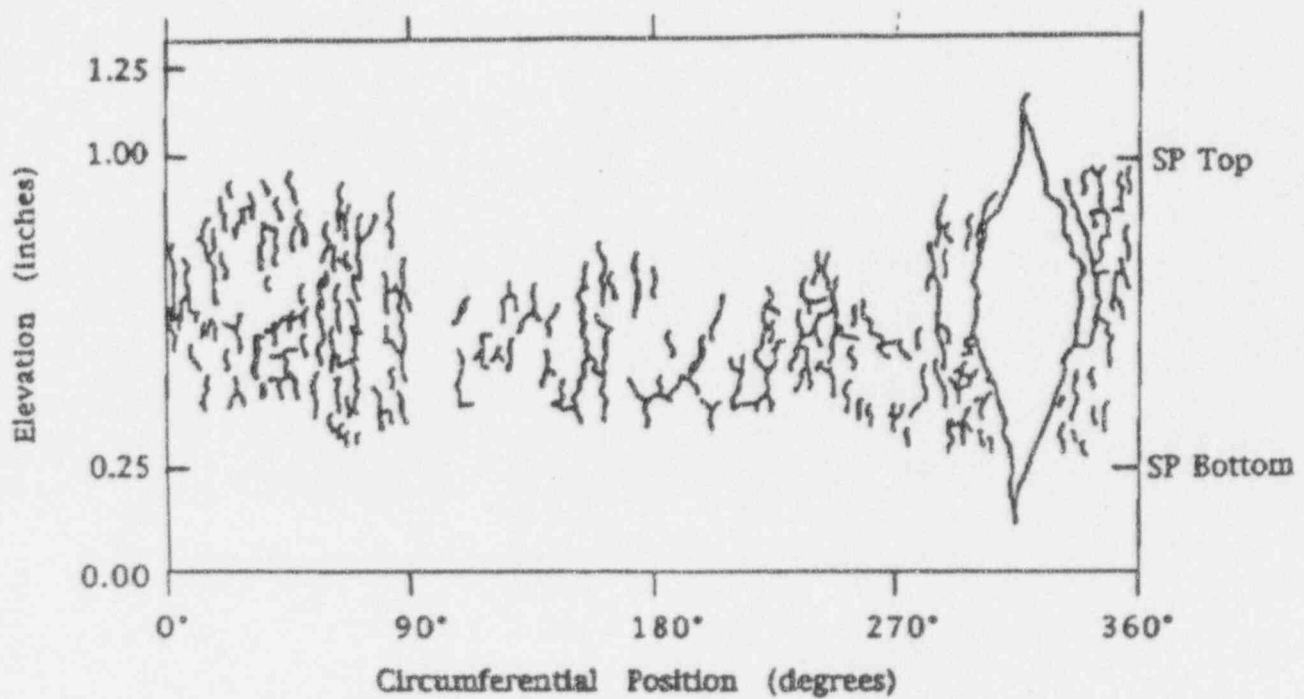
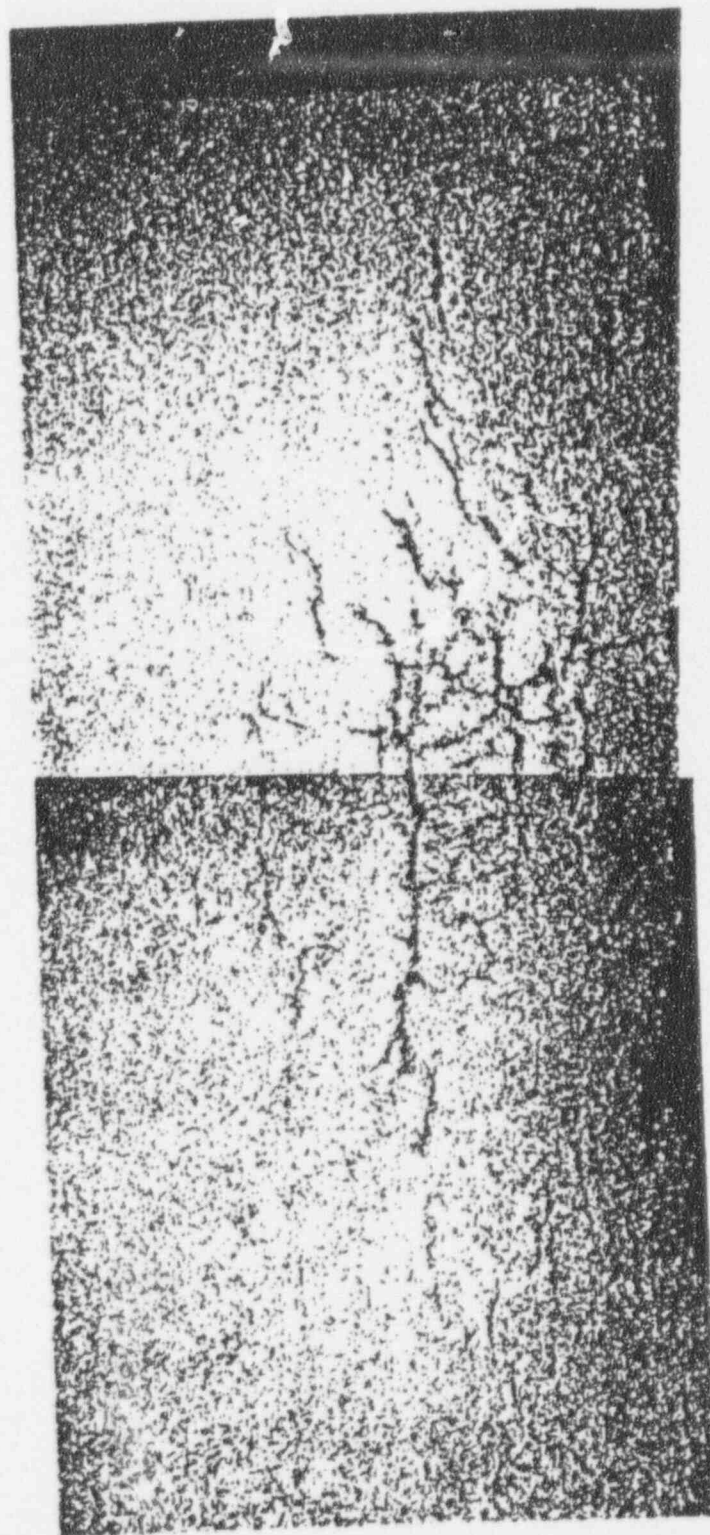


Figure 3-5. Sketch of the OD surface crack distribution found at the seventh support plate (SP7) crevice region of tube R42-C44. Also shown is the location of the burst fracture opening. (The burst opening extended beyond the SP crevice region, but the corrosion cracking on the burst fracture was confined to the crevice region.)



< Fracture Face
(mid-crevice location)

< SP Bottom Location

Figure 3-6. Example of intergranular cellular corrosion (ICC) as observed by radial metallography in the SP5 crevice region of tube R37-C34, 21% depth, 16X magnification.

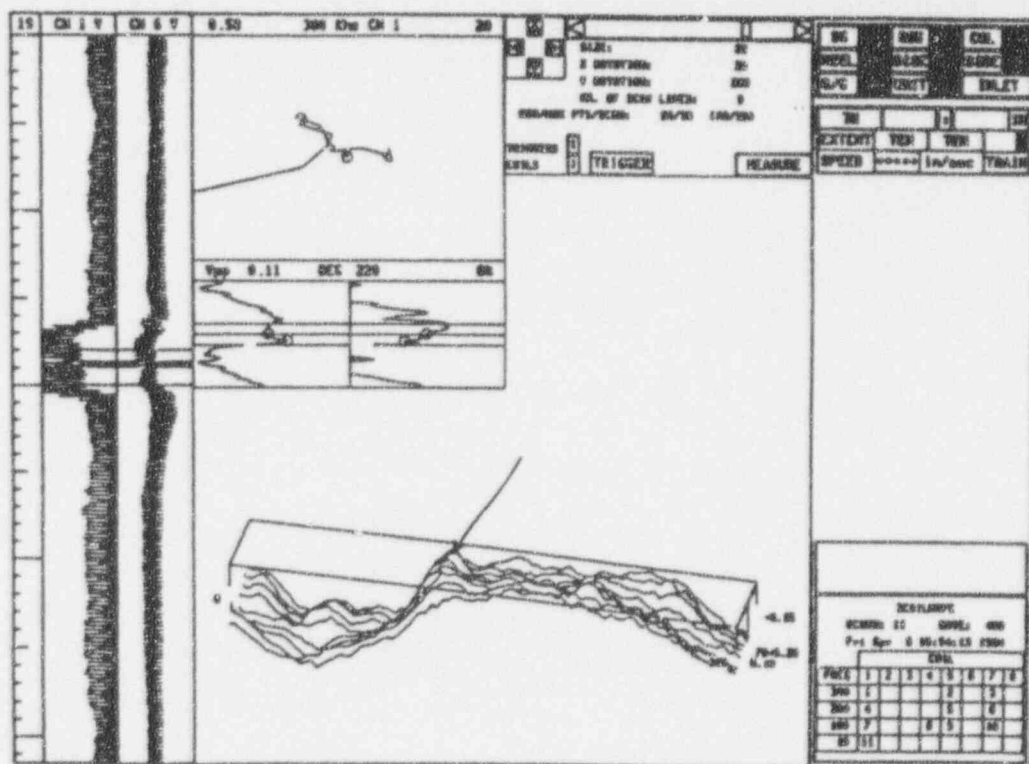
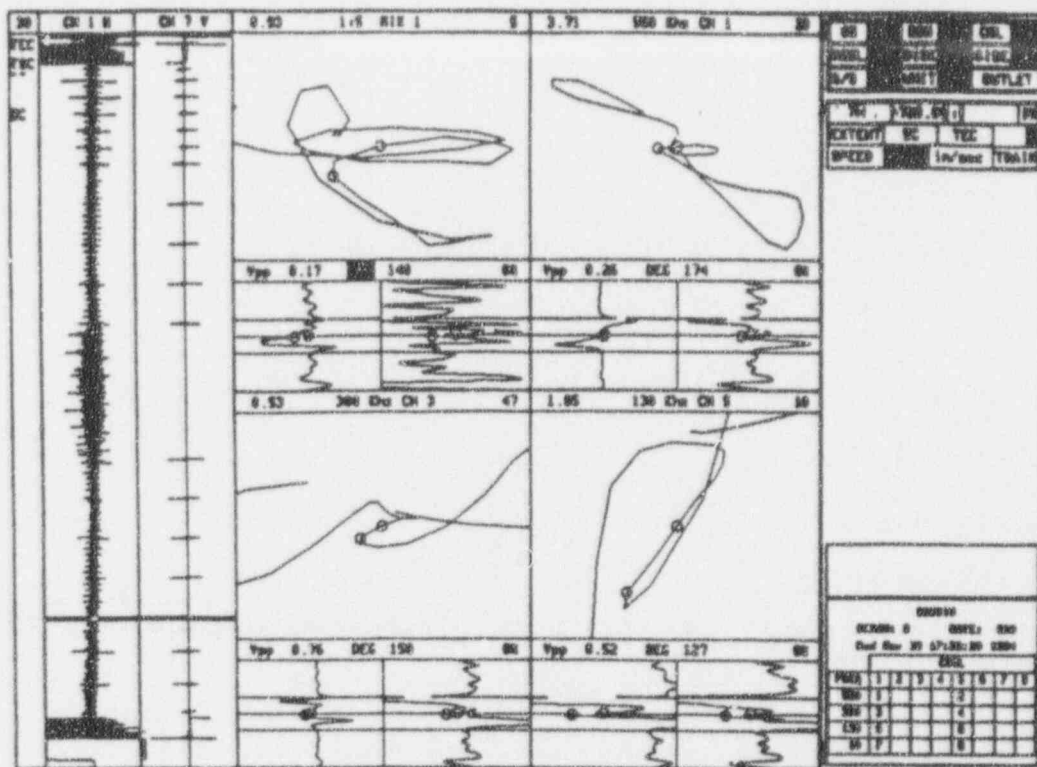


Figure 3-7. Laboratory Re-evaluation of Field Bobbin and RPC Data for R42C44 - 7H

Figure 3-9. Comparison of 3/4" Leak Test Data with CRACKFLO Predictions

4.0 ACCIDENT CONSIDERATIONS

4.1 General Considerations for Accident Condition Analyses

The approach being applied to demonstrate tube integrity at Braidwood-1 is based on applying SLB analyses demonstrating limited TSP displacement to reduce the likelihood of a tube burst in a SLB event to negligible levels. In addition, it is demonstrated that the SLB leak rate, even under the conservative assumption of leak rates for free span indications, is within acceptable limits. The allowable limit on the SLB leak rate is developed in Section 4.8.

Section 4.2 develops the SLB thermal hydraulic loads on the TSPs, which are used in the structural analyses of Sections 4.3 to 4.5 to obtain TSP displacements. Originally, Model D4 SG loads were available for SLB at normal operating conditions and for a very conservative SLB at hot standby conditions. The hot standby loads include conservatism based on low water levels (at level of the top TSP) and include a simultaneous feedwater transient. The potential level of conservatism in the Model D4 hot standby loads is demonstrated by comparing the loads with those obtained from a Model D3 SG analysis with normal water level and no feedwater transient. Both SLB analyses, at normal operating conditions and at conservative hot standby conditions, for TSP displacements developed in Sections 4.3 to 4.5 and were applied in Section 8 of Revision 0 of this WCAP to develop tube burst margins. The TSP displacements are calculated relative to the tube location at the start of the transient, as discussed in Section 4.5. Section 4.4 includes an assessment of the structural integrity of the TSPs and their supports (bar, wedge welds).

Section 4.10 of this report provides updated thermal hydraulic loads on the TSPs obtained from an updated TRANFLO model of the Model D4 SG. Two cases are considered, one for full power operation and another for hot standby; the updated hydraulic loads on the TSPs for these cases are compared to the cases considered in Section 4.2. The updated TSP loads from Section 4.10 are used to update the results of the TSP displacement analysis in Section 4.11. Revised TSP displacements and an assessment of the updated number of tubes falling into each of the displacement groupings used in Section 4.5 for establishing tube burst probabilities are provided in Section 4.11.

Section 4.6 develops the frequencies of occurrence for an SLB at Braidwood-1 at both normal operating and hot standby (Mode 3) conditions. It is shown that the frequency of an SLB at hot standby conditions, for which the TSP displacements are higher, is significantly lower than that for an SLB at normal operating conditions.

For a postulated accident condition combining a LOCA simultaneously with an SSE, it is possible to have some tubes near TSP wedges deformed by the resulting loading condition. Due to the potential for secondary to primary leakage in the combined LOCA plus SSE, the

tubes subject to significant tube deformation near the wedges are excluded from application of the IPC repair limits. The analyses describing this consideration are described in Section 4.7.

Some of the analyses described in this section use the Westinghouse labeling system for numbering TSPs which differs from that applied at Braidwood-1. The following relates the Westinghouse and Braidwood-1 nomenclatures for hot leg TSP identification:

<u>Westinghouse TSP</u>	<u>Braidwood-1 TSP</u>
A	1
C	3
F	5
J	7
L	8
M	9
N	10
P	11

TSP 1 is the Flow Distribution Baffle (FDB). The FDB has large tube to plate clearances (nominal []" diameter) in the central region of the plate and radialized holes (nominal []" width) in the outer region. No indications have been found at the FDB in the Braidwood-1 SGs. For comparison, the Model D3 SG, for which indications have been found at the FDB, has a nominal hole diameter of []".

4.2 Thermal Hydraulic Loads on TSP in a SLB Event

4.2.1 Introduction

A postulated steam line break (SLB) event results in blowdown of steam and water. The fluid blowdown leads to depressurization of the secondary side fluid. Pressure drop develops and exerts hydraulic loads on the tube support plate (TSP) or flow baffle. These hydraulic loads were determined for the Model D4 and D3 steam generator using the TRANFLO Code. This code is a network flow based code that can model the thermal and hydraulic characteristics of fluid through the steam generator internals. TRANFLO code predicts the transient flow rate, pressures and pressure drops.

The hydraulic loads vary with initial conditions and boundary conditions of the SLB event. The significant initial conditions are mode of operation and water level. The important boundary conditions are those associated with feedwater nozzle and steam nozzle; these include the size and location of break, and flow rate through the feedwater nozzle during the event. The most likely initial conditions are of full power operation with a normal water level.

When fluid moves in the tube bundle, water will exert a higher pressure drop across the TSP when compared to steam. Hot standby at zero power provides a solid water pool in the tube bundle while power operation generates a steam and water mixture. Thus, hot standby would be conservative in estimating the hydraulic loads on the TSPs, although the most likely mode of operation is power operation if a SLB event occurred. Previous studies confirmed that the hot standby yields the largest hydraulic loads when compared to full or partial power operation.

Once a SLB event begins, it triggers a rapid depressurization, which leads to water flashing across the water level. The rapid water flashing generates water motion, and the closer the TSP to the water level the higher the flow rate, and thus the larger the pressure drop. Previous parametric evaluations indicate that a lower water level tends to yield higher hydraulic loads on the tube support plates or baffles.

It would be ideal to calculate the hydraulic loads on the TSPs of the Model D4 steam generator under the no load, hot standby conditions. Although there are currently no such calculations, there are other calculations of Model D3 and D4 for developing conservative, bounding loads for the Model D4. This section presents such a task. These bounding loads for the Model D4 and the more applicable Model D3 loads at hot standby with normal water level.

4.2.2 Hydraulic Loads of Model D3 under No Load, Hot Standby with Normal Water Level

In 1993, a TRANFLO calculation of hydraulic loads on the TSP under a SLB event was made for a Model D3 steam generator. The calculation considers the initial conditions of zero load, hot standby and a water level at about normal setting. The following describes the calculation model.

The Model D3 steam generator maintains a normal water level of []" above the top of the tubesheet during no load, hot standby. The computational model considers a water level of []" above the top of the tubesheet. Use of the no load, hot standby and a water level of []" is thus conservative in estimating the pressure loads to tube support plates. Water and steam temperature is initially at 557°F, and primary coolant pressure is at 2350 psia, and secondary side steam pressure is at 1106 psia, and feedwater temperature at 75°F.

A network of nodes and connectors was created to represent the secondary side fluid, tube metal heat transfer and primary coolant. Figures 4-1 and 4-2 show the nodal layout of the secondary side of the Model D3 steam generator. Figures 4-3 and 4-4 present the nodal network of the secondary fluid, primary fluid and tube metal. In the tube bundle area, the space between support plates or baffles forms a fluid node, and a flow connector links the

adjacent nodes. Pressure drops through support plates or baffles are calculated by the code for each flow connector, which represent a plate or baffle.

Blowdown flow induces fluid flow in the secondary side, and thus pressure loads to various TSPs and baffle plates. Figures 4-5 through 4-7 show pressure loads through TSPs and baffle plates outside the preheater. The peak of pressure loads across TSP or baffle plates develops within one second, and it then drops to a small value or becomes a quasi-steady state.

The flow splits take place in the lower tube bundle; it occurs at about TSP L (see Figure 4-1). Plates A, C and G experience downward flow because the fluid leaves in a downward direction from the tube bundle up into the downcomer. Plates above TSP L experiences upward flow as the fluid leaves in the upward direction through the tube bundle. Maximum loads occur at TSPs A, B and T; about []" at the peak for TSP B on the cold leg, []" for TSP A on the hot leg, and []" for TSP T (i.e., the uppermost TSP).

4.2.3 Hydraulic Loads of Model D4 under Full Power with Normal Water Level

Although there are differences in the preheater design between the Model D3 and D4 steam generator, it is judged that there would be no significant differences in the hydraulic loads on the TSPs outside the preheater. It would be ideal to have a TRANFLO calculation for the Model D4 steam generator with initial conditions and boundary conditions like Case 1 for the Model D3. However, no such run is currently available. Calculations are available for hydraulic loads on the TSPs for the Model D4 steam generator under full power operation with a normal water level when a SLB begins.

Figure 4-8 illustrates the nodal layout of the secondary side of the Model D4 steam generator, which is similar to Figure 4-1 for the Model D3. The calculation was made for design analyses in the 1970's. Table 4-1 lists the initial and boundary conditions for three cases for which SLB loads are available; Case 3 will be discussed later.

Results of Case 2 are presented in Figures 4-9 through 4-11. As discussed earlier, hydraulic loads for a steam and water mixture in the tube bundle are less than a solid water pool. Therefore, hydraulic loads of Case 2 for the Model D4 is less than those of Case 1 for the Model D3. When a SLB event initiates from a power operation, the blowdown flow path is essentially in the upward direction from the tubesheet towards the riser barrels. Therefore, hydraulic loads tend to be higher at the upper TSPs, as shown in the above figures. Since the event begins from full power operation, the steam content increases with the bundle height. The uppermost TSP is thus lower in water content, and the resulting hydraulic load is less than the N plate below it. In addition, the highest loads occurs at the TSP L on the hot leg because the flow area is half of a whole TSP and the majority of flow is passing through the hot leg side.

Compared to Case 1 for the Model D3, which experiences flow splits, loads of Case 2 for Model D4 are less even under the situation of no flow splits. The reason for this is because of its relatively mild initial conditions.

4.2.4 Hydraulic Loads of Model D4 under No Load, Hot Standby with a Water Level at the Uppermost TSP and an Excessive Feedwater Flow Transient

The TRANFLO computational model for this case is identical to Case 2 except for its initial and boundary conditions. This calculation of Case 3 uses extremes of both initial and boundary conditions. No load at hot standby is already conservative compared to a most likely mode of full power operation; it considers a water level at the uppermost TSP, which is by itself a very rare transient. In addition, it imposes an excessive feedwater flow transient. As discussed already, a water level at the uppermost TSP generates higher hydraulic loads than a normal water level. An excessive feedwater flow introduces more solid water into the tube bundle, which provides additional source of water for flashing action to trigger more water motion.

Figures 4-12 through 4-14 presents hydraulic loads on various TSPs. Like Case 1, flow splits take place for Case 3 since both cases initiate from a no load, hot standby condition. However, Case 3 yields much higher loads than case 1 because of severe initial and boundary conditions discussed above.

4.2.5 Summary

Table 4-2 summarizes the key parameters regarding the loads. As far as the maximum peak load is concerned Case 2 for Model D4 yields slightly higher loads than Case 1 for Model D3. This is because the flow area for the plate with maximum load is half of the whole plate only, and there is no flow split. The lower TSPs of Case 2 experience hydraulic loads much less than those of Case 1, because there is almost no downward flow split for Case 2.

Peak loads of Case 3 are more than twice those of Case 2. Use of loads of Case 3 is conservative. It is believed that loads for Model D4 would be about the same as those of Case 1 for Model D3, if the same initial and boundary conditions are used in the computational model.

4.3 Structural Modeling for SLB TSP Displacement Analyses

This section summarizes the structural modeling of the Model D4 tube bundle region. A finite element model of the hot leg region of the tube bundle is prepared, and corresponding mass and stiffness matrices are generated. The mass and stiffness matrices are then used in a

subsequent dynamic analysis to determine TSP displacements under SLB loads. Structural members included in the model include all TSPs, the tierods and spacers.¹ Since the present analysis considers only the response of the hot leg to the SLB loading, the finite element model includes 90° of the tube bundle.

4.3.1 Material Properties

A summary of component materials is contained in Table 4-3, with the corresponding material properties summarized in Tables 4-4 through 4-6. The properties are taken from the 1971 edition (through summer 1972 addenda) of the ASME Code, which is the applicable code edition for Braidwood Unit 1. Since temperature dependent properties cannot be used in substructures, properties for the finite element model correspond to the values at 550°F. The material properties for the tube support plates are modified to account for the tube penetrations and flow holes. The density of the TSPs is also modified to account for the added mass of the secondary side fluid.

4.3.2 TSP Support System

The support system for the TSPs is a combination of several support mechanisms. A schematic of the tube bundle region is shown in Figure 4-15, with each of the plates identified. []^a

¹ For the analysis of the Model D3 steam generators under SLB loads, the finite element model also included the shell, wrapper, partition plate, and channel head. Except for the tubesheet, these structures were included to account for support locations for the TSPs and baffle plates. However, compared to the stiffness of the TSPs, baffle plates, and tierods, these structures are essentially infinitely stiff and have insignificant displacements (<0.010) under SLB loads. Therefore, it is acceptable to treat these structures as points of rigid support for the plates, and not include them explicitly in the model.

Regarding the tubesheet, although not considered explicitly in the finite element model, tubesheet displacements are considered in the analysis. Due to similarities in geometry of the tubesheet, shell, and channel head, displacements are scaled from the Model D3 analysis. The tubesheet displacements are quite small relative to the TSP displacements, and scaling of Model D3 displacements is an acceptable approximation. Further discussion of the tubesheet displacements is provided in Section 4.4.

The Model D3 analysis also considered the non-linear interaction between tubes and TSP due to TSP rotation. The present analysis has not incorporated this effect, primarily due to the limited time available to develop the system model. This effect may be considered in subsequent evaluations to limit plate displacements.

[

J^a

The lack of a rigid link between the spacers and TSPs for the outer tierods / spacers results in a non-linear dynamic system. However, the nature of the SLB transient results in an essentially linear system response. During installation a small positive preload is introduced into the tierod/spacer system. As shown in Section 4.2, the plates are subject either to an upward or downward pressure loading, with the exception being Plate J, which sees a both a significant upward and downward loading. Thus, the response is essentially linear either upward or downward. The tierods/spacers have a different stiffness characteristic for upward and downward loads. These differences have been incorporated into the model. For Plate J, the weaker of the two stiffnesses has been incorporated to provide a conservative response.

² [
J^a³ [J^a

The various support locations for the plates are shown in Figures 4-16 through 4-24. Figure 4-16 shows the locations of the tierods and spacers. Plate / wrapper support locations are shown in Figures 4-17 through 4-24. The finite element model representation of the plates and tierods/spacers is shown in Figure 4-25.

4.3.3 Revised Material Properties

As noted earlier, the material properties for the tubesheet and tube support plates are modified to account for the tube penetrations, flow holes, and various cutouts. The properties that must be modified are Young's modulus, Poisson's ratio, and the material density. The density must be additionally modified to account for the added mass of the secondary side fluid.

In calculating revised values for Young's modulus and Poisson's ratio, separate formulations are used for plates with and without flow holes. Due to square penetration patterns, different properties exist in the pitch and diagonal directions. The first step is to establish equivalent parameters for Young's modulus and Poisson's ratio in the pitch and diagonal directions (E_p^*/E , E_d^*/E , ν_d^* , ν_p^*), respectively. The equivalent Young's modulus for the overall plate is taken as the average of the pitch and diagonal directions. The next step in the process is to determine an equivalent value for the shear modulus, G^*/G , for the plate. This is done in a similar manner as for Young's modulus, starting with values in the pitch and diagonal directions, and then taking an average of the two values. The final equivalent value for Poisson's ratio is determined from the relationship between Young's modulus and the shear modulus. A summary of the revised values for Young's modulus and Poisson's ratio is provided in Table 4-7.

There are two aspects to revising the plate density. The first is based on a ratio of solid area to the modeled area. The second aspect corresponds to the plate moving through the secondary side fluid, displacing that fluid, and creating an "added mass" effect. The added hydrodynamic mass is a direct function of the fluid density. Because the dynamic analysis cannot account for the change in fluid density with time, the analysis uses the average density value for the duration of the transient. Results of the calculations to determine effective plate densities are summarized in Table 4-8. This table provides a summary of the actual (structural) and modeled plate masses, the metal and added fluid masses, and the final effective plate densities. The fluid densities correspond to SLB events initiating from hot shutdown conditions (as opposed to full power operation). Calculations were also performed for densities corresponding to full power operation. The change in effective plate densities did not have a significant effect on the dynamic response of the plates.

4.3.4 Dynamic Degrees of Freedom

In setting up the dynamic substructures, it is necessary to define the dynamic degrees of freedom. In order to define dynamic degrees of freedom for the TSPs, two sets of modal calculations are performed for each of the plates. The first set of calculations determine plate mode shapes and frequencies using a large number of degrees of freedom (approximately 120 per plate). The second set of calculations involves repeating the modal analysis, using a significantly reduced set of degrees of freedom (DOF). The reduced DOF are selected to predict all frequencies for a given plate below 50 hertz to within 10% of the frequencies for the large set of DOF. A frequency of 50 hertz was selected as a cutoff, as it is judged that higher frequencies will have a small energy content compared to the lower frequencies. This can be confirmed by noting that the highest frequency content in the first one and a half seconds of the pressure drop time-history input loadings is typically less than 10 hertz. For each of the modal runs, in addition to symmetry boundary conditions along the "Y-axis", and vertical restraint at vertical bar locations, all the plates are assumed to be constrained vertically at tierod/spacer locations.

A sample set of mode shape plots is provided for Plate A. Mode shape plots for the full set of DOF are shown in Figures 4-26 through 4-28, while mode shapes for the reduced set of DOF are shown in Figures 4-29 through 4-31. A comparison of the natural frequencies for the full and reduced sets of DOF for the plates is provided in Table 4-9. Based on the tabular summary, the reduced set of DOF are concluded to provide a good approximation of the plate response. Note that for Plate P, the frequency for Modes 3 and 5 for the reduced set of DOF slightly exceeds the 10% objective for matching frequencies. These variations are not considered to be significant, and the selected DOF are judged to give an acceptable representation of the Plate P response. The reduced set of DOF consists of 8 - 10 DOF for each of the plates.

4.3.5 Displacement Boundary Conditions

The displacement boundary conditions for the substructure generation consist primarily of prescribing symmetry conditions along the "Y" axis for each of the components. Vertical constraint is provided where the plates are constrained by the vertical bars welded to the partition plate and wrapper, and to the tierods at there bottom end. For the TSPs, rotations normal to the plate surface are also constrained, as required by the stiffness representation for the plate elements.

4.3.6 Application of Pressure Loading

The SLB pressure loads act on each of the TSPs. To accommodate this, load vectors are prescribed for each of the plates using a reference load of 1 psi. The reference loads are scaled during the dynamic analysis to the actual time-history (transient) loading conditions, as defined in Section 4.2.

The transient pressures summarized in Section 4.2 are relative to the control volume for the thermal hydraulic analysis. The area over which the hydraulic pressure acts corresponds to the area inside the wrapper minus the tube area. These pressures must be scaled based on a ratio of the plate area in the structural model to the control volume area in the hydraulic model. A summary of the transient pressure drops is given in Section 4.2. These pressure drops were modified as discussed above and applied to the structural model for the dynamic analysis.

4.4 Results of SLB TSP Displacement Analyses

As discussed in Section 4.2, several sets of SLB loads were considered in performing this analysis. In addition to the system analysis, some preliminary single-plate evaluations were performed to estimate the plate response to the applied loadings. Calculations were also performed using the single plate models to estimate the effects of expanding tubes at various locations in the tube bundle to limit plate motions. The results for each set of calculations is summarized within this section of the report.

An overall summary of the limiting displacements for each of the plates for the various cases considered is provided in Table 4-10. The displacements in this table are relative to the initial starting plate positions. The magnitude of the tubesheet displacements and their effect on these results is discussed below.

The first two sets of results in Table 4-10 are for the most limiting SLB loading (SLB with a simultaneous Feedwater Transient) using the single plate models, with and without tube expansion. These results show that tube expansion significantly reduces plate displacement for all of the plates. The third set of results is again for the limiting SLB transient for the full system model. Comparing these results to the single plate models shows that the single plate models provide a good indication of the relative plate motions, but that plate interaction does result in an increase in the plate responses, more for some plates than others.

Comparing the results for the three SLB sets of loads using the system model shows that for the limiting SLB loads, Plates A (1H), C (3H), and J (7H) experience displacements greater

than 0.350 inch. For a transient initiating from normal operation that only Plate J (7H) sees any significant motions, and for the Model D3 SLB loads case, only Plates A (1H) and C (3H) show any significant response. Based on the single plate response to the limiting load with expanded tubes, it is concluded that expansion of a limited number of tubes would be effective in reducing the response of each of these plates to very low levels.

The limiting plate displacements in all cases are limited to a small region of the plate at their outer edge near the tube lane, where the distance between vertical supports is greatest. Displaced geometry plots for Plates A (1H), C (3H), and J (7H) for the limiting set of SLB loads are shown in Figures 4-32 through 4-35. The consistent displacement pattern is apparent for the three plates. Displacement time histories for each of the plates for the limiting transient loads are provided in Figures 4-36 and 4-37. The bottom four plates are shown in Figure 4-36 and the upper four plates in Figure 4-37.

As discussed previously, tubesheet displacements are not significant and were scaled from the Model D3 analysis. The geometry of the tubesheet and supporting structures for the two designs is nearly identical. A summary of key dimensions for the two models of steam generators is provided in Table 4-11. Displacement results for the tubesheet from the Model D3 analysis as a function of distance from plate center for several transient times are summarized in Table 4-12. At the bottom of this table a summary of the tubesheet displacements relative to time zero are presented. The relative displacements are shown to be quite small relative to the plate displacements. This is especially true at the outer edge of the tubesheet where the plate displacements are a maximum.

Since the dynamic analysis is based on elastic response, calculations were performed to assure that the tierods, a significant support element for the plates remain elastic throughout the transient. The dynamics analysis results establish that the stayrods do, in fact, remain elastic throughout the transient. [

]° In both instances, these elongations are well below the yield point for the stayrods.

Also relevant in assessing the appropriateness of the elastic solution, are the stresses in the plates. Thus, in conjunction with the displacement results from the dynamic analysis, stresses are calculated for the hot leg plates at the times corresponding to the maximum plate displacements. The stresses are calculated by extracting displacements from the dynamic analysis for each plate degree of freedom, and then applying those displacements to the finite element model. The finite element code then back-calculates the displacements and stresses for the overall plate model.

In order to extract the appropriate displacements from the tape created by the dynamic analysis, a special purpose computer program is used. This program extracts the displacements for a given plate at specific transient times and writes the resulting nodal displacements to output in a form that can be input directly to the WECAN program as displacement boundary conditions. Using this program, displacement boundary conditions are extracted at the times of maximum relative displacement for Places A (1H), C (3H), and J (7H) at the critical times for the SLB + Excess Feedwater transient and for Plates A (1H) and C (3H) for the Model D3 transient. Note that for Plate J for the SLB + Excess Feedwater transient, stresses are calculated for the times corresponding to both the maximum upward displacement and also for the maximum downward displacement. These are the transients and plates that are judged to be limiting based on the plate displacement results.

Additional boundary conditions corresponding to lines of symmetry and appropriate rotational constraints are also applied to the model. The finite element results give a set of displacement and stress results for the overall plate. The resulting plate stresses, however, correspond to the effective Young's modulus, and must be multiplied by the inverse ratio of effective-to-actual Young's modulus to get the correct plate stresses. The stress multiplication is performed by another special purpose computer program, SRATIO.

In order to interpret the stress results, stress contour plots for the maximum and minimum stress intensities have been made for each plate. The limiting stresses for each of the plates occur for the SLB + Excess Feedwater transient. Plots showing the maximum and minimum stress intensities for Plates A(1H), C(3H), and J(7H) are shown in Figures 4-38 to 4-45, respectively. These plots show the distribution of stress throughout the plate. As expected, the maximum stresses occur near the locations of vertical support, the tierod / spacers and vertical bars. The ASME Code minimum yield strength for the TSP material is 23.4 ksi. Except for one very local area for Plate J corresponding to the upward loading on the plate (Figure 4-42), the stresses are elastic throughout the plate. Recalling that the present analysis does not account for either the wedge support for Plate J at the 10° location, or the potential for tube/plate interaction due to plate rotation, the stresses in Figures 4-42 and 4-43 for Plate J are judged to be conservative. Thus, it is judged that the effective plate stresses will be judged to be elastic for all transient cases.

The plate stresses cannot be compared directly to the material yield strength, as these stresses correspond to an equivalent solid plate. In order to arrive at the plate ligament stresses, additional detailed stress analysis of the plates is required. Such an analysis is outside the scope of this program. The equivalent plate stresses do provide a general guideline as to those areas of the plate that are most limiting from a stress viewpoint. The plate stresses are meaningful in that they indicate that the stresses are generally low throughout the plate, and that the elastic analysis is a good approximation of the transient plate response.

Calculations have also been performed to determine the stresses in the welds between the vertical bars and the partition plate and wrapper. The loads at the various support points are extracted from the static WECAN runs in the form of reaction forces at the times of maximum plate deflection. Loads have been extracted for the limiting plates (based on plate motions) for each of the SLB load cases, and for Plate P, which experiences the highest pressure loads, for the SLB + Excess Feedwater transient.

[

] The corresponding stress intensity is twice the shear stress.

A summary of the reaction forces and corresponding stresses for each of the bar locations for the locations considered is provided in Table 4-13. The results show all of the stresses to be low (<2 ksi) for a faulted event. The allowable stress for the welds is based on $2.4S_m \times 1.5 \times 0.35$ (for fillet welds with visual examination) for carbon steel. S_m at 550°F is 15.5 ksi. The resulting allowable stress intensity is 19.53 ksi, and the weld stresses are acceptable.

Overall, it is concluded that the elastic analysis provides a good approximation of the dynamic response of the TSPs to the applied loading.

4.5 SLB Displacements By Tube Location

In order to establish probabilities for tube burst as a result of relative plate / tube movement, calculations are performed to determine how many tubes are associated with a given displacement magnitude for a given plate. The plate displacements are categorized into groups, starting at 0.35 inch, and increasing in 0.05 inch increments to a maximum displacement > 0.80 inch. It is the relative plate / tube displacement that is of interest, with the tube and plate positions at the start of the SLB transient defined as the reference position. At hot standby, the TSP positions relative to cracks inside the TSP are essentially the same as at cold shutdown. Every known SG cold condition inspection shows ODSCC cracks within the non-dented TSP with a trend towards being centered within the TSP. Therefore, the cold condition TSP location relative to the tubes is essentially the same as for the full power condition where the cracks formed, which is also the position during hot shutdown. These inspections indicate that there is little relative movement between the tubes and plates throughout the operating cycle. Thus, this analysis calculates relative tube / TSP motions based on the tube / plate positions at the initiation of the SLB transient.

The algorithm for calculating the relative displacements is as follows:

$$\Delta D = (D_{t=T} - D_{t=0})_{\text{Plate}} - (D_{t=T} - D_{t=0})_{\text{Tubesheet}}, \text{ where}$$

D_{Plate} = Plate Displacement

$D_{\text{Tubesheet}}$ = Tubesheet Displacement

T = Time of maximum displacement from dynamic analysis

In order to calculate the relative displacements across the full plate, displacement (stress) solutions are performed for the limiting plates at the times of maximum displacement. Calculations were performed for each set of transient loads for those plates where the maximum absolute displacement exceeded 0.350 inch.

The displacement solutions are performed using the finite element representations for the plates. Displacements for the dynamic degrees of freedom for the limiting plates are extracted at the times of interest from a file containing the DOF displacements for the full transient. These displacements are applied to the finite element model as boundary conditions (along with any other appropriate boundary conditions representing symmetry or ground locations), and displacements for the entire plate are then calculated. These results are then combined with the scaled tubesheet displacements, to arrive at a combined relative displacement between the tubes and plates. The combined relative displacements are then superimposed on a tube bundle map, and the results interpolated to arrive at a displacement value for each tube location.

A summary of the number of tubes falling into each of the displacement groupings for the limiting plates is provided in Table 4-14. Note that the numbers of tubes in Table 4-14 correspond to the full plate. The number of tubes in each plate quadrant is one-half of the values listed. A summary of the total number of tubes having displacements > 0.35 inch for each of the SLB loads is provided in Table 4-15. Note that at the top of Table 4-14, the limiting displacements as reported in Table 4-10 are repeated, while the number of tubes where the relative plate/tube displacements exceed 0.350 inch are summarized at the bottom of the table.

Summarized in Table 4-16 is a comparison of the maximum plate displacement to the plate displacement at the limiting tube location (the tube having the highest displacement), R1C1. As can be observed in the displaced geometry plots in Figures 4-32 - 4-35, the displacement gradients at the corner of the plate are high, so the maximum differential displacement at R1C1 is less than the maximum plate displacement reported in Table 4-15.

4.6 SLB Frequency at Hot Standby and Full Power Conditions

In order to identify the frequency of main steamline break in both the hot standby and full power conditions to support the steamline break tube support plate displacement analysis for Braidwood Unit 1, a review of References 4-1 and 4-2 for the Byron Nuclear Power Station Units 1 and 2 was completed.

4.6.1 Secondary Side Breaks

Two main feedline pipe breaks have occurred on Westinghouse designed PWRs. The feedline breaks were downstream of the main feedwater isolation valves (MFWIVs), outside containment. The number of years at criticality calculated for all Westinghouse designed PWRs is 1370 years (Reference 4-1).

Using the Bayes theorem, the mean frequency of occurrence may be determined (Reference 4-2) by:

$$mean = \frac{2r+1}{2t}$$

where r is the number of failures and t is the time interval. Substituting $r = 2$ and $t = 1370$,

$$mean = \frac{2(2)+1}{2(1370)} = \frac{2.5}{1370} = 1.8E-03/year$$

Since no secondary side breaks have occurred, other than these two main feedline breaks, the mean of the frequency for this event is $1.8E-03/year$ (Reference 4-1).

Based on the plant response to steamline/feedline breaks, this event is split into two initiators: (1) secondary side breaks downstream of the main steam isolation valves (MSIVs) or upstream of the MFWIVs and (2) secondary side breaks upstream of the MSIVs or downstream of the MFWIVs. The same frequency is used for both types of steamline/feedline breaks. That is,

Secondary side breaks upstream of MSIVs or downstream of MFWIVs = $1.8E-03/year$
Secondary side breaks downstream of MSIVs or upstream of MFWIVs = $1.8E-03/year$

4.6.2 Hot Standby and Full Power Conditions Evaluations

A review of the operating histories for Braidwood Unit 1 Cycle 3 and 4 was completed to determine the amount of time spent in Mode 3 versus full power operation. The result of this evaluation is shown in Table 4-17. The frequency of Mode 3 operation is defined as:

$$\text{Frequency of Mode 3} = \frac{\text{Days in Mode 3}}{\text{Days in Cycles 3 \& 4}} = \frac{36.1}{959} = 0.038$$

$$\text{Frequency of Mode 1} = 1 - \text{Mode 3} = 0.962$$

The results of these calculations show a frequency in Mode 3 of 0.038 and frequency of Mode 1 of 0.962. Combining these frequencies with the IPE frequency of secondary side break upstream of the MSIVs gives a frequency of secondary side break upstream of the MSIVs in the Mode 3 condition and in the Mode 1 condition of:

$$\text{Mode 3 Secondary Side Break} = (1.8E-03/\text{year}) \times 0.038 = 6.8E-05/\text{yr.}$$

$$\text{Mode 1 Secondary Side Break} = (1.8E-03/\text{year}) \times 0.962 = 1.7E-03/\text{yr.}$$

4.7 Tubes Subject to Deformation in a SSE + LOCA Event

This section deals with accident condition loadings in terms of their effects on tube deformation. The most limiting accident conditions relative to these concerns are seismic (SSE) plus loss of coolant accident (LOCA). For the combined SSE + LOCA loading condition, the potential exists for yielding of the tube support plate in the vicinity of the wedge groups, accompanied by deformation of tubes and subsequent loss of flow area and a postulated in-leakage. Tube deformation alone, although it impacts the steam generator cooling capability following a LOCA, is small and the increase in PCT is acceptable. Consequent in-leakage, however, may occur if axial cracks are present and propagate throughwall as tube deformation occurs. This deformation may also lead to opening of pre-existing tight through wall cracks, resulting in primary to secondary leakage during the SSE + LOCA event, with consequent in-leakage following the event. In-leakage is a potential concern, as a small amount of leakage may cause an unacceptable increase in the core PCT. Thus, any tubes that are defined to be potentially susceptible to deformation under SSE + LOCA loads are excluded from consideration under the IPC.

In the absence of plant specific LOCA and SSE loads for Braidwood Unit 1, a conservative upper bound estimate was made of the maximum number of tubes that would be affected at each wedge location. Using the results of an analysis for another plant having the same model steam generators, a conservative upper bound of []" per wedge group was established for the Braidwood Unit 1 steam generators. A summary of the applicable tubes for each of the wedge locations is provided in accompanying tables and figures.

Braidwood Unit 1 is a four-loop plant. As such, there are two loops with "left-hand" steam generators and two loops with "right-hand" steam generators. These designations refer to the orientation of the nozzles and manways on the channel head. For the purpose of this analysis, "left-hand" units are defined to be those loops where the primary fluid flows from the reactor to the steam generator to the pump and back to the reactor vessel in a counter-clockwise direction. Conversely, for the "right-hand" units, the flow is in the clockwise direction. The left- versus right-hand designation affects the location of the nozzles and manways, and the manner in which the columns are numbered for tube identification purposes. Reference configurations used in identifying wedge locations are shown in Figures 4-46 and 4-47 for the left-hand and right-hand units, respectively. As shown in the figures, for left-hand units, the nozzle and tube column 1 are located at 0°, while for right-hand units they are located at 180°.

Tabular summaries of the tubes that are potentially susceptible to collapse and subsequent in-leakage are summarized in Tables 4-18 to 4-23 for the left-hand units, and in Tables 4-24 to 4-29 for the right-hand units. For the Braidwood Unit 1 steam generators there is a flow distribution baffle, seven tube support plates, and three baffle plates. The plate configuration is shown in Figure 4-15. Plate A corresponds to the flow distribution baffle, Plates B, E, and H are the flow baffles, and Plates C/D, F/G, J/K, and L, M, N, and P are the tube support plates.

Prior analysis for steam generators of similar design show the flow distribution baffle to not impact the wrapper/shell under seismic loads. Thus, it is judged that there will not be any tubes at the flow distribution baffle location that are potentially susceptible to collapse under combined LOCA+SSE. It will be noted that separate summary tables are provided for the lower TSPs, B-K (except E and H where a table common to both is used), and a single table for the upper TSPs L-P. This is due to the orientation of wedge groups for each of the TSP. For the lower TSPs, the wedge groups are rotated in some instances relative to the other TSPs, while for the upper TSPs, the wedge groups have the same angular orientation.

Maps showing the location of the potentially susceptible tubes are provided in Figures 4-48 to 4-57. The maps provide row and column designations relative to the left-hand units. Column numbers for the right-hand units are shown in brackets. Identification of the potentially susceptible tubes is based on crush test results for both Model D and Series 51 steam generators. For both sets of tests, however, wedge / tube configurations identical to those for

the Braidwood Unit 1 steam generators were not tested. As such, it was not possible to identify exactly the []^a that might be limiting at each wedge group. Thus, due to the uncertainties involved, there are generally []^a identified at each wedge group as being limiting.

Finally, Table 4-30 provides an index of the applicable tables and figures identifying the potentially susceptible tubes for each TSP.

4.8 Allowable SLB Leakage Limit

An evaluation has been performed to determine the maximum permissible steam generator primary to secondary leak rate during a steam line break for the Braidwood Nuclear Plant Unit 1. The evaluation considered both pre-accident and accident initiated iodine spikes. The results of the evaluation show that the accident initiated spike yields the limiting leak rate. This case was based on a 30 rem thyroid dose at the site boundary and initial primary and secondary coolant iodine activity levels of 1 $\mu\text{Ci/gm}$ and 0.1 $\mu\text{Ci/gm}$ I-131, respectively. A leak rate of 9.1 gpm was determined to be the upper limit for allowable primary to secondary leakage in the SG in the faulted loop. The SG in each of the three intact loops was assumed to leak at a rate of 150 gpd (approximately 0.1 gpm), the proposed Technical Specification LCO for implementation of IPC. The allowable leak rate will increase in inverse proportion to a reduction in the primary and secondary equilibrium coolant activity.

Thirty rem was selected as the thyroid dose acceptance criteria for a steam line break with an assumed accident initiated iodine spike based on the guidance of the Standard Review Plan (NUREG-0800) Section 15.1.5, Appendix A. Only the release of iodine and the resulting thyroid dose was considered in the leak rate determination. Whole-body doses due to noble gas immersion have been determined, in other evaluations, to be less limiting than the corresponding thyroid doses.

The salient assumptions follow.

- Initial primary coolant iodine activity - 1 $\mu\text{Ci/gm}$ DE I-131

The calculation of primary coolant DE I-131 is based on a mixture of 5 iodine nuclides (I-131 through I-135) and the dose conversion factors of TID-14844, consistent with the Braidwood Technical Specification definition of DE I-131.

- Initial secondary coolant iodine activity - 0.1 $\mu\text{Ci/gm}$ I-131

The calculation of secondary coolant iodine activity is based on actual I-131 activity rather than DE I-131. Although, this is somewhat more conservative than the Technical Specification LCO which is based on DE I-131, secondary coolant activity still accounts for less than 6% (1.75 rem) of the allowable offsite dose.

- Steam released to the environment (0 to 2 hours)
 - from 3 SGs in the intact loops, 416,573 lb
 - from the affected SG, 96,000 lb (the entire initial SG water mass)
- Iodine partition coefficients for primary-secondary leakage
 - SGs in intact loops, 1.0 (leakage is assumed to be above the mixture level)
 - SG in faulted loop, 1.0 (SG is assumed to steam dry)
- Iodine partition coefficients for activity release due to steaming of SG water
 - SGs in intact loops, 0.1
 - SG in faulted loop, 1.0 (SG is assumed to steam dry)
- Atmospheric dispersion factor (SB 0 to 2 hours), $7.70\text{E-}4 \text{ sec/m}^3$
- Thyroid dose conversion factors (I-131 through I-135) utilized in offsite dose calculation, ICRP-30

The activity released to the environment due to a main steam line break can be separated into two distinct releases: the release of the iodine activity that has been established in the secondary coolant prior to the accident and the release of the primary coolant iodine activity that is transferred by tube leakage during the accident. Based on the assumptions stated previously, the release of the activity initially contained in the secondary coolant (4 SGs) results in a site boundary thyroid dose of approximately 1.75 rem. The dose contribution from 1 gpm of primary-to-secondary leakage (4 SGs) is approximately 3 rem. With the thyroid dose limit of 30 rem and with 1.75 rem from the initial activity contained in the secondary coolant, the total allowable primary-to-secondary leak rate is $(30 \text{ rem} - 1.75)/3 \text{ rem}$ per gpm, or 9.4 gpm. Allowing 0.1 gpm per each of the 3 intact SGs leaves $(9.4 - 0.3)$ or 9.1 gpm for the SG on the faulted loop.

4.9 Acceptability of the Use of TRANFLO Code

4.9.1 Background

In the early 1970's, there was a need to accurately predict the steam generator behavior under transient conditions, such as a steam line break (SLB) event; a transient can develop thermal hydraulic loads on the internal components and shell of the steam generator. Structural analyses are required to analyze the adequacy of the individual components and the whole steam generator under various thermal and hydraulic loads. With the assistance of MPR Associates, Westinghouse developed and modified the TRANFLO computer code to conservatively model the thermal and hydraulic conditions within the steam generator under transient conditions.

The secondary side of the steam generator involves water boiling under high pressure during normal operating conditions. During a transient such as a SLB event, it may be subject to vapor generation due to rapid depressurization. Therefore, analysis methods have to recognize this characteristic of two-phase fluid behavior. In the early stage of the computer code development and technology of two phase flow, a homogeneous model was used. For current analyses, a more accurate slip flow model is used which takes into consideration the relative velocity between the liquid and vapor phases. Development of the TRANFLO code reflects this general trend of the two-phase flow modeling. The first version of TRANFLO was a homogeneous model, and it was later updated to a drift flux model to simulate the effect of two-phase slip. Since the original issue of the code, Westinghouse has made several enhancements to the code and has performed the appropriate verification and validation of these changes. These changes do not significantly affect the calculated pressure drops across the steam generator tube support plates.

4.9.2 Acceptability of Application of TRANFLO

The original version of the TRANFLO code (Reference 4-3) was reviewed and approved by the NRC in Reference 4-4. TRANFLO was used as part of the Westinghouse mass and energy release/containment analysis methodology. Specifically, the code was used to predict steam generator (SG) secondary side behavior following a spectrum of steam line breaks. Its output was the prediction of the quality of the steam at the break as a function of time. The quality is calculated as a function of power level, as well as break size. In order to assure that the TRANFLO code evaluates a conservatively high exit quality, Reference 4-4 states that the calculational sequences were reviewed for the determination of "conditions prior to entering into the separation stages. The calculated rate, quality and energy content of the two-phase mixture entering the separation stages must be evaluated conservatively". This review was completed and found to be acceptable, as the NRC staff concludes in

Reference 4-4 that the TRANFLO code is an acceptable code for calculating mass and energy release data following a postulated MSLB. Therefore, it is concluded that the TRANFLO model is appropriate for predicting SG behavior (including tube bundle region) under the range of SLB conditions.

For the current application, TRANFLO is used in conjunction with a structural analysis code to predict TSP movement following the same SLB event. The key data transferred between the transient code and the structural code is the pressure drop across the TSP as a function of time. This pressure drop calculation depends on the fluid conditions in the steam generator and on the adequacy of the loss coefficients along the flow paths. The conditions in the tube bundle as calculated by TRANFLO have been previously reviewed. Further justification of the adequacy of the pressure drop calculation is discussed in Section 4.9.4.

4.9.3 Different Versions of TRANFLO

The original version of the TRANFLO code has been reviewed and approved by the NRC. Westinghouse has continued to update the code with new models that more accurately predict steam generator behavior. Four versions of TRANFLO have been used in calculation. The following are descriptions of each of them.

The Original Version (April 1974)

This is the original homogeneous model, which MPR Associates developed in April 1974. The code predicts mass flow rate, pressure, pressure drop, fluid temperature, steam quality and void fraction. The code document includes results of TRANFLO calculations for a 51 Series steam generator subject to water and steam blowdown due to an SLB event. The document also presents code verification using blowdown test data from pressurized vessels.

Westinghouse documented this version in detail in September 1976, including code verification using vessel blowdown data. Sensitivity analyses were also performed and documented to show that the modelling was conservative. This included sensitivities to loss coefficient.

The TRANFLO code uses an elemental control volume approach to calculate the thermal-hydraulics of a steam and water system undergoing rapid changes. Fluid conditions may be subcooled, two-phase or superheated. The code considers fluid flows being one-dimensional.

Control volumes simulate the geometrical model, and flow connectors allow mass and energy exchange between control volumes. Each nodal volume has mass and energy that are homogeneous throughout the volume. Flow connectors account for flow and pressure drops. The system model allows flow entering or leaving any control volume. This then allows that

feedwater flows into a steam generator and steam flows out of it. The system models also permit a heat source, which then can simulate the tube bundle with hot water flow.

TRANFLO solves for system conditions by satisfying mass, momentum and energy equations for all control volumes. It models the effects of two-phase flows on pressure losses. The code allows a variety of heat transfer correlations for the tube bundle. It covers all regimes from forced convection to subcooled liquid through boiling and forced convection to steam.

The Drift-Flux Version (November 1980)

This version implements a drift-flux model to better simulate relative flow velocity between water and steam. For example, it allows a realistic simulation of counter-current flow of steam and water. It required modification of the mass, momentum and energy equations of the two-phase flow. A capability is provided for monitoring calculated variables for convenient examination of results.

TRANFLO Version 1.0 (November 1991)

This version accepts transient data of parameters as direct inputs, rather than supplying input subroutines, as used in the drift-flux version. It also improves printouts and plots. This version maintains the drift-flux model, and includes the addition of thermal conductivity of Alloy 690 tubing.

TRANFLO Version 2.0 (January 1993)

This version provides an option for two inlets of feedwater flow into the steam generator. It involves minor changes to a subroutine for specifying feedwater flow. This version is used for separate inlets of simultaneous feedwater flow from main and auxiliary feedwater nozzle.

4.9.4 Verification of Loop Pressure Drop Correlations

As discussed earlier, an accurate prediction of mass and energy release from the vessel means that the TRANFLO code properly calculates local thermal-hydraulics in various nodes (i.e., elemental control volume and flow connector). It is critical to accurately simulate the pressure drop inside a steam generator that consists of various components, such as the tube bundle with tube support plates, moisture separators, and downcomer. Hydraulic loads on various components depend on accurate pressure drop calculations. Thus, it is important to verify the pressure drop calculations through the circulation loop.

The TRANFLO code uses the same pressure drop correlations as the Westinghouse GENF code, which is a performance program. The GENF code predicts one-dimensional steady

state conditions, which include pressure drops along the circulation flow loop. Both laboratory tests and field data validate the accuracy of the GENF code. The GENF code is used extensively for steam generator performance analysis and has been shown to accurately predict operating steam generator conditions.

When provided with all geometrical input and operating conditions, GENF calculates the steam pressure, steam flow rate, circulation ratio, pressure drops, and other thermal-hydraulic data. The circulation ratio is a ratio of total flow through the tube bundle to feedwater flow. For a dry and saturated steam generator, there exists a hydrostatic head difference between the downcomer and the tube bundle. This head difference serves as the driving head to circulate flow between them (see Figure 4-58). The driving head is constant for given operating specifications, such as power level and water level. The total pressure drop through the circulation loop is equal to the driving head.

Pressure drops depend on loss coefficient and flow rate (i.e., velocity). Loss coefficient consists of friction loss and form loss; the majority of the loss is due to the form loss in the steam generator. Since the driving head is constant, a higher loss coefficient means a lower circulation flow rate and a lower circulation ratio. A lower loss coefficient yields a higher circulation ratio. Therefore, an accurate prediction of the circulation ratio depends on an accurate loss coefficient.

Model boiler and field tests are used in qualifying the loss coefficients in the flow loop of the steam generator. For example, the major contributors of the pressure drop are the primary separator and tube support plates. The loss coefficient of the primary separator has been verified using model boilers and field steam generators (Reference 4-5). Similarly, loss coefficients of tube support plates have been developed using test data; Figure 4-59 presents the correlation of the loss coefficient and test data.

Figure 4-60 shows a typical comparison between predicted and actual measured circulation ratio. There is good agreement in circulation ratio between the prediction and measurement.

The TRANFLO model uses the same loss coefficient correlations as GENF code. This provides assurance in properly calculating the pressure drops throughout the steam generator.

4.9.5 Summary

This section presents a summary of the adequacy of the TRANFLO code for its current applications. Blowdown test data of simulated reactor vessels validate the adequacy of the code in predicting the steam and water blowdown transient. The NRC has accepted the TRANFLO code in calculating mass and energy release to the containment during a steam generator blowdown due to feed or steam line break.

As part of its review, the NRC accepted the code's ability to accurately predict local thermal-hydraulics in the vessel. The calculated pressure agrees well with the measured vessel pressure. Flow through the internals of the steam generator depends on accurate prediction of pressure drops, which relies on the accuracy of the loss coefficients along the flow paths. Test data of pressure drops from model boiler and field steam generators have been applied to verify the correlations for the loss coefficients.

Westinghouse has made modifications to the code to better predict steam generator behavior following a SLB event. Westinghouse has performed the verification and validation consistent with the methods approved by the NRC staff for the original version.

In conclusion, the TRANFLO code is a verified program for adequately predicting thermal-hydraulic conditions during the blowdown transient of a steam generator due to a feed or steam line break.

4.10 Updated Model D4 SG SLB Thermal Hydraulic Loads on TSPs

4.10.1 Introduction

Section 4.2 provides bounding thermal hydraulic loads on TSPs using the existing results calculated by TRANFLO code. This section presents an updated TRANFLO model of the Model D4 steam generator and the resulting thermal hydraulic loads on the TSPs.

4.10.2 Updated TRANFLO Model and Its Initial and Boundary Conditions

Three bounding cases (Cases 1 to 3) are presented in Section 4.2. Three additional cases of the updated TRANFLO model have been calculated. One of them is initiated from hot standby and the other two from full power operation. Table 4-31 lists the initial and boundary conditions for these three cases. In addition, the model considers a guillotine break and a Moody discharge coefficient of unity for both cases.

Calculations for an initiation from hot standby are identified as Case 4. Sensitivity studies were conducted for initiation from full power, these are identified as Case 5 and Case 6. As known, characteristics of two-phase flow depend on void fraction, and so does the pressure drop of two-phase flow. Initial void fractions in the tube bundle were estimated according to performance parameters predicted by the Westinghouse performance code for steam generators. Case 5 documents a run with lower initial void fractions in the tube bundle than typically expected for full power operation. Case 6 documents a run with typical initial void fractions in the tube bundle for Braidwood Unit 1 at full power operation. For Case 6, the estimated void fractions were adjusted slightly to bring steady state TSP pressure drops of the

Westinghouse SG performance code into agreement with initial pressure drops of the TRANFLO code.

The updated TRANFLO computer model is composed of a network of nodes and connectors that represent the secondary side fluid, tube metal heat transfer and primary coolant. Figures 4-61 and 4-62 show the nodal layout of the secondary side of the Model D4 steam generator. Figures 4-63 and 4-64 present the nodal network of the secondary fluid, primary fluid and tube metal. The computational model consists of the following elements:

1. 31 nodes (i.e., Nos. 22 through 52) for secondary fluid.
2. 44 fluid connectors (i.e., Nos. 23 through 66) for secondary fluid.
3. 21 nodes (i.e., Nos. 1 through 21) for primary coolant.
4. 22 fluid connectors (i.e., Nos. 1 through 22) for primary coolant.
5. 21 heat transfer nodes (i.e., Nos. 1 through 21) for tube.
6. 42 heat transfer connectors (i.e., Nos. 1 through 42) from primary to secondary fluid.

4.10.3 Loss Coefficient of Pressure Drop through TSPs

In the tube bundle area, the space between TSPs forms a fluid node, and a flow connector is used to link the adjacent nodes. Pressure drops through tube support plates or baffles are calculated by the code for each flow connector that represents a plate or baffle. For example, flow connector 41 links fluid Nodes 32 and 31. Tube support plate M is the boundary between Nodes 32 and 31. Pressure drop through TSP M is thus calculated along the flow connector 41. This connector consists of three segments. Segment 1 is from the center of Node 32 to the bottom side of the TSP M, Segment 2 is from the bottom side to the top side of the TSP M, and Segment 3 from the top side of the TSP M to the center of Node 31.

Pressure load on each TSP is a result of the form loss pressure drop. The form loss pressure drop depends on the form loss coefficient and flow rate across the plate. As discussed in Section 4.9, the TRANFLO model uses the verified correlation for determining the form loss coefficient for tube support plate. The form loss coefficient is assigned to the appropriate segment of a flow connector. For example, the form loss coefficient for TSP M is assigned to Segment 2 of the flow connector 41. It should be noted that the pressure drop across a TSP, as calculated from the form loss, is less than the pressure drop between the nodes below and above the plate.

4.10.4 Hydraulic Loads of the Updated Model D4

Figures 4-65, 4-66 and 4-67 show hydraulic loads through various tube support plates for a SLB event initiated from hot standby. Figures 4-68, 4-69 and 4-70 show hydraulic loads

through various tube support plates for a SLB event initiated from full power operation. Note that Figures 4-68, 4-69, and 4-70 present both Case 5 and Case 6, respectively. Please also note that water level is at the normal setting (i.e., at 487" above the top of the tubesheet) rather than at the uppermost tube support plate (i.e., at 280" above the top of the tubesheet).

The load on the uppermost TSP (i.e., P plate) is slightly higher for Case 4 (hot standby) than Case 5 (full power). However, the remaining TSPs all have higher loads for Case 5. Case 6 has higher pressure drops in the upward flow direction than Case 5, but the opposite is true for the downward flow direction. When compared to a hot standby with a water level at the uppermost TSP, the loads on all TSPs for the hot standby case are much higher than for the full power at a normal water level (i.e., 487"). This is indirectly evidenced by Figure 4-71; a relative peak pressure drop across the uppermost TSP as a function of water level for an initiation from hot standby.

4.10.5 Load Comparison

Table 4-32 summarizes peak loads for all six cases. The first three cases are discussed in Section 4.2 as bounding loads. The last three cases are the loads from the updated TRANFLO model for the Model D4 steam generators of Braidwood Unit 1. As seen, Case 3 serves as the bounding load for the last three cases. A summary of the peak pressure drops across each plate for each of the six cases is given in Section 8, Table 8-9.

4.11 Updated Model D4 SG SLB TSP Displacement Analyses

This section presents updated results for the TSP displacement analysis. As discussed in Section 4.10, three additional sets of transient loadings have been considered. In addition, the following changes have been made to the modeling of the tube bundle region. First, the channel head, tubesheet, and lower shell have been added to the model in order to calculate the tubesheet displacements directly, rather than scale the results from prior analyses, as was done for the initial sets of loads. Second, the non-linear interfaces between the TSP and spacers have been incorporated in the model. Previously, depending on the direction of the loading on the individual plates, some of the plate / spacer interfaces were treated as linear (pinned) connections. Third, the upward support provided to Plates A(1H), C(3H), and J(7H) by the wedges located at the 10° location (see Figures 4-17, 4-18, and 4-20) is included; note that the wedges provide upward support only. Finally, TSP and tubesheet displacements are calculated both for time = 0, and for the subsequent transient loads. Previously, only the transient displacements were calculated.

4.11.1 Material Properties

An expanded summary of the component materials including the tubesheet, channel head, and shell, which were added to the model, is contained in Table 4-33. Material properties for the tubesheet, channel head, and shell are summarized in Tables 4-34 through 4-36. The properties are taken from the 1971 edition (through summer 1972 addenda) of the ASME Code, which is the applicable code edition for Braidwood Unit 1. The material properties for the tubesheet are subsequently modified to account for the tube penetrations.

4.11.2 TSP Support System / Finite Element Model

The support system for the TSPs is discussed in Section 4.3.2. With the exception of incorporating the wedge support for Plates A(1H), C(3H), and J(7H) at the 10° location, and incorporating the TSP / spacer non-linearities, there have not been any changes to the support system.

The finite element model representation of the tube bundle, with the addition of the channel head, tubesheet, and lower shell, is shown in Figure 4-72. Vertical support for the model is defined to be consistent with the vertical support locations on the channel head for the overall steam generator.

4.11.3 Revised Material Properties

As noted earlier, the material properties for the tubesheet are modified to account for the tube penetrations. The properties that are modified are Young's modulus, Poisson's ratio, and the material density. The formulations for revising Young's Modulus and Poisson's ratio are discussed in Section 4.3.3. The density modification for the tubesheet is based solely on an area ratio of the actual perforated tubesheet to the equivalent solid plate.

4.11.4 Dynamic Degrees of Freedom

The dynamic degrees of freedom (DOF) used in the analysis are essentially unchanged from the prior calculations. Several DOF have been added for Plates A(1H), C(3H), and J(7H) to account for the potential of having additional wedge support for these plates, as discussed above. The additional DOF have been defined using the same methodology as discussed in Section 4.3.4. Briefly, this methodology involves performing two modal analyses, one with a large number of DOF and one with a reduced set of DOF, and matching frequencies for modes less than 50 hertz. The final set of DOF defined for these plates is a combination, or union, of the sets of DOF resulting from the two possible support conditions, with and without wedge support.

4.11.5 Displacement Boundary Conditions

The displacement boundary conditions for the TSPs are unchanged from the prior calculations (Section 4.3.5). Symmetry boundary conditions have been added for the tubesheet, channel head and lower shell.

4.11.6 Application of Pressure Loading

The application of the SLB pressure loadings is described in Section 4.3.6. Other than adding a load vector to the substructure generation for the tubesheet, no changes have been made to the application of the pressure loads.

4.11.7 Results of SLB TSP Displacement Analyses

An updated summary of the limiting displacements for each of the plates is provided in Table 4-37. Note that results for the single plate model cases are not shown in this table, but can be found in Table 4-10. The displacement results for the new load cases show relative plate / tubesheet displacements at the time of maximum plate displacements.

The results for the new load cases show Plate C (3H) to be limiting. The displacements for the other plates are all less than 0.3 inch. Comparing these results to the prior cases shows a re-distribution of the limiting displacements away from Plate J to Plate C. This is due to lower pressure loads on Plate J, as well as the added support in the vertical direction provided by the wedge at 10°.

The limiting plate displacements are still confined to a small region of the plates at the outer edge near the tube lane, where the distance between vertical supports is greatest. Displaced geometry plots for Plate C (3H) for each of the new load cases are shown in Figures 4-73 through 4-75. Displacement time histories for each of the plates for the SLB from Hot Shutdown are shown in Figures 4-76 and 4-77, for SLB from Full Power in Figures 4-78 and 4-79, and for SLB from Full Power with prototypic void fraction in Figures 4-80 and 4-81.

Since the dynamic analysis is based on elastic response, it is necessary to show that the tierods remain elastic throughout the transient. The dynamic analysis results establish that the stayrods do, in fact, remain elastic throughout the transient. [

]ª In both instances, these elongations are well below the yield point for the stayrods.

Also relevant in assessing the appropriateness of the elastic solution, are the stresses in the plates. Based on a comparison of maximum DOF displacements, it is concluded that the limiting event in terms of plate stress is the SLB + Excess Feedwater transient. The plate stresses are shown in Section 4.4 to be generally low throughout the plate, and that the elastic analysis is a good approximation of the transient plate response.

Similarly, stresses in the welds between the vertical bars and the partition plate and wrapper will be bounded by the results for the SLB + Excess Feedwater transient. A summary of the reaction forces and corresponding stresses for each of the bar locations for the initial set of transient loads is provided in Table 4-13. The allowable stress intensity for the welds is 19.53 ksi, and the weld stresses are acceptable.

Overall, it is concluded that the elastic analysis provides a good approximation of the dynamic response of the TSPs to the applied loading.

4.11.8 SLB Displacements By Tube Location

An updated summary of the number of tubes falling into each of the displacement groupings used for establishing burst probabilities (see Section 4.5 for further discussion) is provided in Table 4-38. Note that the numbers of tubes in Table 4-38 correspond to the full plate. The number of tubes in each plate quadrant is one-half of the values listed. There are no tubes with relative tube / tubesheet displacements that exceed 0.35 inch for SLB from full power with prototypic void fraction, thus this transient is not included in Table 38. A summary of the total number of tubes having displacements > 0.35 inch for each of the SLB loads is provided in Table 4-39. Note that at the top of Table 4-39, the limiting displacements as reported in Table 4-37 are repeated, while the number of tubes where the relative plate/tube displacements exceed 0.350 inch are summarized at the bottom of the table.

Summarized in Table 4-40 is a comparison of the maximum displacement anywhere on the plate (usually the edge) to the maximum plate displacement at the tube location having the highest displacement, R1C1. Note that the displacement at the edge of the plate represents the change in differential tubesheet displacement from time = 0. This relative displacement from time = 0 is the appropriate displacement for calculating the plate displacement relative to the cracks formed at operating conditions as described below. The results in Table 4-39, on the other hand represent the differential plate and tubesheet displacement at the time of maximum plate displacement. As can be observed in the displaced geometry plots in Figures 4-73 through 4-75, the displacement gradients at the corner of the plate are high, so the maximum differential displacement at R1C1 is less than the maximum plate displacement.

The calculations to estimate the SLB tube burst probabilities are based on the change in the relative plate/tube position from their positions at the initiation of the SLB transient. The ODS/CC indications are formed on the tube within the TSP at normal operating conditions.

Relative to cold shutdown conditions, the TSP is displaced (relative to a fixed location on the tube) by the net effect of the secondary flow pressure difference across the plate plus the bow of the tubesheet. (Thermal expansion effects also marginally influence the TSP/tube displacements relative to cold shutdown, but these effects are negligible for SLB displacements at normal operating conditions.) The tubesheet bow displaces all axial locations on the tubes by the amount of the bow, while the TSP displacements closely match the bow of the tubesheet only at the locations of the tierods. The secondary flow pressure difference across the TSP tends to displace the plate in the upward direction relative to the tube. The net displacement of the plate is the sum of the tubesheet bow interaction through the tierods and the pressure differential. Therefore, the movement of the plate relative to the tube is the difference between the net plate displacement and tubesheet bow. For the Model D4 SG, the relative plate to tube displacements at normal operating conditions are not large, as shown in Figures 4-78 through 4-81 at time = 0 for the location with maximum SLB displacement. These relative displacements are typically ≤ 0.06 inch, as shown in the figures. The relative displacements for hot standby conditions (Figures 4-76, 4-77) are not significantly different, which indicates that the full power TSP displacements due to the pressure differential across the plate are not large. Thus, it would be expected for the Model D4 SGs that the indications would be inside the TSP at both cold and hot conditions, independent of whether or not the plates are effectively clamped to the tubes as a result of crevice deposits. The net SLB displacement of the plate relative to the ODSCC on the tube is then the change in relative plate to tube (or tubesheet) displacement between a time in the SLB and time = 0. This is reflected in the algorithm given in Section 4.5 for calculating the relative SLB plate to tube displacement. The updated relative plate displacements of Tables 4-37 and 4-39 are used in Section 8 for estimating SLB tube burst probabilities.

4.12 References

- 4-1. "Quantification of Byron IPE Steamline/Feedline Break Frequency", CN-COA-92-537-R1, Appendix R1-B, April 1993.
- 4-2. "Byron IPE Initiating Event Calculations and Notebook - Draft", CN-COA-92-537-R0, December 1993.
- 4-3. R. E. Land, "TRANFLO Steam Generator Code Description", Westinghouse Nuclear Energy Systems, WCAP-8821, September 1976.
- 4-4. Memo from C. O. Thomas to E. P. Rahe, "Proprietary Content Review of SER on WCAP-8821 and WCAP-8822", October 14, 1982.
- 4-5. P. W. Bird and P. J. Prabhu, "Review of Primary Separator Loss Coefficient", WTD-TH-80-010, July 1980.

Table 4-1

**Initial and Boundary Conditions of the TRANFLO Calculation Models
for Model D3 and D4 Steam Generator**

<u>Case</u>	<u>SG Model</u>	<u>Initial Conditions</u>		<u>Boundary Conditions</u>	
		<u>Mode of Operation</u>	<u>Water Level</u>	<u>Steam Nozzle Flow Limiter</u>	<u>FeedwaterFlow</u>
1	D3	Hot Standby	@ ~ Normal Setting	Yes	Small
2	D4	Full Power	@ Normal Setting	Yes	Full Flow
3	D4	Hot Standby	@ Uppermost TSP	Yes	Excessive

Table 4-2

Peak Pressure Drop at Different Tube Support Plates
(Hot Leg Only for Half Plate)

Parameter	SG & Case <u>D3 - 1</u>	SG & Case <u>D4 - 2</u>	SG & Case <u>D4 - 3</u>
Flow splits within tube bundle	Yes	No	Yes
TSP with max peak Dp	[] ^a
Peak Dp @ uppermost TSP			
Max peak Dp, psi			
Peak max Dp @ bottom Plate			
Dp @ Hot Leg Top TSP			

Table 4-3

Summary of Component Materials

Component	Material
Tube Support Plate	SA-285 Grade C
Stayrod	SA-106 Grade B
Spacer	SA-106 Grade B
Tube	Inconel 600

Table 4-4

**Summary of Material Properties
SA-285, Gr. C**

PROPERTY	CODE ED	TEMPERATURE						
		70	200	300	400	500	600	700
Young's Modulus	71	27.90	27.70	27.40	27.00	26.40	25.70	24.80
Coefficient of Thermal Expansion	71	6.07	6.38	6.60	6.82	7.02	7.23	7.44
Density	---	0.284	0.283	0.283	0.282	0.281	0.281	0.280
		7.35	7.33	7.32	7.30	7.28	7.26	7.25

PROPERTY	UNITS
Young's Modulus	psi x 1.0E06
Coefficient of Thermal Expansion	in/in/deg. F x 1.0E-06
Density	lb/in ³
	lb-sec ² /in ⁴ x 1.0E-4

Table 4-5

Summary of Material Properties
SA-106, Gr. B

PROPERTY	CODE ED.	TEMPERATURE						
		70	200	300	400	500	600	700
Young's Modulus	71	27.90	27.70	27.40	27.00	26.40	25.70	24.80
Coefficient of Thermal Expansion	71	6.07	6.38	6.60	6.82	7.02	7.23	7.44
Density	---	0.284	0.283	0.283	0.282	0.281	0.281	0.280
		7.35	7.33	7.32	7.30	7.28	7.26	7.25

PROPERTY	UNITS
Young's Modulus	psi x 1.0E06
Coefficient of Thermal Expansion	in/in/deg. F x 1.0E-06
Density	lb/in ³
	lb-sec ² /in ⁴ x 1.0E-4

Table 4-6

**Summary of Material Properties
SB-166**

PROPERTY	CODE ED.	TEMPERATURE						
		70	200	300	400	500	600	700
Young's Modulus	71	31.70	30.90	30.50	30.00	29.60	29.20	28.60
Coefficient of Thermal Expansion	71	7.13	7.40	7.56	7.70	7.80	7.90	8.00
Density	---	---	0.306	0.305	0.305	0.304	0.303	0.302
		---	7.923	7.905	7.886	7.867	7.847	7.828

PROPERTY	UNITS
Young's Modulus	psi x 1.0E06
Coefficient of Thermal Expansion	in/in/deg. F x 1.0E-06
Density	lb/in ³
	lb-sec ² /in ⁴ x 1.0E-4

Table 4-7

Summary of Equivalent Plate Properties

Plate	Reference Young's Modulus	Effective Young's Modulus	Effective Poisson's Ratio
A - Inside 32" Radius	2.605E+07	4.810E+06	0.2466
A - Outside 32" Radius	2.605E+07	5.850E+06	0.2654
C, F, J, L, M, N, P*	2.605E+07	2.470E+06	0.6445

* - These plates have flow holes, resulting in a significantly reduced value for Young's Modulus

Table 4-8

Summary of Effective Plate Densities

a

Comparison of Natural Frequencies Full Versus Reduced DOF

a

Summary of TSP Displacements for Postulated SLB Events for Model D3 and D4 Steam Generators*

Postulated SLB Events for Model D3 and D4 Steam Generators*

Table 4-11

**Comparison of Component Dimensions
Model D3 versus Model D4 Steam Generators**

Dimension	Model D3	Model D4
Shell ID	[] a
Shell Thickness		
Channel Head Bowl Radius		
Channel Head Thickness		
Tubesheet Thickness		
Hole Diameter		
Number Holes		
Tube Pitch		

Table 4-12

**Summary of Tubesheet Displacements
Model D3 SLB Analysis**

a

Table 4-13

Summary of Vertical Bar Stresses
Model D4 Steam Generators

a

Table 4-14

Summary of Number of Tubes Having Different Displacement Magnitudes
Model D4 Steam Generator
Steam Line Break Load Cases

a

Table 4-15

Summary of Tubes Having Relative Tube / Plate Displacements
That Exceed 0.400 inch

a

Comparison of Maximum Displacement at Plate Edge and at Limiting Tube Location

1

Table 4-17

Braidwood Unit 1 Mode 3 Durations

Event	Offline Date	Hours in Mode 3	Online Date	Online Days
Cycle 3				
A1R02	N/A	360 *	5/18/91	
A1F19	7/16/91	0	7/27/91	60
A1F20	10/9/91	0	10/14/91	74
A1F21	11/6/91	54	11/11/91	24
A1F22	2/5/92	62	2/7/92	86
A1F23	3/21/9	8	3/21/92	43
A1R03	9/1/92	26*	N/A	165
	Hours in Mode 3 = 510 Days in Mode 3 = 21.2		Online Days = 452 Days in Cycle = 472	
Cycle 4				
A1R03	N/A	56*	11/3/92	
A1M03	11/20/92	124	11/25/92	18
A1F24	1/7/93	38	1/14/93	44
A1M04	5/29/93	35	5/30/93	136
A1F25	6/2/93	65	6/7/93	4
A1F26	10/24/93	21	11/11/93	140
A1R04	3/4/94	18*	N/A	114
	Hours in Mode 3 = 357 Days in Mode 3 = 14.9		Online Days = 456 Days in Cycle = 487	

* Mode 3 times associated with planned refueling outages.

Cycle 3 percent of time spent in Mode 3 = 4.50%.

Cycle 3 percent of time spent in Mode 3 minus Refuelling Mode 3 hours = 1.09%.

Cycle 4 percent of time spent in Mode 3 = 3.05%.

Cycle 4 percent of time spent in Mode 3 minus Refuelling Mode 3 hours = 2.42%.

Tubes Potentially Susceptible to Collapse and In-Leakage
TSP C, D
Left-Hand Unit

— a

Table 4-19

Tubes Potentially Susceptible to Collapse and In-Leakage
TSP F, G
Left-Hand Unit

a

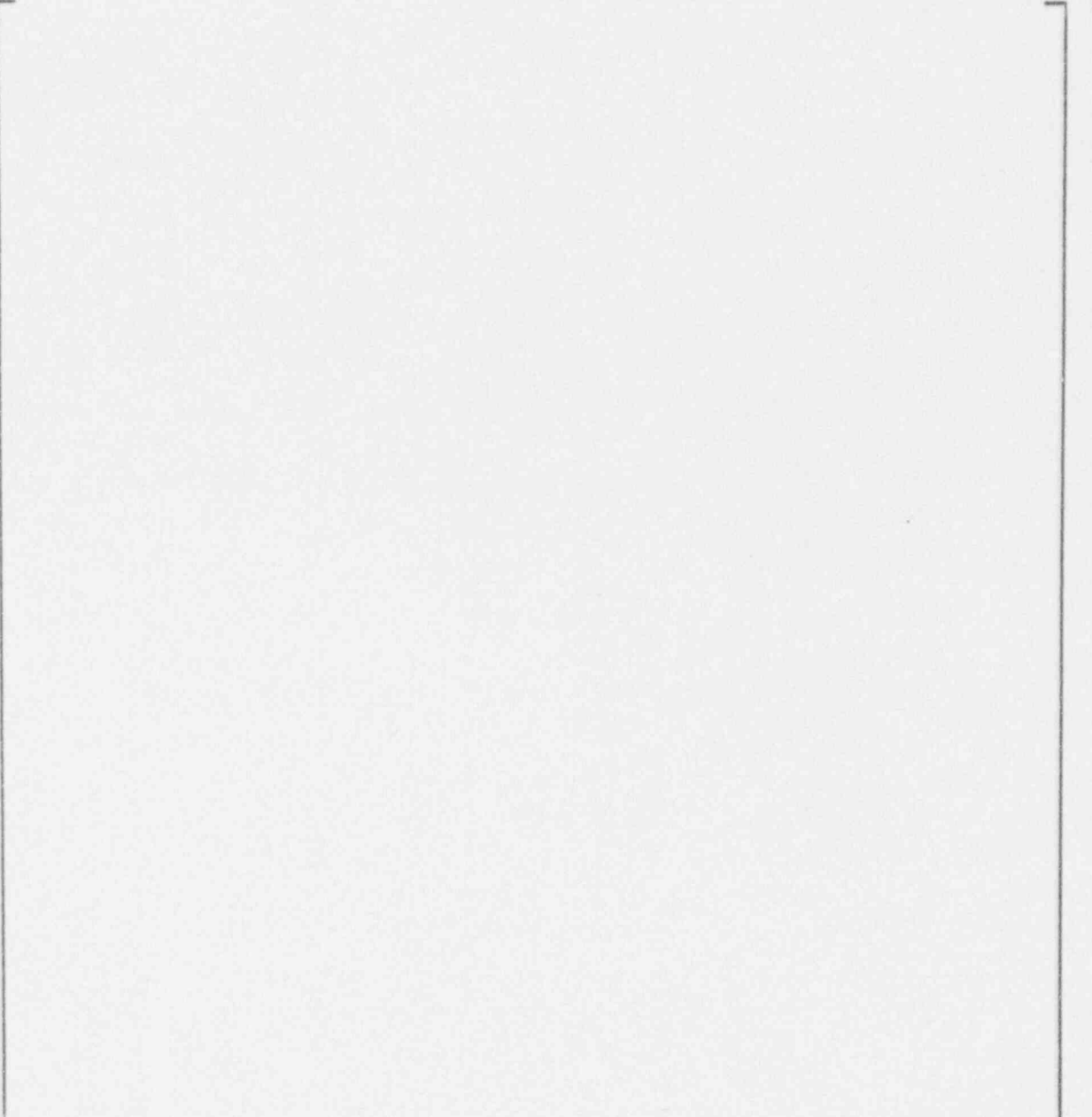
Table 4-20

Tubes Potentially Susceptible to Collapse and In-Leakage
TSP J, K
Left-Hand Unit

a

Tubes Potentially Susceptible to Collapse and In-Leakage
TSP L-P
Left-Hand Unit

DISK 215 - BRDWD\TBL42 - 04/19/94



Tubes Potentially Susceptible to Collapse and In-Leakage
TSP E, H
Left-Hand Unit

TSP E, H
Left-Hand Unit

1

Table 4-24

Tubes Potentially Susceptible to Collapse and In-Leakage
TSP C, D
Right-Hand Unit

a

Table 4-25

Tubes Potentially Susceptible to Collapse and In-Leakage
TSP F, G
Right-Hand Unit

a

Table 4-26

Tubes Potentially Susceptible to Collapse and In-Leakage
TSP J, K
Right-Hand Unit

a

Tubes Potentially Susceptible to Collapse and In-Leakage
TSP L-P
Right-Hand Unit

a

Tubes Potentially Susceptible to Collapse and In-Leakage
TSP B
Right-Hand Unit

Table 4-29

Tubes Potentially Susceptible to Collapse and In-Leakage
TSP E, H
Right-Hand Unit

a

Table 4-30

Table and Figure Index for TSP Row/Column Identification

TSP	Summary Tables		Tube Map Figures
	Left-Hand SG	Right-Hand SG	
B	4-22	4-28	4-48, 4-49
C	4-18	4-24	4-48, 4-49
D	4-18	4-24	4-50, 4-51
E	4-23	4-29	4-52, 4-53
F	4-19	4-25	4-54, 4-55
G	4-19	4-25	4-50, 4-51
H	4-23	4-29	4-52, 4-53
J	4-20	4-26	4-48, 4-49
K	4-20	4-26	4-48, 4-49
L	4-21	4-27	4-56, 4-57
M	4-21	4-27	4-56, 4-57
N	4-21	4-27	4-56, 4-57
P	4-21	4-27	4-56, 4-57

Table 4-31

Initial and Boundary Conditions of the Updated TRANFLO
Calculation Models for Model D4 Steam Generator

<u>Case</u>	<u>SG Model</u>	<u>Mode of Operation</u>	<u>Initial Conditions</u>		<u>Boundary Conditions</u>	
			<u>Water Level</u>		<u>Steam Nozzle Flow Limiter</u>	<u>Auxiliary Feedwater Flow</u>
4	D4	Hot Standby	[]
5*	D4	Full Power				
6**	D4	Full Power				

Notes:

- * A run with lower initial void fractions in the tube bundle than the typical values expected for full power.
- ** A run with typical initial void fractions in the tube bundle for Braidwood Unit 1 at full power operation.

Table 4-32

Peak Pressure Drop at Different Tube Support Plates
(Hot Leg Only for Half Plate)

Case	1	2	3	4	5*	6*
SG	D3	D4	D4	D4	D4	D4
Identification	D3-1	D4-2	D4-3	D4-4	D4-5	D4-6
Operating Condition	Hot Standby	Full Power	Hot Standby with Excess Feedwater	Hot Standby	Full Power	Full Power
Water Level	[]
Flow splits within tube bundle						
TSP with max peak Δp	Bottom	HL TSP L	Uppermost	Uppermost	HL TSP L	HL TSP L
Peak Δp at uppermost TSP, psi	[]
Max peak Δp , psi						
Peak Δp at bottom plate	[]
Δp at HL TSP L (Elev. of Top TSP of Preheater)						
	1.18	2.53	3.39	0.58	2.01	3.67

* See Table 4-31 for description of differences in initial void fraction between Case 5 and Case 6.

Table 4-33

Expanded Summary of Component Materials

Component	Material
Channel Head	SA 216 Grade WCC
Tubesheet	SA-508 Class 2a
Shell	SA-533 Grade A Class 2
Tube Support Plate	SA-285 Grade C
Stayrod	SA-106 Grade B
Spacer	SA-106 Grade B
Tube	Inconel 600

Table 4-34

Summary of Material Properties
SA-216, Gr. WCC

PROPERTY	CODE ED.	TEMPERATURE						
		70	200	300	400	500	600	700
Young's Modulus	71	27.90	27.70	27.40	27.00	26.40	25.70	24.80
Coefficient of Thermal Expansion	71	6.07	6.38	6.60	6.82	7.02	7.23	7.44
Density	---	0.283	0.282	0.282	0.281	0.280	0.280	0.279
		7.324	7.303	7.287	7.269	7.252	7.234	7.215

PROPERTY	UNITS
Young's Modulus	psi x 1.0E06
Coefficient of Thermal Expansion	in/in/deg. F x 1.0E-06
Density	lb/in ³
	lb-sec ² /in ⁴ x 1.0E-4

Table 4-35

Summary of Material Properties
SA-508, Class 2a

PROPERTY	CODE ED.	TEMPERATURE						
		70	200	300	400	500	600	700
Young's Modulus	71	29.90	29.50	29.00	28.60	28.00	27.40	26.60
Coefficient of Thermal Expansion	71	6.07	6.38	6.60	6.82	7.02	7.23	7.44
Density	---	0.283	0.282	0.282	0.281	0.280	0.280	0.279
		7.324	7.303	7.287	7.269	7.252	7.234	7.215

PROPERTY	UNITS
Young's Modulus	psi x 1.0E06
Coefficient of Thermal Expansion	in/in/deg. F x 1.0E-06
Density	lb/in ³
	lb-sec ² /in ⁴ x 1.0E-4

Table 4-36

**Summary of Material Properties
SA-533, Grade A Class 2**

PROPERTY	CODE ED.	TEMPERATURE						
		70	200	300	400	500	600	700
Young's Modulus	71	29.90	29.50	29.00	28.60	28.00	27.40	26.60
Coefficient of Thermal Expansion	71	6.07	6.38	6.60	6.82	7.02	7.23	7.44
Density	---	0.283	0.282	0.282	0.281	0.280	0.280	0.279
		7.324	7.303	7.287	7.269	7.252	7.234	7.215

PROPERTY	UNITS
Young's Modulus	psi x 1.0E06
Coefficient of Thermal Expansion	in/in/deg. F x 1.0E-06
Density	lb/in ³
	lb-sec ² /in ⁴ x 1.0E-4

Updated Summary of TSP Displacements for Postulated SLB Events for Model D3 and D4 Steam Generators

1

** Updated results for this case reflect re-distribution of pressure loads and revised support conditions and prototypic void fraction.

Table 4-38

Updated Summary of Number of Tubes Having Different Displacement Magnitudes
Model D4 Steam Generator
Steam Line Break Load Cases

a

Table 4-39

Summary of Tubes Having Relative Tube / Plate Displacements
That Exceed 0.350 inch

- (1) Low Water Level
- (2) Controlled Water Level

* Updated results for this case reflect re-distribution of pressure loads and revised support conditions.

Table 4-40

Comparison of Maximum Displacement at Plate Edge and at Limiting Tube Location

a

- * Displacement relative to tubesheet from time = 0.
- ** Prototypic void fraction

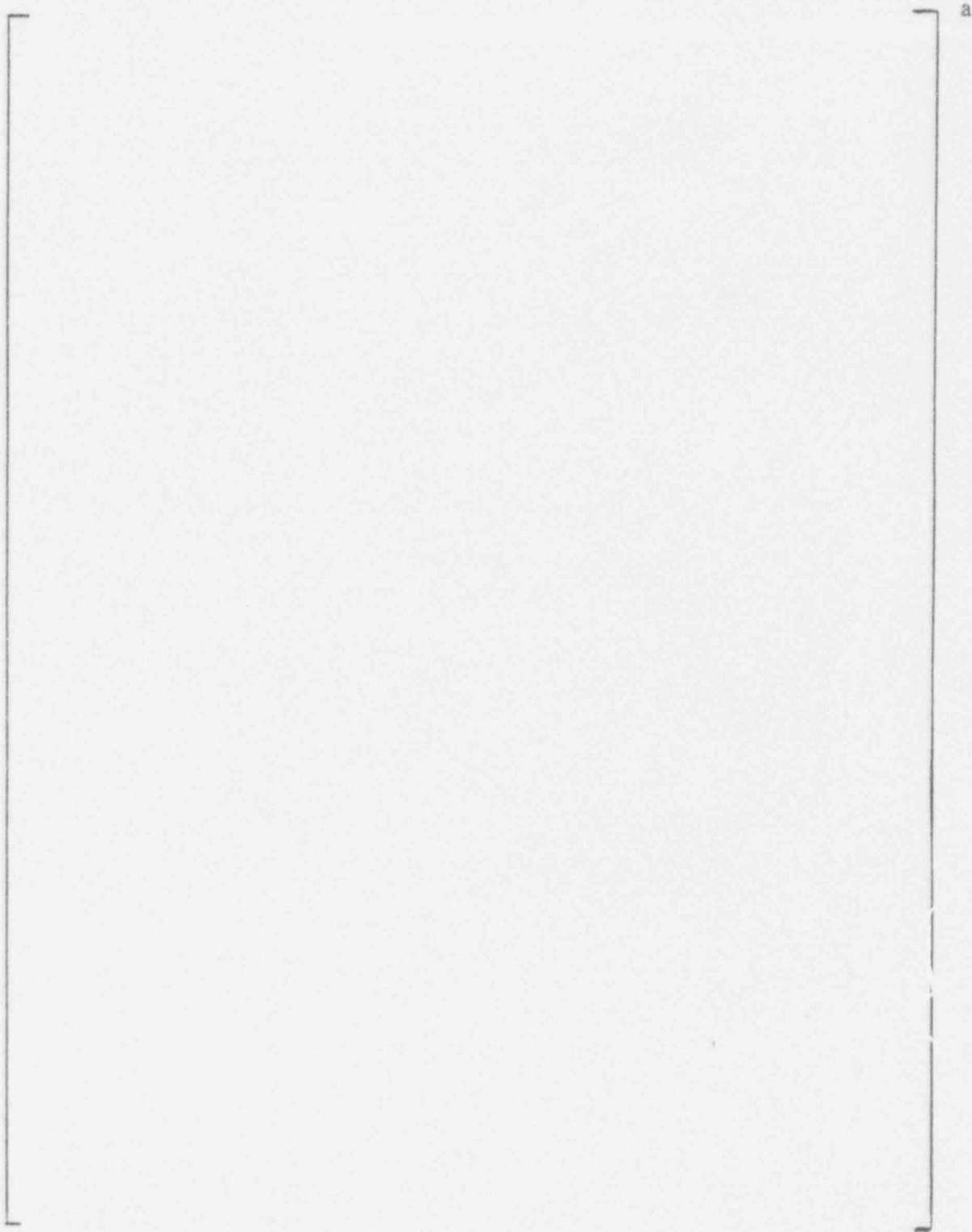


Figure 4-1. Secondary Side Nodes, and Tube Support Plate Identification (See Figure 4-2 for Preheater Detail)

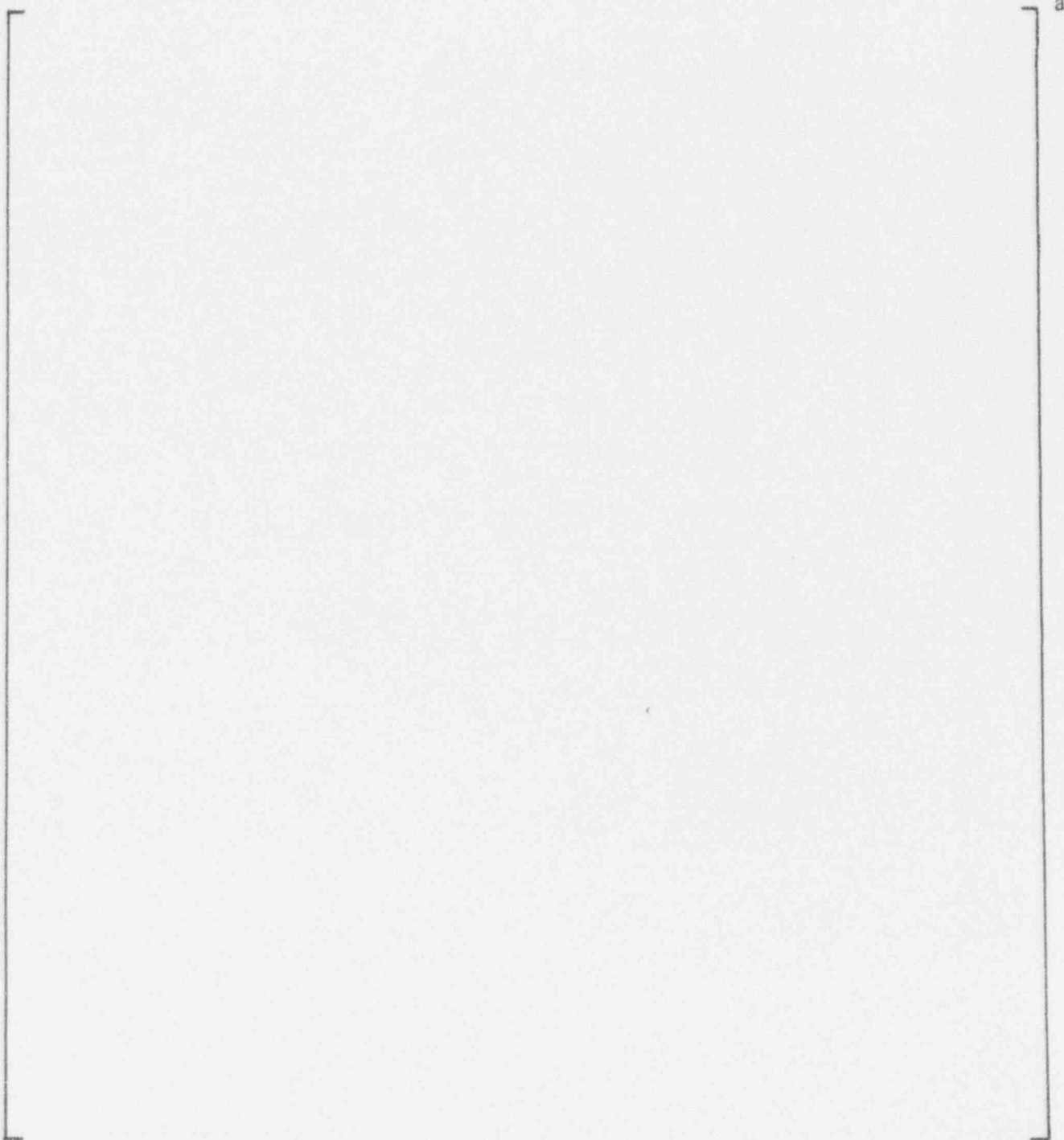


Figure 4-2. Preheater Nodes, and Baffle Identification of Model D3 Steam Generator

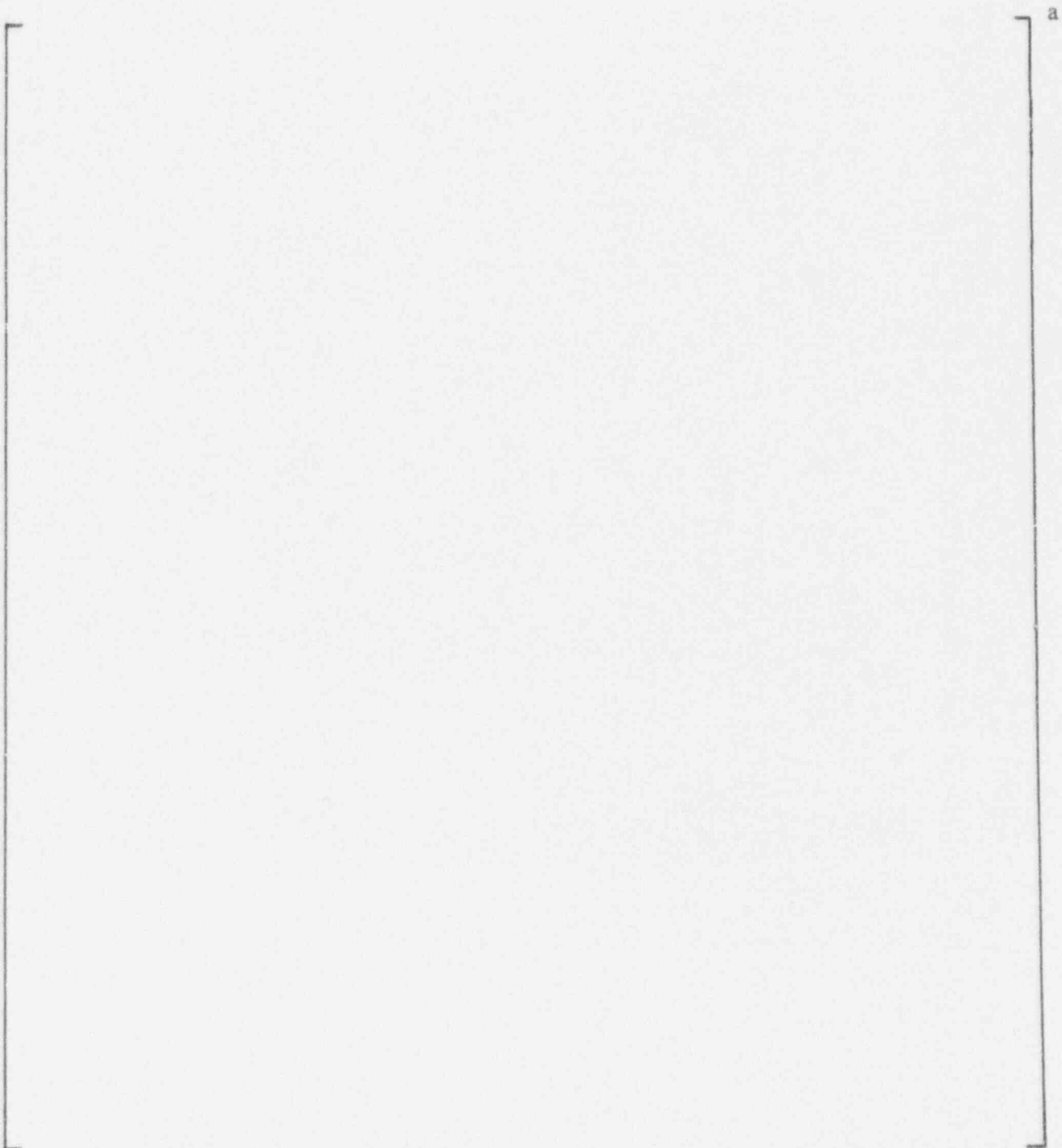


Figure 4-3. Secondary Side Fluid Nodes and Flow Connectors for Model D3 Steam Generator

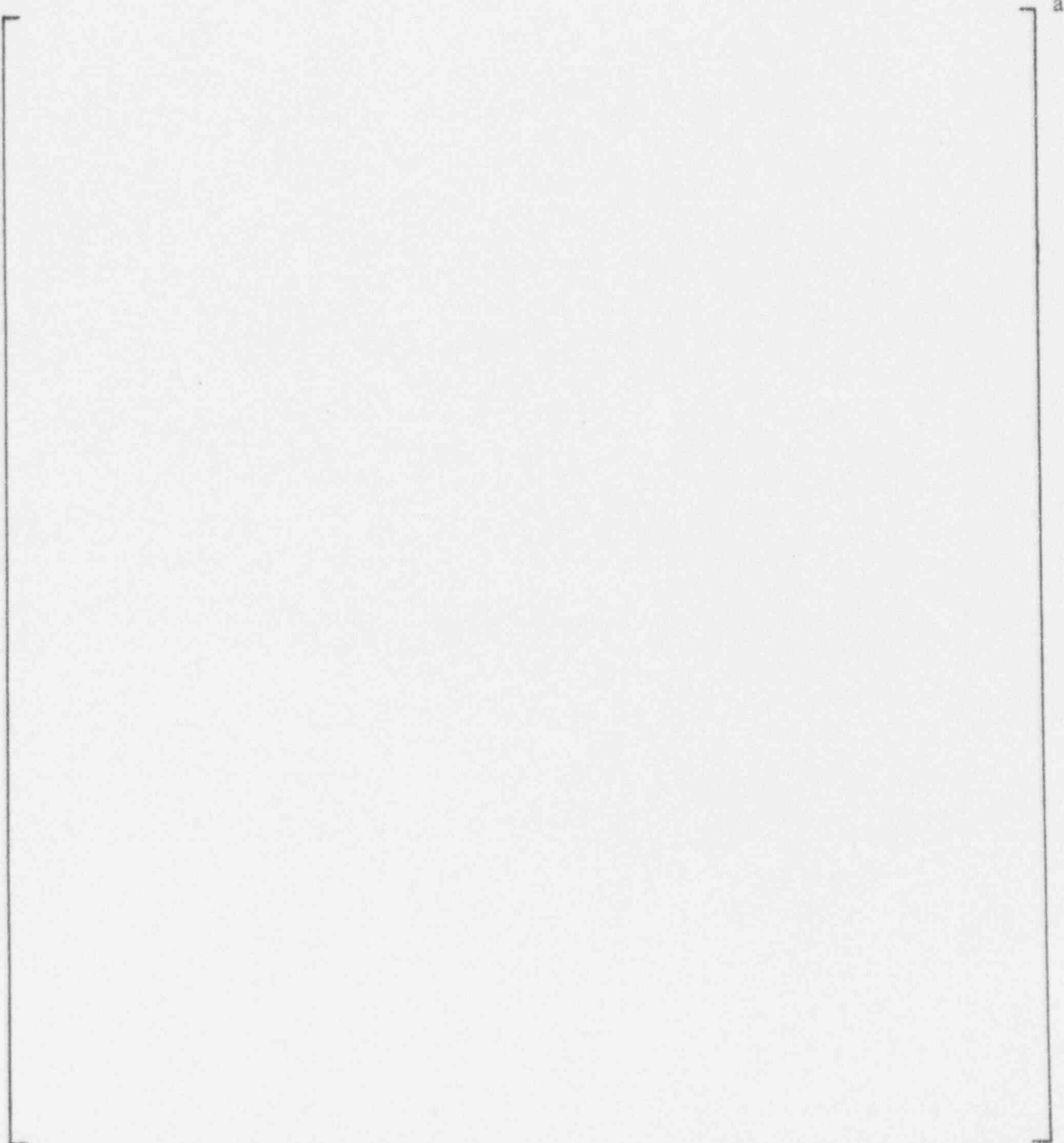


Figure 4-4. Primary Fluid Nodes and Its Flow Connectors, Metal Heat Nodes and Its Heat Transfer Connectors, and Secondary Fluid Modes Within Tube Bundle



Figure 4-5. Pressure drop through tube support plates T, S and R during steam line break of a Model D3 (Case 1; ■ - TSP T, □ - TSP S, ◆ - TSP R)



Figure 4-6. Pressure drop through tube support plates Qhot, L and G during steam line break of a Model D3 (Case 1; ■ - TSP Qhot, □ - TSP L, ◆ - TSP G)



Figure 4-7. Pressure drop through tube support plates Qhot, L and G during steam line break of a Model D3 (Case 1; ■ - TSP C, □- TSP A)

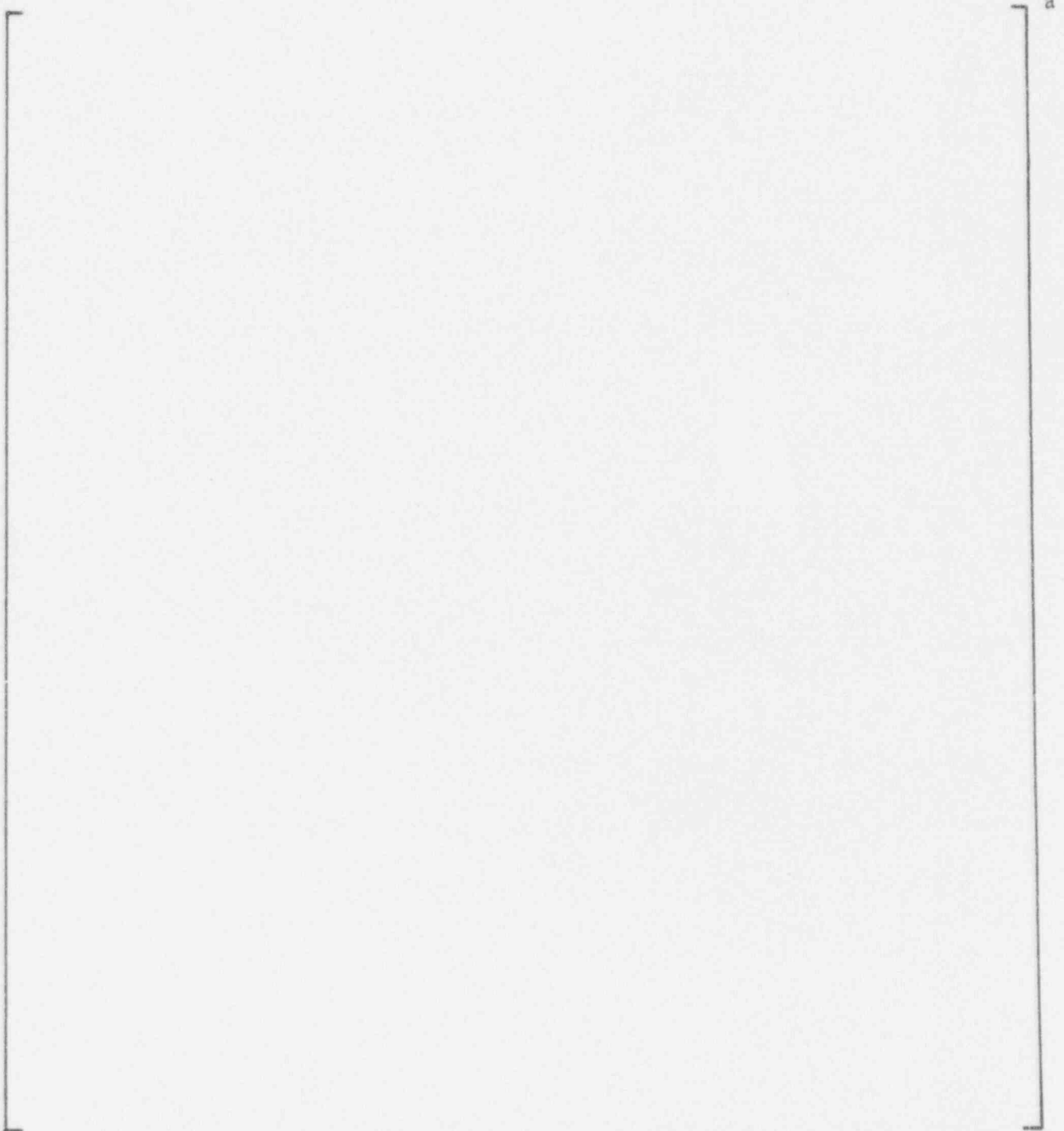


Figure 4-8. Secondary Side Nodes and Tube Support Plates Identification of TRANFLO Model for Model D4 Steam Generator



Figure 4-9 Pressure drop through tube support plates M, N and P during steam line break of a Model D4 (case 2; □ - TSP N, ■ - TSP P, ◆ - TSP M)



Figure 4-10 Pressure drop through tube support plates L, J and F during steam line break of a Model D4 (Case 2; □ - TSP J, ■ - TSP L, ◆ - TSP F)



Figure 4-11. Pressure drop through tube support plates A and C during steam line break of a Model D4 (Case 2; □ - TSP A, ■ - TSP C)



Figure 4-12. Pressure drop through tube support plates M, N and P during steam line break of a Model D4 (Case 3; ■ - TSP P, □ - TSP N, ◆ - TSP M)



Figure 4-13. Pressure drop through tube support plates M, N and P during steam line break of a Model D4 (Case 3; ■ - TSP L, □ - TSP J, ◆ - TSP F)



Figure 4-14. Pressure drop through tube support plates M, N and P during steam line break of a Model D4 (Case 3; ■ - TSP C, □ - TSP A)

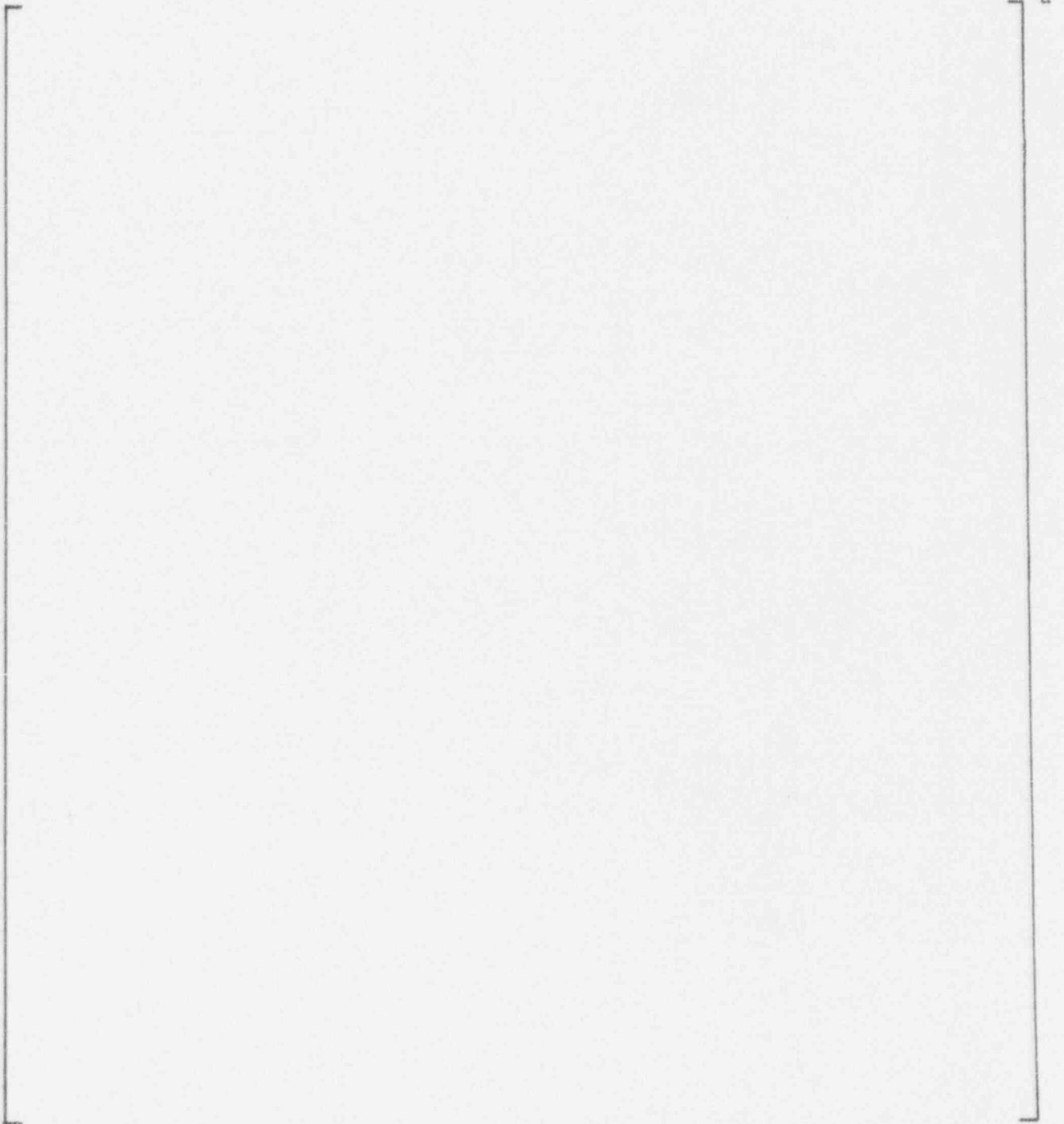


Figure 4-15. Tube Bundle Geometry

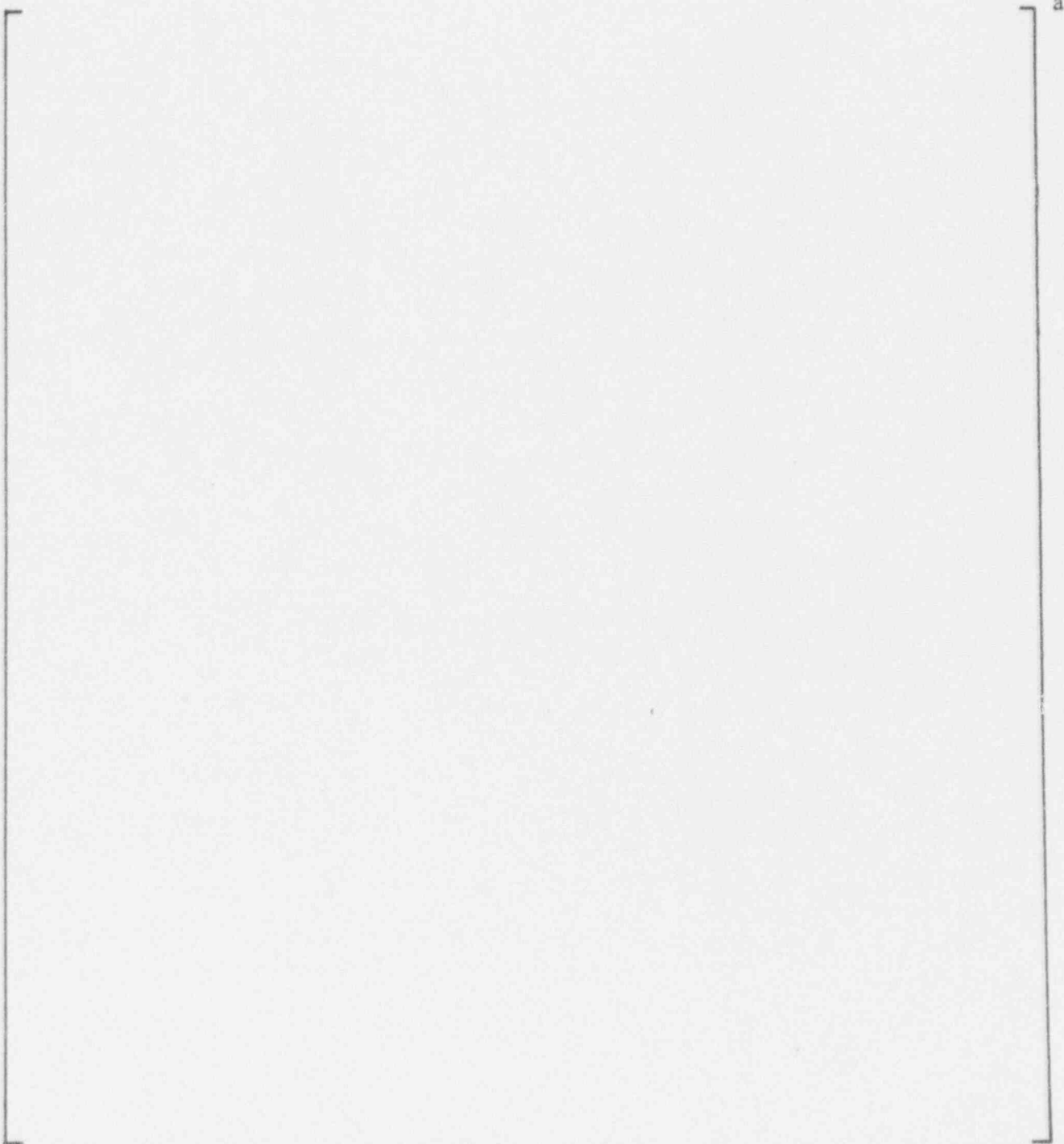


Figure 4-16. Tierod / Spacer Locations

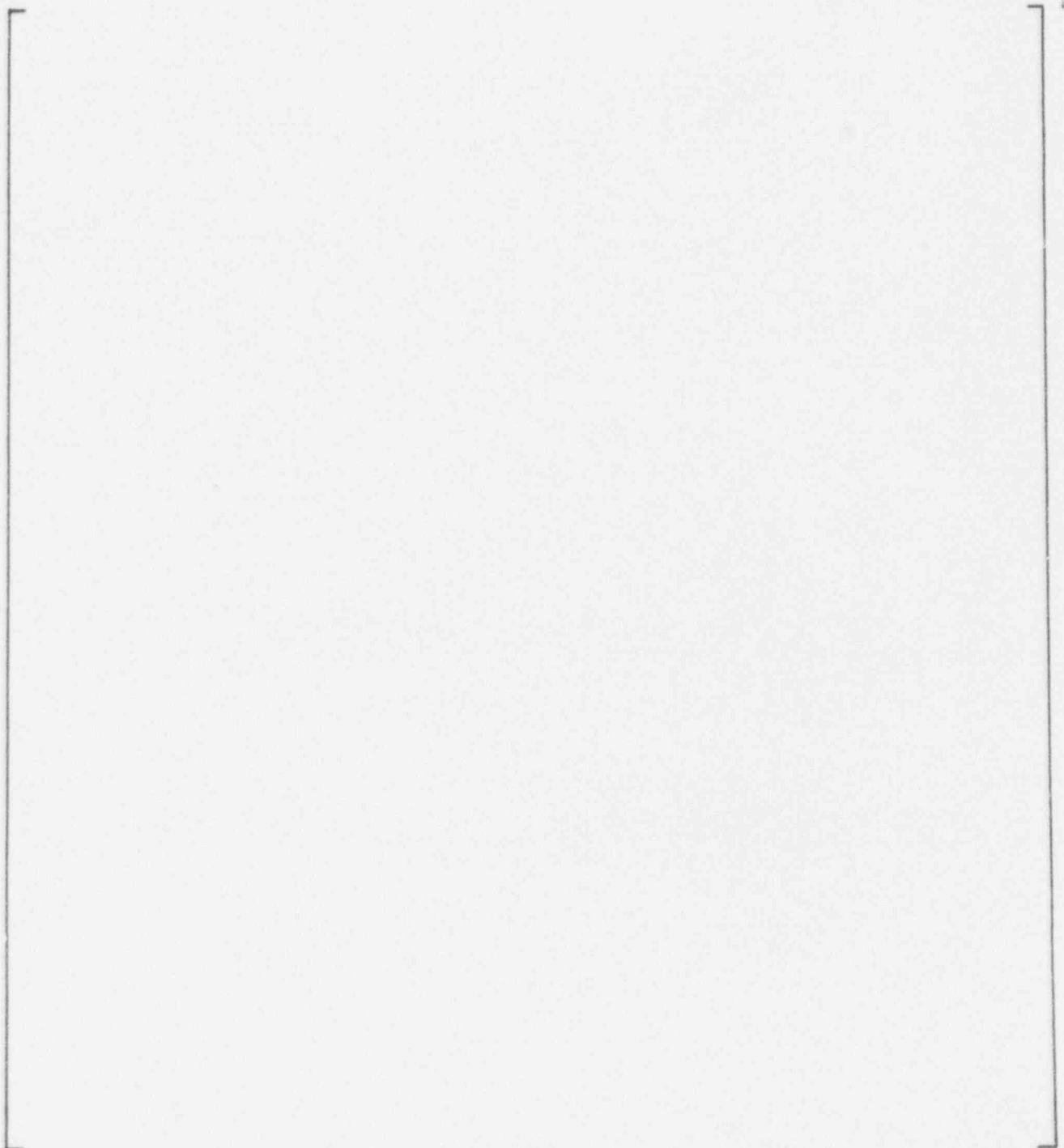


Figure 4-17. Plate A (1H) Support Locations

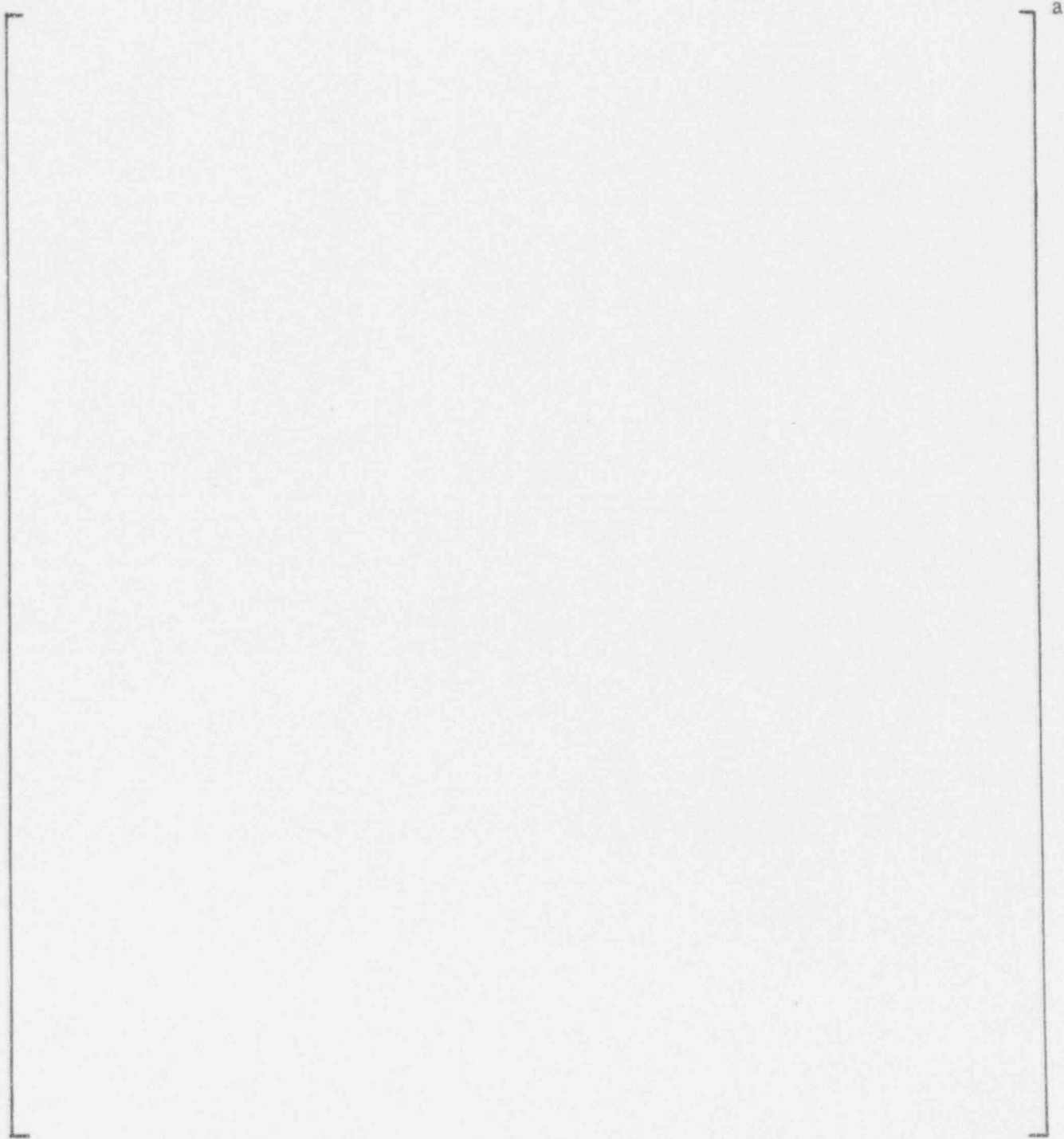


Figure 4-18. Plate C (3H) Support Locations

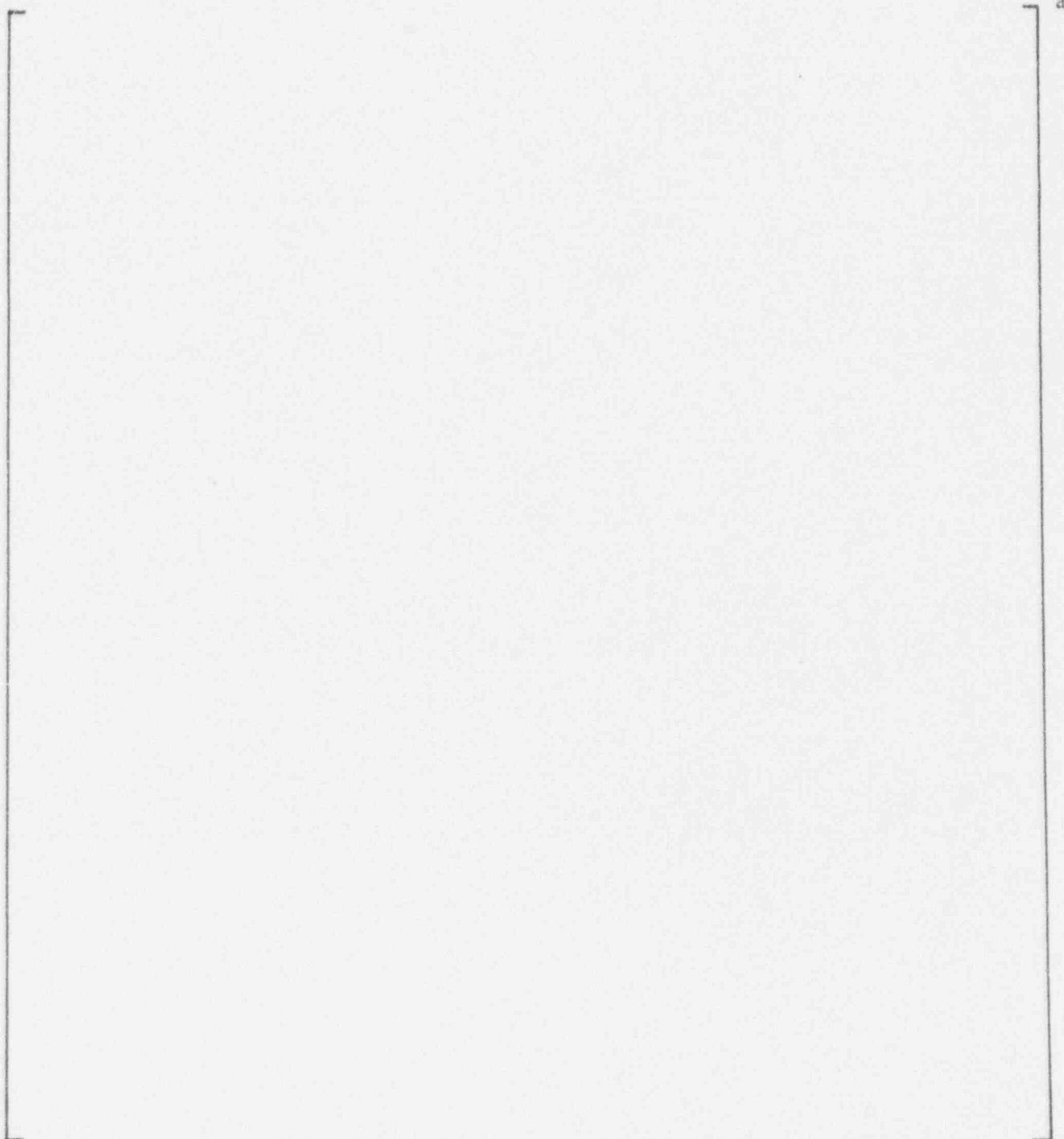


Figure 4-19. Plate F (5H) Support Locations

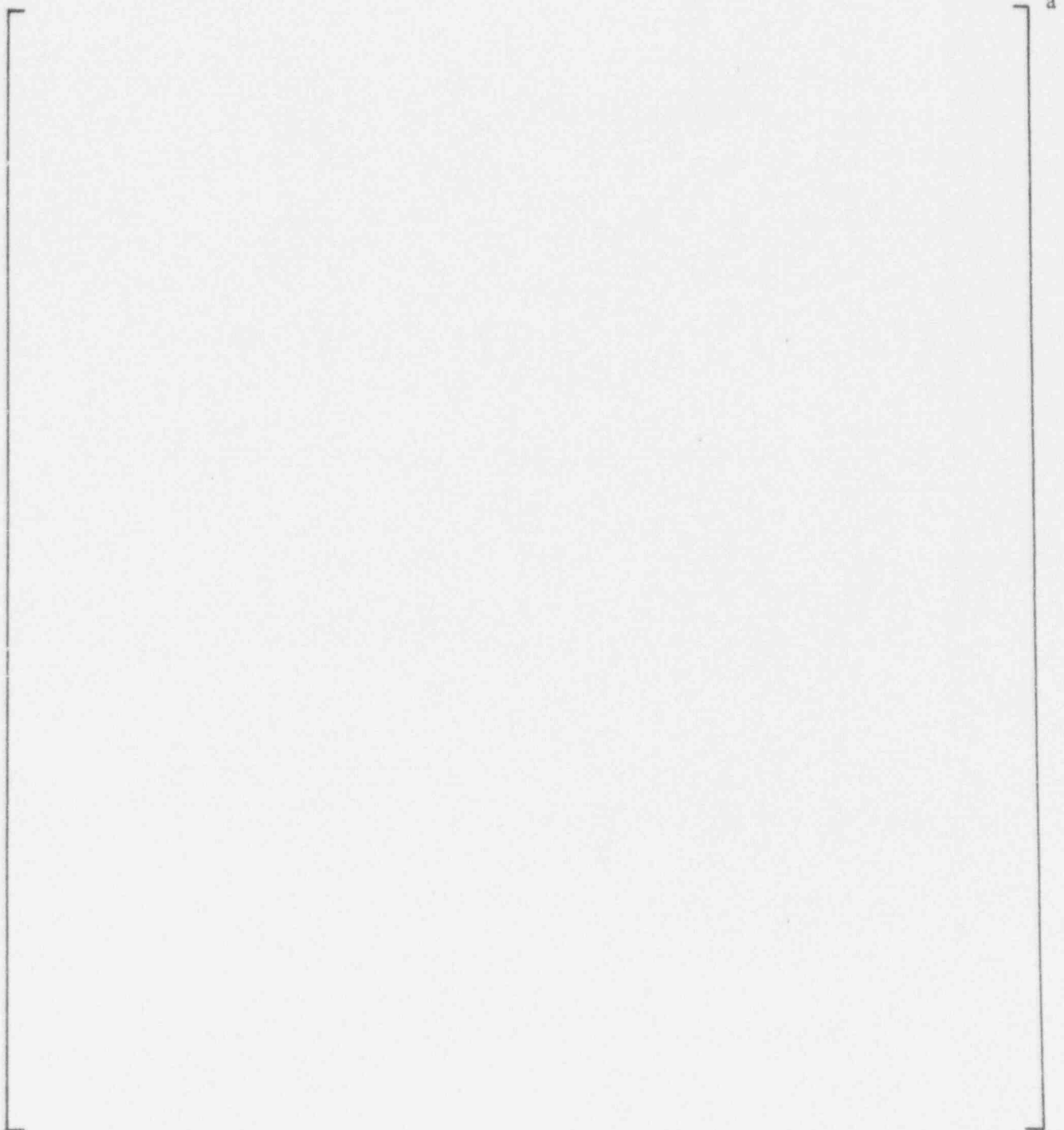


Figure 4-20. Plate J (7H) Support Locations

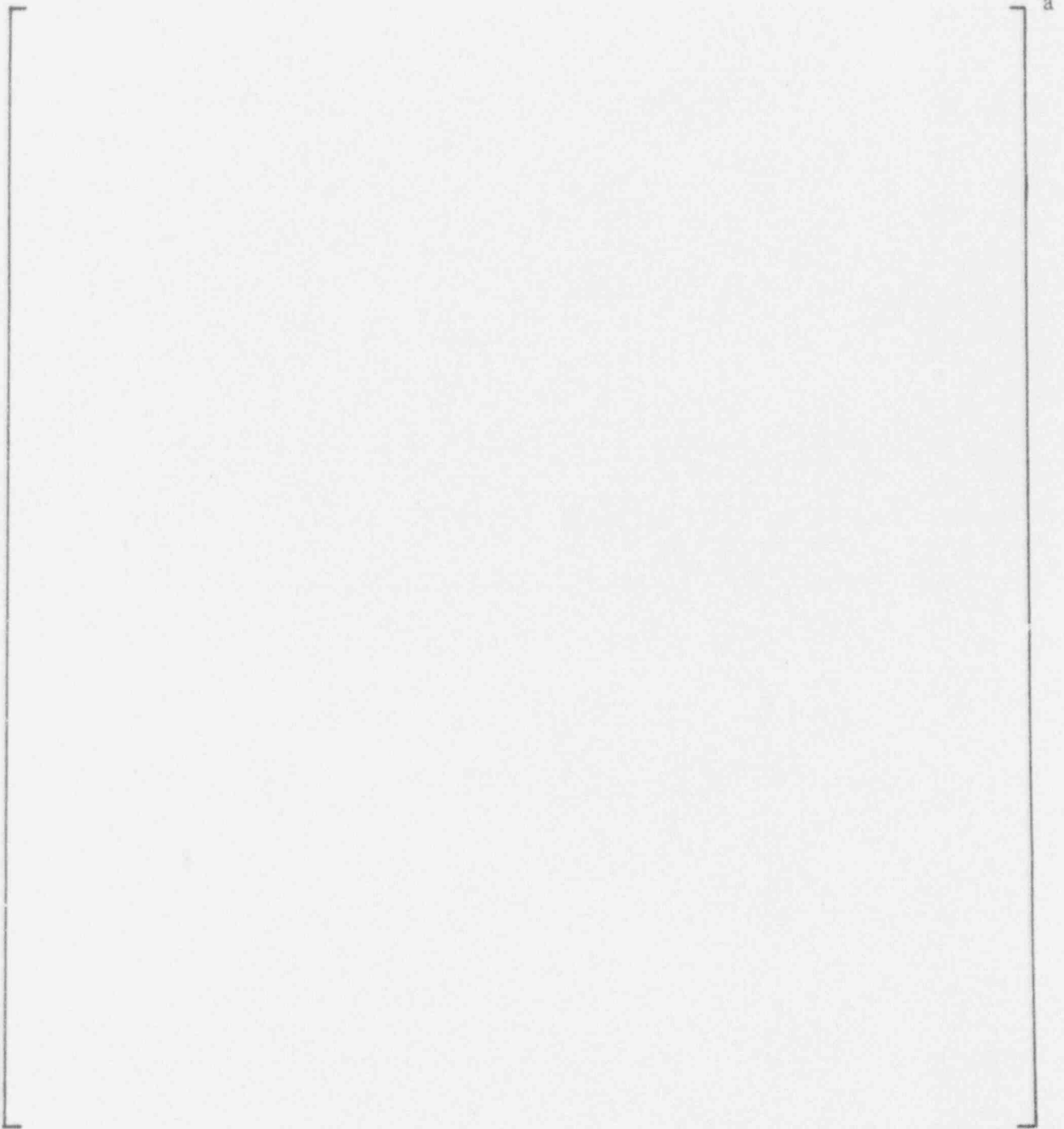


Figure 4-21. Plate L (8H) Support Locations

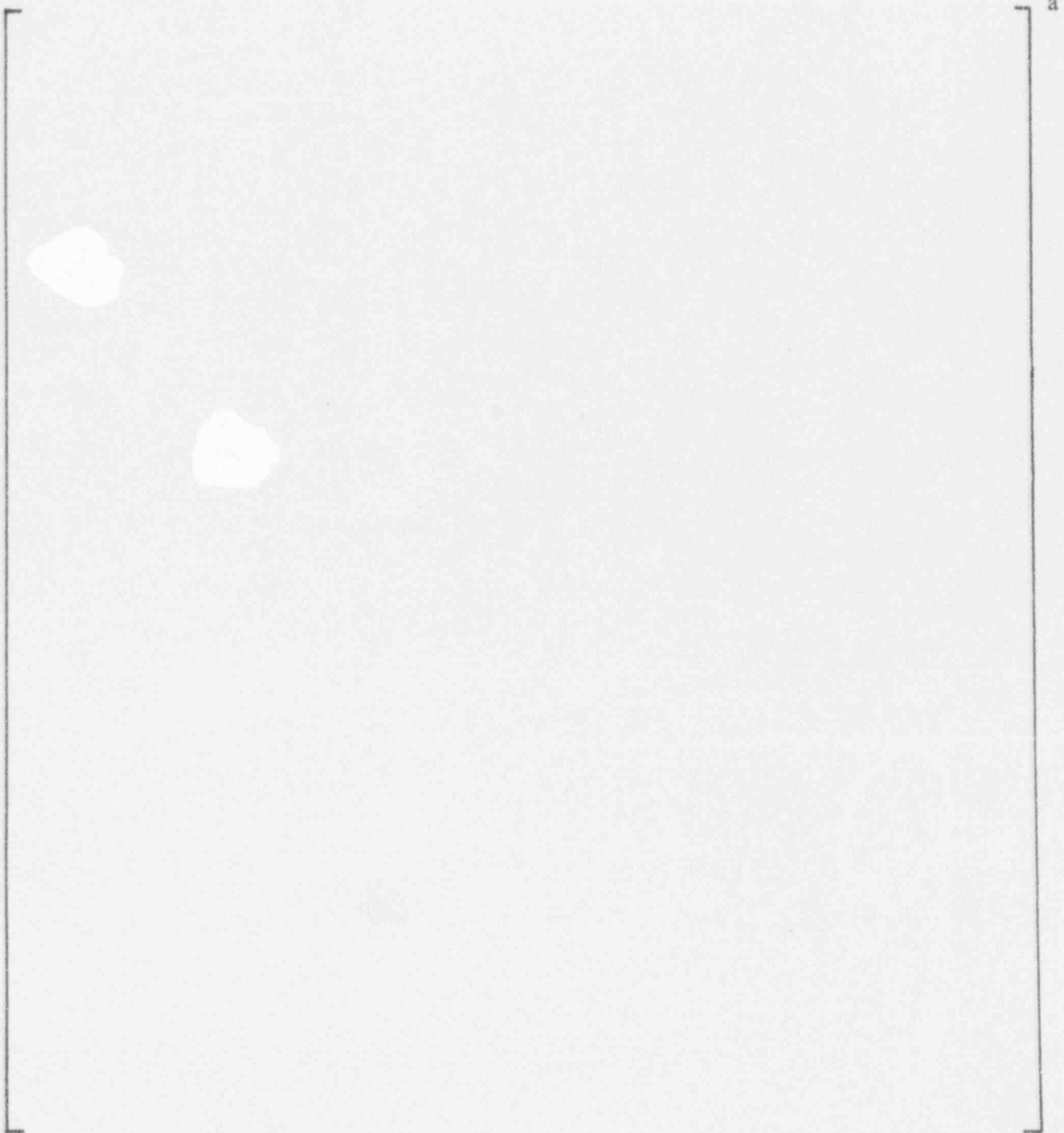


Figure 4-22. Plate M (9H) Support Locations

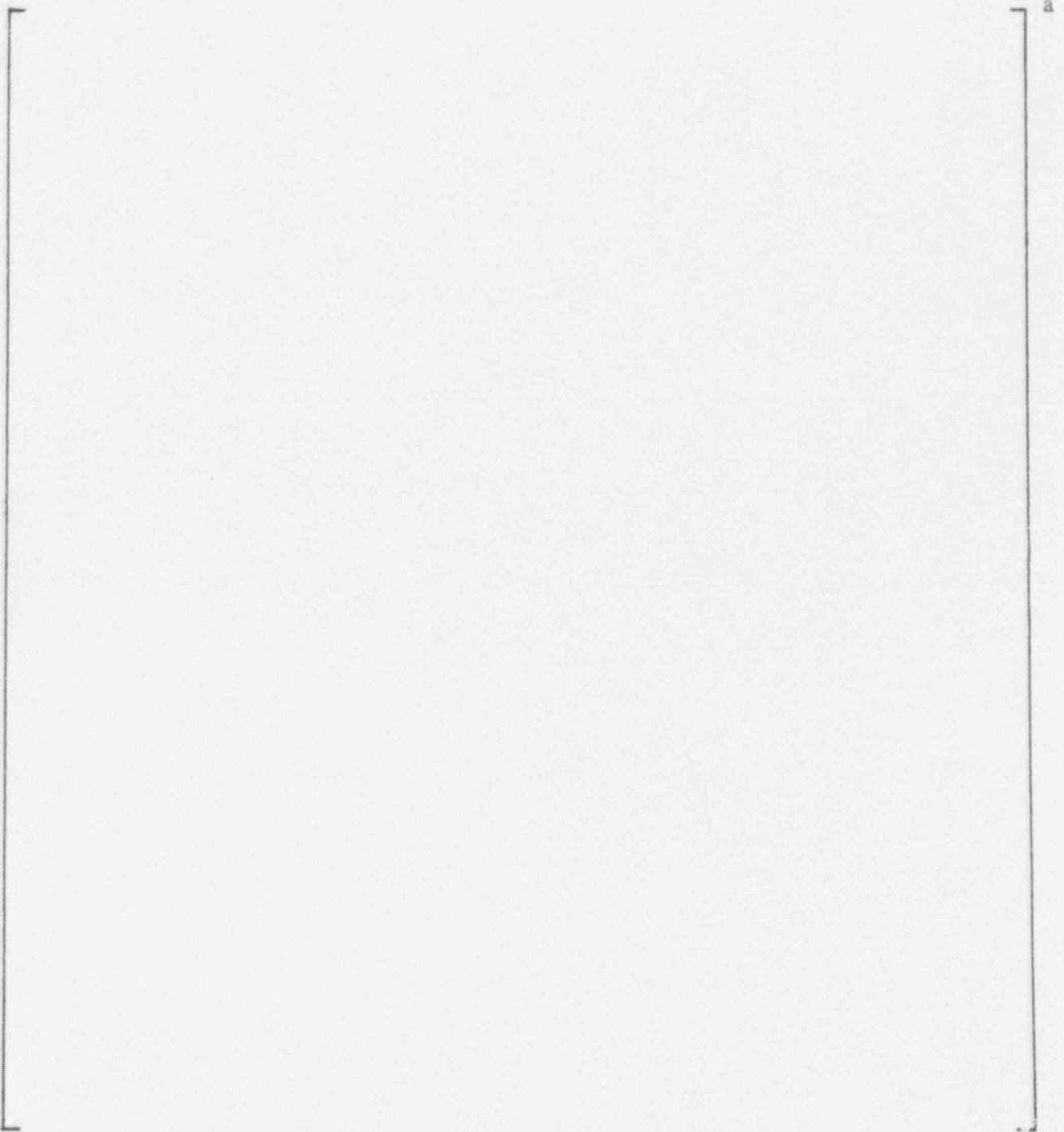


Figure 4-23. Plate N (10H) Support Locations

a

Figure 4-24. Plate P (11H) Support Locations

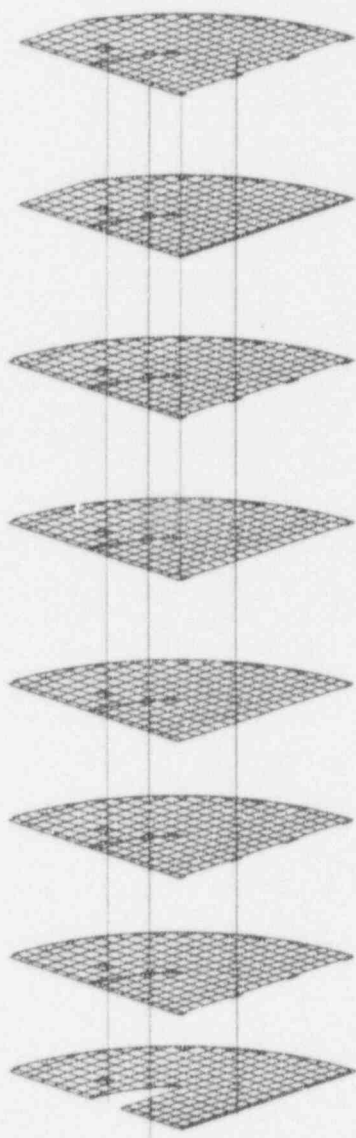


Figure 4-25. Overall Finite Element Model Geometry

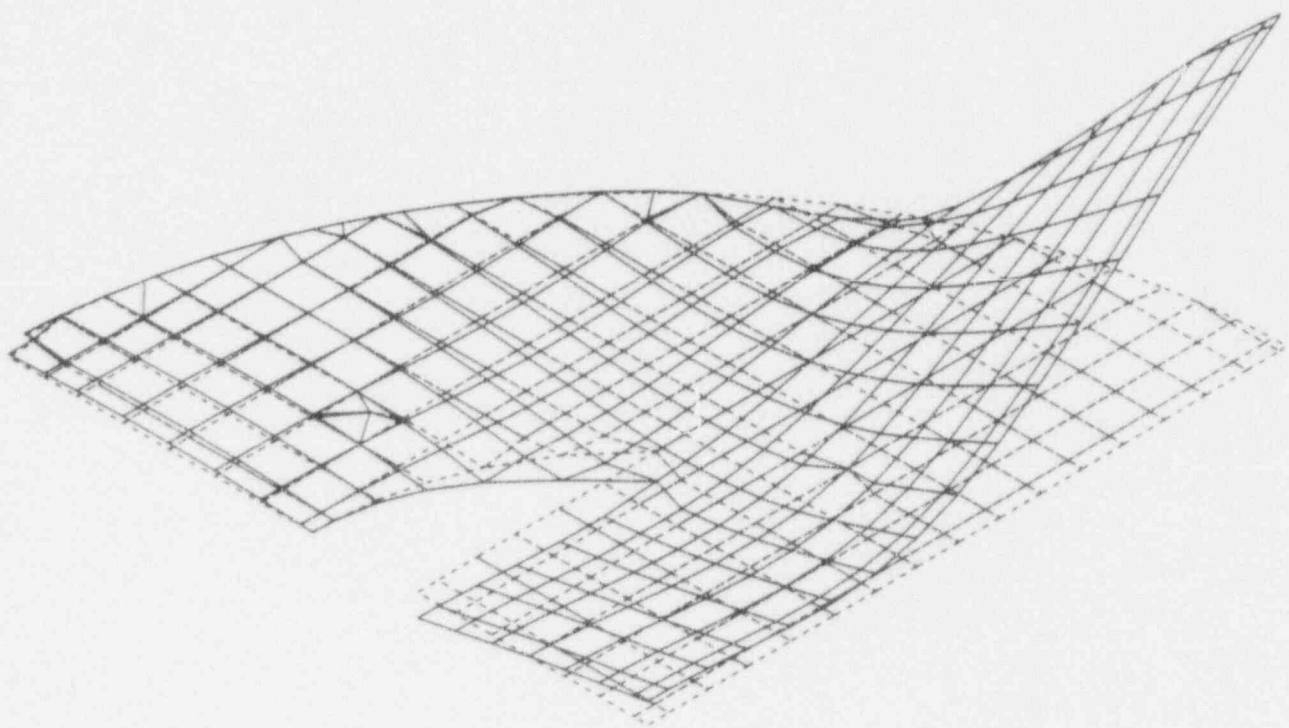


Figure 4-26. Mode Shape Plot - Plate A
Full Set of DOF
Mode 1

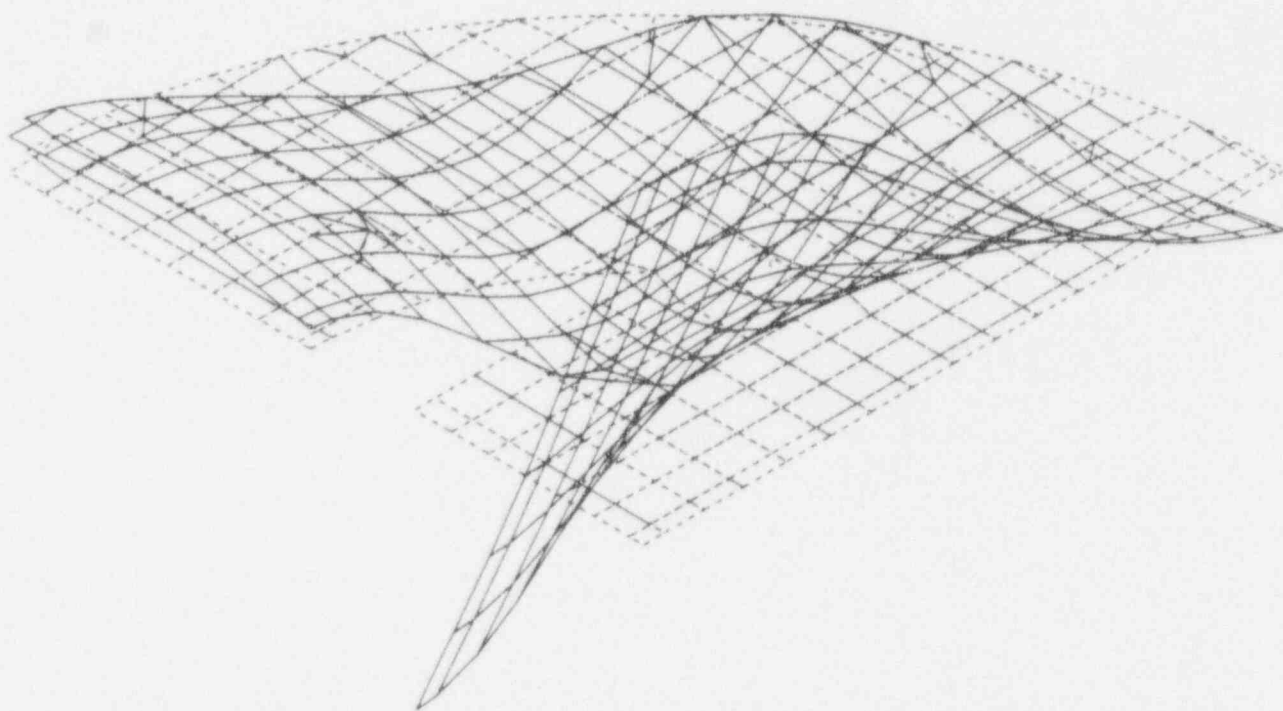


Figure 4-27. Mode Shape Plot - Plate A
Full Set of DOF
Mode 2

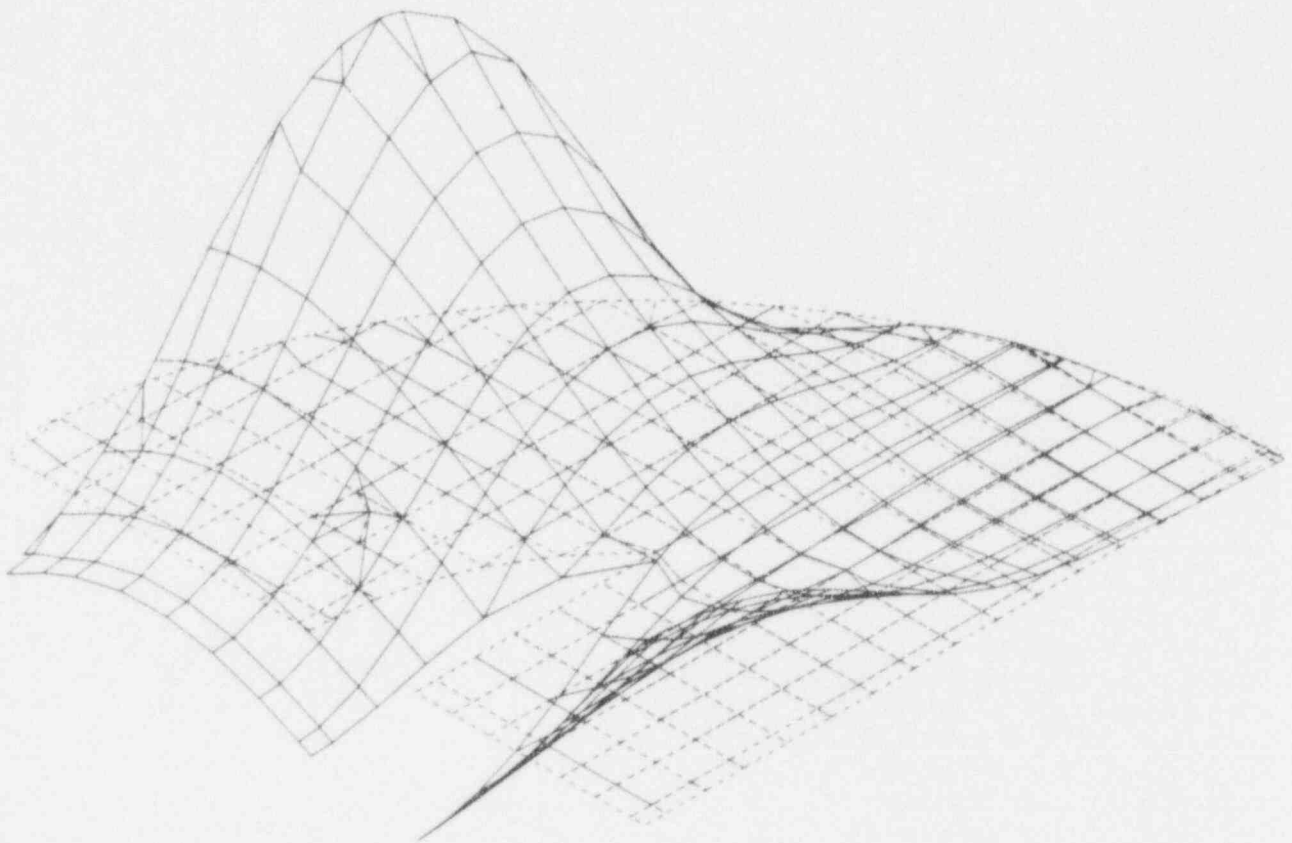


Figure 4-28. Mode Shape Plot - Plate A
Full Set of DOF
Mode 3

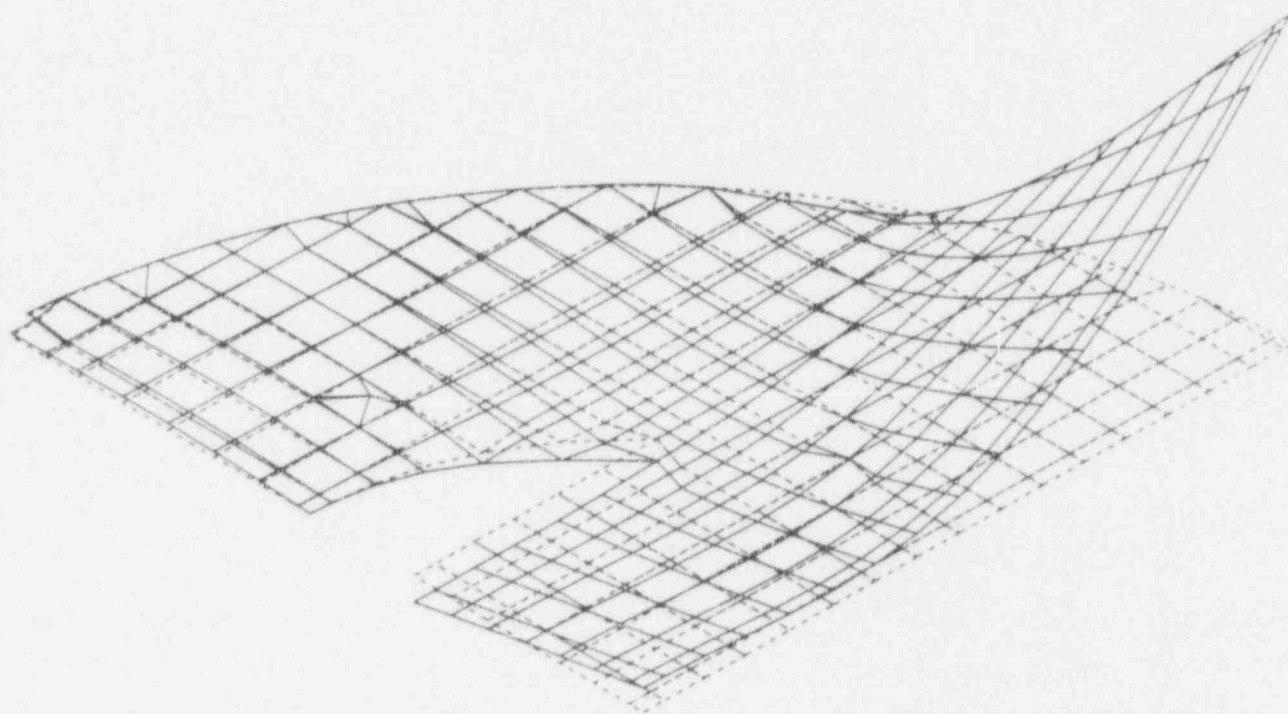


Figure 4-29. Mode Shape Plot - Plate A
Reduced Set of DOF
Mode 1

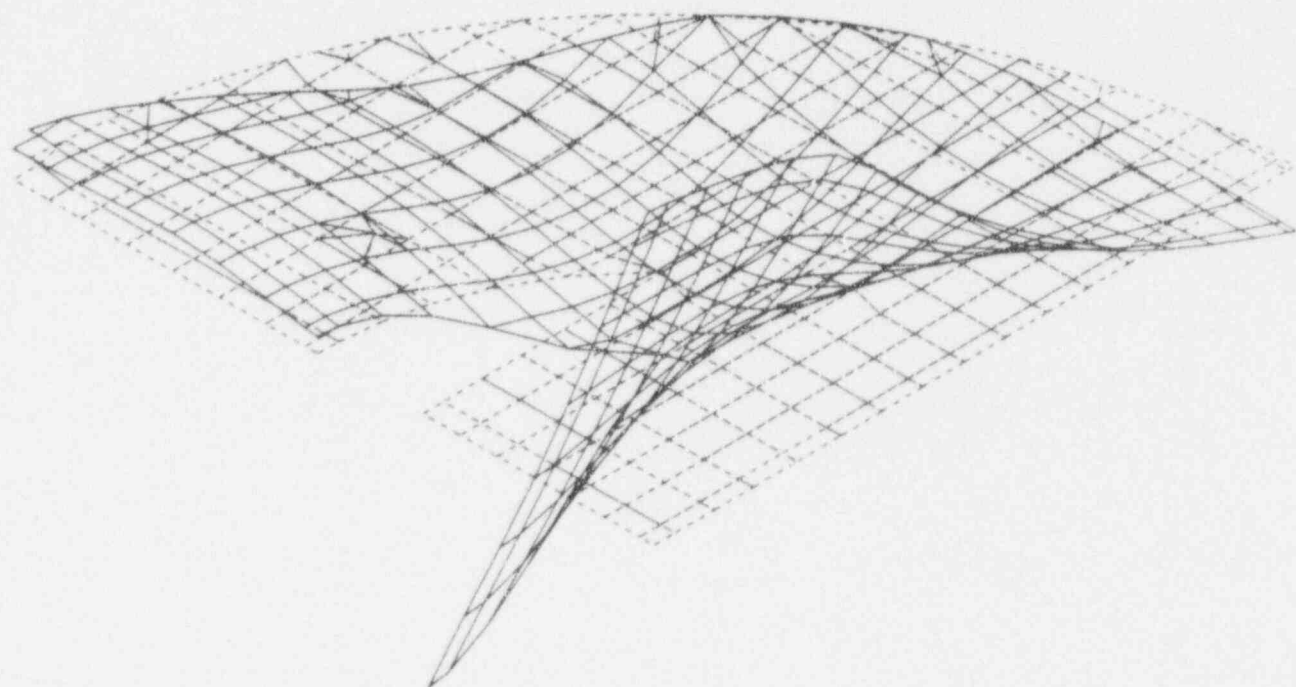


Figure 4-30. Mode Shape Plot - Plate A
Reduced Set of DOF
Mode 2

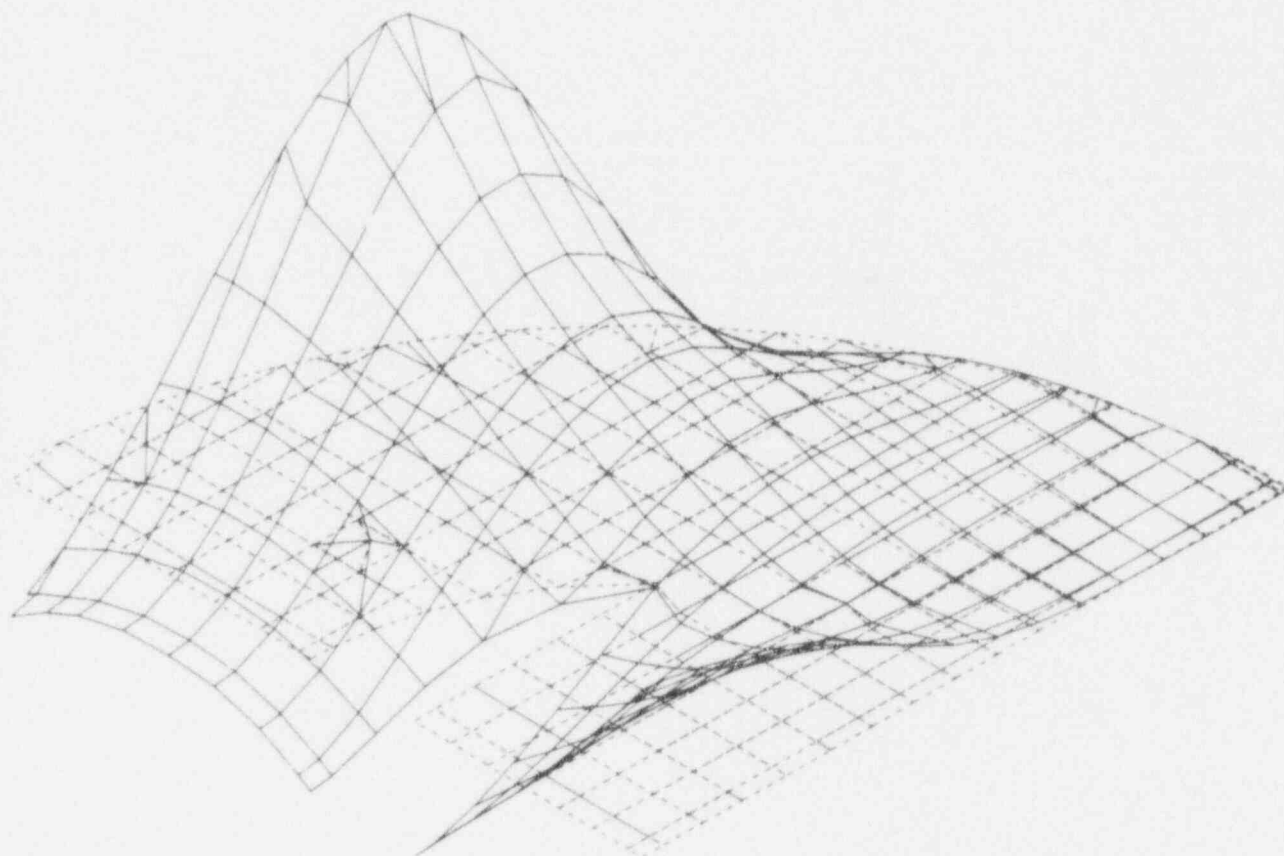


Figure 4-31. Mode Shape Plot - Plate A
Reduced Set of DOF
Mode 3

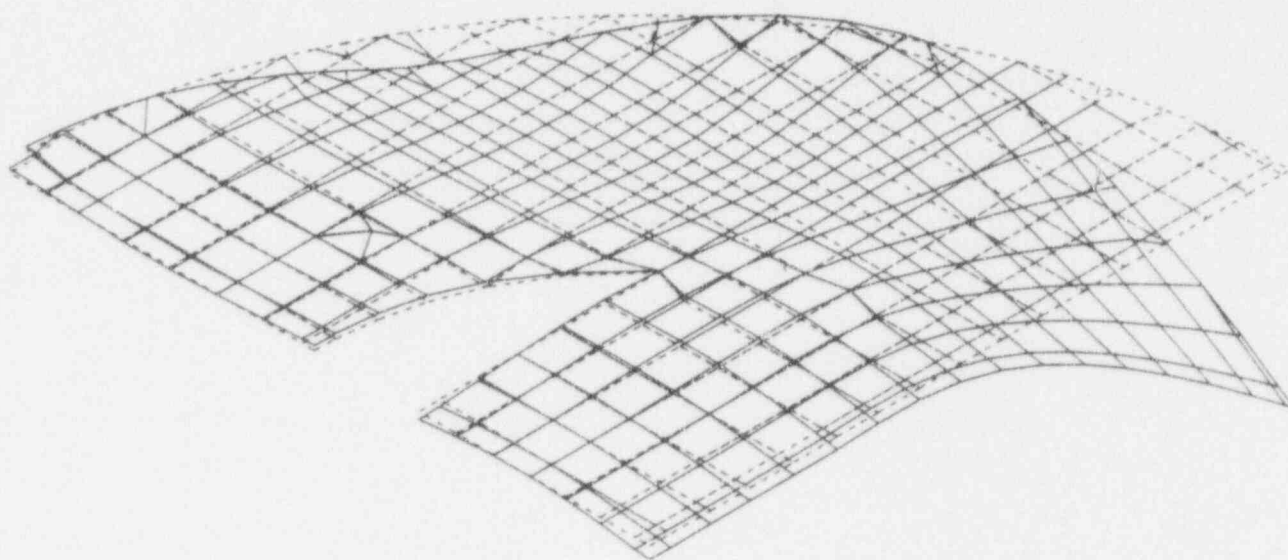


Figure 4-32. Displaced Geometry
Plate A(1H) : Time = 0.902 sec
SLB + Excess Feedwater Transient

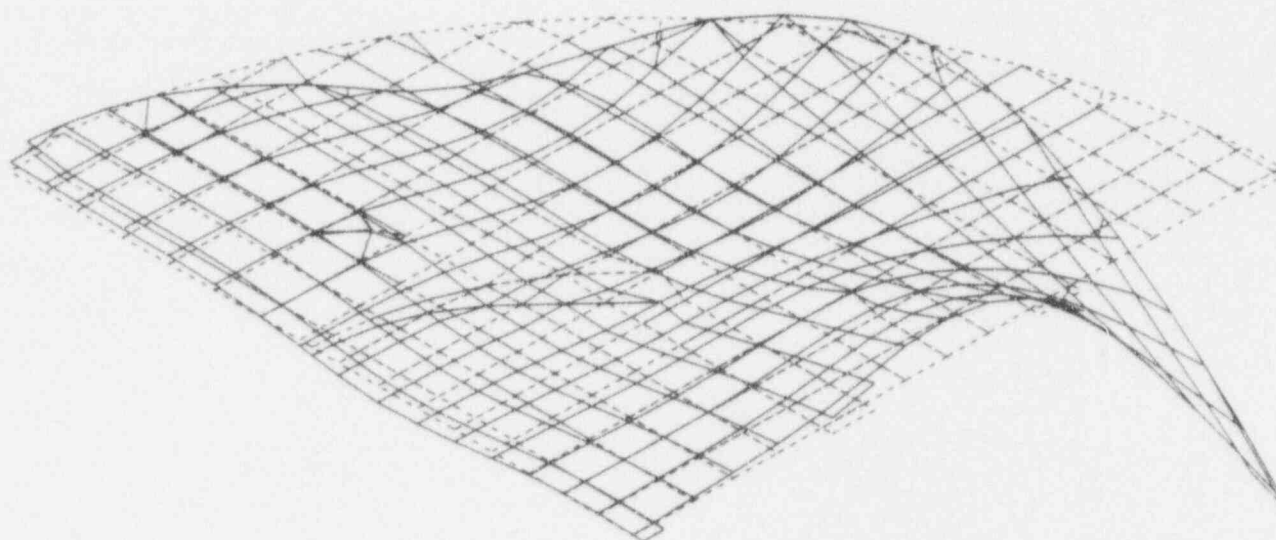


Figure 4-33. Displaced Geometry
Plate C(3H) : Time = 1.886 sec
SLB + Excess Feedwater Transient

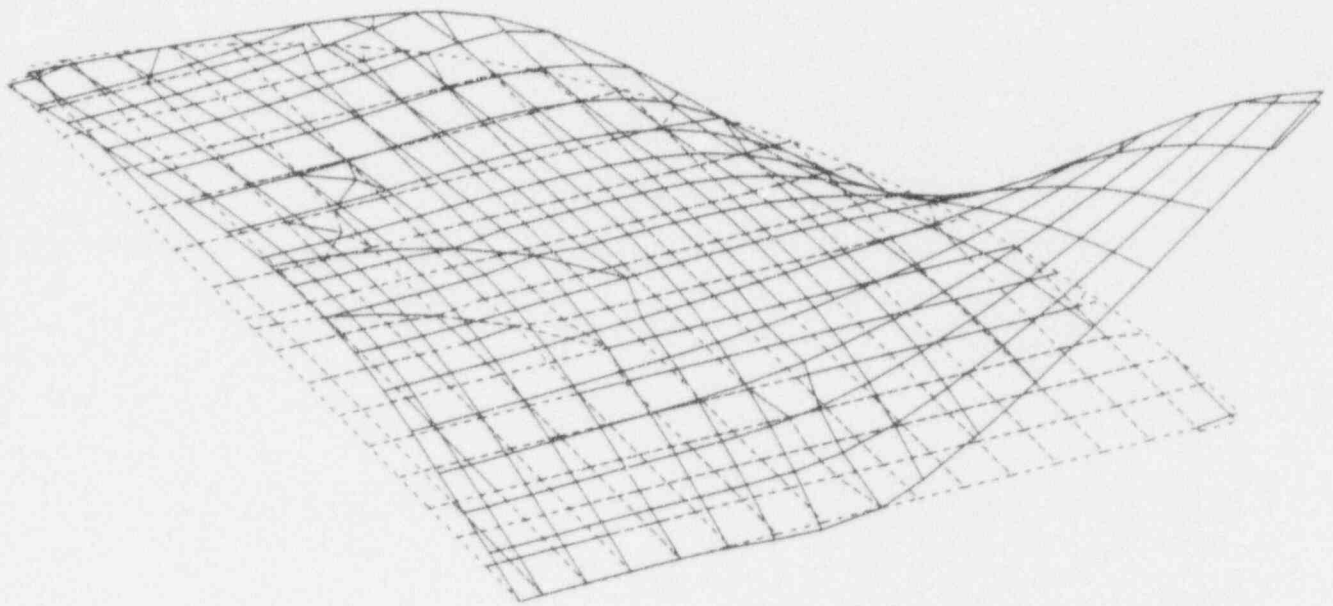


Figure 4-34. Displaced Geometry
Plate J(7H) : Time = 0.264 sec
SLI + Excess Feedwater Transient

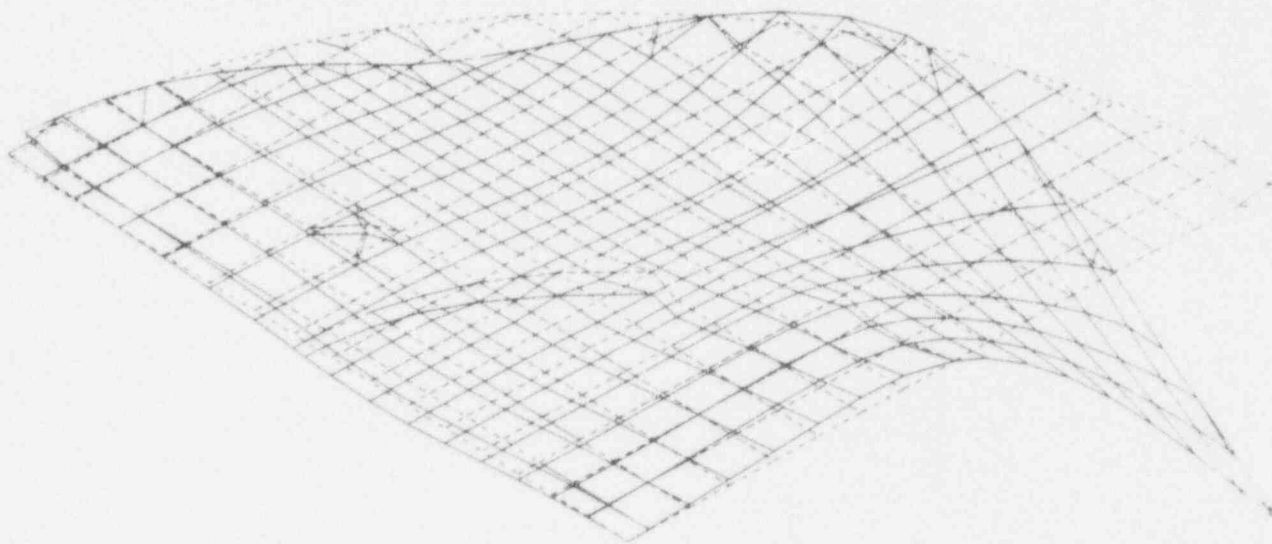


Figure 4-35. Displaced Geometry
Plate J(7H) : Time = 1.926 sec
SLB + Excess Feedwater Transient

**Figure 4-36. Displacement Time History Response
SLB + Excess Feedwater Transient
Plates A(1H), C(3H), F(5H), J(7H)**

**Figure 4-37. Displacement Time History Response
SLB + Excess Feedwater Transient
Plates L(8H), M(9H), N(10H), P(11H)**

a

Figure 4-38
Maximum Stress Intensity
SLB + Excess Feedwater Transient
Plate A (1H)

Figure 4-39
Minimum Stress Intensity
SLB + Excess Feedwater Transient
Plate A (1H)

a

Figure 4-40
Maximum Stress Intensity
SLB + Excess Feedwater Transient
Plate C (3H)

Figure 4-41
Minimum Stress Intensity
SLB + Excess Feedwater Transient
Plate C (3H)

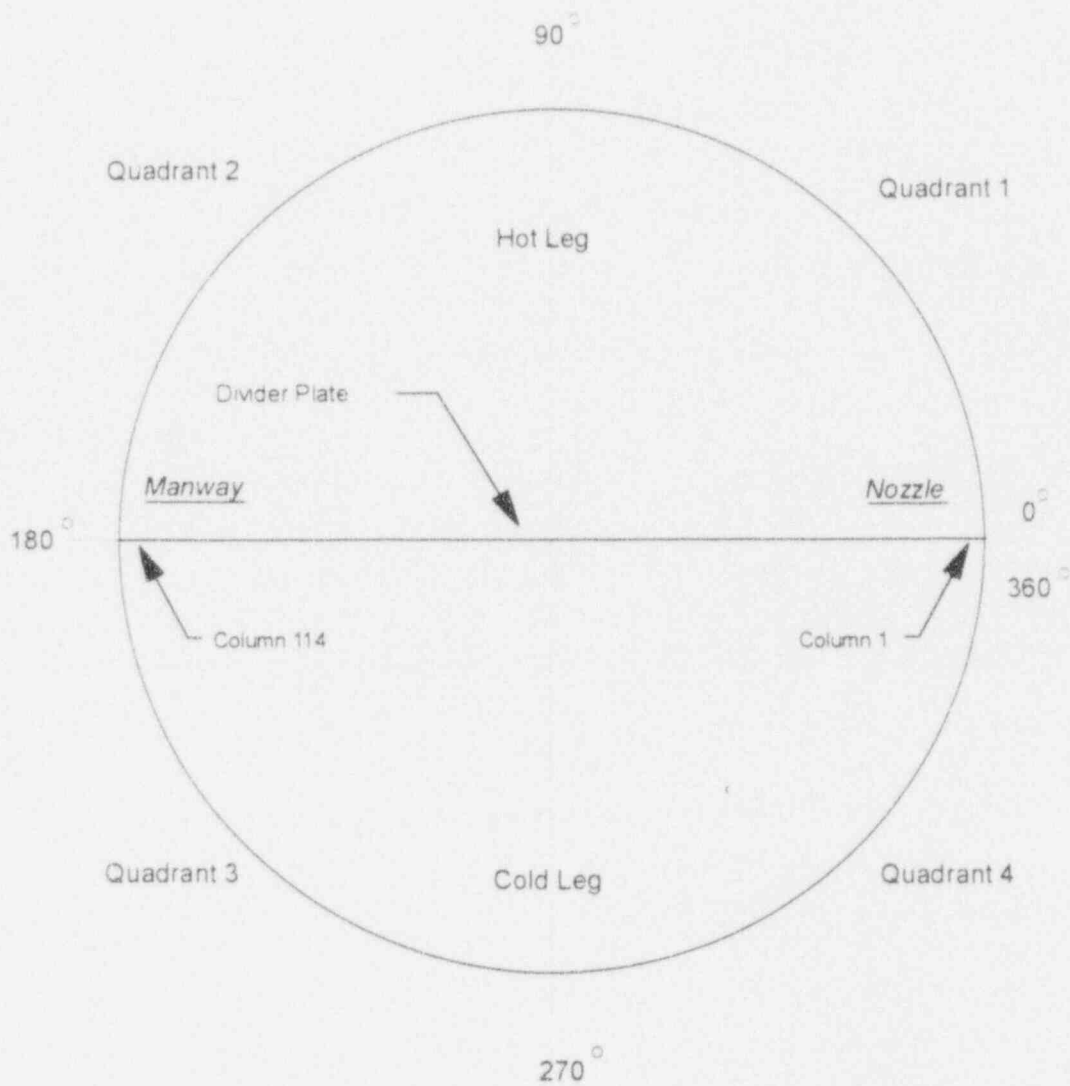
Figure 4-42
Maximum Stress Intensity
SLB + Excess Feedwater Transient
Plate J (7H) (Maximum Upward Response)

Figure 4-43
Minimum Stress Intensity
SLB + Excess Feedwater Transient
Plate J (7H) (Maximum Upward Response)

a

Figure 4-44
Maximum Stress Intensity
SLB + Excess Feedwater Transient
Plate J (7H) (Maximum Downward Response)

Figure 4-45
Minimum Stress Intensity
SLB + Excess Feedwater Transient
Plate J (7H) (Maximum Downward Response)



**Figure 4-47. Reference Configuration
Looking Down on Steam Generator
Right-Hand Unit**

Figure 4-48. Tubes Potentially Susceptible to Collapse and In-Leakage
Braidwood Unit 1
TSP C, J
Quadrant 1

Figure 4-49. Tubes Potentially Susceptible to Collapse and In-Leakage
Braidwood Unit 1
TSP C, J
Quadrant 2

a

Figure 4-50. Tubes Potentially Susceptible to Collapse and In-Leakage
Braidwood Unit 1
TSP D, G
Quadrant 3

Figure 4-51. Tubes Potentially Susceptible to Collapse and In-Leakage
Braidwood Unit 1
TSP D, G
Quadrant 4

Figure 4-52. Tubes Potentially Susceptible to Collapse and In-Leakage
Braidwood Unit 1
TSP E, H
Quadrant 3

Figure 4-53. Tubes Potentially Susceptible to Collapse and In-Leakage
Braidwood Unit 1
TSP E, H
Quadrant 4

a

Figure 4-54. Tubes Potentially Susceptible to Collapse and In-Leakage
Braidwood Unit 1
TSP F
Quadrant 1

Figure 4-55. Tubes Potentially Susceptible to Collapse and In-Leakage
Braidwood Unit 1
TSP F
Quadrant 2

a

Figure 4-56. Tubes Potentially Susceptible to Collapse and In-Leakage
Braidwood Unit 1
TSP L, M, N, P
Quadrant 1

a

**Figure 4-57. Tubes Potentially Susceptible to Collapse and In-Leakage
Braidwood Unit 1
TSP L, M, N, P
Quadrant 2**

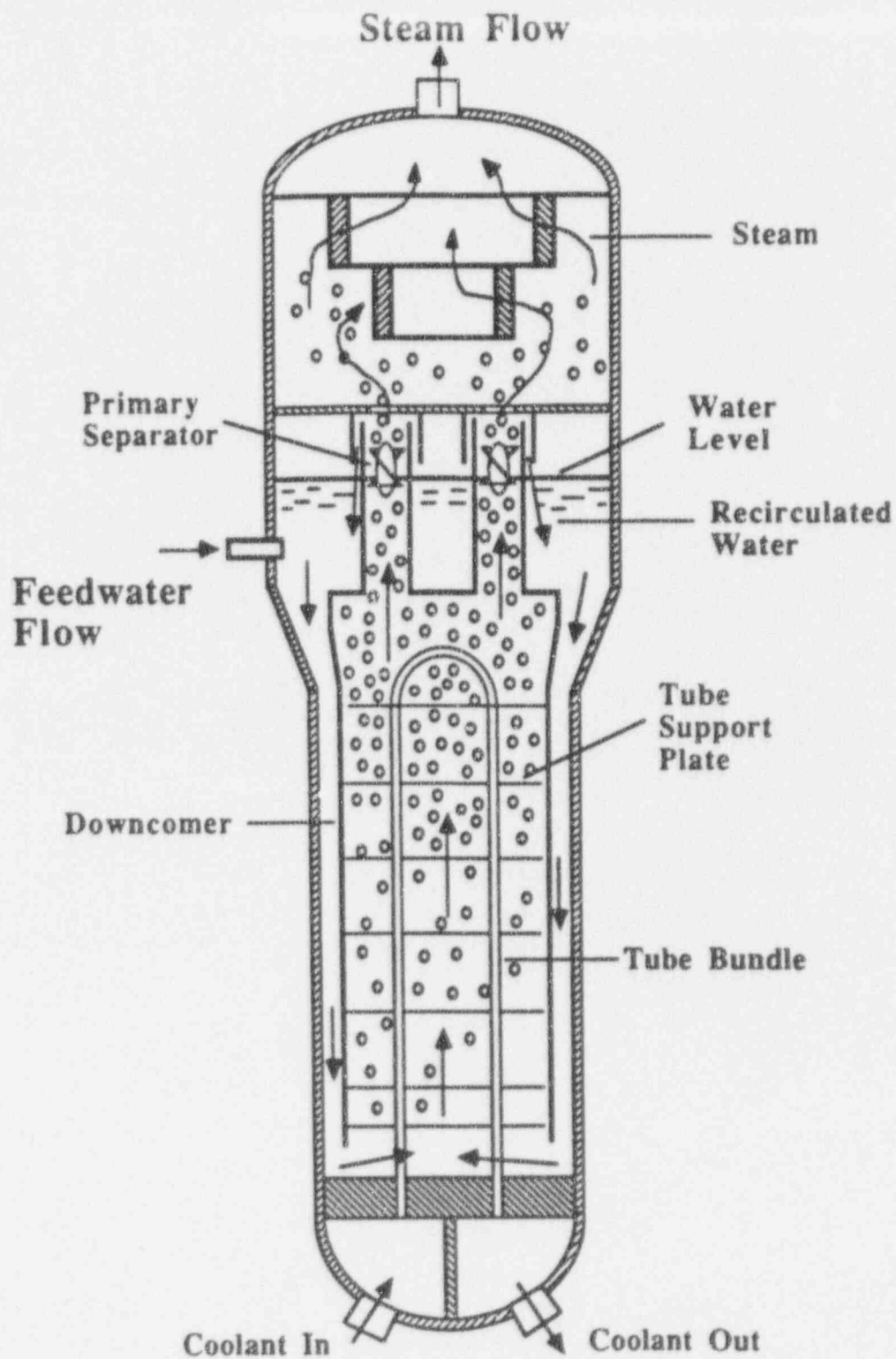


Figure 4-58. Diagram of Flow Circulation During Power Operation

a,b

Figure 4-59. Counterbored Structural Quatrefoil Loss Coefficients

a,b

Figure 4-60. GENF Verification, Circulation Ratio Versus Load

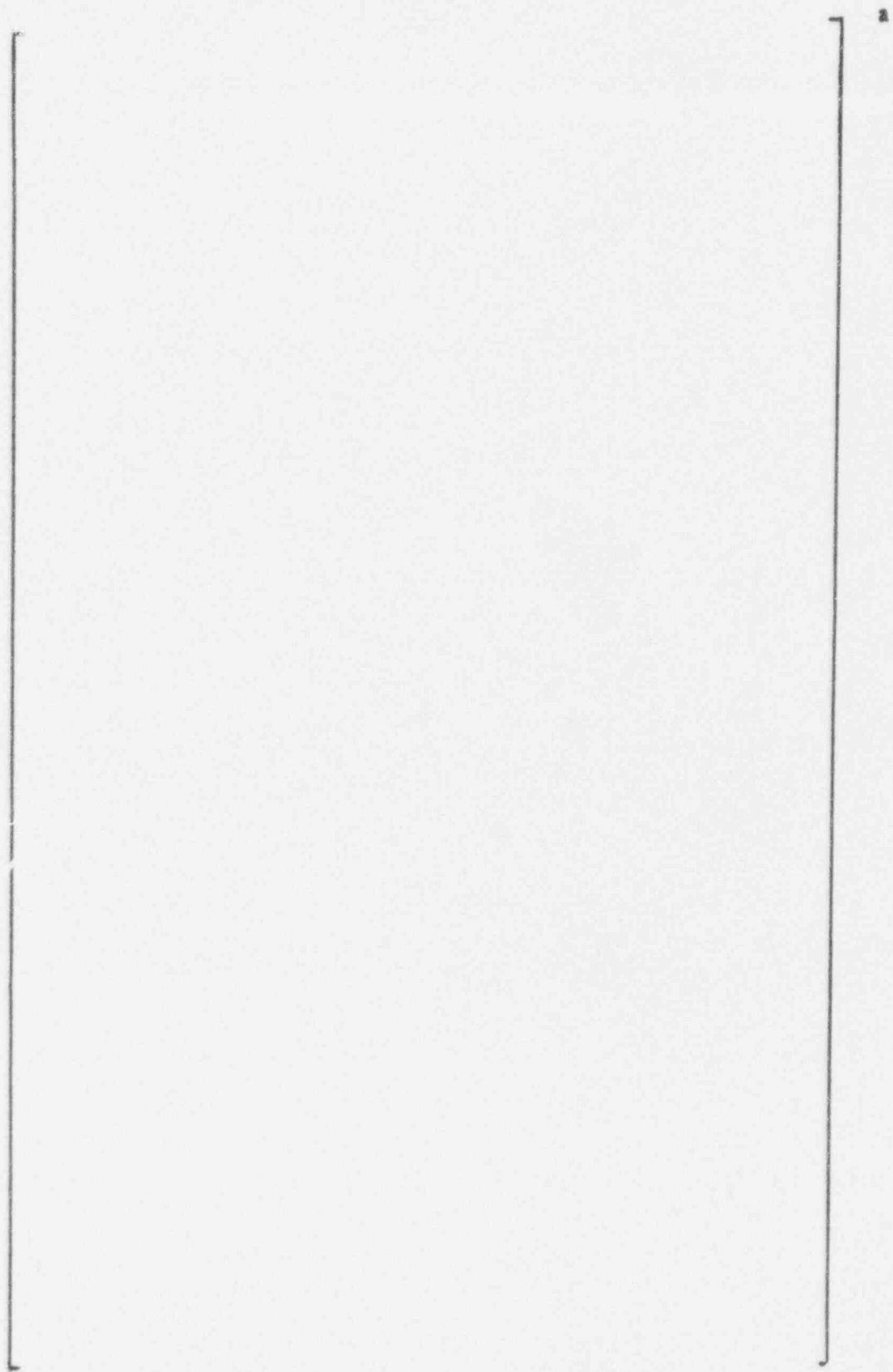


Figure 4-61 Secondary Side Nodes, and Tube Support Plates
Identification of Model D4

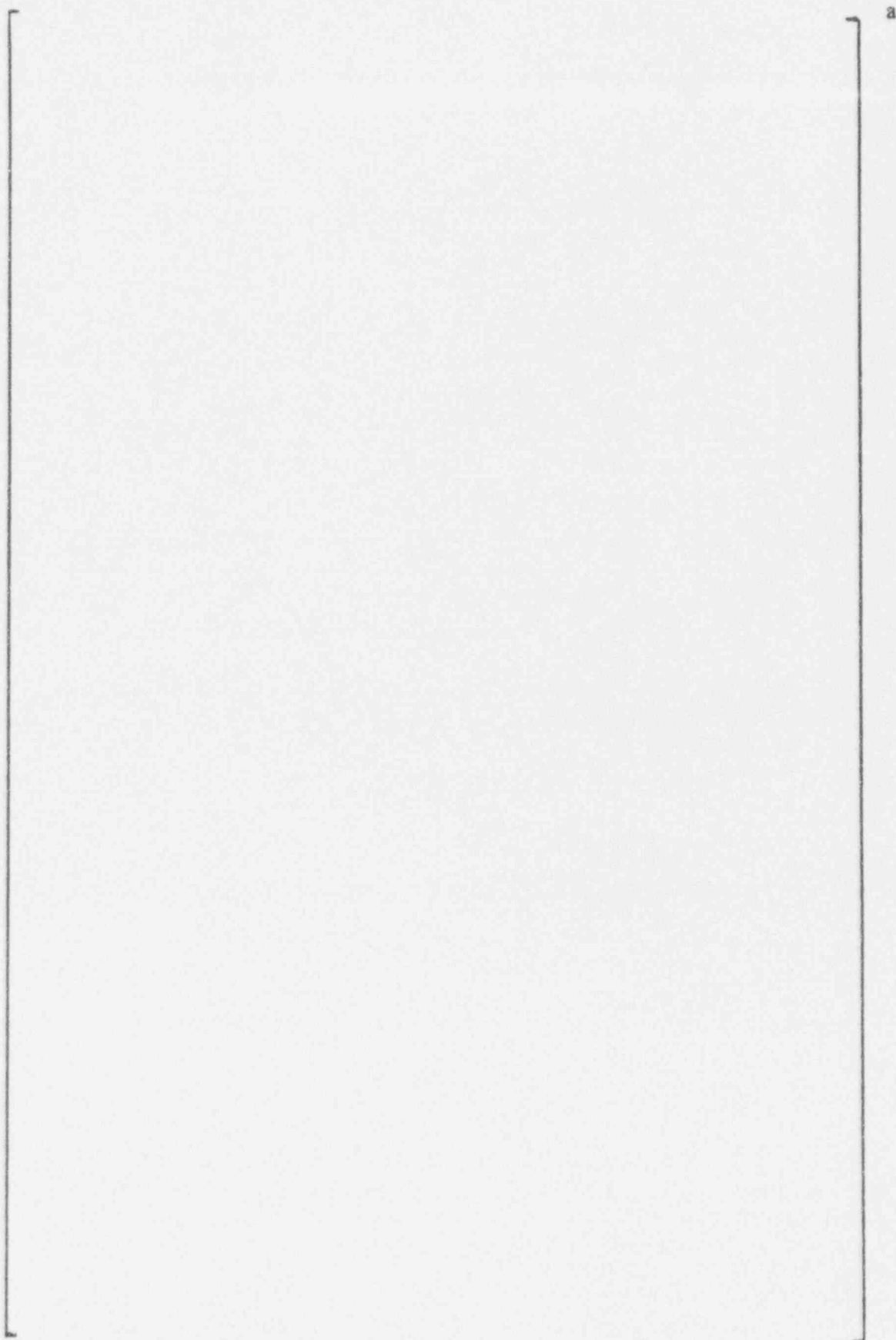


Figure 4-62 Preheater Nodes, and Baffle Identification of Model D4 Steam Generator

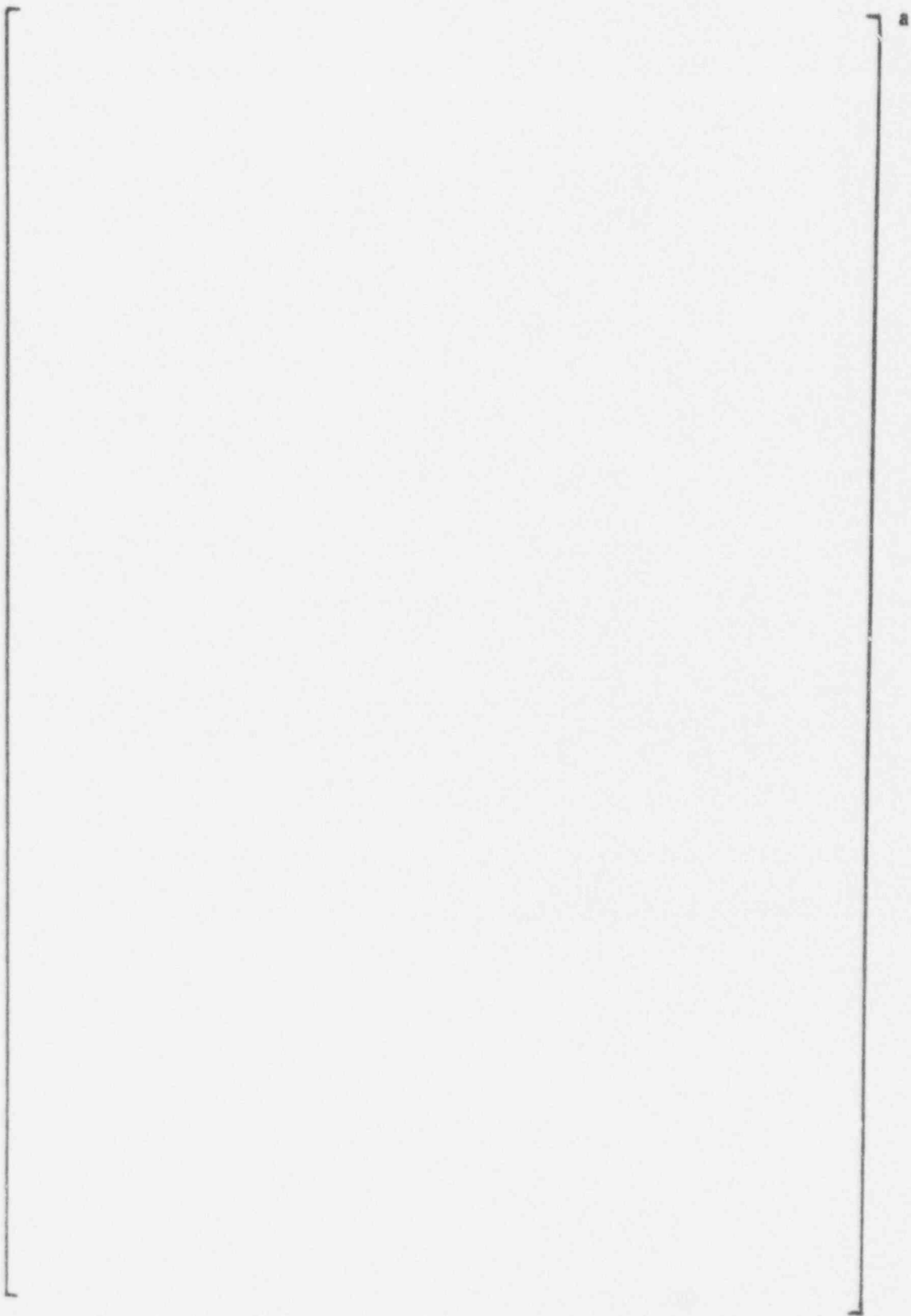


Figure 4-63 Primary Fluid Nodes and Its Flow connectors, Metal Heat Nodes and Its Heat Transfer Connectors, and Secondary Fluid Nodes within Tube Bundle (Model D4)

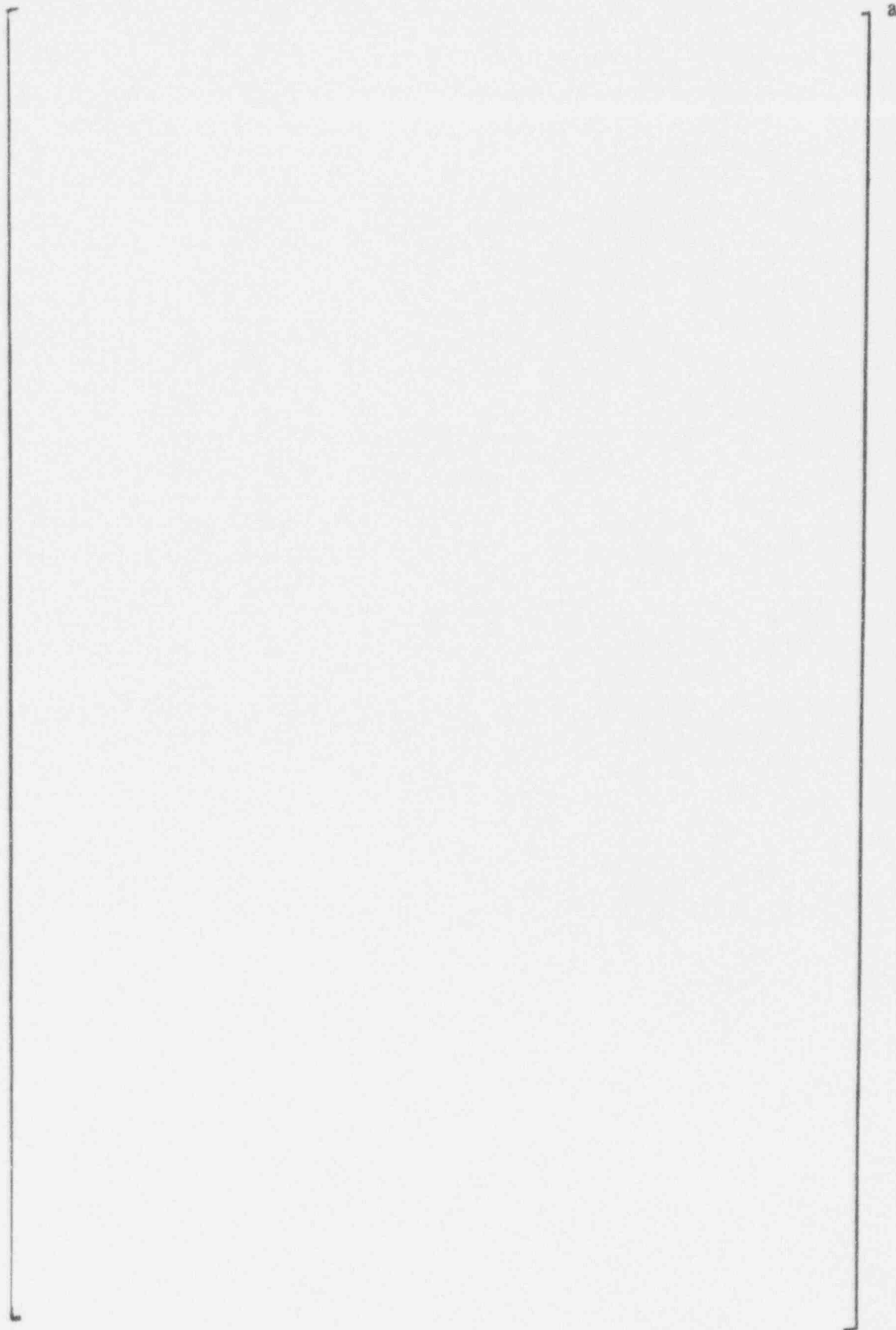


Figure 4-64 Secondary Side Fluid Nodes and Flow Connectors for Model D4 Steam Generator

65

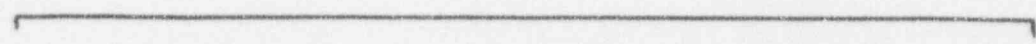


Figure 4-65 Pressure drop through tube support plates P, N, and M

Figure 4-66 Pressure drop through tube support plates L, J, and F

Figure 4-67 Pressure drop through tube support plate, C and A

Figure 4-68 Pressure drop through tube support plates P, N and M

Figure 4-69 Pressure drop through tube support plates L, J and F

Figure 4-70 Pressure drop through tube support plates C and A

Figure 4-71 Relative peak pressure drop across the uppermost TSP as a function of water level; water level ranging from the uppermost TSP (280") to Mid Deck (544"); This is a study for Model D4 SG

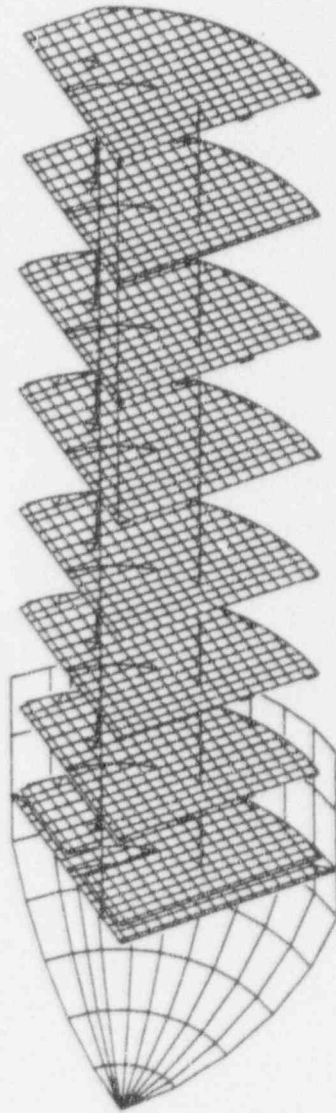
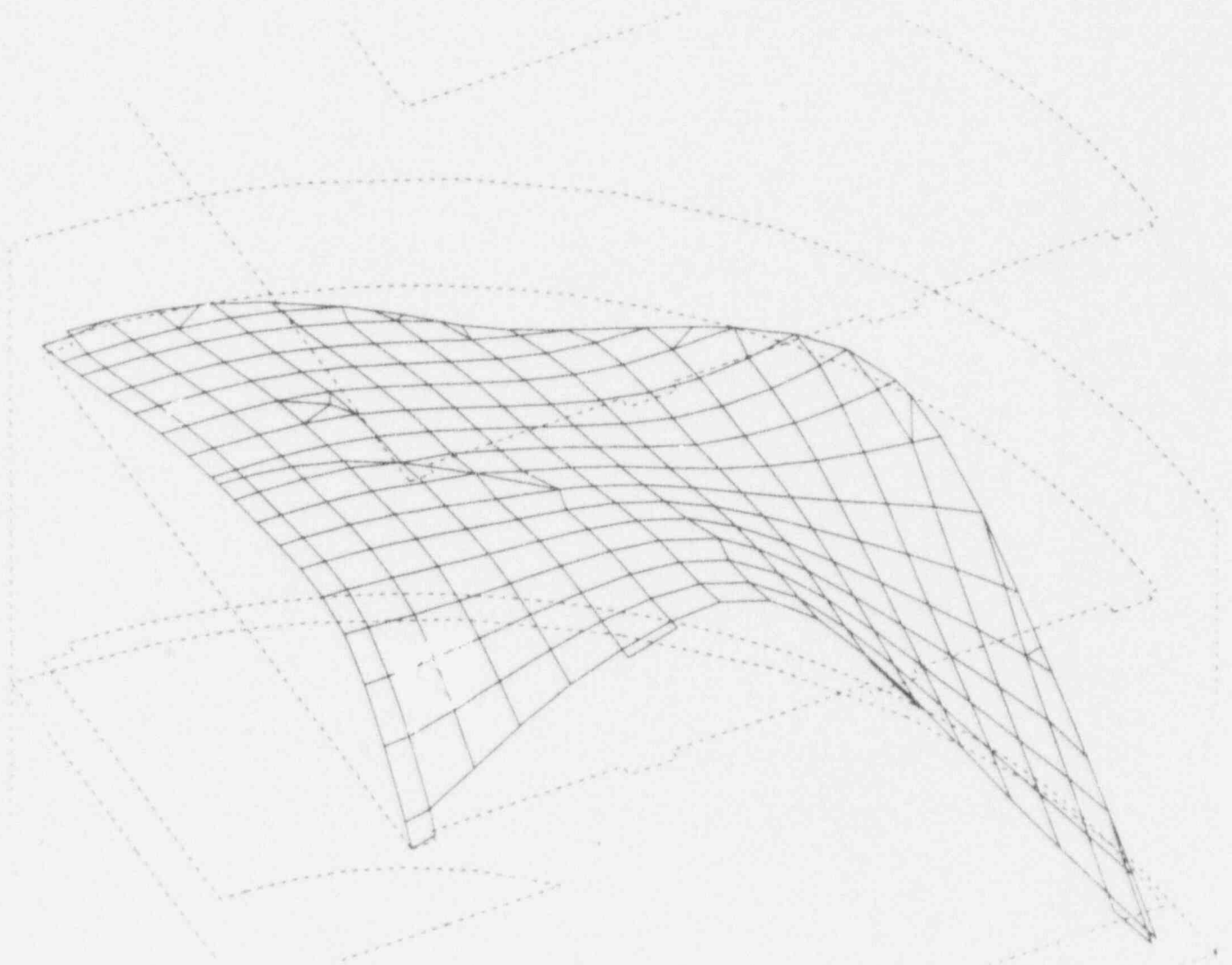


Figure 4-72. Overall Finite Element Model Geometry



**Figure 4-73. Displaced Geometry
Plate C(3H) : Time = 1.9694 sec
SLB Transient From Hot Shutdown**

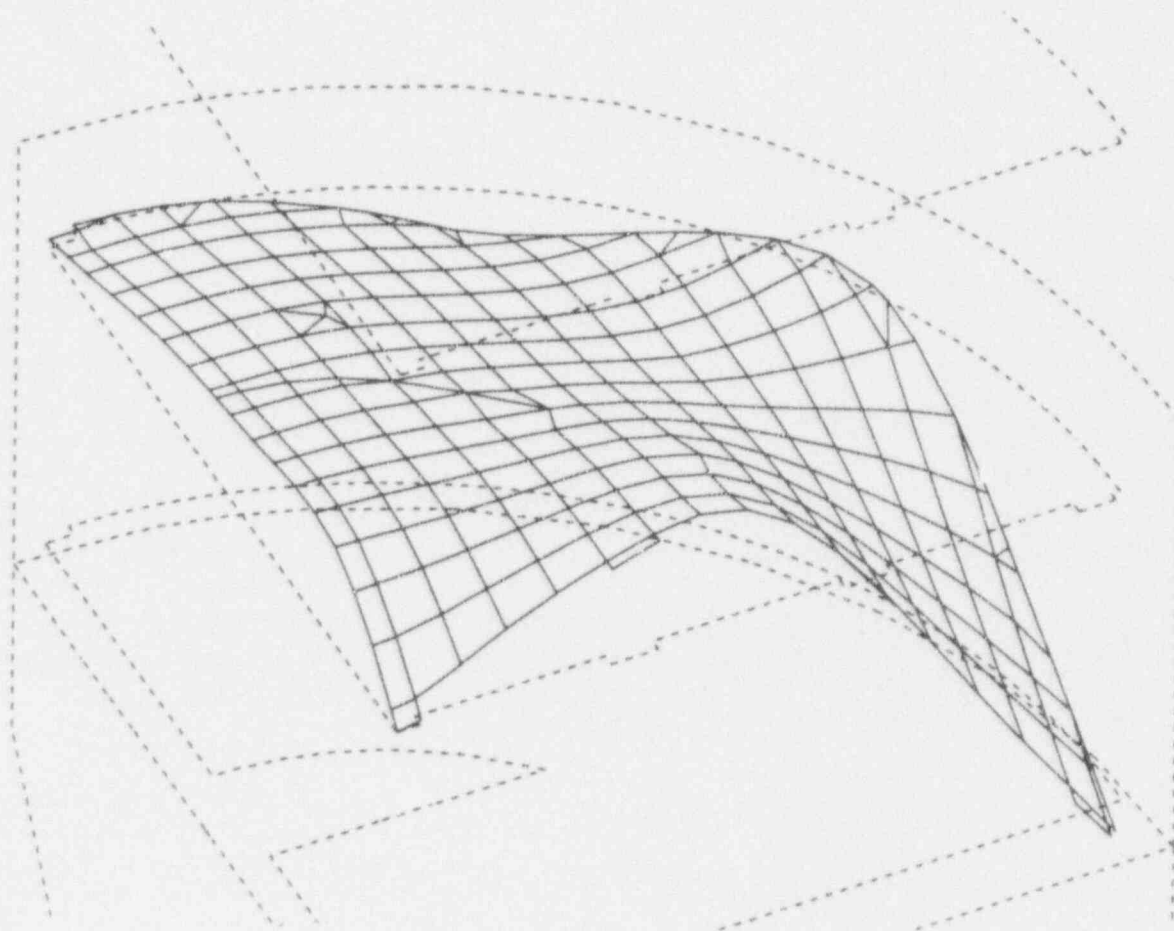


Figure 4-74. Displaced Geometry
Plate C(3H) : Time = 2.6622 sec
SLB Transient from Full Power

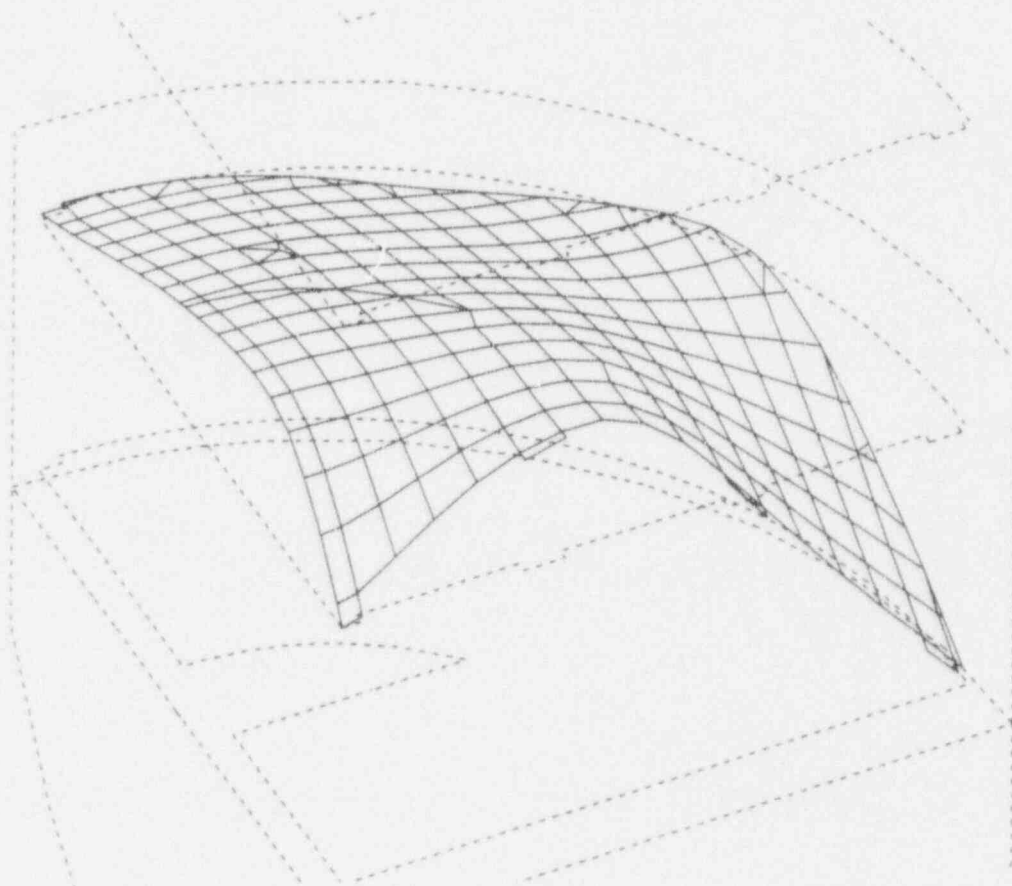


Figure 4-75. Displaced Geometry
Plate C(3H) : Time = 2.7080 sec
SLB Transient from Full Power
Prototypic Void Fraction

Figure 4-76. Relative Tube / Tubesheet Displacement Time History Response
SLB Transient From Hot Standby
Plates A(1H), C(3H), F(5H), J(7H)

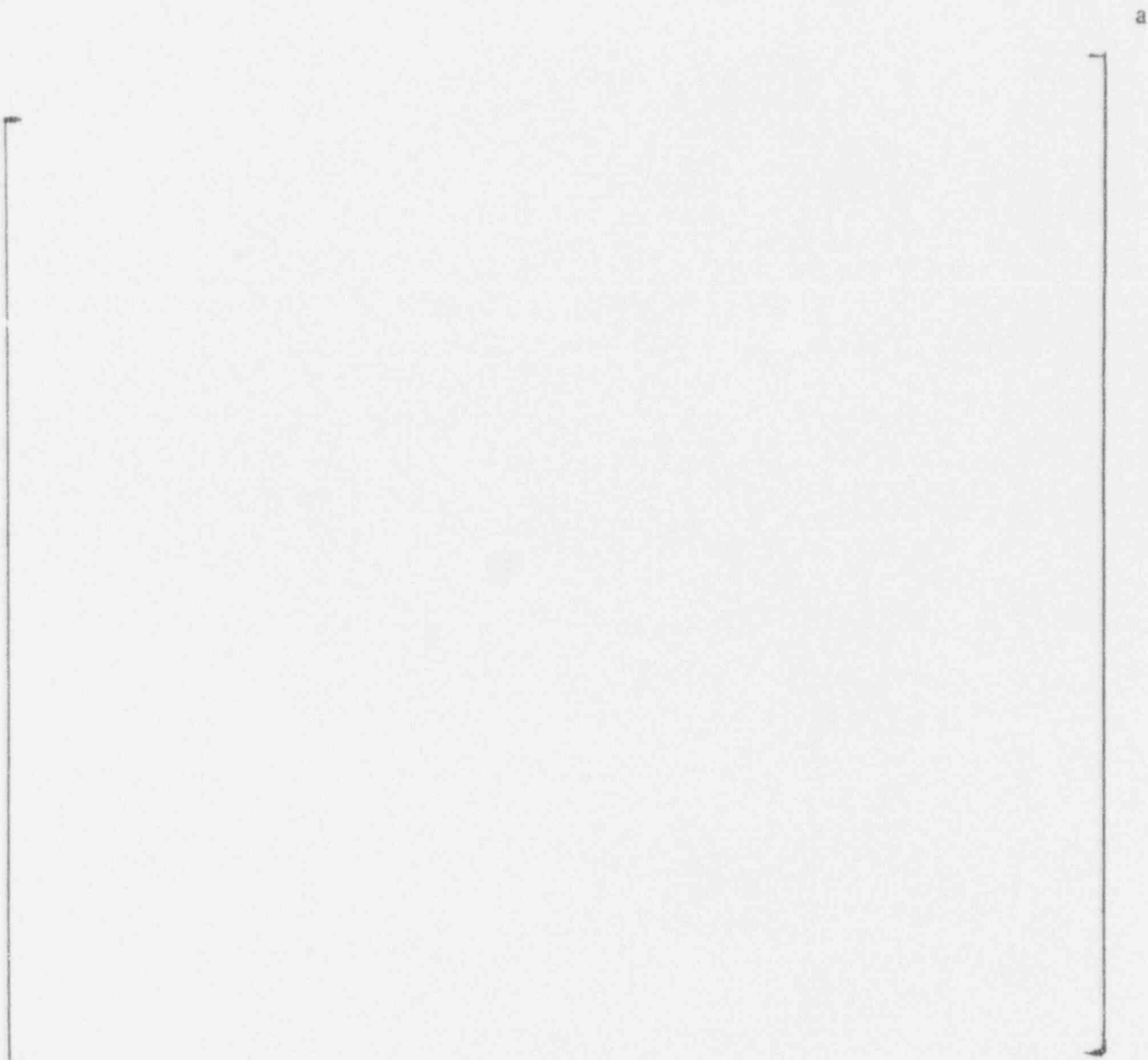


Figure 4-77. Relative Tube / Tubesheet Displacement Time History Response
SLB Transient From Hot Standby
Plates L(8H), M(9H), N(10H), P(11H)




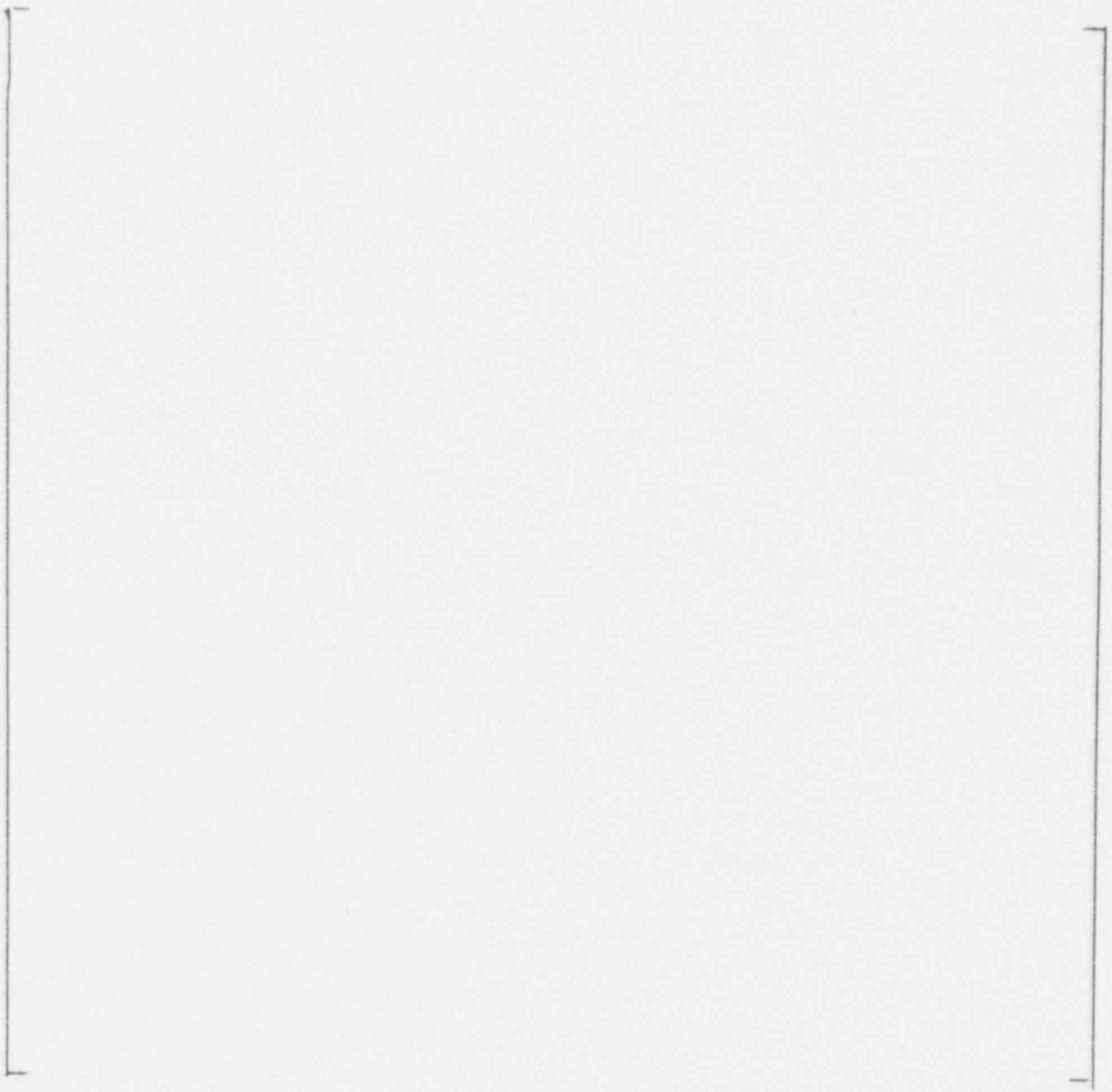
Figure 4-78. Relative Tube / Tubesheet Displacement Time History Response
SLB Transient From Full Power
Plates A(1H), C(3H), F(5H), J(7H)



**Figure 4-79. Relative Tube / Tubesheet Displacement Time History Response
SLB Transient From Full Power
Plates L(8H), M(9H), N(10H), P(11H)**

a

**Figure 4-80. Relative Tube / Tubesheet Displacement Time History Response
SLB Transient From Full Power
Prototypic Void Fraction
Plates A(1H), C(3H), F(5H), J(7H)**



**Figure 4-81. Relative Tube / Tubesheet Displacement Time History Response
SLB Transient From Full Power
Prototypic Void Fraction
Plates L(8H), M(9H), N(10H), P(11H)**

5.0 DATABASE SUPPORTING ALTERNATE REPAIR CRITERIA

This section describes the database supporting the alternate repair criteria (ARC) burst and leak rate correlations. The database for 3/4 inch diameter tubing is described in EPRI Report NP-7480-L, Volume 2 (Reference 5-1). However, at the February 8, 1994 NRC/Industry meeting, the NRC presented resolution of industry comments on draft NUREG-1477. The NRC identified guidelines for application of leak rate versus voltage correlations and for removal of data outliers in the burst and leak rate correlations. This section applies the NRC guidance on removal of outliers to update the database for the 3/4 inch tubing correlations.

5.1 Data Outlier Evaluation

At the February 8 meeting, the NRC provided the following guidance for removal of data outliers:

- Data can be deleted in case of an invalid test.
- Any morphology criteria for deleting outliers must be rigorously defined and applied to all the data.
- Criteria for deleting outliers must be able to be unambiguously applied by an independent observer.
- It is acceptable to modify data or a model in a conservative manner.

Based on the above NRC guidance, the outlier evaluation of Reference 5-1 is updated in this section. Consistent with the NRC guidance, criteria for removal of outliers are defined in this section and applied to the database. These criteria were developed and approved by the EPRI Adhoc Alternate Repair Criteria (ARC) Committee. Consistent with Reference 5-1, only conservative outliers which are high on the burst correlation or low on the leak rate correlation are evaluated for removal from the database. Although the outliers are conservative in this manner, their retention in the database can increase the uncertainties from the regression analyses such that their removal from the database can lead to non-conservatisms in analyses applying uncertainties at upper or lower tolerances.

Criterion 1 for outlier removal applies to invalid data including unacceptable specimens, invalid measurements, etc. To describe the invalid test condition, Criteria 1a to 1e are defined as described in Table 5-1. Table 5-1 provides examples of invalid data that are applicable to the EPRI database.

Criterion 2 for outlier removal applies to specimens with atypical or non-prototypic crack morphology. Criterion 2a applies to specimens with atypical ligament morphology while Criterion 2b applies to severe degradation significantly exceeding the EPRI database. The specific criteria for deleting outliers based on morphology considerations are given in Table 5-2. Table 5-2 also includes the indications excluded from the correlations based on Criterion 2b. No 3/4" indications were removed from the database based on Criterion 2a. Specimen 598-1 is excluded by Criterion 2b. This data point's voltage is more than 40 volts higher than the next largest specimen. There is insufficient data at the high voltage (64.9 volts) to assess the prototypicality of the specimen or applicability to the database. This singular point may unduly influence the correlations without comparable voltage data to define the appropriate trend in the data at these high voltages. Based on destructive examination results providing identification of remaining uncorroded ligaments, the criteria of Table 5-2 can be unambiguously applied by an independent observer and thus satisfies the NRC guidance for removal of data outliers.

Criterion 3 for outlier removal applies to specimens with abnormal leakage behavior due to a suspected test problem. In the performance of leak tests, the crack can become plugged by deposits resulting in abnormally low leak rates or a measurement error could occur. For these cases, the cause for the measurement error is not as apparent as for Category 1 and the test results must be evaluated for apparent errors. It is not appropriate to include the spread in leak rates resulting from plugging of cracks in leak tests in the leak rate correlation and each leak rate measurement should be evaluated against the criteria of this section before including the data in the database. Table 5-3 defines Criterion 3 provides for either SLB leak rates insignificantly greater than normal operating leak rates or for leak rates much lower than expected for the throughwall crack length found by destructive examination as a basis for excluding data from the correlations. Also included in Table 5-3 are the 3/4" tubing specimens excluded from the database by this criterion and the basis for exclusion.

Criterion 3 applies to extreme cases of low leak rate outliers, such as more than a factor of 50 lower than predicted by verified analytical models. In addition, the factor of 50 criterion applies only to specimens which have no remaining uncorroded ligaments within the throughwall length of the crack. The principal effects causing lower than expected variation in leak rates are remaining ligaments in the crack face, tortuosity (oblique steps in the crack, surface irregularities) and presence of deposits. These effects tend to lower leakage for modest throughwall crack lengths. All three effects become smaller as crack length increases and crack opening increases. Longer throughwall cracks tend to have lost the ligaments by corrosion; the wider crack openings reduce the influence of surface irregularities and reduce the potential for deposits plugging the crack. From the database, "long" cracks appear to be about > 0.3 " throughwall as above this length, the variability from predicted leak rates as a function of length appears to be smaller (see Figure 5-1). For 0.3" throughwall cracks, the

crack width is about 1 mil at 2560 psid and increases to about 10 mils for a 0.5" long crack. Thus, crack lengths < 0.3" are more susceptible to plugging from deposits.

From Figure 5-1, it is seen that model boiler specimens 598-3 and 604-2 have very low leak rates for their respective throughwall crack lengths. The remaining data are reasonably clustered with trends similar to that expected as shown for the CRACKFLO analyses in Figure 5-1. There is no indication through spread in the data that other specimens are significantly influenced by probable deposits in the crack face. Criterion 3 has been applied to specimen 598-3 to eliminate this indication from the leak rate correlation, as this specimen is more than a factor of 100 lower than the mean of the other data at about the 0.27" crack length of this specimen. Criterion 3 has not been applied to specimen 604-2, as this specimen is not clearly a factor of 50 less than the mean of the data, although the leak rate is apparently affected by deposits.

Criterion 3 can be unambiguously applied by an independent observer to all measured leak rates given the results from leak rate measurements and/or destructive examinations and thus satisfies the NRC guidance for removal of outliers. This criterion is applied only to low leak rate measurements. For conservatism, high leak rate measurements are not considered for removal from the database.

Based on Criteria 1 to 3 as described in Tables 5-1 to 5-3, the EPRI database of Reference 5-1 was reviewed for identification of data outliers to be removed from the database. Tables 5-4 to 5-6 summarize the data points removed from the database applied to the burst, leak rate and probability of leak correlations, respectively.

Data were removed from the EPRI database in Reference 5-1 based on the same technical considerations, although less formal, as the criteria of Tables 5-1 to 5-3. However, the updated criteria lead to no changes from Reference 5-1. Plant S pulled tube R28C41 was deleted from the database of Reference 5-1 and would also be deleted by the more explicit criteria of this section. However, special considerations have been applied to this indication as described below.

Special Consideration for Plant S Pulled Tube R28C41

Plant S pulled tube R28C41 had leak rates exceeding the initial hot cell leak rate facility capacity at pressure differentials near SLB conditions. Test results are given in Table 5-7. Measured leak rates of 43.4 and 95.1 l/hr at 2335 and 2650 psid, respectively, exceeded facility capacity and are not valid measurements. At 1500 psid, a measured leak rate of 12.3 l/hr was within the facility capability (~ 25 l/hr) and represents a valid measurement. The facility capacity was increased and attempts to reach 2650 psid for a valid leak rate measurement (i.e., without hysteresis effects) were not successful as the leakage exceeded the

new facility capacity. At the first 2650 psi unsuccessful leak test, the cracks were plastically deformed such that succeeding tests below 2650 psi are not directly applicable due to the crack opening or hysteresis effect. As a consequence of not having an acceptable SLB leak rate measurement, this data point was not included in the EPRI leak rate database of Ref. 5-1.

This indication is given special consideration, per NRC request, because of the crack morphology for this indication. The crack face had a 5% ID ligament about 0.31" long separating throughwall cracks in an overall, near throughwall crack length of 0.67" and a total crack length of 0.80". Destructive examination results for the crack length versus depth are given in Table 5-8. The uncorroded ligaments where the crack depth is 95% (Ligaments 1 and 2) include the widest (0.013") ligament and tend to reinforce the remaining 5% wall thickness against tearing. Based on the increase in voltage after the tube pull, it is known that some ligaments were torn as a result of the tube pull. The initial leak rate was measured at 1500 psid. A pressurization to 2650 psi followed, but leak rates were too high to be measured in that facility. Leak rate tests performed in a facility with larger flow capacity can be used to estimate the effective through wall crack length and the leak rate at steam line break conditions. The method applied herein was developed by Paul Hernalsteen of Laborelec. The general methodology is based on the fact that the initial pressurization to 2650 results in a crack opening that has a significant plastic opening component. Subsequent measured leak rates, performed at lower pressure differentials, are affected by the plastic deformation which resulted from the pressurization to 2650 psid.

The evaluations described below are based on crack opening areas calculated by the CRACKFLO Code. SLB leak rates calculated for R28C41 by CRACKFLO are in very good agreement with results obtained by Hernalsteen using the LABOLEAK Code. Differences in crack openings calculated by the two codes are small.

The process used for the evaluation of the test results on the pulled tube included the following steps. These steps are summarized in Table 5-9 and use the test results from Table 5-7. For each step, the plastic and elastic crack opening widths are presented in Table 5-9 along with the crack lengths and leak rate.

1. Figure 5-2 shows CRACKFLO leak rates at the conditions of Test 1. Based on the measured leak rate for this test, 12.3 l/hr, a crack length of 0.38 inches is inferred. This length is greater than the 0.26 inch length of 100% depth (Table 5-8) determined assuming that ligaments 3 and 4 were torn during the tube pull. Thus, tearing of ligaments with modest throughwall crack extension was probable from the tube pulling operations.
2. The pressurization to 2650 psid (Test 3) is assumed to have introduced an irreversible minimum plastic opening in the existing crack. Using CRACKFLO, the plastic opening

area was calculated as a function of crack length. These results are presented in Figure 5-3, along with a curve fit to the calculations. The curve fit was used to develop a modified version of CRACKFLO which maintains the minimum plastic opening resulting from the pressurization to 2650 psid and combines it with an additional elastic opening due to the pressure differential of subsequent tests.

3. Using the modified CRACKFLO code with plastic crack opening at 2650 psid, the leak rate as a function of crack length was determined for the conditions of Test 4, Table 5-7. The results are presented in Figure 5-4. The figure shows that a crack length of 0.42 inch is inferred from the measured leak rate of 79.8 l/hr. Some additional tearing of the ligaments and throughwall crack extension from the 2650 psid pressurization is suggested by the throughwall crack length increase from 0.38 to 0.42 inch between Tests 1 to 3 and Test 4.
4. The modified code, a 0.42 inch crack length and the conditions for Test 6 give a leak rate of 114 l/hr at 1615 psid. This is substantially less than the 448 l/hr measured for this test, suggesting significant tearing of the crack has occurred from thermal cycling and pressurization between Tests 4 and 6.
5. Destructive examination of the tube after a tube burst test indicated a crack length up to 0.67 inches was possible. Using this crack length, a leak rate of 375 l/hr is obtained for the conditions of Test 6. This value is reasonably close to the measured leak rate of 448 l/hr. For this calculation CRACKFLO was used since the plastic opening area, 2.0×10^{-3} inch, was greater than the 1.5×10^{-3} inch calculated to be present after the pressurization to 2650 psid. Thus it is expected that complete tearing of all ligaments and the 5% wall thickness occurred between Tests 4 and 6.
6. Using the desired steam line break conditions (2560 psid and 616 °F primary temperature) for the EPRI database, the as-pulled crack length of 0.38 inch (Step 1) is expected to have torn to 0.42 inch and a leak rate of 111 l/hr is calculated.

The estimated leak rate for Plant S tube R28C41 at SLB conditions (2560 psid) is therefore 111 l/hr. This result is reasonably consistent with Plant S tube R33C20, which was measured in the large capacity facility. Tube R33C20 had a throughwall corrosion length of 0.33", compared to the 0.26" continuous length for R28C41. Both indications likely had ligament tearing and crack extension from tube pulling and pressurization to 2560 psid. The measured leak rate for R33C20 at 2560 psid was 137 l/hr, compared to the estimate of 111 l/hr for R28C41.

Based on similar analyses using a few runs with the LABOLEAK code and analytical ratios of crack areas between 2650 and 1200 psid, Paul Hernalsteen of Laborelec estimated a

R28C41 throughwall crack length of 0.475 inch at 2650 psid and predicted a leak rate of 123 l/hr at 2560 psid. This result is in very good agreement with the CRACKFLO estimate of 111 l/hr.

To bound the CRACKFLO and LABOLEAK analyses, a SLB leak rate of 125 l/hr at 2560 psid is assigned to R28C41 for the EPRI database.

5.2 Database for ARC Correlations

No new data for 3/4 inch diameter tubing has been obtained since the preparation of Reference 5-1. The data of Reference 5-1 are updated for the present application based on the outlier evaluation of Section 5.1 above. Table 5-10 summarizes the data having burst pressure and leak rate tests. Table 5-11 summarizes the data for use in the probability of leak correlation.

5.3 NDE Uncertainties

For IPC applications, NDE uncertainties are required to support projections of EOC voltage distributions, SLB leak rates and SLB tube burst probabilities as discussed in Section 8.0. The database supporting NDE uncertainties is described in Reference 5-1, and NDE uncertainties for IPC/APC applications are given in the EPRI repair criteria report (Reference 5-2). From Reference 5-2, the NDE uncertainties are comprised of uncertainties due to the data acquisition technique, which is based on use of the probe wear standard, and due to analyst interpretation, which is sometimes called the analyst variability uncertainty.

The data acquisition (probe wear) uncertainty has a standard deviation of 7.0% about a mean of zero and has a cutoff at 15%, with implementation of the probe wear standard requiring probe replacement at 15% differences between new and worn probes. ASME standards cross-calibrated against the reference laboratory standard and the probe wear standard were implemented in the Braidwood-1 EOC-4 inspection.

The analyst interpretation (analyst variability) uncertainty has a standard deviation of 10.3% about a mean of zero. Typically, this uncertainty has a cutoff at 20% based on requiring resolution of analyst voltage calls differing by more than 20%. However, as of the February 8, 1994 meeting, the NRC has not accepted the 20% cutoff on the analyst interpretation uncertainty. Pending a further resolution of this issue with the NRC, the analyst interpretation uncertainty was applied for Braidwood-1 without a cutoff. For EOC voltage projections, separate distributions are applied for probe wear with a cutoff at 15% and the analyst interpretation with no cutoff.

5.4 References

- 5-1. "Steam Generator Tubing Outside Diameter Stress Corrosion Cracking at Tube Support Plates - Database for Alternate Repair Criteria, Volume 2: 3/4-Inch Diameter Tubing", NP-7480-L, Volume 2, October 1993.
- 5-2. "PWR Steam Generator Tube Repair Limits - Technical Support Document for Outside Diameter Stress Corrosion Cracking at Tube Support Plates", TR-100407, Revision 1, Draft Report, August 1993.

Table 5-1

Criteria 1a to 1e for Excluding Data from Correlations

Criterion 1a: Unacceptable Bobbin Voltage Measurement

- Excludes specimen from all applications
- Examples: Welded specimen extension influences voltage measurement, specimen damage prior to test completion

Criterion 1b: Unacceptable Burst Test

- Excludes specimen only from burst correlation
- Examples: Incomplete burst test (e.g. leak but not burst), test malfunction, burst inside TSP

Criterion 1c: Unacceptable Leak Test

- Excludes specimen from leak rate correlation and requires prob. of leak evaluation
- Examples: Leak rate exceeded facility capacity, test malfunction

Criterion 1d: Unacceptable Leak Data Due to Tube Pull Damage

- Excludes specimen from leak rate correlation and requires prob. of leak evaluation
- Requires analyses to demonstrate uncorroded ligament would not have torn at accident conditions
- Example ID ligament torn during tube pull as demonstrated by post-pull voltage and higher than expected leak rates at or below normal operating conditions. Structural analysis shows uncorroded ligament would not be expected to tear at accident conditions.

Criterion 1e: Unacceptable Data for Estimating Probability of Leak

- Prob. of leak (yes/no) cannot be confidently estimated from destructive exam crack morphology and leak test not performed
- Examples: Short TW corrosion cracks such as < 0.1 " which normally do not leak at SLB conditions. No destructive exam data available for estimating prob. of leak

Table 5-2

Criteria 2a and 2b for Excluding Data from Correlations

Criterion 2a: Atypical Ligament Morphology

- Cracks having ≤ 2 uncorroded ligaments in shallow cracks $< 60\%$ maximum depth should be excluded from the database as having bobbin voltages significantly higher than the dominant database which shows more uncorroded ligaments in shallow cracks
 - Results in atypical voltages and associated specimens are excluded from all corr.
 - No 3/4" specimens are excluded from the database due to this criterion

Criterion 2b: Severe Degradation

- Exclude data points having bobbin voltages > 20 volts larger than next data point from correlations, as singular data points at the tail of distributions can have undue influence on regression correlation. In this case, there is insufficient data at comparable voltages to assess the prototypicality of the crack morphology and applicability to the database.
 - Results in atypical voltages and associated specimens are excluded from all corr.
 - Excludes 3/4" model boiler specimen 598-1 (64.9 volts) which is > 40 volts larger than the next highest voltage point (22 volts)

Table 5-3

Criterion 3 for Excluding Data from Correlations

Criterion 3: Suspected Test Error

- Data are excluded from only the SLB leak rate versus voltage correlation if either or both of the following criteria are satisfied
- Leak rates at SLB pressure differentials should be at least 10% higher than that measured at normal operating pressure differentials for free span leak tests
 - No 3/4" specimens are excluded from the database for this criterion
- For throughwall cracks with no ligaments, the measured leak rate should be within a factor of less than about 50 of the mean measured leak rate at the associated throughwall crack length
 - For 3/4" tubing, this criterion excludes model boiler specimen 598-3 (0.27" TW, 0.02 l/hr leak rate). The measured leak rate for this specimen with no remaining ligaments is more than a factor of 100 less than the mean measured leak rate for a 0.27" crack length
 - The most limiting specimen compared to this criteria retained in the database is model boiler specimen 604-2 (0.19"TW, 0.05 l/hr), for which the mean measured leak rate is about 0.2 to 0.3 l/hr

Table 5-4

Basis for Excluding Data from the 3/4" Burst Correlation

Tube	TSP	Basis for Excluding Indications from Tube Burst Correlation	Exclusion Category	EPRI* Report Section
Plant E-4				
R19C35	2	Burst inside TSP. Yields much higher burst pressure than free span burst tests of ARC data base.	1b	4.4
R45C54	2	Burst inside TSP	1b	
R47C66	2	Burst inside TSP	1b	
Plant S				
R28C41	1	Incomplete burst test - burst opening length less than macrocrack length (no tearing)	1b	2.5, 4.5
Plant R-1				
R7C71	3	Test recorder malfunction	1b	2.2, 4.3
R5C112	2,3	Incomplete burst test	1b	
R10C6	2,3	Incomplete burst test	1b	
R10C69	2,3	Incomplete burst test	1b	
R20C46	2,3	Incomplete burst test	1b	
R7C47	3	Incomplete burst test	1b	
Model Boiler Specimens				
591-3		Unacceptable specimen preparation due to bobbin voltage influenced by cracks in model boiler Teflon spacer below TSP as well as cracking within TSP. This results in two bands of cracks.	1a	5.6
598-1		Bobbin voltage (64.93 volts) and three large throughwall indications not prototypic of field indications and single data point >20 volts unduly influences burst correlation.	2b	5.6
593-4, 595-4, 596-1, 597-4, 603-4, 604-4		These bobbin NDD specimens all burst at a welded joint made to extend the specimen length for burst testing and are not valid tests. These data have been excluded from the 3/4 inch data base discussed in the EPRI report.	1b	
* EPRI Report NP-7480-L, Vol. 2 (Reference 5-1)				

Table 5-5

Basis for Excluding Data from the 3/4" Leak Rate Correlation

Tube	TSP	Basis for Excluding Indications from Leak Rate Correlation	Exclusion Category	EPRI* Report Section
Plant R-1				
R5C112	3	Max. corrosion depth of 97%. Remaining TW ligament torn during tube pull as indicated by post-pull voltage and leak at 500 psi. Analyses indicate ligament would not have torn at accident conditions.	1d	2.2, 4.3
Plant B-1				
R4C61	5	No leakage identifiable during pressure test above SLB conditions. Test accuracy not sufficient to conclude no leakage.	1e	2.2, 4.3
Model Boiler Specimens				
591-3		Unacceptable specimen preparation due to bobbin voltage influenced by cracks in model boiler Teflon spacer below TSP as well as cracking within TSP. This results in two bands of cracks.	1a	5.6
598-1		Bobbin voltage (64.93 volts) and three large throughwall indications not prototypic of field indications and single data point >20 volts unduly influences correlation.	2b	5.6
598-3		Specimen had no operating leakage and 0.02 l/hr at SLB conditions. Crack was found to be 0.27" TW with no ligaments for which leak rate of 5 to 20 l/hr would be expected, based on the mean of the measured data. It is concluded that crack became plugged by deposits or a measurement error was made.	3	
* EPRI Report NP-7480-L, Vol. 2 (Reference 5-1)				

Table 5-6

Basis for Excluding Data from the 3/4" Prob. of Leak Correlation

Tube	TSP	Basis for Excluding Indications from Prob. of Leak Correlation	Exclusion Category	EPRI* Report Section
Plant R-1				
R7C47	2	No destructive exam data or burst test to estimate probability of leakage.	1e	4.3
R5C112	3	Max. corrosion depth of 97%. Remaining TW ligament torn during tube pull as indicated by post-pull voltage and leak at 500 psi. Analyses indicate ligament would not have torn at accident conditions.	1d	2.2, 4.3
Plant B-1				
R4C61	5	No leakage identifiable during pressure test above SLB conditions. Test accuracy not sufficient to conclude no leakage.	1e	2.2, 4.3
Model Boiler Specimens				
591-3		Unacceptable specimen preparation due to bobbin voltage influenced by cracks in model boiler Teflon spacer below TSP as well as cracking within TSP. This results in two bands of cracks.	1a	5.6
598-1		Bobbin voltage (64.93 volts) and three large throughwall indications not prototypic of field indications and single data point >20 volts unduly influences correlation.	2b	5.6
* EPRI Report NP-7480-L, Vol. 2 (Reference 5-1)				

Table 5-7
Plant S R28C41 Leak Rate Tests

<u>Test</u>	<u>Primary Conditions</u> <u>Temperature</u> (°F)	<u>Pressure</u> (psia)	<u>Differential</u> <u>Pressure</u> (psid)	<u>Secondary</u> <u>Pressure</u> (psia)	<u>Leak Rate</u> (l/hr)
<u>Initial Series</u>					
1	612	2000	1500	500	12.3
2		2650	2335	315	> 43 *
3		2850	2650	200	> 96 *
<u>Second Series</u>					
4	550	1930	1200	730	78.9
5	560	2375	1535	840	321
6	580	2550	1615	935	448
7	550	2500	1375	1125	478 **

* Leak rate exceeded facility capacity.

** Note increase in leak rate at low pressure differential which indicates additional deformation of crack opening.

Table 5-8

Plant S SG Tube Macrocrack Profile for R28C41

<u>Tube, Location</u>	<u>Length vs. Depth</u> <u>(inch/% throughwall)</u>	<u>Ductile Ligament</u> <u>Location</u>
R28C41, FDB	0.00 / 0	
	0.07 / 100	
	0.13 / 100	
	0.19 / 95 ←	Ligament 1, 0.013" wide
	0.25 / 95	
	0.32 / 95 ←	Ligament 2, 0.004" wide
	0.38 / 95	
	0.44 / 100	
	0.52 / 100 ←	Ligament 3, 0.007" wide
	0.60 / 100	
	0.70 / 100 ←	Ligament 4, 0.008" wide
	0.75 / 70	
	0.80 / 0	

Table 5-9
Evaluation Summary, R28C41 Tube Leak Rate Tests

<u>Case</u>	<u>Crack Opening</u> <u>Plastic</u> <u>Elastic</u> (x 10 ⁻³ in)		<u>Crack</u> <u>Length</u> (in.)	<u>Leak Rate</u> (l/hr)
Before Pressurizing to 2650 psi ΔP				
<u>Step 1</u>				
Crack Length inferred from measured leak rate at ΔP=1500 psi	0.12	0.65	0.38	12.3*
After Pressurizing to 2650 psi ΔP				
<u>Step 3</u>				
Crack Length inferred from measured leak rate at ΔP=1200 psi and 550 °F	1.5	0.65	0.42	79.8*
<u>Step 4</u>				
Leak rate for a crack length of 0.42" at ΔP=1615 psi & 580 °F	1.5	0.86	0.42	114
		Measured leak rate		448*
<u>Step 5</u>				
Crack Length = 0.67 in. at ΔP=1615 psi & 580°F assumed	2.0	2.6	0.67	375
Calculated Leak Rate at 2560 psi ΔP (Step 3 length of 0.42")				
<u>Step 6</u>				
Leak rate for a crack length of 0.42" at ΔP=2560 psi & 616 °F	1.4	1.4	0.42	111

* Measured leak rates - see Table 5-7

Table 5-10

Burst Pressure and Leak Rate Data Base for 3/4 Inch Tubing

Plant	Row/Col or Specimen No.	TSP	Bobbin Volts	Bobbin Depth	RPC Volts	Destructive Exam Max. Depth	Length (1)	SLB Leak (2) Rate (l/hr) 2560 psid	Adjusted Burst (3) Pressure (ksi)	Correlation (4) Application Leak Rate	Burst
-------	----------------------------	-----	-----------------	-----------------	--------------	-----------------------------------	------------	--	--	--	-------

e

Table 5-10

(continued)

Burst Pressure and Leak Rate Data Base for 3/4 Inch Tubing

Plant	Row/Col or Specimen No.	TSP	Bobbin Volts	Bobbin Depth	RPC Volts	Destructive Exam Max. Depth	Length (1)	SLB Leak (2) Rate (l/hr) 2560 psid	Adjusted Burst (3) Pressure (ksi)	Correlation (4) Application Leak Rate	Burst
-------	----------------------------	-----	-----------------	-----------------	--------------	-----------------------------------	------------	--	--	--	-------

e

Table 5-10
(continued)

Burst Pressure and Leak Rate Data Base for 3/4 Inch Tubing

Plant	Row/Col or Specimen No.	TSP	Bobbin Volts	Bobbin Depth	RPC Volts	Destructive Exam Max. Depth	Length (1)	SLB Leak (2) Rate (l/hr) 2560 psid	Adjusted Burst (3) Pressure (ksi)	Correlation (4) Application Leak Rate	Burst
-------	----------------------------	-----	-----------------	-----------------	--------------	-----------------------------------	------------	--	--	--	-------

e

Table 5-11: Database for Probability of Leak for 3/4" Diameter Tubes					
Plant or Model Boiler Sample Number	Bobbin Amplitude (V)	Probability of Leak	Plant or Model Boiler Sample Number	Bobbin Amplitude (V)	Probability of Leak

e

Figure 5-1
Comparison of 3/4" Leak Test Data with CRACKFLO Predictions

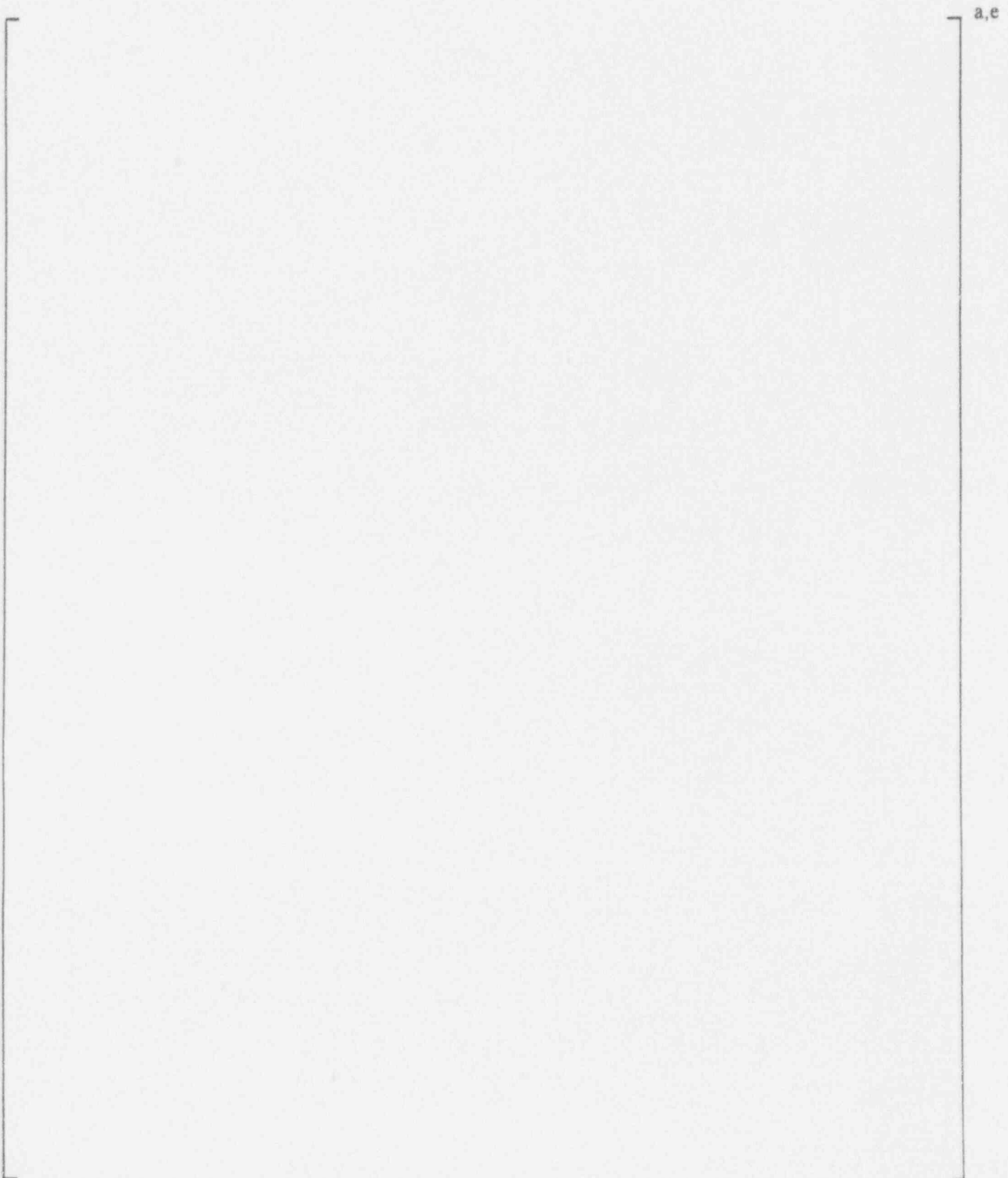


Figure 5-2

**As Pulled Tube Leak Rate
1500 psi Pressure Drop**

a,e

Figure 5-3

**Plastic Correction Area
2650 psi Pressure Difference**

a,e

Figure 5-4

Modified Code Leak Rate
1200 psi Pressure Drop

a,e

6.0 BURST AND SLB LEAK RATE CORRELATIONS

6.1 EPRI ARC Correlations

As part of the development of alternate repair criteria (ARC), correlations have been developed for tubes containing ODSCC indications at TSP locations between the bobbin amplitude, expressed in volts, of those indications and the free-span burst pressure, the probability of leak, and the free-span leak rate for indications that leak, References 6.1 and 6.2. The database used for the development of the correlations is presented and discussed in Reference 6.2. Guidelines for the identification and exclusion of inappropriate data, termed *outliers*, are provided in Reference 6.3. In addition to the aforementioned, an empirical correlation curve for the burst pressure as a function of crack length has been developed for tubes with free-span, through-wall, axial cracks. In 1993, the NRC issued draft NUREG-1477, Reference 6.4, for public comment. The draft NUREG delineated a set of guidelines for criteria to be met for the application of Interim Plugging Criteria (IPC) for ODSCC indications. The criteria guidelines permitted the use of, with adequate justification, a burst pressure to bobbin amplitude correlation and a probability of leak to bobbin amplitude correlation. The criteria guidelines did not permit the use of a leak rate to bobbin amplitude correlation for the estimation of end of cycle (EOC) total leak rates. In essence, References 6.1 and 6.2 provided comments on the Reference 6.4 guidelines. Reference 6.5 provided an NRC response and position relative to resolving the differences between References 6.1 & 6.2 and Reference 6.4, along with responses to other public comments. Of significance to this report, is that Reference 6.5 indicated that a correlation between leak rate and bobbin amplitude could be employed if the correlation could be statistically justified at a 95% confidence level, and provided direction for the development of guidelines, e.g., Reference 6.3, that could then be employed for the identification and exclusion of outlying experimental data. Subsequent discussions with NRC personnel have revealed potential issues associated with the manner in which the leak rate to bobbin amplitude correlation is used, thus, the potential leak rate during a postulated steam line break (SLB) is herein estimated by alternate Monte Carlo and deterministic methods to demonstrate that either method yields acceptable results.

The purpose of this section is to provide information and justification for all of the correlations developed in support of the application of an IPC for the Braidwood 1 nuclear power plant. Information is first presented relative to the correlation of burst pressure to bobbin amplitude and to through-wall crack length, followed by a discussion of the correlation between the probability of leak and the bobbin amplitude, and lastly a discussion of the correlation of leak rate to bobbin amplitude. The use of each of the correlations is also documented.

6.2 Burst Pressure versus Bobbin Voltage Correlation

The bobbin coil voltage amplitude and burst pressure data presented in the EPRI database report for 3/4" tubes, Reference 6.2, were used to estimate the degree of correlation between the burst pressure and bobbin voltage amplitude. The details of performing the correlation analysis, and subsequent regression analysis to estimate the parameters of a log-linear relationship between the burst pressure and the bobbin amplitude, are provided in the EPRI database report. The evaluations examined the scale factors for the coordinate system to be employed, the detection and treatment of outliers, the order of the regression equation, the potential for measurement errors in the variables, and the evaluation of the residuals following the development of a relation by least squares regression analysis. The results of the analyses indicated that an optimum linear, first order relation could be obtained from the regression of the burst pressure on the common logarithm (base 10) of the bobbin amplitude voltage.

A linear, first order equation relating the burst pressure to the logarithm of the bobbin amplitude was developed. Examination of the residuals from the regression analysis indicated that they are normally distributed, thus verifying the assumption of normality inherent in the use of least squares regression. The regression curve (line) is given by

$$\begin{aligned} P_{B_i} &= a_0 + a_1 \log(V_i) \\ &= 7.822 - 3.077 \log(V_i), \end{aligned} \tag{6.1}$$

where the burst pressure is measured in *ksi* and the bobbin amplitude is in *volts*. The *index of determination* for the regression was 80.7%, thus the correlation coefficient is 0.90, which is significant at a >99.999% level. This means that the *p-value* for the slope of the line is < 0.001%. The estimated standard deviation of the residuals, i.e., the error of the estimate, s_p , of the burst pressure was 0.95 *ksi*. A summary of the results from the regression analysis is provided in Table 6-1.

The data base and the regression curve are illustrated on Figure 6-1. Using the regression relationship, a lower 95% prediction bound for the burst pressure as a function of bobbin amplitude was developed. These values were further reduced to account for the lower 95%/95% tolerance bound for the Westinghouse data base of tubing material properties at 650°F. Both of these are also depicted on Figure 6-1. Using this reduced lower prediction bound, the bobbin amplitude corresponding to a *free-span* burst pressure of 3657 psi was found to be 4.54 V. The value of 3657 psi results from considering a SLB differential pressure of 2560 psi divided by 0.7 in accord with the guidelines of RG 1.121, Reference 6.6.

6.3 Burst Pressure versus Through-Wall Crack Length Correlation

For a tube with a mean radius of r_m and a thickness t , the normalized burst pressure as a function of the actual burst pressure, P_B , is given by

$$P_{bar} = \frac{P_B r_m}{(S_Y + S_U) t} \quad (6.2)$$

Thus, P_{bar} is the ratio of the maximum Tresca stress intensity, taking the average compressive stress in the tube to be $P_B/2$, to twice the flow strength of the material. The normalizing parameter for crack length, a , is given by

$$\lambda = \frac{a}{\sqrt{r_m t}}, \quad (6.3)$$

a form which arises in the theoretical solutions. The burst pressure as a function of axial crack length for a specific tube size is then easily obtained from the non-dimensionalized relationship.

Examination of the normalized burst pressure data indicated that a variety of functional forms would result in similar fit characteristics. An exponential function, i.e.,

$$P_{bar} = b_0 + b_1 e^{-\frac{\lambda}{b_2}}, \quad (6.4)$$

was finally selected based on the combination of maximizing the goodness of fit, and minimizing the number of coefficients in the function. Equation (6.4) was also found to be advantageous in that it can easily be inverted to yield λ as a function of P_{bar} . For the data analyzed, the coefficients of equation (6.4) were found to be

$$P_{bar} = 0.0615 + 0.534 e^{-\frac{\lambda}{3.611}} \quad (6.5)$$

The index of determination for the fit was 98.3%, with a standard error of the estimate of 0.015. The F distribution statistic for the regression, the ratio of the mean square due to the regression to the mean square due to the residuals, was 4625. Thus, the fit of the equation to the data is excellent. Note that this does not mean that equation (6.4) is the true form of a

functional relationship between the two variables, only that it provides an excellent description of the relationship. Equation (6.4) was then rearranged to yield the inverse relation

$$\lambda = -3.611 \ln \left(\frac{P_{bar} - 0.0615}{0.534} \right), \quad (6.6)$$

for the normalized crack length as a function of normalized burst pressure.

In order to present the results in a form directly applicable to the Braidwood 1 tubes, the normalized relationships were converted for 0.750" diameter by 0.043" thick tubes having a flow stress of 71.6 ksi, the average of the Westinghouse database. The converted data base, the regression curve, and the regression curve adjusted for lower 95%/95% tolerance limit material properties are shown on Figure 6-2.

Using the regression results, the probability of burst during SLB was estimated as a function of crack length. The mean estimate of the burst pressure is given by the regression equation as

$$P_B = \frac{P_{bar} t}{R_m} (S_Y + S_U). \quad (6.7)$$

An unbiased estimate of the variance of P_B which accounts for the variation in P_{bar} about the regression curve and the variation in $S_Y + S_U$ can be calculated as

$$V(P_B) = \left(\frac{2t}{R_m} \right) \left[P_{bar}^2 V(S_f) + \bar{S}_f^2 V(P_{bar}) - V(P_{bar}) V(S_f) \right], \quad (6.8)$$

where V is used to represent an unbiased estimate of the variance of the respective term in parentheses, and S_f , the flow stress for Alloy 600 material, is one-half of the sum of the yield and ultimate strengths. Taking the standard deviation of the burst pressure as the square root of the estimated variance allows for the estimation of the probability of burst using a Student's t -distribution. Specifically, the difference between the estimated burst pressure for a given crack length, a , and the SLB pressure is divided by the estimated standard deviation of the burst pressure to obtain a t -deviate. The probability of occurrence of the value of t is then an estimate of the probability of burst for that crack length during a SLB. The number of degrees of freedom used in estimating the probability of occurrence of a t -deviate greater than t is conservatively taken as the lesser of the number of degrees of freedom of P_{bar} or S_f . An alternate estimate of the probability of burst can be obtained by simulating P_{bar} and S_f independently. In this case, a large number of values of P_{bar} and S_f are independently

calculated using randomly generated independent t -variates and the respective estimated standard deviations of P_{bur} about the regression curve and S_y about the mean of the database. These are then combined using equation (6.7) to obtain a burst pressure for a single simulation. The number of occurrences of the calculated burst pressure being less than the SLB pressure is then an estimate of the probability of burst. Based on the specific simulation results, an upper bound for the estimate of the probability of burst may then be made using non-parametric methods. The results of the calculational and the Monte Carlo simulation determinations are depicted on Figure 6-3. Also shown are the 99% upper confidence bounds for the Monte Carlo estimated values. The calculational procedure is seen to lead to a conservative estimate of the probability of burst for a given crack length. An examination of the distribution of the burst pressures from the Monte Carlo simulations reveals that is skewed right. Thus, the tail of the distribution is shorter for the lower burst pressures, hence the lower probabilities of burst.

6.4 NRC Draft NUREG-1477 SLB Leak Rate POD and Uncertainty Methodology

The NRC methodology of draft NUREG-1477 obtains the number of indications that are to be considered as being returned to service, N , as:

$$N = N_d + N_{nd} - N_r = N_d + \frac{1 - \text{POD}}{\text{POD}} N_d - N_r = \frac{N_d}{\text{POD}} - N_r, \quad (6.9)$$

where, N_d = number of detected bobbin indications
 N_r = number of repaired indications
 N_{nd} = number of indications not detected by the bobbin inspection
 POD = probability of detection (0.6 for NRC methodology).

The above adjustments for POD have been incorporated in the BOC and EOC voltage distributions so that no further adjustments are required for the leakage calculation. Section 3.3 of draft NUREG-1477 states that the total leak rate, T , should be determined as:

$$T = \mu P + Z \sqrt{\sigma^2 P + \mu^2 P - \sum_i (N_i P_i^2)}, \quad (6.10)$$

where, μ = mean of the leak rate data independent of voltage
 σ = standard deviation of the leak rate data independent of voltage
 P_i = probability that a tube leaks for the i^{th} voltage bin
 N_i = number of indications (after POD adjustment) in the i^{th} voltage bin
 $P = \sum_i (N_i P_i)$ = expected number of indications that leak summed over all voltage bins
 Z = standard normal distribution deviate (establishes level of confidence on leakage).

For the total leakage, the first term of the above equation represents a mean expected leak rate while the square root term is an effective standard deviation for the total leakage based on the variance of the product of the probability of leak and the predicted leak rate. Draft NUREG-1477 recommends that Z be applied as 2, which corresponds to a level of confidence of 98%, while Reference 6.5 indicates that Z may be taken as 1.645, corresponding to a confidence level of 95%.

6.5 Probability of Leakage Correlations

Historically, the probability of leakage has been evaluated by segregating the model boiler and field data into two categories, i.e., specimens that would not leak during a SLB and those that would leak during a SLB. These data were analyzed to fit a sigmoid type equation to establish an algebraic relationship between the bobbin amplitude and the probability of leak. The specific algebraic form used to date has been the logistic function with the common logarithm of the bobbin amplitude employed as the regressor variable, i.e., letting P be the probability of leak, and considering a logarithmic scale for volts, V , the logistic expression is:

$$P(\text{leak} | V) = \frac{1}{1 + e^{-[\beta_1 + \beta_2 \log(V)]}} \quad (6.11)$$

This is then rearranged as:

$$\ln\left(\frac{P}{1-P}\right) = \beta_1 + \beta_2 \log(V), \quad (6.12)$$

to permit an iterative, linear, least squares regression to be performed to find the maximum likelihood estimators, b_1 and b_2 , of the coefficients, β_1 and β_2 .

Reviews of those evaluations, e.g., NUREG-1477, have resulted in the NRC requesting that alternate sigmoid function forms be investigated, and that the evaluations also consider the potential dependence to be on the bobbin amplitude instead of the logarithm of the bobbin amplitude. NUREG-1477 specifically mentions that the cumulative normal, or Gaussian, distribution function and the Cauchy distribution function be investigated. Discussions with NRC personnel led to the stipulation that these functions be analyzed and used in predicting the end-of-cycle leak rate for the Braidwood 1 plant steam generator tube indications. Reference 6.7 has acknowledged that any non-conservatism associated with the exclusive use of the log-logistic function would be expected to be small in comparison to the conservatism inherent in the methodology used to estimate the radiological consequences of leakage associated with a postulated SLB. On this basis, the evaluation and results presented herein for alternative function forms is considered to be for information only.

The use of the logistic function for the analysis of dichotomous data is standard in many fields. The differential form assumes that the rate of change of the probability of leak is proportional to the product of the probability of leak and the probability of no leak. As noted, the function is sigmoidal in shape, and is similar to the cumulative normal function, and likewise similar to using a probit model (which is a normal function with the deviate axis shifted to avoid dealing with negative values). In principle, any distribution function that has a cumulative area of unity could be fit as the distribution function, a limitless number of possibilities. Trying to identify a latent, or physically based, distribution for the probability of leak would be considered to be unrealistic and unnecessary. For most purposes the logistic and normal functions will agree closely over the mid-range of the data being fitted. The tails of the distributions do not agree as well, with the normal function approaching the limiting probabilities of 0 and 1 more rapidly than the logistic function. Thus, relative to the use of the normal distribution, the use of the logistic function is conservative. Given its wide acceptance in multiple fields it was judged that the logistic function would be suitable for use in determining a probability of leak as a function of voltage.

In addition, consideration was given as to whether the bobbin amplitude or the logarithm of the bobbin amplitude should be used. Since the logistic, normal and Cauchy distribution functions are unbounded, the use of volts would result in a finite probability of leak from non-degraded tubes, and would be zero only for $V=-\infty$. By contrast, the use of the logarithm of the voltage results in a probability of leak for non-degraded tubes of zero. Clearly, the second situation is more realistic than the first, especially in light of the fact that a voltage threshold is a likely possibility. To comply with the NRC request, however, each distribution function was fitted to the data using the logarithm of the bobbin amplitude and the bobbin amplitude as the regressor.

The three functions to be evaluated fall into a category of models referred to as *Generalized Linear Models* (GLMs). This simply means that the models can be transformed into a linear form, e.g., equation (6.12). The left side of equation (6.12) is referred to as the link function for the logistic model. For the normal or cumulative Gaussian distribution function, the model to be fitted is:

$$P(leak) = \frac{1}{\sqrt{2\pi}} \int_{-\infty}^{\beta_1 + \beta_2 \log(V)} e^{-\frac{z^2}{2}} dz, \quad (6.13)$$

and the model to be fitted for the Cauchy distribution function is:

$$P(leak) = \frac{1}{2} + \frac{1}{\pi} \tan^{-1}[\beta_1 + \beta_2 \log(V)]. \quad (6.14)$$

The link function for the Gaussian function is:

$$\eta = \Phi^{-1}(P) = \beta_1 + \beta_2 \log(V), \quad (6.15)$$

while the link function for the Cauchy function is:

$$\eta = \tan \left[\pi \left(P - \frac{1}{2} \right) \right] = \beta_1 + \beta_2 \log(V). \quad (6.16)$$

To fit the equation forms to the bobbin amplitude rather than log of the amplitude, V is substituted for $\log(V)$. Each equation was fitted to the data using an iterative least squares technique, which results in the maximum likelihood estimates of the parameters.

The results of all of the regression analyses are summarized in Table 6-2. The coefficients of the equations are provided along with the elements of the variance-covariance matrix for the coefficients. In addition, the deviance for each solution is also given. One accepted measure of the goodness of the solution or fit for GLMs is the deviance, given by,

$$D = 2 \sum_{i=1}^n \left\{ P_i \ln \left[\frac{P_i}{P(V_i)} \right] + (1 - P_i) \ln \left[\frac{1 - P_i}{1 - P(V_i)} \right] \right\} \quad (6.17)$$

where P_i is the probability associated with data pair i and $P(V_i)$ is the calculated probability from V_i . The deviance is used similar to the residual sum of squares in linear regression analysis and is equal to the error, or residual, sum of squares (SSE) for linear regression. For the probability of leak evaluation P_i is either zero or one, so Equation (6.17) may be written

$$D = -2 \sum_{i=1}^n \left\{ P_i \ln[P(v_i)] + (1 - P_i) \ln[1 - P(v_i)] \right\}. \quad (6.18)$$

Since the deviance is similar to the SSE, lower values indicate a better fit, i.e., the lower the residual sum of squares the more of the variation of the data is considered to be explained by the regression equation. The smallest deviances, 28.9, were obtained from the logistic and normal function fits. The deviances for the remaining four functions ranged from 32.5 to 33.8, about 12% to 17% higher than for the first two functions. For similar calculations performed using 7/8" tube data, the deviances obtained using either of the Cauchy forms were about 15% to 20% higher than for the other four functions. These differences are not considered to be numerically significant in themselves relative to selecting the best form of a fitting function.

The results of fitting each of the equations are depicted on Figures 6-4 and 6-5. A comparison of the results shown on Figure 6-4 with those shown on Figure 6-5 indicates that the use of the logarithm of the volts results in a spreading of the functions with the probability of leak at, say, 3 volts being higher for the logarithmic forms. In the very low voltage range, less than 1 volt, the probability of leak is lower for the logarithmic forms. This is because the tails must extend to $-\infty$. In general, the Cauchy cumulative distribution function has longer tails than either the logistic or normal functions. It also rises much more sharply in the middle of the data range. The regression results on Figure 6-2 illustrate the non-realistic nature of the Cauchy fit for the non-logarithmic form, in spite of its similar deviance value. Examination of the figures indicates that the Cauchy distribution is significantly less representative of the data in the regions where the no-leak and leak test data overlap.

A listing of probability of leak results for selected volts is provided in Table 6-3. Up to a bobbin amplitude of 1 volt, predictions based on the log-normal function are less than predictions based on the log-logistic function. For very high voltages the Cauchy distribution forms rise to a probability of leak of one slower than the other distribution functions.

Taken in conjunction with the leak rate versus voltage correlation, the choice of a probability of leak function is relatively moot. The final total leak rate values tend to differ by only a few percent across the spectrum of POL functions.

6.6 SLB Leak Rate Versus Voltage Correlation for 3/4" Tubes

The bobbin coil and leakage data previously reported were used to determine a correlation function between the SLB leak rate and the bobbin amplitude voltage. Since the bobbin amplitude and the leak rate would be expected to be functions of the crack morphology, it is to be expected that a correlation between these variables would exist. Previous plots of the data on linear and logarithmic scales indicated that a linear relationship between the logarithm of the leak rate and the logarithm of the bobbin amplitude would be an appropriate choice for establishing a correlating function via least squares regression analysis. Thus, the functional form of the correlation is

$$\log(Q) = b_3 + b_4 \log(V), \quad (6.19)$$

where Q is the leak rate, V is the bobbin voltage, and b_3 and b_4 are estimates obtained from the data of some coefficients, β_3 and β_4 . The final selection of the form of the variable scales, i.e., log-log, was based on performing least squares regression analysis on each possible combination and examining the square of the correlation coefficient for each case. The largest index of determination, 58.2%, was found for the $\log(Q)$ on $\log(V)$ regression. The second largest index, for Q on V , was found to be on the order of 24%, clearly indicating the appropriate choice of scales to be log-log.

A summary of the results of the regression analysis is provided in Table 6-4, and illustrated on Figure 6-6. The number of data points used for the above evaluations was 40 and the number of degrees of freedom (dof) 38. The obtained value of r^2 of 58.2% is significant at a level of >99.99999% based on an F distribution test of the ratio of the mean square of the regression to the mean square of the error. This can also be interpreted as the probability that the log of the leak rate is correlated to the log of the bobbin amplitude. An alternate interpretation is that if the variables are really uncorrelated and the testing was repeated many times, an index of determination equal to or greater than that obtained from the analyzed data would be expected to occur randomly in only <0.000001% of those tests. The conclusion to be drawn from these results is that it is very likely that the variables are correlated.

At the February 8, 1994, meeting between the NRC, EPRI, and NUMARC, information was presented by the NRC that the "use of linear regression is acceptable if shown to be valid at a 5% level with [a] p-value test." The p -value is the conditional probability of observing a computed statistic, e.g., the F distribution value reported above, as large or larger than the observed value, under the condition that there is no relationship. In this case, a small p -value is evidence supporting the hypothesis that there is a correlation between $\log(Q)$ and $\log(V)$. The p -values for the estimated parameters of Equation (6.19) are also given in Table 6-4. For the slope of the regression equation, the conditional probability that the slope is zero is <0.000001%. The conditional probability that the intercept is zero is 0.01%. The validity of the regression is judged by the p -value associated with the slope. Since this is significantly less than the 5% value stipulated above the regression is concluded to be valid, and the use of linear regression is acceptable.

The expected, or arithmetic average (AA), leak rate, Q , corresponding to a voltage level, V , was also determined from the above expressions. Since the regression was performed as $\log(Q)$ on $\log(V)$ the regression line represents the mean of $\log(Q)$ as a function of bobbin amplitude. This is not the mean of Q as a function of V . The residuals of $\log(Q)$ are expected to be normally distributed about the regression line. Thus, the median and mode of the $\log(Q)$ residuals are also estimated by the regression line. However, Q is then expected to be distributed about the regression line as a log-normal distribution. The regression line still estimates the median of Q , but the mode and mean are displaced. The corresponding adjustment to the normal distribution to obtain the AA of Q for a log-normal distribution is

$$Q = E\{Q | V\} = 10^{b_1 + b_4 \log(V) + \frac{\ln(10)}{2} \sigma^2}, \quad (6.20)$$

for a given V , where σ^2 is the estimated variance of $\log(Q)$ about the regression line. The variance of the expected leak rate about the regression mean is then obtained from

$$\text{Var}(Q) = Q^2 \left[10^{\ln(10) \sigma^2} - 1 \right]. \quad (6.21)$$

To complete the analysis for the leak rate, the expected leak rate as a function of $\log(V)$ was determined by multiplying the AA leak rate by the probability of leak as a function of $\log(V)$. The results of this calculation are also depicted on Figure 6-6 for a steam line break differential pressure of 2560 psi.

6.6.1 Analysis of Regression Residuals

As previously noted, the correlation coefficients obtained from the analyses indicate that the log-log regressions at the various SLB ΔP s are significant at a level greater than 99.8%. Additional verification of the appropriateness of the regression was obtained by analyzing the regression residuals, i.e., the actual variable value minus the predicted variable value from the regression equation. A plot of the $\log(Q)$ residuals as a function of the predicted $\log(Q)$ was found to be nondescript, indicating no apparent correlation between the residuals and the predicted values. A cumulative probability plot of the residuals on normal probability paper approximated a straight line, thus verifying the assumption inherent in the regression analysis that the residuals are normally distributed. Given the results of the residuals scatter plots and the normal probability plots, it is considered that the regression curve and statistics can be used for the prediction of leak rate as a function of bobbin amplitude, and for the establishment of statistical inference bounds.

6.7 SLB Leak Rate Analysis Methodology

The leak rate versus voltage correlation can be simulated in conjunction with the EOC voltage distributions obtained by Monte Carlo methods, or by applying the POL and leak rate correlations to the EOC voltage distribution obtained by Monte Carlo methods as applied for the draft NUREG methodology. This second approach is a hybrid that joins Monte Carlo and deterministic calculations. Parallel analyses verified that the full Monte Carlo leak rates and the direct application of the correlations to the EOC voltage distribution yield essentially the same results. Thus, it is adequate to apply the correlations to the EOC voltage distributions.

The determination of the end of cycle leak rate estimate proceeds as follows. The beginning of cycle voltages are estimated using the methodology provided in draft NUREG-1477. The distribution of indications is binned in 0.1V increments. The number of indications in each bin is divided by 0.6 to account for POD. The resulting number of indications in each bin is reduced by the number of indications plugged in each bin. The final result is the beginning of cycle distribution used for the Monte Carlo simulations. The NDE uncertainty and growth rate distributions are then independently sampled to estimate an end of cycle distribution, also reported in bins of 0.1V increment. Given the EOC voltage distribution the calculational steps to obtain an estimate of the total leak rate are as follows:

- (1) For each voltage bin, the leak rate versus bobbin amplitude correlation is used to estimate an expected, or average, leak rate for indications in that bin.

- (2) The probability of leakage correlation is then used to estimate the mean probability of leak for the indications in each bin.
- (3) The relationships derived in Appendix C of draft NUREG-1477 for the variance of the product of the probability of leak with the leak rate and for the total leak rate are then used to estimate the expected total leakage and variance for the sum of the indications in each bin as a function of the correlation means and estimated variances for the leak rate and probability of leak.

To account for the variances of the coefficients of the regression equation for the leak rate, the σ used in equations (6.20) and (6.21) is that from the predictive distribution for the logarithm of the leak rate as a function of bobbin amplitude, i.e., for each voltage, V_i , an effective standard deviation of the regression error, σ_i , is calculated as

$$\sigma_i = \sigma_e \sqrt{1 + \frac{1}{N} + \frac{[\log(V_i) - \overline{\log(V)}]^2}{\sum_j [\log(V_j) - \overline{\log(V)}]^2}}, \quad (6.22)$$

where N is the number of data pairs in the regression analysis, and σ_e is an unbiased estimate of σ . The expected total leak rate from all of the indications in all of the bins is

$$T = \sum_{i=1}^{N_B} \frac{n_i}{1 + e^{-[b_1 + b_2 \log(V_i)]}} 10^{b_3 + b_4 \log(V_i) + \frac{\ln(10)}{2} \sigma_i^2}, \quad (6.23)$$

where N_B is the number of bins, and n_i is the number of indications in the bin with bobbin amplitude V_i . Thus, the expected total leakage for the entire distribution is obtained as the sum of the expected leak rates for each bin.

In order to estimate an upper confidence bound for the total leak rate an expression is needed for the variance of the total leak rate. There are two sources of variance to be considered, the variance about the predicted expected value and the variance of the predicted expected value; the estimated total variance about the predicted expected value being the sum of the two. The variance of the total leak rate about the predicted expected value is

$$V(T) = \sum_{i=1}^{N_B} n_i \left\{ P_i Q_i^2 \left[e^{\ln(10) \sigma_i^2} - 1 \right] + Q_i^2 P_i (1 - P_i) \right\}, \quad (6.24)$$

where P_i is the probability of leak from equation (6.11). As noted, an additional variance term is added in order to estimate the contribution to the variance from the correlation between the

individual leak rates, i.e., from the covariance, which arises as a consequence of using the regression equations. Thus, the second term accounts for the variances of the positions of the regression equations. A linearized approximation (via Taylor's Theorem) of the variance of the mean of the regression prediction, T_μ , is given by

$$\mathbf{V}(T_\mu) = \sum_{i=1}^{N_s} n_i \left\{ \frac{dT}{d\beta_j} \right\}_i^T \begin{bmatrix} [\text{Cov}(\beta_1, \beta_2)] & 0 & 0 \\ 0 & [\text{Cov}(\beta_3, \beta_4)] & 0 \\ 0 & 0 & \mathbf{V}(\sigma_i^2) \end{bmatrix} \left\{ \frac{dT}{d\beta_j} \right\}_i, \quad (6.25)$$

where the derivative of the total leak rate vector contains five elements for $j=1, \dots, 5$, and the *Covariance Matrix* is a square 5×5 matrix consisting of the estimated variances and covariances of the estimated individual regression coefficients and σ_i . Note that here $[\text{Cov}(\beta_1, \beta_2)]$ and $[\text{Cov}(\beta_3, \beta_4)]$ are each 2×2 matrices, where the β 's are estimated by b_1 through b_4 , and recall that σ_i is an estimate of β_5 . The variance of the variance is estimated as

$$\mathbf{V}(\sigma_i^2) = \frac{2 \sigma_i^4}{n - 2}, \quad (6.26)$$

where n is the number of data pairs used in the leak rate regression analysis. The standard deviation of the total leak rate is then taken as the square root of the variance of the total leak rate. The upper bound 95% confidence limit on the total leak rate is then obtained as the expected total leak rate plus 1.645 times the standard deviation of the total leak rate. The results obtained with this approach have been compared to results obtained from the Monte Carlo simulation without significant differences being observed. For a calculation utilizing only equation (6.24), the total leak rate from SG "D" at the EOC is estimated to be 3.0 GPM. By including the variance from equation (6.25), the estimated total leak rate was estimated to be 3.1 GPM. The value obtained from the Monte Carlo simulation of the total leak rate was 3.2 GPM, as described in Section 6.8.1 below. Thus, for the distribution analyzed, the contribution of terms associated with the covariance, i.e., the uncertainty of the prediction of the mean total expected leak rate, is small (being on the order of 3%) when compared to the variance of the total leak rate about the mean value. The results obtained provide independent verification of the Monte Carlo and hybrid techniques.

6.8 Simulation of Equation Parameter Uncertainties

The estimated, total end of cycle leak rate can also be calculated using Monte Carlo techniques, e.g., the method documented in the EPRI ODSCC report (TR-10047, Rev. 1). In the Monte Carlo analysis the variation in the parameters, i.e., coefficients, and the variation of the dependent variable about the regression line is simulated. A 95% confidence bound on the total leak rate from SG "D" of Braidwood 1 was calculated using a Monte Carlo simulation to

verify the results from the deterministic analysis. The approach used for the simulation is different from that discussed in the EPRI ODSCC report. While both methods simulate the variation of each parameter of the correlation equations, the method discussed herein also simulated the effect of the covariance of the individual indication leak rates. Each of the methods is discussed herein in order to provide clarification regarding their use. In order to simplify the discussion of the Monte Carlo techniques, different nomenclature is used from that of the previous section, i.e., Q_i is used to represent the common logarithm of the leak rate, and V_i is used to represent the common logarithm of the bobbin amplitude. Thus, the following model is used to describe a working relationship between the logarithm of the leak rate and the logarithm of the bobbin amplitude,

$$Q_i = b_3 + b_4 V_i + \epsilon, \quad (6.27)$$

where ϵ is the estimated error of the residuals, assumed to be from a population that has a zero mean, and a variance that is not dependent on the magnitude of V_i . The coefficients, b_3 and b_4 , are the estimates from the regression analysis of some true coefficients, β_3 and β_4 , representing the intercept and slope of the equation, respectively.

6.8.1 Monte Carlo Simulation of the Total Leak Rate for Braidwood 1

The method used by Westinghouse for simulating the total leak rate is the outcome of a series of technical discussions held with the NRC. The method differs from that reported in prior WCAP reports, wherein the predictive distribution was simulated and covariance terms were ignored. It is noted that, although both methods yielded similar results (within ~3%) for Braidwood 1, the method described herein is more statistically accurate. This small difference in the total leak rate results is because the contribution of the covariance terms relative to the variance terms is relatively small for the correlations used herein. In summary, random versions of the POL and leak rate correlations are generated and used to calculate the sum of the leak rates for all of the indications in a SG to obtain a single simulated value of the total leak rate. This process is repeated to obtain a distribution of the total leak rate from 10,000 simulations of the correlation equations. A non-parametric 95% confidence bound on the total leak rate is then estimated from the distribution of total leak rates.

At the start of each SG simulation, i.e., the calculation of a single total leak rate, a random value for the *standard deviation of the errors for the population* is calculated from the χ^2 distribution, the degrees of freedom from the data, and the standard deviation of the regression errors. This is used to calculate random values for the parameters of the regression equation, which remain constant for the entire SG simulation. The variation of the regression predictions are accounted for by randomly estimating the POL from a uniform distribution, and by adding the product of a random normal deviate and the standard deviation of the errors for the population to the predicted logarithm of the leak rate, for each individual indication in the SG

distribution. The total leak rate for the SG simulation is calculated as the sum of the leak rates from all of the indications in the SG. The expression for the total leak rate is

$$T = \sum_{i=1}^N R_i(\beta_1, \beta_2) Q_i(\beta_3, \beta_4, \beta_5), \quad (6.28)$$

where

- N = the total number of indications in the SG at EOC,
- $R_i(\beta_1, \beta_2)$ = 0 or 1 is the POL from a single indication, i , in a tube,
- $Q_i(\beta_3, \beta_4, \beta_5)$ = is the conditional leak rate of indication i , i.e., the leak rate if the indication is leaking,
- β_1, β_2 = the coefficients of the POL equation,
- β_3, β_4 = the coefficients of the leak rate versus bobbin amplitude equation, and
- β_5 = the standard error of the log of the leak rate about the correlation line, also referred to herein as σ .

To simulate the total leak rate from all of the indications in the generator, random coefficients for the probability of leak, POL, and leak rate correlation equations are generated, and then those coefficients are used to simulate the POL and leak rate for each indication. The POL, R_i , for each indication, i , is simulated as,

$$R_i(\beta) = \begin{cases} 1 & \text{if } U_i < \text{logit}(\beta_1 + \beta_2 \log(V_i)) \\ 0 & \text{otherwise} \end{cases}, \quad (6.29)$$

where U_i is an independent draw from a uniform distribution. The step of determining an integer value for the POL accounts for the variation of the distribution of probabilities about the log-logistic regression line. Discussion of the generation of β_1 and β_2 is left until after the discussion of the coefficients for the leak rate equation.

Leak Rate versus Bobbin Amplitude Simulation

To simulate the leak rate from the regression line, random coefficients β_3 and β_4 must be simulated. Each of these has a variance that is dependent on the variance of the error of the log of the leak rate about the regression line. Thus, the first step is to simulate a random error variance by picking a random χ^2 deviate for $n-2$ degrees of freedom and then calculating a random error variance, σ^2 , for the correlation equation from the regression error variance as

$$\sigma^2 = \frac{(n-2)}{\chi_{(n-2), \text{random}}^2} \hat{\sigma}^2 = f_v \hat{\sigma}^2, \quad (6.30)$$

where n is the number of data pairs used to calculate the regression coefficients, and f_V is defined by equation (6.30). This is now one possible variance for the *population* of log-leak rates about a correlation equation. Thus, it is appropriate to use the normal distribution to obtain random values for the parameters of the correlation equation. The distribution of β_3 and β_4 will be bivariate normal. Since they are correlated, although each is normally distributed marginally, they are not free to vary independently. If a value for the slope is determined first, then the distribution of the intercept values will be conditional on that value of the slope. The degree of correlation is indicated by the off-diagonal entry in the parameter covariance matrix calculated from the regression analysis. The entries of the covariance matrix of the parameters, V_{11} , V_{12} , and V_{22} , for the correlation equation to be used for a SG simulation are obtained from the corresponding estimated matrix obtained from the regression analysis as

$$V_{ij} = f_V \hat{V}_{ij}, \quad (6.31)$$

where the caret, " \wedge ", indicates an estimate from the regression data. A bivariate normal intercept for the simulation correlation is then calculated from the regression equation intercept as

$$\beta_3 = b_3 + Z_1 \sqrt{V_{11}}, \quad (6.32)$$

and the bivariate normal slope is calculated from the regression slope as

$$\beta_4 = b_4 + Z_1 \frac{V_{12}}{\sqrt{V_{11}}} + Z_2 \sqrt{V_{22} - \frac{V_{21}^2}{V_{11}}}, \quad (6.33)$$

where Z_1 and Z_2 are random univariate normal deviates, i.e., from a population with a mean of zero and a variance of one. We now have β_3 , β_4 , and σ for use in simulating all of the leak rates from each of the indications in the SG for one simulation of the total leak rate. For each simulation of an individual indication, i , the leak rate will be

$$Q_i(\beta) = 10^{\beta_3 + \beta_4 \log(V_i) + \beta_5 Z_i}, \quad (6.34)$$

with Z_i representing the i^{th} value from N independent draws from a standard normal distribution. Once the probabilities of leak have been calculated, the total leak rate for one simulation is then calculated using equation (6.28). It is noted that each simulation of T requires the generation of one β vector, N binomial variates R_i , and a maximum of N log-normal variates Q_i . In practice, a value for the leak rate only needs to be generated for each indication that is leaking, i.e., when $R_i = 1$.

Probability of Leak Simulation

The generation of the coefficients of the POL relation to be used in the simulation of the total leak rate proceeds in the same manner as for the coefficients of the leak rate relation. The elements of the covariance matrix are obtained from the GLM regression analysis and used with the estimated coefficients in equations like (6.32) and (6.33) to obtain β_1 and β_2 for a random population POL equation. However, for the simulation of the POL, there is no term of the form $Z_i \sigma$ in the simulation of the total leak rate. This exception is due to the fact that the data are binary. In effect, this additional term is being simulated through the use of the random sampling to determine if R_i is 0 or 1 in equation (6.29).

It is noted that the elements of the covariance matrix obtained from the GLM regression are scaled to a mean square error (mse) of 1. This is because the mse for the binary variables is asymptotically 1. A check of this assumption can be made by calculating an estimate of the square root of the mse from the regression results as

$$\hat{\sigma} = \sqrt{\frac{1}{n-2} \sum_i \frac{(y_i - \mu_i)^2}{\mu_i(1 - \mu_i)}}, \quad (6.35)$$

where the y_i 's are the observed probabilities of leak, either zero or one, from the leak and burst testing, and the μ_i 's are the calculated probabilities of leak from the *logistic* regression equation. A significant departure from 1 for this quantity could be indicative of an inadequate model. For the simulation of the POL data for 3/4" tubes the root mse was found to be 1.1. This is not significantly different from 1.

A 95% confidence bound on the total leak rate from SG "D" at the end of the fuel cycle was found to be 3.2 GPM. This is in very close agreement with the value found using the deterministic estimate.

6.8.2 EPRI Monte Carlo Simulations

The simulation methodology documented in the EPRI ODSCC report, Reference 6.1, was also used for the estimation of a EOC leak rate for the Braidwood 1 SG "D". The resulting value, 3.1 GPM is provided for information since this analysis was not the reference methodology employed for the evaluation of the Braidwood SG's. Thus, the following discussion of the EPRI model is also for information purposes to clarify how it relates to the methodology employed. Application of the EPRI model involves two major steps. In the first step, an EOC leak rate table as a function of BOC volts is generated from Monte Carlo simulations of NDE uncertainties, plant specific growth rates, and uncertainties associated with the correlation analyses. In the second step, the total leak rate is estimated as the sum of the individual EOC leak rates from each indication using the tabulated leak versus BOC volts values.

Using the EPRI methodology, the probe wear and analyst variability are randomly sampled to obtain a random BOC voltage corresponding to a measured BOC voltage. The growth curve is then entered to obtain a random growth for the length of the cycle. This is then added to the BOC voltage to obtain a random EOC voltage. The POL and leak rate versus volts correlations are sampled to obtain a random POL and leak rate for that indication. The expected leak rate from the indication is then taken as the POL times the leak rate. The simulation is repeated several thousand times to obtain an EOC distribution of leak rate at each voltage level, typically in 0.1 volt increments. From the distribution, a non-parametric 95% confidence bound for 95% of the population of the leak rates is determined at each voltage level. These are then used to estimate the EOC leakage from the distribution of BOC indications.

The POL for a specified EOC indication voltage is obtained from the correlation equation as

$$R_i = \frac{1}{1 + e^{-[\beta_1 + \beta_2 \log(V_i) + Z_i \eta_i]}} \quad (6.36)$$

where β_1 and β_2 are the coefficients from the POL regression analysis, $Z_i \sim N(0,1)$, and η_i is the estimated standard deviation given by

$$\eta_i = \sqrt{V_{11} + [2V_{12} + V_{22} \log(V_i)] \log(V_i)} \quad (6.37)$$

where the V_{ij} 's are the elements of the covariance matrix of the coefficients.

For each indication simulated, the coefficients of the leak rate versus voltage equation are generated. The slope of the regression equation is sampled using a random t -variate, followed by simulation of the intercept. Finally, the regression residual error is sampled with a random t -variate. Random t -variates are used instead of random normal variates because the standard deviation of the population of residuals is estimated, and not known, from the regression analysis. A two-sided $100 \cdot (1-\alpha)\%$ confidence band for the true slope, β_4 , of the regression equation is given by

$$\beta_4 = b_4 \pm t_{v, 1-\alpha/2} \sqrt{\frac{\sigma_e^2}{\sum (V_j - \bar{V})^2}} \quad (6.38)$$

where b_4 is the estimated slope from the regression analysis, v is the number of degrees of freedom used for the determination of σ_e , the estimated standard deviation of the residuals. Thus, by randomly sampling the t -distribution with v degrees of freedom, t_v , random values of

the slope can be generated from equation (6.38), where the sign of the random t -variate governs the sign of the second expression, i.e.,

$$\beta_4 = b_4 + t_v \sqrt{\frac{\sigma_e^2}{\sum_j (V_j - \bar{V})^2}} \quad (6.39)$$

The coefficients of the regression equation, i.e., equation (6.27), are not statistically independent. Thus, selecting a random value for the intercept must account for the already selected slope. In this case, a joint $100 \cdot (1-\alpha)\%$ confidence ellipse for the coefficients is given by

$$(\beta_3 - b_3)^2 + 2\bar{V}(\beta_3 - b_3)(\beta_4 - b_4) + \frac{\sum V_j^2}{n}(\beta_4 - b_4)^2 \leq \frac{2\sigma_e^2 F_{2,v}}{n}, \quad (6.40)$$

where β_3 and β_4 are the true, but unknown, coefficients of the regression equation. Thus, given the random slope from equation (6.39), a random F -distribution value, F , for 2 and v degrees of freedom, is selected and equation (6.40) is solved (considering the equality) to obtain a random value for β_3 . Since there are multiple roots of equation (6.40), i.e.,

$$\beta_3 = b_3 - \bar{V}(\beta_4 - b_4) \pm \sqrt{(\beta_4 - b_4)^2 \left[\bar{V}^2 - \frac{\sum V_j^2}{n} \right] + \frac{2\sigma_e^2 F_{2,v}}{n}}, \quad (6.41)$$

an additional random selection must be made to account for the sign of the radical in equation (6.41). It is also noted that the selection of a random F deviate may result in the radical of (6.41) being imaginary. In this case, it is necessary to sample F until the radical is real. To complete the leak rate versus voltage correlation for the simulation, only the variation about the regression line remains. The standard error, σ_e , from the regression analysis has been shown to be approximately normally distributed with a mean of zero. Since the true variance of the residual population is estimated, the distribution is simulated using a random t -variate, and the final leak rate for each simulation case is given by

$$Q_i = 10^{\beta_3 + \beta_4 V_i + t_v \sigma_e} \quad (6.42)$$

It is noted that the method described in the EPRI ODSCC report indicates that the effective standard deviation of the residuals, σ_i , from equation (6.22) is to be used instead of the actual standard deviation of the residuals, σ_e , in equation (6.42). This is considered to be an unnecessary conservatism because the variance of the coefficients would enter equation (6.42) twice, i.e., through the simulation of β_3 and β_4 and through σ_i . The net effect would be to

slightly over estimate the leak rate for each individual indication. For the simulation result reported previously herein, equation (6.42) was used.

In summary, the EPRI simulation essentially uses the predictive distribution to simulate the EOC leak rate. This ignores the potential contribution due to the covariance of the individual POL times leak rate values, however, this is likely compensated for by taking each individual EOC leak rate at a 95% confidence level, and the fact that the contribution from the covariance terms is small. Westinghouse has previously reported results, in prior WCAP reports, based on directly simulating the predictive distribution. Results obtained using this method, 3.0 and 3.1 GPM for two independent simulations, were comparable to the result obtained using the methodology described in Section 6.8.1. Thus, the EPRI methodology of Reference 6.1 results in a predicted total leak rate of 3.1 GPM, which is in excellent agreement with the 3.2 GPM result obtained by the Monte Carlo methods of Section 6.8.1, and the 3.1 GPM result from the hybrid method. In conclusion, either of the three methods is adequate for the SLB leak rate analysis.

6.9 Effect of Braidwood 1 Pulled Tubes' Results on Burst & Leak Rate Correlations

The purpose of this section is to report on evaluations performed which utilized the results of leak rate and burst testing of tube sections which were removed from Braidwood Unit 1 in the spring of 1994. The Braidwood 1 pulled tube data for ARC applications is given in Table 3-6. A total of eight (8) tube sections which exhibited bobbin amplitudes greater than zero volts, based on the field inspection data, were tested to determine their probability of leak during SLB, and their burst pressure. Three (3) of the specimens were found to exhibit a probability of leak of one and measurements were made of the leak rate at multiple differential pressures, including conditions similar to those expected during a postulated steam line break (SLB). The outcomes of these tests, see Table 6-5, were compared to the database of similar test results for 3/4" outside diameter steam generator tubes, and the effect of including the new test data in the database evaluated. The results of these comparisons and evaluations are discussed in what follows.

Burst Pressure vs. Bobbin Amplitude

A total of eight (8) burst test were performed on tube specimens which exhibited non-zero bobbin amplitudes at locations corresponding to the in-plant elevations of the tube support plates. A plot of the Braidwood 1 specimens' burst pressures is depicted on Figure 6-7 relative to the correlation developed for the reference database (EPRI), which is shown on Figure 6-1. A visual examination of the indicates that all of the burst pressures measured fall within the scatterband of the reference data about the reference regression line. The burst pressure for specimen R42C44-7 is somewhat higher than would have been expected, but not significantly so, cf. the uppermost data point at a bobbin amplitude of ~2.2 volts. Likewise, the burst pressure for specimen R42C44-3 is somewhat lower than would be expected, but totally within

the range of the data scatter in the relative vicinity of a bobbin amplitude of 4 volts. Thus, the visual examination doesn't indicate any significant departures from the reference database. Although the upper bound is not shown, all of the data fall within a 90% non-simultaneous prediction band about the regression line (the one-sided 95% prediction curve depicted is the lower bound of a two-sided 90% prediction band). Since a two-sided simultaneous prediction band for the eight data points would be wider than the non-simultaneous band, no statistically significant anomalies are indicated.

Since the Braidwood 1 burst pressure data are not indicated to be from a separate population from the reference data, the regression analysis of the burst pressure on the common logarithm of the bobbin amplitude was repeated with the additional data included. A comparison of the regression results obtained by including those data in the regression analysis is provided in Table 6-6. The intercept of the burst pressure, P_B , as a linear function of the common logarithm of the bobbin amplitude regression line is increased by 0.2%, and the slope is decreased by ~1%, i.e., the slope is a larger negative number. The regression line obtained by including these data in the regression analysis is also shown on Figure 6-7. The intersection of the two regression lines occurs at ~3 volts. Thus, for bobbin amplitudes less than 3 volts the predicted burst pressure would be slightly higher than the value obtained using the reference regression line. There is also a decrease of ~1% in the standard error of the residuals. The effect of this change would be reflected in a smaller deviation of the 95% prediction line from the regression line. The net effect of both of these changes on the SLB structural limit, using 95%/95% lower tolerance limit material properties, would be to increase it by 0.04 volts, i.e., from 4.54 volts to 4.58 volts, which is judged to be not significant. The decrease in the standard error of the residuals would also slightly reduce the probability of burst for bobbin indications less than 12.6 volts, and slightly increase the probability of burst for indications with amplitudes greater than 12.6 volts. Based on the judged insignificant change in the structural limit, the change in the probability of burst would also likely not be significant.

Probability of Leak

The same eight data points examined relative to the burst pressure correlation were also examined relative to the reference correlation for the PoL as a function of the common logarithm of the bobbin amplitude. Figure 6-8 illustrates the Braidwood 1 data relative to the database and the reference correlation. Specimen R42C44-5, with a bobbin amplitude of 2.1 volts exhibits some tendency away from the bulk of the data for which the PoL is unity, i.e., based on the bobbin amplitude it would have been expected to have a PoL of about 5%. However, the associated leak rate for this indication is very small, being 0.84 lph or 0.0037 gpm. One specimen from the reference database exhibited leakage at a lower amplitude level. All of the other specimens exhibited PoL behavior in line with expectations indicated by the reference regression curve. Based on the visual examination, there appears to be no significant evidence of irregular results, i.e., outlying behavior is not indicated.

In order to assess the effect of the new data on the correlation curve, the database was expanded to include the Braidwood 1 data and the *Generalized Linear Model* regression (see Section 6.5) of the PoL on the common logarithm of the bobbin amplitude was repeated. A comparison of the correlation parameters with those for the reference database is shown in Table 6-7. These results indicate a 9% reduction in the *logistic* intercept parameter and an 8% reduction in the *logistic* slope parameter. In order to assess whether or not these changes are significant the reference correlation and the new correlation were also plotted on Figure 6-8. An examination of Figure 6-8 reveals essentially no change, in an absolute sense, in the correlation below a bobbin amplitude of 1 volt, or above a bobbin amplitude of about 15 volts. The PoL is greater than the reference correlation in the range of 1 volt to almost 6 volts, and slightly less in the range of 6 volts to about 15 volts. A listing of comparative values is provided in Table 6-8. At 1 volt the increase in the PoL is on the order of 0.003. The maximum increase in the PoL is 0.04, from 0.23 to 0.27, at an amplitude of 3 volts.

To assess the single effect (ignoring the effect of the change on the leak rate correlation) of the above changes to the PoL function on the total leak rate, a recalculation of the leak rate as reported in Table 8-1 was performed. Using the reference correlation of the leak rate to the bobbin amplitude, the 95% confidence bound for the total leak rate is increased by 0.01%. This is not an unexpected result, since the information presented in Table 8-2 shows that when the total leak rate is determined using the leak rate to bobbin volts correlation the resulting value can be quite insensitive to the form of the PoL function.

Leak Rate vs. Bobbin Amplitude

As previously noted, three (3) of the removed tube specimens exhibited leakage under SLB conditions. The leak rates are provided in Table 6-5, and depicted on Figure 6-9. All of the results fall well within the spread of the reference data. The actual leak rates range from ~40% to ~75% below the median prediction (the regression fit on the plot) of the regression. It is implied from the visual examination, using the relative distance of the 95% confidence bound on the arithmetic average from the arithmetic average, that all of the data points would fall well within a 90% non-simultaneous, two-sided prediction band. Thus, the visual appearance of the data do not indicate any departure from the database and strongly support the trend of the prior correlation.

As for the previously discussed correlations, a regression analysis was performed to assess the influence of the Braidwood 1 data on the leak rate to bobbin amplitude correlation. The results of repeating the regression analysis with the Braidwood 1 data included are given in Table 6-9. Inclusion of the Braidwood 1 data results in a 8% decrease in the logarithmic intercept parameter and a 4% increase in the logarithmic slope parameter. In addition, the standard error of the logarithmic residuals is decreased by ~3%, the index of determination of the regression is increased by about 10%, and the *p*-value for the slope parameter is reduced by about two orders of magnitude. Thus, the addition of the data increases the strength of the correlation. A

plot of the correlation with the Braidwood 1 data included in the regression is depicted on Figure 6-9 along with the correlation reported in Section 6.6 of this report. The net effect of including the new data is to reduce the expected, i.e., arithmetic average, leak rate for bobbin amplitudes less than ~20 volts. It is also noted that the slope of a line joining the three added data points is almost parallel to the reference database regression line.

The dual effect of the Braidwood 1 data on the total leak rate, by considering both the PoL and the leak rate correlations to bobbin volts, was estimated by repeating the calculation of Table 8-1 as per the above discussion on the effect of the data on the PoL. For this case the revised coefficients as reported in Table 6-7 and Table 6-9 were used. The net effect was found to be a 14% decrease in the 95% confidence bound for the total EOC leak rate during a postulated SLB. Since the increase due to the modified PoL function coefficients was insignificant, the net effect of the Braidwood 1 data on the total expected leak rate is a 14% reduction.

General Conclusions

The review of the effect of the Braidwood 1 data indicates that the burst pressure, the probability of leak, and the leak rate correlations to the common logarithm of the bobbin amplitude would not be significantly changed by, and are conservative relative to, inclusion of the data. It is therefore concluded that the correlations reported in the previous sections of this document should not be revised at this time. It is further concluded that the conclusions given in Revision 0 to this document would not be significantly affected by repeating all of the analyses for which results are reported herein in Section 8.

6.10 References

The references used in this report section are:

- 6.1 TR-100407, Revision 1 (draft), "PWR Steam Generator Tube Repair Limits - Technical Support Document for Outside Diameter Stress Corrosion Crack at Tube Support Plates," Electric Power Research Institute, August 1993.
- 6.2 NP-7480-L, Volume 2, "Steam Generator Tubing Outside Diameter Stress Corrosion Cracking at Tube Support Plates - Database for Alternate Repair Limits, Volume 2: 3/4 Inch Diameter Tubing," Electric Power Research Institute, October, 1993.
- 6.3 EPRI Letter, "Exclusion of Data from Alternate Repair Criteria (ARC) Databases Associated with 7/8 inch Tubing Exhibiting ODSCC," D. A. Steininger (EPRI) to J. Strosnider (USNRC), April 22, 1994 [to become Appendix E of Reference 6.2].

- 6.4 NUREG-1477 (draft), "Voltage-Based Interim Plugging Criteria for Steam Generator Tubes - Task Group Report," United States Nuclear Regulatory Commission (NRC), June 1, 1993.
- 6.5 [United States Nuclear Regulatory Commission] Meeting with EPRI, NUMARC, "Resolution of Public Comments on Draft NUREG-1477," United States Nuclear Regulatory Commission, February 8, 1994.
- 6.6 Regulatory Guide 1.121 (draft), "Bases for Plugging Degraded PWR Steam Generator Tubes," United States Nuclear Regulatory Commission, issued for comment in August, 1976.
- 6.7 Docket STM-50-456, "Safety Evaluation by the Office of Nuclear Reactor Regulation Related to Amendment No. to Facility Operating License No. NPF-72 Commonwealth Edison Company Braidwood Station, Unit No. 1," United States Nuclear Regulatory Commission, May, 1994.

Table 6-1: Regression Analysis Results -
Burst Pressure vs. log(Bobbin Amplitude)
3/4" x 0.050" Alloy 600 MA SG Tubes
(Reference $\sigma_f = 75$ ksi)

Parameter	Value	Value	Parameter
b_1	-3.077	7.822	b_0
SE b_1	0.175	0.136	SE b_0
r^2	80.7%	0.955	SE P_B
F	306.1	73	DoF
SS _{reg}	279.03	66.55	SS _{res}
Pr(F)	8.0E-28	29.46	SS _{log(V)}
p ₁ -value	8.0E-28	1.6E-62	p ₀ -value

Table 6-2: Results of Regression Fits of Logarithmic Forms
of POL Distribution Functions to 3/4" OD Tube Data
@ 620°F and $\Delta P = 2560$ psi

Parameter	Log-Logistic Values	Log-Normal Values	Log-Cauchy Values
b_1	-5.5998	-2.7157	-13.8413
b_2	9.1924	4.6317	21.3183
V_{11}	2.1145	0.3664	46.5125
V_{12}	-2.9538	-0.4985	-71.2114
V_{22}	4.5779	0.7993	110.22
Deviance	32.52	33.84	32.43
Results of Regression Fits of Non-Logarithmic Forms of POL Distribution Functions to 3/4" OD Tube Data.			
Parameter	Logistic Values	Normal Values	Cauchy Values
b_1	-5.3890	-2.8544	-10.5327
b_2	1.1945	0.6395	2.3085
V_{11}	1.4958	0.2905	24.4371
V_{12}	-0.3141	-0.0617	-5.3943
V_{22}	0.0787	0.0169	1.2223
Deviance	28.87	28.94	32.47

Table 6-3: Sample Results for Probability of Leak for 3/4" SG Tubes @ 620°F and $\Delta P = 2560$ psi						
Volts	Log-Logistic Function	Log-Normal Function	Log-Cauchy Function	Logistic Function	Normal Function	Cauchy Function
0.1	3.77E-07	1.02E-13	9.05E-03	5.12E-03	2.63E-03	3.08E-02
0.2	5.99E-06	1.32E-09	1.11E-02	5.77E-03	3.20E-03	3.15E-02
0.3	3.02E-05	1.39E-07	1.27E-02	6.49E-03	3.88E-03	3.22E-02
0.4	9.53E-05	2.57E-06	1.42E-02	7.31E-03	4.68E-03	3.30E-02
0.5	2.32E-04	1.98E-05	1.57E-02	8.23E-03	5.63E-03	3.38E-02
0.6	4.81E-04	9.09E-05	1.71E-02	9.26E-03	6.74E-03	3.47E-02
0.7	8.90E-04	2.98E-04	1.85E-02	1.04E-02	8.05E-03	3.55E-02
0.8	1.52E-03	7.77E-04	2.00E-02	1.17E-02	9.57E-03	3.65E-02
0.9	2.42E-03	1.71E-03	2.15E-02	1.32E-02	1.13E-02	3.75E-02
1.0	3.68E-03	3.31E-03	2.30E-02	1.49E-02	1.34E-02	3.85E-02
2.0	5.56E-02	9.32E-02	4.26E-02	4.74E-02	5.76E-02	5.33E-02
5.0	6.95E-01	6.99E-01	7.59E-01	6.42E-01	6.34E-01	7.52E-01
7.0	8.97E-01	8.85E-01	9.25E-01	9.51E-01	9.48E-01	9.44E-01
10.0	9.73E-01	9.72E-01	9.58E-01	9.99E-01	1.00E+00	9.75E-01

Table 6-4: Regression Analysis Results:
log(Leak Rate) vs log(Volts)
for 3/4" x 0.043" Alloy 600 SG Tubes
@ 620°F and $\Delta P = 2560$ psi

Parameter	Value	Value	Parameter
b_4	3.132	-1.888	b_3
SE b_4	0.431	0.425	SE b_3
r^2	58.2%	0.653	SE log(Q)
F	55.88	38	DoF
SS _{reg}	22.56	16.21	SS _{res}
Pr(F)	<0.000001%	2.300	SS _{log(V)}
p ₁ -value	<0.000001%	0.01%	p ₀ -value

Table 6-5: Results of Leak Rate and Burst Testing of Tubes
Removed from Braidwood Unit 1

Specimen ID	Bobbin Amplitude (Volts)	Burst Pressure for $\sigma_t = 75$ ksi (ksi)	Probability of Leak During SLB	Leak Rate During SLB (lph)
R16C42-3	3.12	6.501	0	
R16C42-5	0.21	10.809	0	
R27C43-3	4.99	5.236	1	0.84
R37C34-3	1.04	9.002	0	
R37C34-5	10.4	4.917	1	12.83
R42C44-3	3.73	4.868	0	
R42C44-5	2.09	6.424	1	0.041
R42C44-7	0.28	9.157	0	

Table 6-6: Effects of the Braidwood Unit 1 Data on the
Burst Pressure vs. Bobbin Volts Correlation

$$P_B = \alpha_1 + \alpha_2 \log(\text{Volts})$$

Parameter	Reference Database Value	Database with Braidwood 1 Data
α_1	7.822	7.838
α_2	-3.077	-3.109
σ_{Error}	0.955	0.944
p Value for α_2	$8 \cdot 10^{-28}$	$4 \cdot 10^{-31}$
r^2	80.7%	81.3%

Table 6-7: Effect of Braidwood Unit 1 Data on the Probability of Leak Correlation

$$Pr(Leak) = \left\{ 1 + e^{-[\beta_1 + \beta_2 \log(Voltr)]} \right\}^{-1}$$

Parameter	Reference Database Value	Database with Braidwood 1 Data
β_1	-5.600	-5.035
β_2	9.192	8.457
V_{11}	2.115	1.437
V_{12}	-2.954	-2.043
V_{22}	4.578	3.286
Pearson σ_{Error}	1.2	0.87
Note: Parameters V_{ij} are elements of the covariance matrix of the coefficients, β_k , of the above regression equation.		

Table 6-8: Effect of Braidwood 1 Data on the Probability of Leak as a Function of Bobbin Amplitude		
Bobbin Amplitude (Volts)	PoL (Reference)	PoL (w/Braidwood)
0.60	0.0005	0.0010
0.70	0.0009	0.0018
0.90	0.0024	0.0044
1.00	0.0037	0.0065
2.00	0.0556	0.0766
3.00	0.2290	0.2689
5.00	0.6954	0.7060
6.00	0.8254	0.8243
7.00	0.8974	0.8920
9.00	0.9598	0.9541

Table 6-9: Effects of Braidwood Unit 1 Data on the Leak Rate vs. Bobbin Volts Correlation $\log(\text{Leak Rate}) = \beta_3 + \beta_4 \log(\text{Volts})$		
Parameter	Reference Database Value	Database with Braidwood 1 Data
β_3	-1.888	-2.044
β_4	3.132	3.272
$\beta_5 (\sigma_{\text{Error}})$	0.653	0.636
p Value for β_4	$1 \cdot 10^{-8}$	$1 \cdot 10^{-10}$
r^2	58.2%	64.1%

Figure 6-1: Burst Pressure vs Bobbin Amplitude
EPRI Database , @ 650°F, Reference Flow Stress = 75 ksi

a,c

Figure 6-2: Burst Pressure vs. Crack Length
0.750" x 0.043", Alloy 600 MA Steam Generator Tubes @ 650°F, Average Flow Stress

a,e

Figure 6-3: Probability of Burst vs. Through-Wall Crack Length
3/4" x 0.043" Alloy 600 MA SG Tubes

a,c

Figure 6-4: Probability of Leak for 3/4" SG Tubes
Comparison of Logarithmic Forms of Logistic, Normal & Cauchy Functions

Figure 6-5: Probability of Leak for 3/4" SG Tubes
Comparison of Non-Logarithmic Forms of Logistic, Normal & Cauchy Functions

a,c

Figure 6-6: 2560 psi SLB Leak Rate vs. Bobbin Amplitude
3/4" x 0.043" Alloy 600 SG Tubes, Model Boiler & Field Data (EPRI)

a,c

Figure 6-7: Burst Pressure vs Bobbin Amplitude
EPRI Database, Reference $\sigma_r = 75$ ksi

a,c

6 - 40

Figure 6-8: Probability of Leak for 3/4" SG Tubes @ 650°F, $\Delta P = 2560$ psi
Comparison of Braidwood '94 Data with EPRI Reference Database

a,c

6 - 41

Figure 6-9: SLB Leak Rate vs. Bobbin Amplitude
3/4" x 0.043" Alloy 600 SG Tubes @ 650°F, $\Delta P = 2560$ psi

a,c

6 - 42

7.0 BRAIDWOOD-1 EDDY CURRENT INSPECTION RESULTS

7.1 General

The March-April 1994 refueling shutdown was accompanied by 100% full length bobbin probe inspection of all four steam generators. In anticipation of the potential finding of significant ODSCC at support plate intersections, the ASME standards were calibrated to be consistent with IPC guidelines (such as incorporated into Appendix A of WCAP-13854), wear standards were employed to allow tracking of voltage measurement variation, and the eddy current analysts were required to demonstrate their capability to report and to measure indication voltages. TSP indications have been assessed against the prior inspection conditions at the corresponding locations to develop voltage growth rates for the preceding periods of operation.

Previous inspections of the Braidwood-1 steam generator tubes were conducted in November 1993 during an unplanned outage (SG C only), in September 1992 (EOC-3), and in April 1991 (EOC-2); the EOC-1 inspection in September 1989 was not included in the growth rate studies. For each indication reported during the 1994 inspection, both the 1993 (SG C) and the 1992 (all SGs) data were reevaluated to determine, as far as possible, the pre-existing signal amplitude which could be attributed to any detectable precursor condition. Only if a possible flaw indication was observed in the earlier inspection was a growth point calculated for the particular 1994 indication; i.e. no assumptions were made about prior year signal voltages. Because of the unplanned outage during Cycle 4, comparisons in SG C were made to both the 1993 and 1992 inspection results; furthermore, 1992 data for tubes reported in 1993 were compared to obtain an estimate of the partial cycle (4a) growth rate. Cycle 4b growth was determined by comparing the 1993 and 1994 data for SG C only; an overall Cycle 4 growth rate based on comparison of 1994 with 1992 data was also calculated. All the tubes plugged in 1992 were used to develop growth rate data for Cycle 3 by reanalyzing the 1991 data. Table 7-1 presents a summary tabulation of all the growth rates on a per cycle as well as a per Effective Full Power Year (EFPY) basis; also shown for each case are the number of comparisons used, the average BOC voltages, the voltage growth (ΔV), and the length of the operating period in EFPY. For each cycle evaluated, the data was subdivided into indication populations less than 0.75 volt and those equal to or greater than 0.75 volt. This was done to demonstrate the consistency in behavior with prior cases, which have consistently shown higher average percentage growth rates for low voltage indications.

The distribution of the TSP ODSCC indications among the four SGs for the 1994 inspection is shown in Table 7-2, which tabulates the number of indications for each TSP elevation for which indications were observed. For the D4 SGs of Braidwood-1, the 1H level represents the Flow Distribution Baffle (FDB), a plate with oversize tube holes and no flow holes; for this reason the incidence of ODSCC is expected to be low in the absence of unusual

circumstances. In fact, none of the indications reported in Braidwood-1 occur at this elevation. The support levels above are numbered in the cold leg order, i.e., the next hot leg TSP is designated 3H since its height corresponds to the 3rd preheater plate. The remaining TSPs are designated 5H, 7H, 8H, 9H, 10H, and 11H. Thus, though some probability of encountering ODSCC signals at the upper plates exists, it is expected that most of the indications will be observed in TSPs 3H, 5H, and 7H. These levels are in the relatively hotter internal temperature zone of the tubes (maximum in the hot leg tubesheet and decreasing with elevation up to the apexes of the U-bends, thereafter decreasing as the cold leg elevation decreases).

7.2 Inspection Results

7.2.1 March 1994 Inspection

During the scheduled refueling outage (A1R04), all tubes in service were tested full length with bobbin probes. Each distorted support plate indication (DSI) and all TSP indications characterized as a percent (%) call were subjected to confirmatory MRPC testing to assess the consistency of the underlying tube condition with prior cases of TSP ODSCC, and to determine the severity of the indication with respect to the repair criteria. The TSP bobbin indications confirmed by MRPC testing numbered 1567 among the four SGs, 470 in SG A, 76 in SG B, 642 in SG C, and 379 in SG D. The total number of TSP intersections subjected to MRPC testing on the basis of possible ODSCC indications was 2733, distributed among the four SGs; this represents a 57% rate of confirmation of the bobbin calls. It is considered that only those intersections which exhibit detectable ODSCC with pancake coil inspections warrant scrutiny with respect to plugging criteria, whether under Tech. Spec. criteria or under the alternate basis represented by the Interim Plugging Criteria. Two SG C bobbin field calls confirmed as NDD by RPC inspection are not included in the statistics of this report. These indications were more appropriately called permeability variations or residual signals, and inclusion of these two indications would result in misleading growth data.

The axial distribution of TSP ODSCC indications, as expected, exhibits the strong correlation with height above the tubesheet. With the exception of the 1H level (FDB), a strong concentration of the bobbin and MRPC indications are observed at 3H (58%), 5H (28%), and 7H (10%). Figure 7-1 presents the numerical distributions of the TSP ODSCC with respect to elevation in histogram form. The bobbin amplitude distributions associated with the ODSCC indications are presented together with the cumulative distribution curves in Figures 7-2 to 7-6 for the individual SGs and for the composite of all four SGs. Figure 7-7 gives the cumulative RPC confirmation fraction of the bobbin indications as a function of bobbin voltage. As expected, the probability that the RPC probe will detect degradation increases with the bobbin voltage, which increases with the depth and length and number of cracks present. Table 7-3

provides detailed RPC confirmation statistics as a function of bobbin voltage for each of the individual SGs, as well as cumulative confirmation data for the four SG composite results.

An RPC sampling plan was performed to inspect TSP intersections with dent signals greater than 5 volts and artifact/residual signals that could potentially mask bobbin indications of about 1.0 volt. Denting in Braidwood-1 is minor and most of the dents represent mechanical dings rather than corrosion induced denting. The RPC sampling plan was performed on all identified hot leg dents > 5.0 volts in SGs A and B. It included 21 dents (18 in SG A, 3 in SG B) at TSP intersections. There are only 6 dents in SG C (one additional dent was in a tube plugged for other causes) and 2 in SG D left in service above 5 volts that were not RPC inspected. The RPC sample included 40 mix residuals in SG A and 41 in SG B. The mix residuals inspected had greater than a one volt signal and were manually selected to represent the larger residual signals. In addition to this RPC sampling plan, 85 intersections with no bobbin indications were RPC inspected. No RPC flaw indications were found in the RPC sampling plan. In both this RPC sample and the RPC inspection of bobbin flaw indications, no circumferential indications or indications extending outside of the TSP thickness were detected.

Limiting the RPC sampling to only SGs A and B left only 8 dented TSP intersections uninspected in SGs C and D. Reviews of data from previous outages indicate that all 8 of these dent indications were present. The uninspected dent indications lead to a negligible risk of leakage or rupture due to the small number of dents, the fact that no flaw indications were found at the inspected dent locations and the fact that a conservative POD of 0.6, independent of voltage, is applied for the SLB leak rate and tube burst probability estimates. Similarly, uninspected mix residuals in SGs C and D would have negligible concern for leakage or burst considerations.

The two dents in SG D have bobbin voltages of 19.1 and 5.1 volts. The bobbin data for these indications have been reviewed for the 1989, 1991, 1992 and 1994 inspections. There have been no discernable changes in the dent voltages or phase angles. In all inspections, the phase angles are within 3 degrees of the expected 180 degrees for a dent. If a flaw were present, some change to the voltage and phase angle would be expected. Thus, it is judged that the dents are not growing in size and there is a low likelihood of a flaw being present in the dents. SG D is the most limiting SG for tube leakage and burst considerations. Since only two uninspected dents are present, even the assumption of a flaw being present in the dent (a flaw too small to influence the phase angle of the dent) would have negligible influence on leakage or burst. The $POD = 0.6$ adjustment results in 7.3 indications (actual indications plugged) above 2.7 volts left in service and 2 indications above 5.0 volts left in service. The contributions of these postulated indications to leakage and burst probability would be expected to exceed that of a potential indication in the two dented intersections not RPC inspected. SG C is not a limiting SG for leakage or burst considerations due to the

lower voltages (maximum of 2.74 volts found in the 1994 inspection) and lower growth rates found for this SG compared to SG D. Even if indications were postulated in the six uninspected dents left in service, the additional indications would be very unlikely to cause the leakage or burst probability to approach that for SG D. It can be further noted that the presence of a crack within a dented TSP would result in no or very small leakage due to the constraint provided by the dent, as shown by leak testing in the EPRI database report. If the postulated indication extended more than about 0.2" from the dent, the crack indication would be detectable by bobbin inspection. For these additional reasons, leakage or burst potential would be negligible for uninspected dents.

7.2.2 Prior Inspections: November 1993 and September 1992

The 1993 inspection of SG C was conducted in conjunction with an unplanned outage. This 100% full length inspection with bobbin probes was conducted with 610 mil standard bobbin coils, using standards which were subsequently normalized to the laboratory standard which serves as the reference for 3/4" alloy 600 tubing. Using the prevailing industry guidelines for reporting bobbin indications, 116 percent-type indications were reported, along with 300 DSIs. The percent-type indications were removed from service after confirmation with MRPC, and the DSIs were continued in service without MRPC verification. This was considered prudent in light of the A1R04 refueling outage scheduled 4 months later. Since the November 1993 testing was not conducted as a Tech. Spec. inspection, there was no extension of the testing to the other SGs.

The 1993 bobbin indication distributions for number vs. TSP elevation and number vs. amplitude are given in Figure 7-8 and in Table 7-4. Once again, the temperature/elevation dependency of the ODSCC incidence is apparent, and the distribution of amplitudes shows the predominance of low voltage (<1) signals accompanied by a low frequency tail of larger amplitude signals.

During A1R03, the September 1992 inspection, all four SGs were subjected to 100% full length bobbin inspection, again using site-specific bobbin interpretation guidelines consistent with the prevailing industry approach in plants not implementing the IPC. In this inspection, as in A1R04, all bobbin percent (%) and DSI indications reported were subjected to MRPC examination; 166 tubes with bobbin TSP indications confirmed by MRPC testing were removed from service. DSI signals reported on 79 intersections were continued in service after obtaining NDD (no detectable degradation) results from MRPC testing and analysis. The reported distribution of bobbin indications for A1R03 are given in Table 7-5 and Figure 7-9 for the elevation dependency, and the amplitude spectrum of the plugged tube indications is shown in Figure 7-10. It is apparent that the bobbin inspection data for 1992, 1993 and 1994 reflect similar patterns of tube degradation, proceeding for the most part at modest rates in terms of bobbin amplitudes, but progressively involving more tubes.

7.3 TSP Voltage Growth Rates

The progression of ODSCC indications at the TSPs is determined by re-evaluation of prior inspection EC records at the locations identified with indications in the 1994 inspection. In most cases, some element of the precursor is identified as corresponding to the flaw signal reported in 1994. However, it should be noted that rather conservative analysis criteria are invoked to accomplish this task. In this process analysts are required to forego the behavior criteria they may have employed to screen out low signal-to-noise indications, and to report possible flaw-like behavior in the TSP mix residual regardless of clarity. Review of the growth data identifies any anomalous growth data, and these are subjected to further scrutiny to eliminate spurious data.

The evaluation of voltage growth based on reevaluating the prior inspection data for all indications found during the latest inspection is the same approach used for other IPC/APC evaluations. This method of growth evaluation includes the largest growth values (typically repaired at the EOC) for each cycle, and can result in large, conservative average growth values. However, because of tube repair and the occurrence of new indications, there are differences in the population of tubes when comparing growth rates between cycles. This introduces some uncertainty in assessing growth trends between cycles, such as those which may be due to chemistry improvements. A more desirable growth evaluation would track the same population of indications for multiple cycles to more accurately assess growth trends. However, if the last inspection indications are tracked back in time, the larger prior cycle indications which were repaired are not included in the analysis and this method can lead to an underestimate of average prior cycle growth. This method has been applied to SG C over the first and second parts of Cycle 4 as described below. A third option for evaluating growth would be to track the latest inspection results back in time and to add plugged tubes into the population evaluated for prior cycles. This method has not been systematically evaluated. A more systematic evaluation of these three options would be desirable to assess the best option for evaluating both cycle-to-cycle growth trends and the influence of operational chemistry improvements. Such an evaluation has not been performed for Braidwood-1 in this report.

The operational periods for which growth values were determined included Cycle 3 - plugged tubes only; Cycle 4a (9/92-10/93) - SG C only but in three subgroups: all plugged tubes at 10/93, all indications reported at 10/93, and all indications reported at 4/94; Cycle 4b (11/93-4/94) for SG C only for all indications reported in 4/94, and the overall Cycle 4 for all four SGs. For each of these periods, growth data for indications <0.75 volt and those ≥ 0.75 volt were contrasted with the composite growth data for all indications. Table 7-6 shows a summary of the growth rates developed in this fashion for all four SGs. Figure 7-11 illustrates the overall growth/amplitude relationship for all the comparisons obtained in A1R04.

Figure 7-12 presents the same data combined with the elevation (temperature) effect. The dominance of the lower TSP levels in the incidence of the ODSCC indications is also reflected in the growth rates.

The distribution of the growth rate data, expressed as volts difference in the amplitude readings for 2 inspections, are tabulated (Table 7-6) in 0.1 volt bins up to 3 volts, 0.2 volt bins from 3 volts to 5 volts, and in 0.5 volt intervals up to the maximum observed change. For each bin the number of indications is entered along with the corresponding cumulative probability value. Voltage growth distributions are reported on a per EFPY basis. The voltage growth histograms for each of the operational periods evaluated are presented in Figures 7-13 to 7-18 on a composite basis for the prior cycles and on an individual SG basis for the Cycle 4 data. It is seen that for the A1R04 inspection, the average voltage growth rate for the composite of four SGs is 49% per EFPY, or 0.24 volt average growth per EFPY on an average BOC amplitude of 0.48 volt. The maximum growth was observed in SG A, 76% per EFPY, 0.36 volt growth on the average BOC amplitude of 0.47 volt. The largest individual growth observations for Cycle 4 are listed in Table 7-7. For indications with appreciable BOC amplitude readings, i.e., those from 0.75 volt and up, average growth is but a fraction of the composite, 26% in SG A and approximately 16% for the overall population. These estimates are strongly weighted by the SG C results, which exclude the tubes plugged in 11/93 (EOC-4a), for which higher growth rates were observed. The decrease noted in the EOC-4 data and the EOC-4b data correlate with secondary system chemistry changes implemented at Braidwood-1 since the A1R03 outage.

While the voltage growth rates prior to 1993 appear to be larger than those observed in other domestic plants, they fall well below growth rates observed in European plants. Three cases of tube leakage attributable to TSP ODSCC have been reported in Europe, though none has approached even Tech. Spec. leakage limits. None of the domestic plants affected by TSP ODSCC has experienced tube leakage in the absence of denting, notwithstanding indication amplitudes as high as 10.5 volts, and one occurrence of 22 volts.

7.4 Historical Operating Chemistry

Braidwood Unit 1 is currently in its fourth refueling outage. The unit has typically operated in the load follow manner of operation (Figures 7-19 through 7-21). Frequent changes in plant output requirements have resulted in power swings and plant shutdowns on occasion in the past. During periods of operation with chemistry imbalances, more frequent shutdowns with chemistry cleanup prior to restart can result in more limited accumulation of contaminant species in crevice regions subject to superheated conditions. Braidwood Unit 1 has experienced periods of elevated steam generator sodium to chloride molar ratios during prior operating cycles. Operating with these elevated ratios enhances the possibility of developing

caustic crevice conditions conducive to initiation and propagation of Alloy 600 alkaline stress corrosion cracking. Figures 7-19 through 7-27 show the power history, steam generator blowdown sodium to chloride molar ratios, and steam generator blowdown sodium and chloride concentrations during power operation for Braidwood Unit 1 during Cycles 2 through 4. During Cycle 2, SG blowdown sodium to chloride molar ratios (Figure 7-22) were slightly higher than molar equivalency with ratios typically less than 2. These ratio values fluctuated along with variations in plant operating conditions and minor contaminant ingresses - condenser leakage and demineralizer leakage. It should be noted that ratios maintained in this range can lead to development of caustic conditions in steam generator crevice regions. During Cycle 3, SG blowdown sodium to chloride molar ratios (Figure 7-23) were very elevated - both with respect to prior cycles of operation and with respect to good operating chemistry conditions. It is believed that this notable increase is likely to primarily be due to increased attention paid to SG blowdown cation conductivity values and attempts to lower them. As chloride concentration affects cation conductivity, lower chloride concentrations resulted in lower cation conductivity and, consequently, higher sodium to chloride molar ratios. Sodium concentrations were elevated during the first half of Cycle 3 (Figure 7-26). As these concentrations were decreased during the latter part of the fuel cycle, however, chloride concentrations were also decreased. Sodium to chloride molar ratios typically in the range of 2 to 3 and up to 5, as observed during Cycle 3, are strongly indicative of potentially caustic environment development in SG crevice regions as described above. During Cycle 4, a period of operation with higher molar ratios around 2 to 3 was followed by attempts to control molar ratio by modification of blowdown demineralizer operation and, subsequently, ammonium chloride addition (Figure 7-24). Ammonium chloride addition had the greatest effectiveness at Braidwood Unit 1 in controlling steam generator blowdown sodium to chloride molar ratios in the desired band. The success of this method at controlling crevice chemistry appears to be positive as a result of shutdown hideout return evaluations performed in May and at the end of the cycle.

Hideout return data obtained during Cycle 4 has been evaluated to ascertain the success of the molar ratio control program in modifying the steam generator crevice pH environment. Molar ratios of highly soluble species (sodium, potassium, and chloride) indicate a decreasing trend over the entire cycle (Figure 7-28). In addition, it has been reported that the crevice pH calculated by the MULTEQ program indicates an approximate 1.5 pH unit reduction to around 7.5 prior to the end of cycle shutdown. The end of cycle shutdown indicated more acidic conditions and lower molar ratio due to the occurrence of circulating water leakage.

7.5 Relationship Between Operating Chemistry and ODSCC Growth

Corrective actions taken at Braidwood Unit 1 specifically to slow the progression of Alloy 600 tubing ODSCC include molar ratio chemistry control and boric acid addition beginning in

April 1994. Molar ratio chemistry control was initiated during Cycle 4 in December 1992, following nearly two months of plant operation with elevated sodium to chloride molar ratios. Molar ratio control chemistry was begun by varying blowdown demineralizer operations to obtain greater breakthrough of anionic species. These operations have had some success in minimizing sodium leakage from the demineralizers; however, the operational sodium to chloride molar ratio was not able to be fully controlled. When it became apparent that operating in this manner was not achieving the desired degree of control, the decision was made to add ammonium chloride to adjust the sodium to chloride molar ratio in the steam generator blowdown. This method achieved a high degree of control over the operating steam generator blowdown sodium to chloride molar ratio. However, it was not apparent whether the desired result of neutral to slightly acidic hideout return chemistry would be achieved by operating in the identified control band of $\text{Na/Cl} = 0.3 - 0.6$. Following a hideout return evaluation at the end of May 1993, the Na/Cl control band was lowered to 0.2 to 0.4 to further alter the steam generator operating environment. The result of this change is demonstrated in Figure 7-29. Hideout return chemistry data reflect the success of the molar ratio control program in modifying the steam generator environment to the desired degree as indicated by the trends in hideout return chemistry.

Boric acid addition has been identified as the next step to be employed at Braidwood Unit 1 to control Alloy 600 ODSCC progression. Boric acid will be used during the startup for the fifth fuel cycle in April, 1994. Laboratory and operating PWR plant data indicate the usefulness of boric acid as a contributor to the overall corrosion control program. It is anticipated that the use of boric acid will take Braidwood Unit 1 one step further in their goal of minimizing ODSCC growth rates.

Overall, the chemistry review indicates that the high molar ratios of Cycle 3 (4/91-9/92) and the early part of Cycle 4 (up to 1/93) are most likely to be associated with caustic crevice conditions and increased potential for ODSCC initiation and growth. Molar ratios since February 1993 and particularly since the May 1993 reduction in the control band are supportive of reduced potential for ODSCC growth. Since voltage growth rates across the complete Cycle 4 operating period involve both high and low molar ratio operation, the growth rates cannot be readily related to chemistry improvements. However, the SG C growth data of Table 7-1 for Cycle 4a (includes high molar ratio period) and Cycle 4b (low molar ratio period) can provide some insight on the influence of reduced molar ratio on crack growth. SG C had an average growth rate of 39%/EFY for Cycle 4a and 27%/EFY for Cycle 4b. This reduction in growth rates for Cycle 4b is supportive of the chemistry improvements in the reduction of growth rates. Cycle 5 experience, which will include boric acid addition, will provide more conclusive data for assessing the influence of chemistry enhancements on growth rates.

7.6 Pulled Tube Eddy Current Data

TSP intersections from 4 tubes were removed from the Braidwood-1 SGs to provide the basis for application of Interim Plugging Criteria and to demonstrate the consistency of the Braidwood-1 experience with other plants in which those criteria have been accepted. From SG A, 2 tubes (R37C43 and R42C44) were pulled, and from SG D, 2 tubes (R37C34 and R16C42). Tube R42C44 was cut above the 7H intersection, permitting the extraction of 4 intersections at the 1H, 3H, 5H and 7H elevations. The three remaining tubes were cut below the 7H TSP level on inlet side, permitting the extraction of 9 additional intersections (total of 13), 3 at each of the 1H, 3H, and 5H elevations. Bobbin and RPC data were collected for each of the removed intersections, which resulted in 6 field bobbin indications with corresponding RPC confirmations and 7 NDD intersections. The bobbin field EC graphics for each of the intersections are given in Figures 7-30 to 7-42. The corresponding RPC field graphics for the tubes reported to have bobbin indications are given in Figures 7-43 to 7-48. Table 7-8 summarizes the field analysis results for each of the intersections. With the exception of the 1.04 volt indication at the 3H level on R37C34 and the 2.09 volt indication at TSP-CH on R42C44, the field calls represent voltages in excess of the full APC limit calculated for the 3/4" tubes in Braidwood-1. The 5H level on R16C42 is considered as representing a possible bobbin indication of 0.61 volt, but field RPC was reported as NDD, suggesting the absence of significant ODSCC; evaluation of the tube metallography for this tube may provide some insight into the relative sensitivities of the bobbin and RPC probes for the less developed areas of ODSCC.

Table 7-1 Average Voltage Growth for Braidwood Unit 1

Cycle 4 9/92 - 3/94		Average ΔV				% Growth	
All S/G's	#Indications	Average V_{BOC}	ΔV	efpy	$\Delta V/efpy$	% per cycle	% per efpy
Entire Voltage Range	2654	0.49	0.26	1.147	0.23	53%	48%
$V_{BOC} < .75$	2289	0.41	0.29		0.25	69%	60%
$V_{BOC} \geq .75$	365	0.94	0.13		0.11	14%	16%

S/G A							
Entire Voltage Range	680	0.47	0.41		0.36	86%	75%
$V_{BOC} < .75$	586	0.39	0.43		0.37	113%	97%
$V_{BOC} \geq .75$	94	0.95	0.28		0.24	29%	25%

S/G B							
Entire Voltage Range	261	0.48	0.17		0.15	36%	31%
$V_{BOC} < .75$	230	0.41	0.16		0.14	39%	34%
$V_{BOC} \geq .75$	31	0.94	0.22		0.19	23%	20%

S/G C							
Entire Voltage Range	1030	0.5	0.19		0.17	38%	34%
$V_{BOC} < .75$	876	0.42	0.24		0.21	57%	50%
$V_{BOC} \geq .75$	154	0.95	-0.06		-0.05	-6%	5%

S/G D							
Entire Voltage Range	683	0.49	0.27		0.24	55%	49%
$V_{BOC} < .75$	597	0.43	0.27		0.24	63%	56%
$V_{BOC} \geq .75$	86	0.92	0.29		0.25	31%	27%

Cycle 3 Plugged Tubes

4/91 to 9/92 All S/G's

Entire Voltage Range	167	0.62	0.62	1.12	0.55	100%	89%
$V_{BOC} < .75$	145	0.43	0.65		0.58	151%	135%
$V_{BOC} \geq .75$	22	0.92	0.42		0.38	46%	41%

Cycle 4a - Plugged Tubes

9/92 to 10/93 S/G C

Entire Voltage Range	128	0.71	0.67	0.852	0.79	94%	141%
$V_{BOC} < .75$	71	0.54	0.69		0.81	128%	191%
$V_{BOC} \geq .75$	57	0.92	0.65		0.76	71%	105%

Cycle 4a - All Indications

9/92 to 10/93 S/G C

Entire Voltage Range	428	0.62	0.33	0.852	0.39	53%	79%
$V_{BOC} < .75$	315	0.51	0.31		0.36	61%	91%
$V_{BOC} \geq .75$	113	0.92	0.36		0.42	39%	58%

9/92 to 10/93 to 3/94 - All 1994 Indications Cycle 4a and 4b

S/G C - Cycle 4a

Entire Voltage Range	1010	0.5	0.16	0.852	0.19	32%	48%
$V_{BOC} < .75$	857	0.42	0.19		0.22	45%	68%
$V_{BOC} \geq .75$	153	0.95	-0.01		-0.01	-1%	-2%

S/G C - Cycle 4b

Entire Voltage Range	1069	0.66	0.03	0.295	0.10	5%	16%
$V_{BOC} < .75$	737	0.5	0.07		0.24	14%	46%
$V_{BOC} \geq .75$	332	1.02	-0.04		-0.14	-4%	-13%

Table 7-2. Braidwood #1 TSP ODSCC Indications (A1R04) March, 1994

TSP	Steam Generator A				Steam Generator B				Steam Generator C				Steam Generator D				All Steam Generators			
	#	Volts Max.	Volts Ave.	Growth volts	#	Volts Max.	Volts Ave.	Growth volts	#	Volts Max.	Volts Ave.	Growth volts	#	Volts Max.	Volts Ave.	Growth volts	#	Volts Max.	Volts Ave.	Growth volts
1H	0				0				0				0				0			
3H	344	4.99	0.86	0.37	134	4.25	0.68	0.13	708	2.38	0.72	0.21	403	8.82	0.82	0.3	1590	8.82	0.78	0.27
5H	238	8.33	0.95	0.5	116	2.75	0.59	0.23	235	2.46	0.62	0.16	180	10.44	0.75	0.28	770	10.44	0.75	0.26
7H	91	2.42	0.8	0.35	18	1.37	0.6	0.13	94	2.10	0.64	0.25	77	1.24	0.58	0.17	280	2.74	0.67	0.26
8H	28	3.46	0.83	0.44	3	0.44	0.41	0.08	20	0.92	0.55	0.24	23	1.59	0.57	0.25	74	3.46	0.66	0.31
9H	3	1.02	0.77	0.37	1	0.39	0.39	0.13	1	0.63	0.63	0.1	9	0.53	0.43	0.16	14	1.02	0.51	0.2
10H	2	0.76	0.63	0.22	0				1	0.45	0.45	0.18	1	0.67	0.67	0.43	4	0.76	0.6	0.26
11H	0				0				0				1	0.52	0.52		1	0.52	0.52	

Table 7-3

Braidwood Unit 1 1994 TSP Inspection Summary

bin	S/G A				S/G B				S/G C				S/G D				Combined Population			
	Bobbin		RPC		Bobbin		RPC		Bobbin		RPC		Bobbin		RPC		Bobbin		RPC	
	#ind	cpdf	#obs	%Conf.	#ind	cpdf	#obs	%Conf.	#ind	cpdf	#obs	%Conf.	#ind	cpdf	#obs	%Conf.	#ind	cpdf	#obs	%Conf.
0	0	0.00	0		0	0.00			0	0.00			0	0.00			0	0.00	0	
0.1	1	0.14	0	0.00	0	0.00	0		1	0.09	0	0.00	0	0.00			2	0.07	0	0.00
0.2	6	0.99	0	0.00	5	1.84	0	0.00	7	0.76	1	14.29	3	0.43	0	0.00	21	0.84	1	4.76
0.3	49	7.93	11	22.45	21	8.56	4	19.05	51	5.57	13	25.49	31	4.90	5	16.13	152	6.41	33	21.71
0.4	64	17.00	22	32.81	51	28.31	6	11.76	124	17.28	41	33.06	83	16.86	13	15.86	322	18.20	82	25.47
0.5	92	30.03	46	47.83	43	44.12	9	20.93	156	32.01	68	43.59	111	32.05	39	34.82	402	32.92	162	40.30
0.6	92	43.06	56	56.70	48	61.76	16	33.33	160	47.12	89	55.63	107	48.27	56	52.34	407	47.82	217	53.32
0.7	68	52.69	49	70.59	27	71.69	8	29.63	142	60.53	86	60.56	93	61.67	51	54.84	330	59.90	194	58.79
0.8	45	59.07	26	57.78	25	80.88	8	24.00	117	71.58	86	73.50	68	71.47	41	59.42	255	69.24	159	62.35
0.9	51	66.29	41	80.39	23	89.34	7	30.43	92	80.26	74	80.43	38	76.95	28	73.68	204	76.71	150	73.53
1	44	72.52	38	66.36	3	90.44	1	33.33	64	86.31	57	89.06	34	81.84	29	85.29	145	82.02	125	86.21
1.1	34	77.34	25	73.53	6	92.65	5	83.33	41	90.18	31	75.61	41	87.75	36	87.80	122	86.49	97	79.51
1.2	25	80.88	22	88.00	6	94.85	4	66.67	31	93.11	29	93.55	18	90.35	18	100.00	80	89.42	73	91.25
1.3	25	84.42	25	100.00	2	95.59	0	0.00	18	94.81	17	94.44	14	92.36	13	92.86	59	91.58	55	93.22
1.4	14	86.40	14	100.00	2	96.32	1	50.00	22	96.88	18	81.82	9	93.66	9	100.00	47	93.30	42	89.36
1.5	11	87.96	10	90.91	0	96.32	0		8	97.64	7	87.50	6	94.52	5	83.33	25	94.21	22	88.00
1.6	9	89.24	9	100.00	2	97.06	2	100.00	7	98.30	6	85.71	4	95.10	3	75.00	22	95.02	20	90.91
1.7	13	91.08	13	100.00	0	97.06	0		3	98.58	3	100.00	6	95.97	6	100.00	22	95.83	22	100.00
1.8	8	92.21	8	100.00	2	97.79	2	100.00	3	98.87	3	100.00	3	96.40	2	66.67	16	96.41	15	93.75
1.9	7	93.20	7	100.00	0	97.79	0		3	99.15	3	100.00	4	96.97	4	100.00	14	96.92	14	100.00
2	6	94.05	6	100.00	0	97.79	0		2	99.34	2	100.00	3	97.41	3	100.00	11	97.33	11	100.00
2.1	5	94.76	5	100.00	2	98.53	1	50.00	1	99.43	1	100.00	0	97.41			8	97.62	7	87.50
2.2	8	95.89	8	100.00	0	98.53			3	99.72	3	100.00	4	97.98	4	100.00	15	98.17	15	100.00
2.3	3	96.32	3	100.00	0	98.53			0	99.72	0		1	98.13	1	100.00	4	98.32	4	100.00
2.4	1	96.46	1	100.00	0	98.53			1	99.81	1	100.00	0	98.13			2	98.39	2	100.00
2.5	4	97.03	4	100.00	1	98.90	1	100.00	1	99.91	1	100.00	1	98.27	1	100.00	7	98.65	7	100.00
2.6	2	97.31	2	100.00	0	98.90			0	99.91	0		1	98.41	1	100.00	3	98.76	3	100.00
2.7	1	97.45	1	100.00	0	98.90			0	99.91	0		0	98.41			1	98.79	1	100.00
2.8	0	97.45	0		1	99.26	1	100.00	1	100.00	1	50.00	1	98.56	1	100.00	3	98.90	3	100.00
2.9	0	97.45	0		0	99.26			0	100.00			1	98.70	1	100.00	1	98.94	1	100.00
3	3	97.88	3	100.00	0	99.26			0	100.00			0	98.70			3	99.05	3	100.00
3.2	3	98.30	3	100.00	0	99.26			0	100.00			1	98.85	1	100.00	4	99.19	4	100.00
3.4	2	98.58	2	100.00	0	99.26			0	100.00			1	98.99	1	100.00	3	99.30	3	100.00
3.6	3	99.01	3	100.00	0	99.26			0	100.00			0	98.99			3	99.41	3	100.00
3.8	1	99.15	1	100.00	1	99.63	1	100.00	0	100.00			1	99.14	1	100.00	3	99.52	3	100.00
4	2	99.43	2	100.00	0	99.63			0	100.00			2	99.42	2	100.00	4	99.67	4	100.00
4.2	1	99.58	1	100.00	0	99.63			0	100.00			0	99.42			1	99.71	1	100.00
4.4	0	99.58	0		1	100.00	1	100.00	0	100.00			1	99.57	1	100.00	2	99.78	2	100.00
4.6	0	99.58	0		0	100.00			0	100.00			0	99.57			0	99.78	0	
4.8	0	99.58	0		0	100.00			0	100.00			0	99.57			0	99.78	0	
5	1	99.72	1	100.00	0	100.00			0	100.00			0	99.57			1	99.82	1	100.00
5.5	0	99.72	0		0	100.00			0	100.00			1	99.71	1	100.00	1	99.85	1	100.00
6	1	99.86	1	100.00	0	100.00			0	100.00			0	99.71			1	99.89	1	100.00
6.5	0	99.86	0		0	100.00			0	100.00			0	99.71			0	99.89	0	
7	0	99.86	0		0	100.00			0	100.00			0	99.71			0	99.89	0	
7.5	0	99.86	0		0	100.00			0	100.00			0	99.71			0	99.89	0	
8	0	99.86	0		0	100.00			0	100.00			0	99.71			0	99.89	0	
8.5	1	100.00	1	100.00	0	100.00			0	100.00			0	99.71			1	99.93	1	100.00
9	0	100.00	0		0	100.00			0	100.00			1	99.86	1	100.00	1	99.96	1	100.00
9.5	0	100.00	0		0	100.00			0	100.00			0	99.86			0	99.96	0	
10	0	100.00	0		0	100.00			0	100.00			0	99.86			0	99.96	0	
10.5	0	100.00	0		0	100.00			0	100.00			1	100.00	1	100.00	1	100.00	1	100.00
706				470	272			76	1059			641	694			379	2731			

Table 7-4. Braidwood Unit 1 10/93 Inspection S/G C Only

Elevation	Number of Indications
1H	0
3H	346
5H	75
7H	23
8H	2
9H	1
10H	1
11H	1
Note: All Bobbin Indications: No RPC Confirmations	

**Table 7-5. Braidwood Unit 1 9/92 Inspection
TSP Indication Distribution in Plugged Tubes**

Elevation	A	B	C	L	Total
1H	0	0	0	0	0
3H	32	18	94	49	193
5H	14	5	15	15	49
7H	5	3	5	2	15

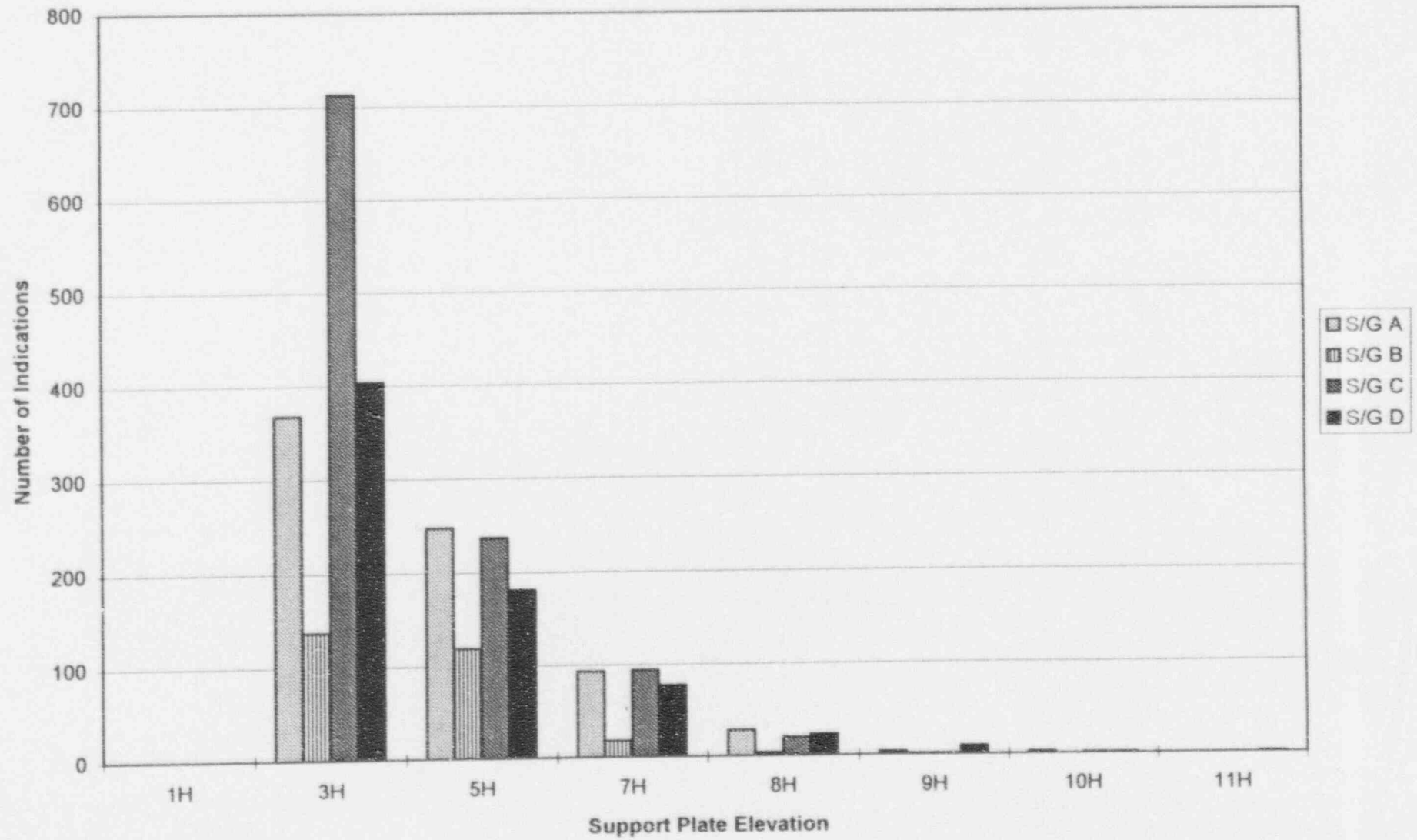
Table 7-7. Braidwood Unit 1 Summary of Largest Bobbin Voltage Growth Rates for Cycle 4

S/G	Tube		Elevation	EOC 4 Signal Size		Boc 4 Bobbin	Growth	New Ind.
	Row	Col		Bobbin	RPC			
D	37	34	5H	10.44	8.62	0.68	9.76	Yes
D	23	12	3H	8.82	8.78	0.76	8.06	Yes
A	45	41	5H	8.33	8.25	1.66	6.67	Yes
A	18	23	5H	5.54	6.72	0.50	5.04	Yes
A	27	43	3H	4.99	4.82	0.32	4.67	Yes
D	12	9	3H	5.02	4.01	0.76	4.26	Yes
D	11	9	3H	4.28	5.16	0.39	3.89	Yes
B	7	9	3H	4.25	4.13	0.55	3.70	Yes
D	19	7	3H	3.95	3.79	0.29	3.66	Yes
A	6	91	5H	4.18	2.01	0.68	3.50	DSI 0.52V No RPC Conf.
A	8	60	3H	3.91	3.29	0.47	3.44	Yes
A	29	88	3H	3.91	1.55	0.49	3.42	Yes
D	35	29	3H	3.62	1.21	0.32	3.30	Yes
A	6	19	8H	3.46	3.05	0.41	3.05	Yes
A	43	35	5H	3.52	3.53	0.49	3.03	Yes
D	33	20	3H	3.83	3.68	0.80	3.03	DSI 0.73V No RPC Conf.
A	5	13	5H	3.30	0.9	0.49	2.81	Yes
A	37	88	3H	2.99	3.35	0.27	2.72	Yes
A	30	24	5H	2.93	2.02	0.28	2.65	Yes
B	15	88	3H	3.62	5.64	1.00	2.62	Yes
A	42	44	3H	3.73	3.11	1.13	2.60	Yes
D	11	12	3H	3.21	3.41	0.63	2.58	Yes
D	16	42	3H	3.12	3.43	0.54	2.58	Yes
A	45	55	3H	3.02	2.79	0.59	2.43	Yes
A	33	75	3H	3.04	3.08	0.65	2.41	Yes
A	32	85	3H	2.46	1.62	0.21	2.25	Yes
A	42	54	5H	2.56	2.31	0.34	2.22	Yes
A	47	75	5H	3.44	0.4	1.23	2.21	Yes
A	35	42	3H	2.96	3.07	0.76	2.2	Yes
D	2	105	3H	2.84	2.32	0.67	2.17	Yes
D	32	27	5H	2.48	2.52	0.36	2.12	Yes
A	45	26	7H	2.42	2.32	0.34	2.08	Yes
A	4	12	5H	3.06	3.19	1.01	2.05	Yes
A	4	16	3H	3.23	2.08	1.18	2.05	Yes
A	10	67	5H	2.48	1.56	0.43	2.05	Yes
C	20	24	3H	2.38	1.56	0.35	2.03	Yes

Table 7-8					
Braidwood Unit 1 A1RO4 Pulled Tube EC Results					
Tube	I.D.	Bobbin Voltage	Bobbin Call	RPC Call	RPC Voltage
SG A					
R27C43	1H	-	NDD	NDD	-
	3H	4.88	85%	SAI	5.28
	5H	-	NDD	NDD	-
R42C44	1H	-	NDD	NDD	-
	3H	3.73	68%	MAI	3.24 max.
	5H	2.09	49%	SAI	1.62
	7H	-	NDD	NDD	-
SG D					
R37C34	1H	-	NDD	NDD	-
	3H	1.04	92%	SAI	0.31
	5H	10.44	82%	SAI	8.77
R16C42	1H	-	NDD	NDD	-
	3H	3.12	70%	MAI	1.70 max.
	5H	0.61 *	NDD	NDD	-

* Indication not reported in field inspection.

Figure 7-1 Braidwood Unit 1 Number of Indications as Function of Elevation



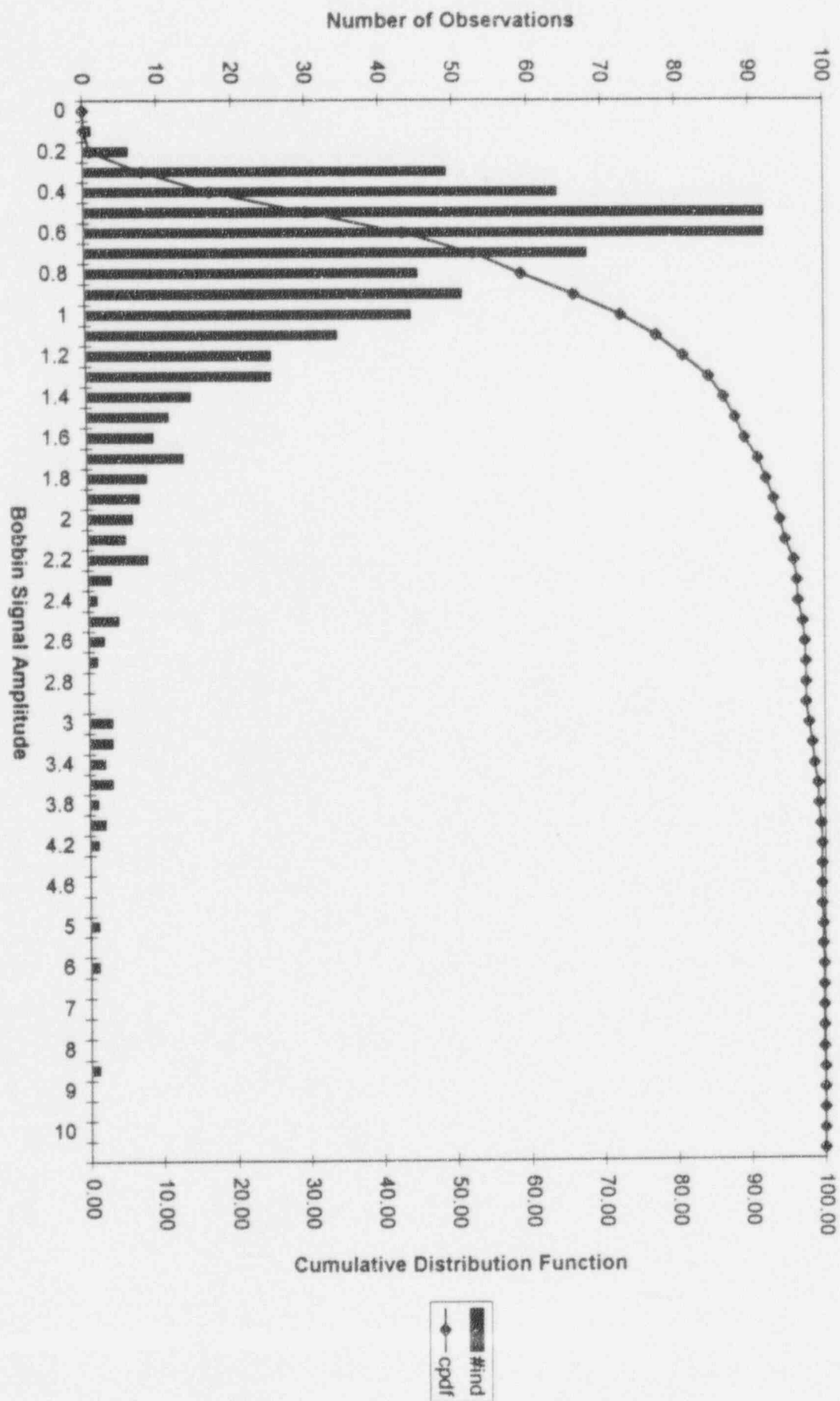


Figure 7-2 Braidwood Unit 1 S/G A Bobbin Statistics 4/94 Inspection

Figure 7-3 Braidwood Unit 1 S/G B Bobbin Statistics 4/94 Inspection

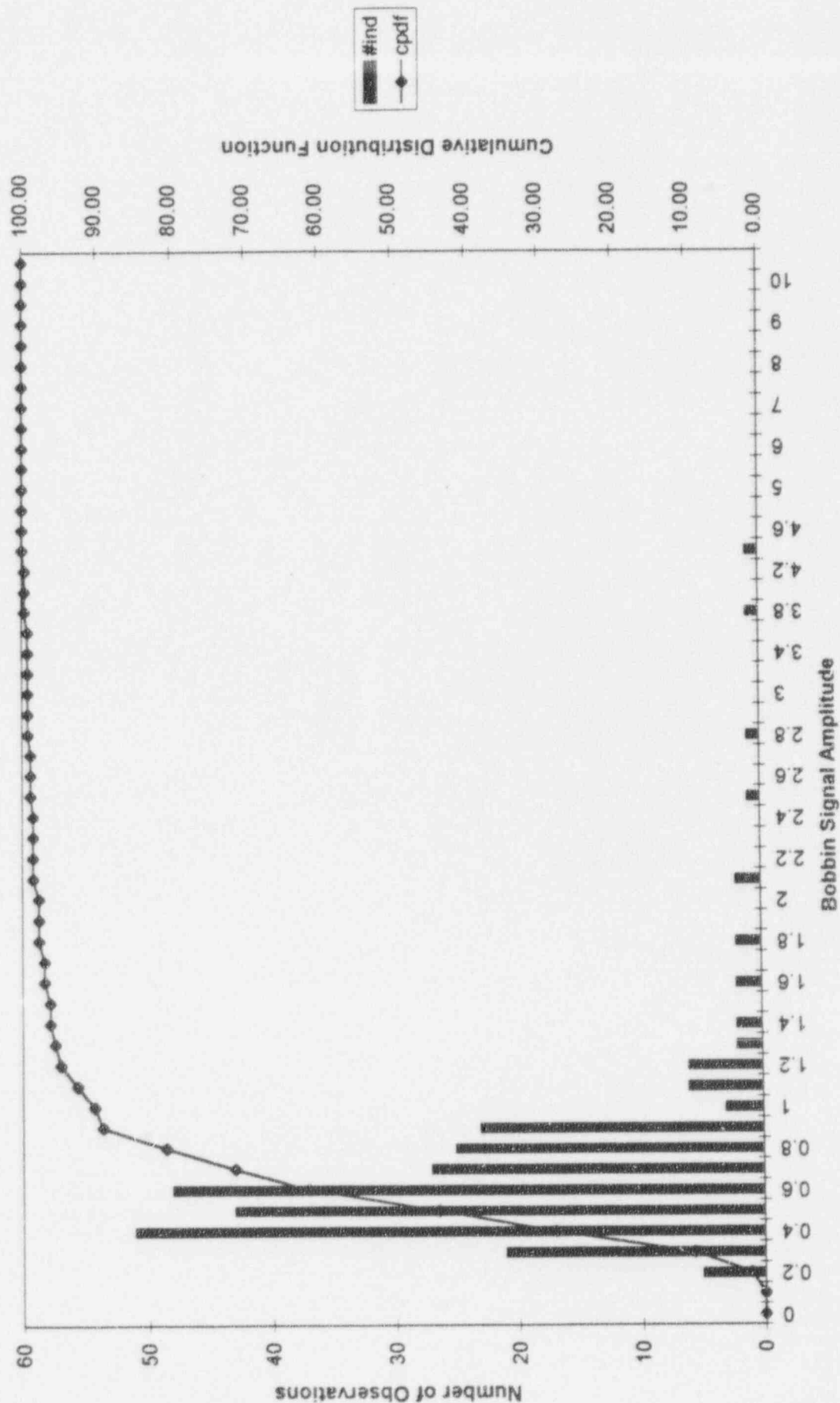
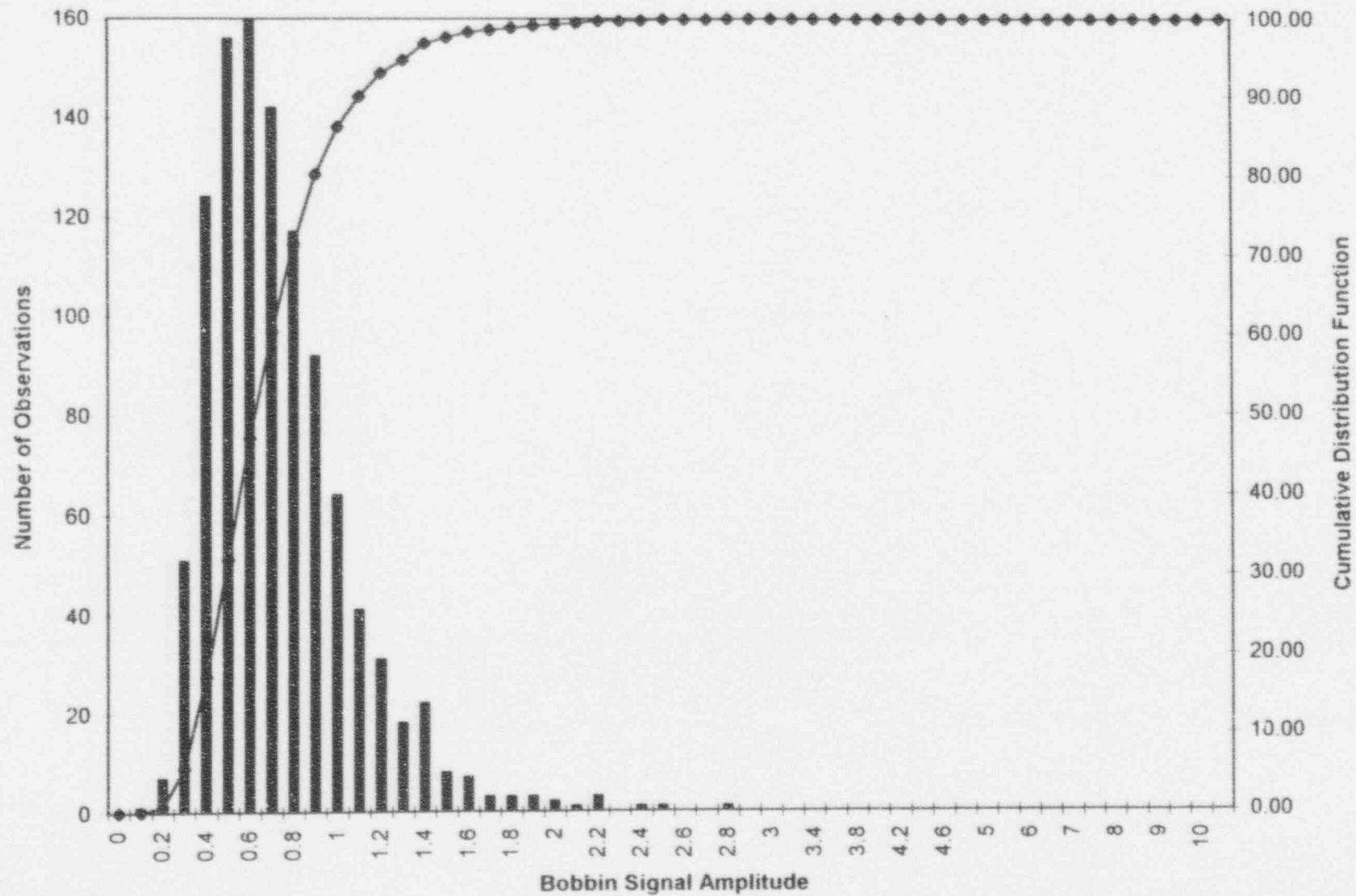


Figure 7-4 Braidwood Unit 1 S/G C Bobbin Statistics 4/94 Inspection



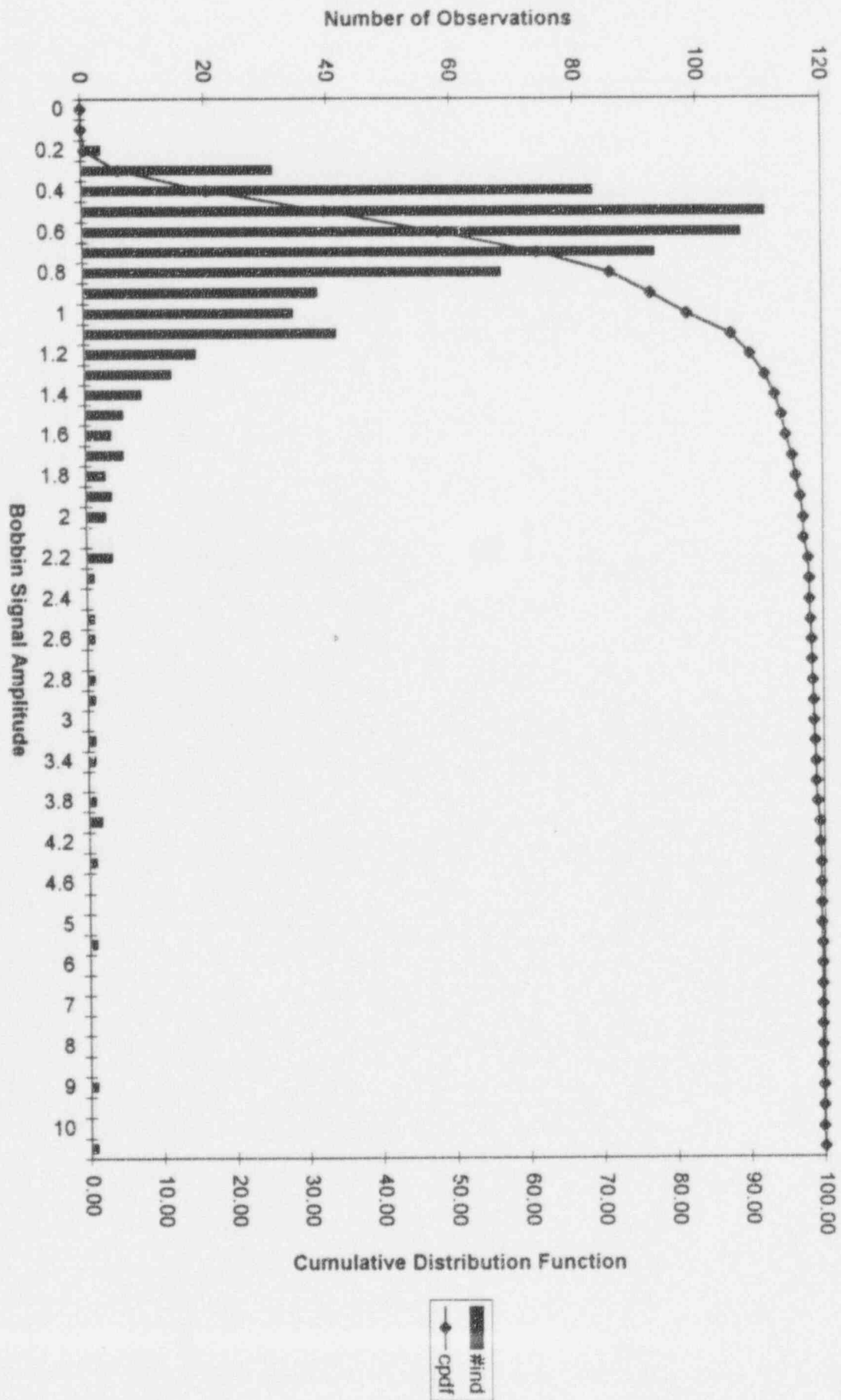


Figure 7-5 Braidwood Unit 1 S/G D Bobbin Statistics 4/94 Inspection

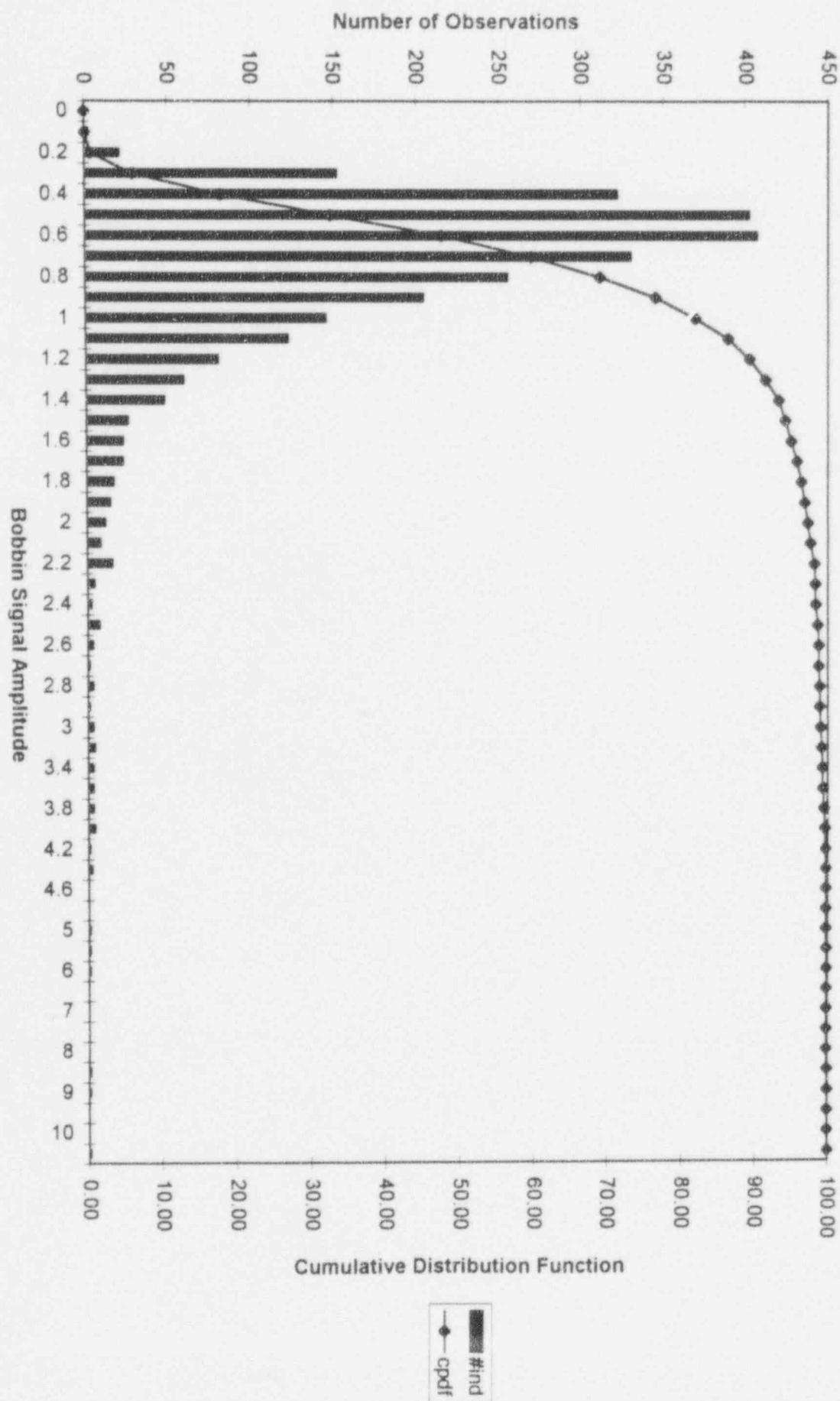


Figure 7-6 Braidwood Unit 1 All S/G's - Bobbin Statistics 4/94 Inspection

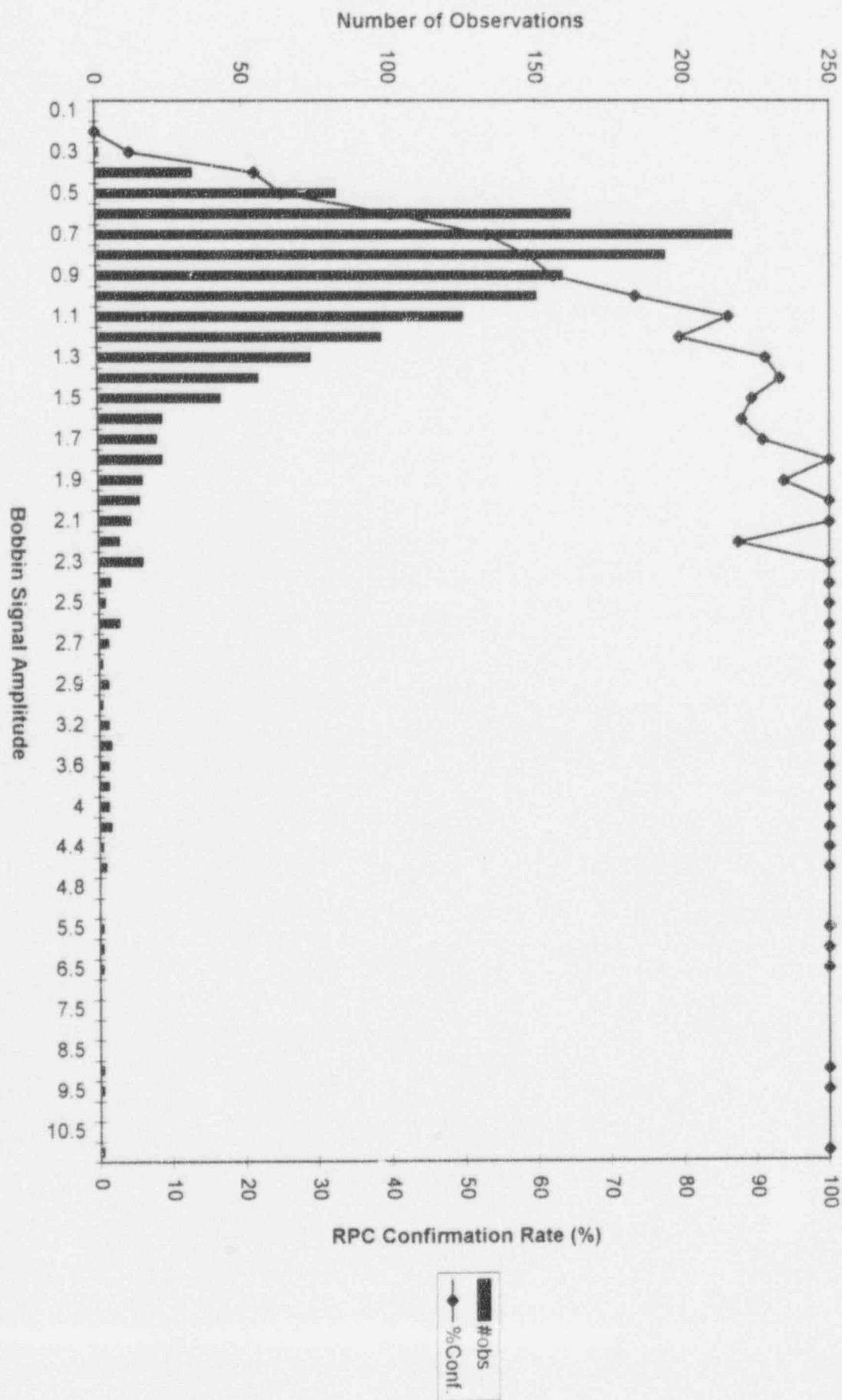


Figure 7-7 Braidwood Unit 1 All S/G's RPC Statistics 4/94 Inspection

Figure 7-8. Braidwood Unit 1 SG C TSP Amplitude Distribution

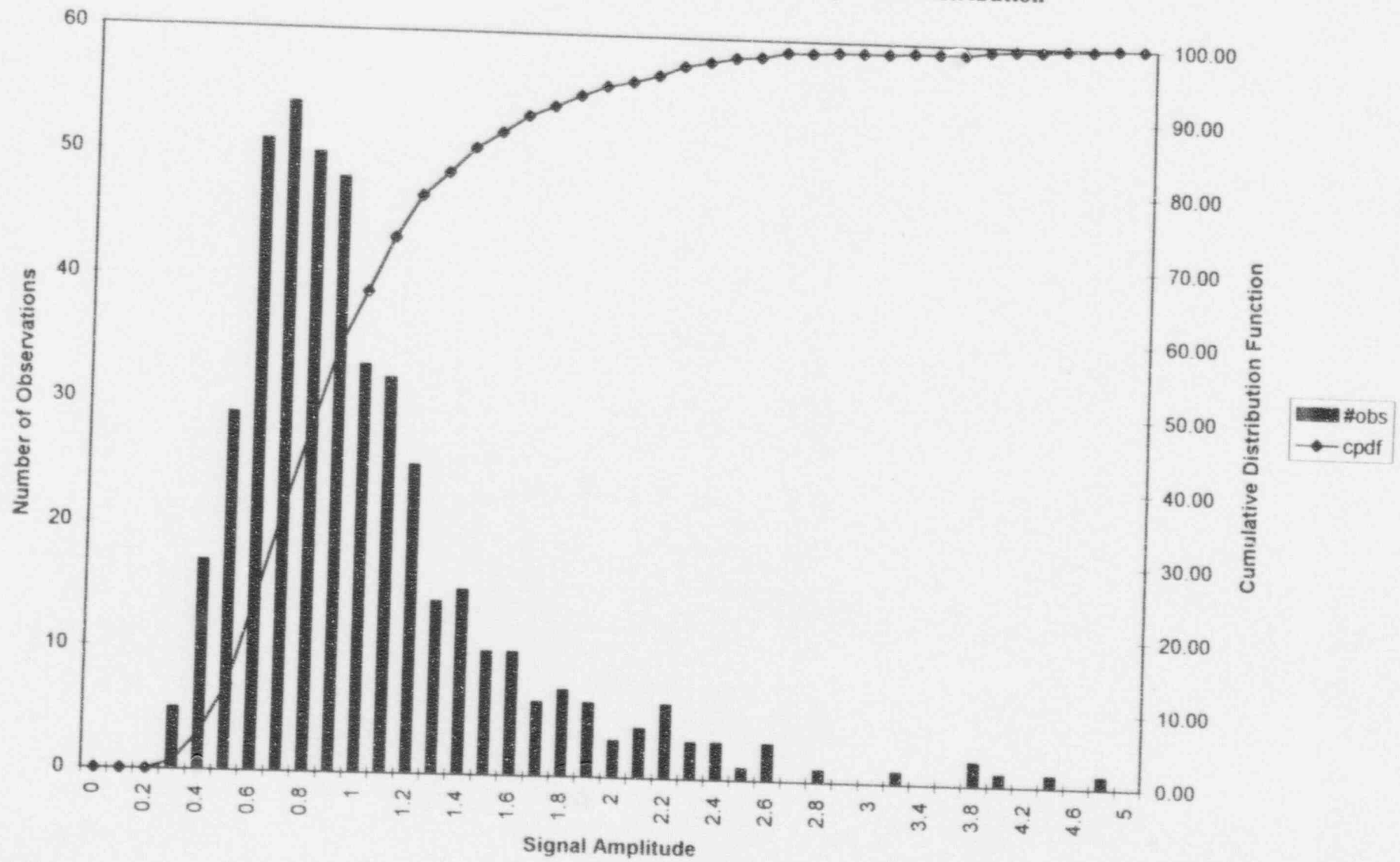


Figure 7-9. Braidwood Unit 1 9/92 TSP Indication Distribution

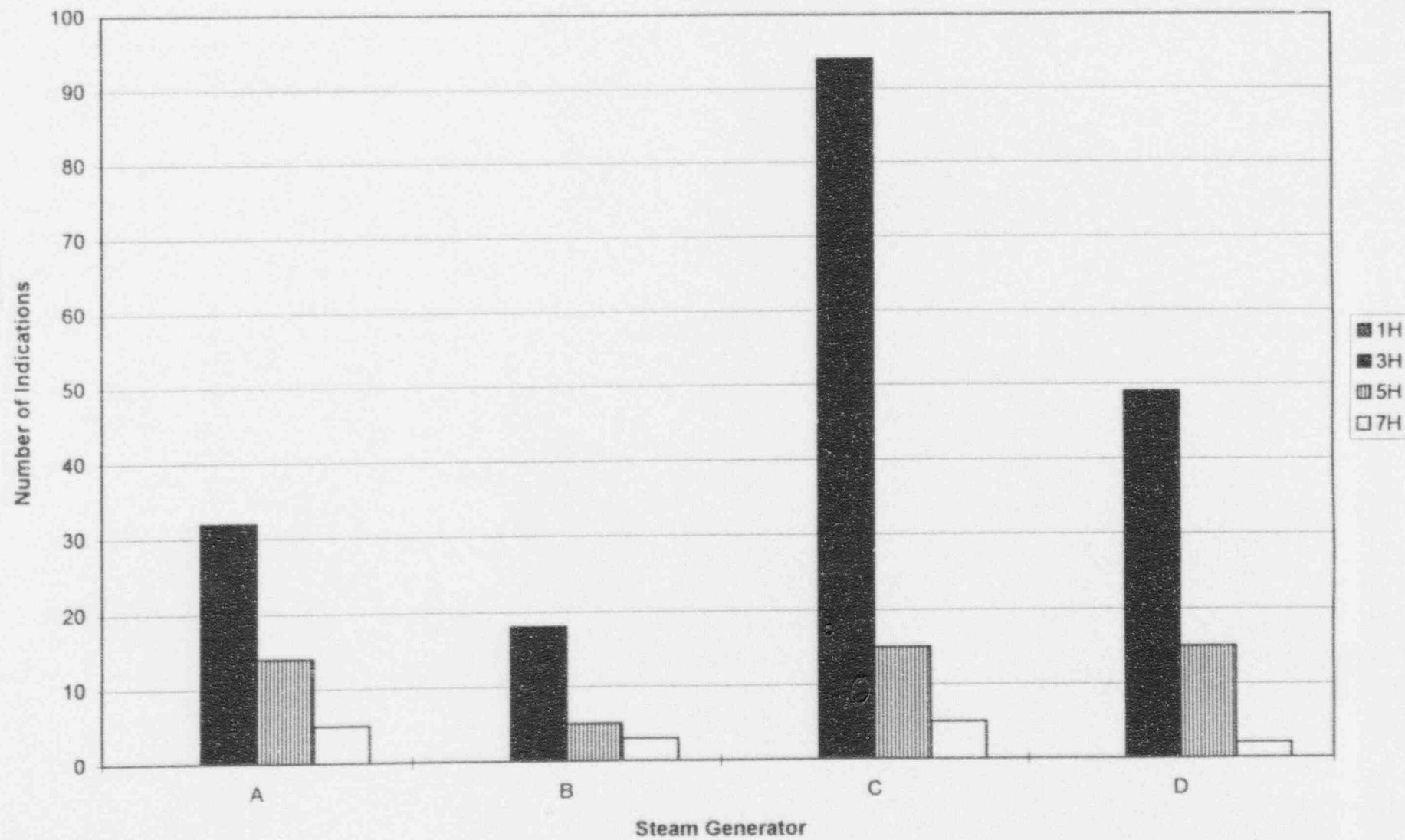


Figure 7-10. Braidwood Unit 1 9/92 Inspection Amplitude Distribution of Confirmed Bobbin Indications

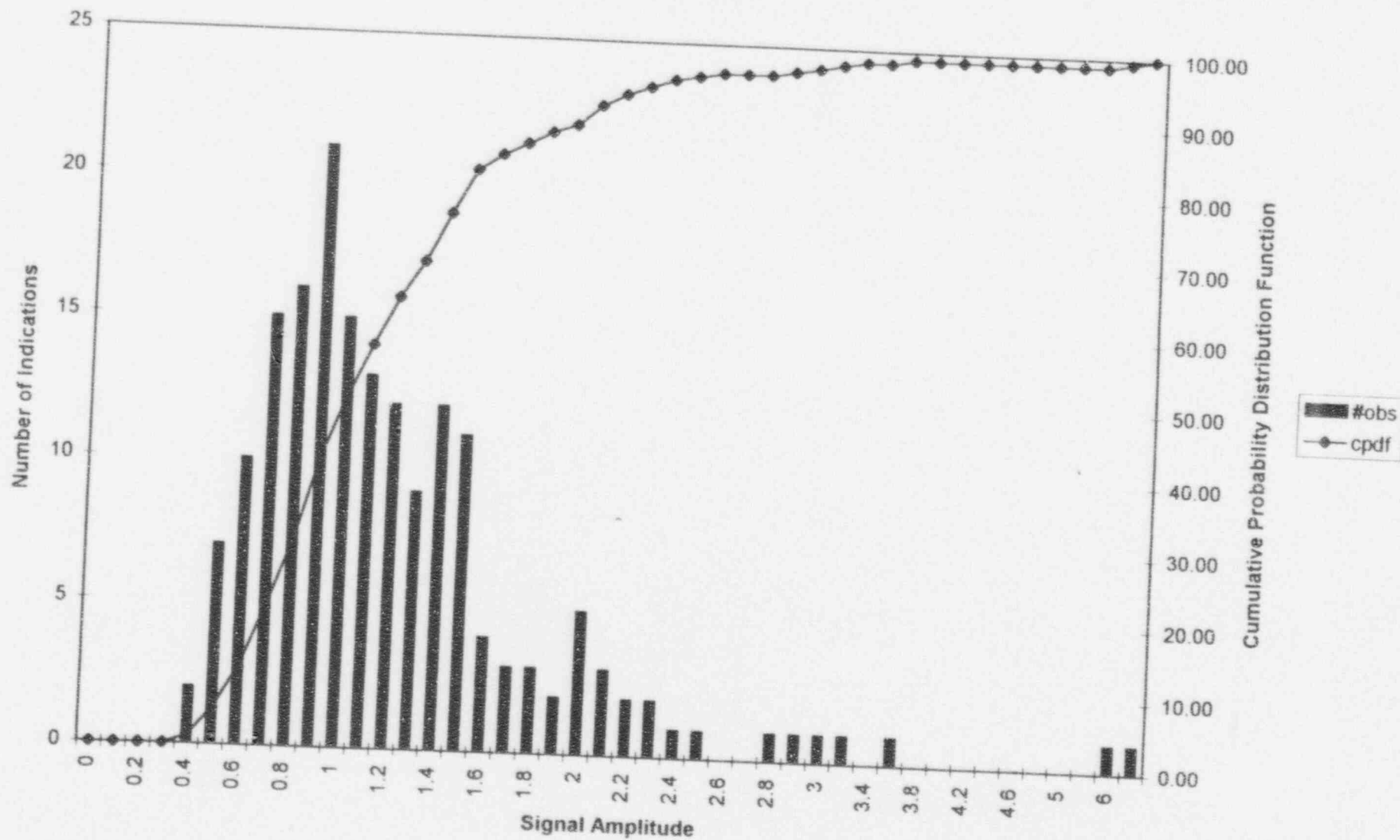
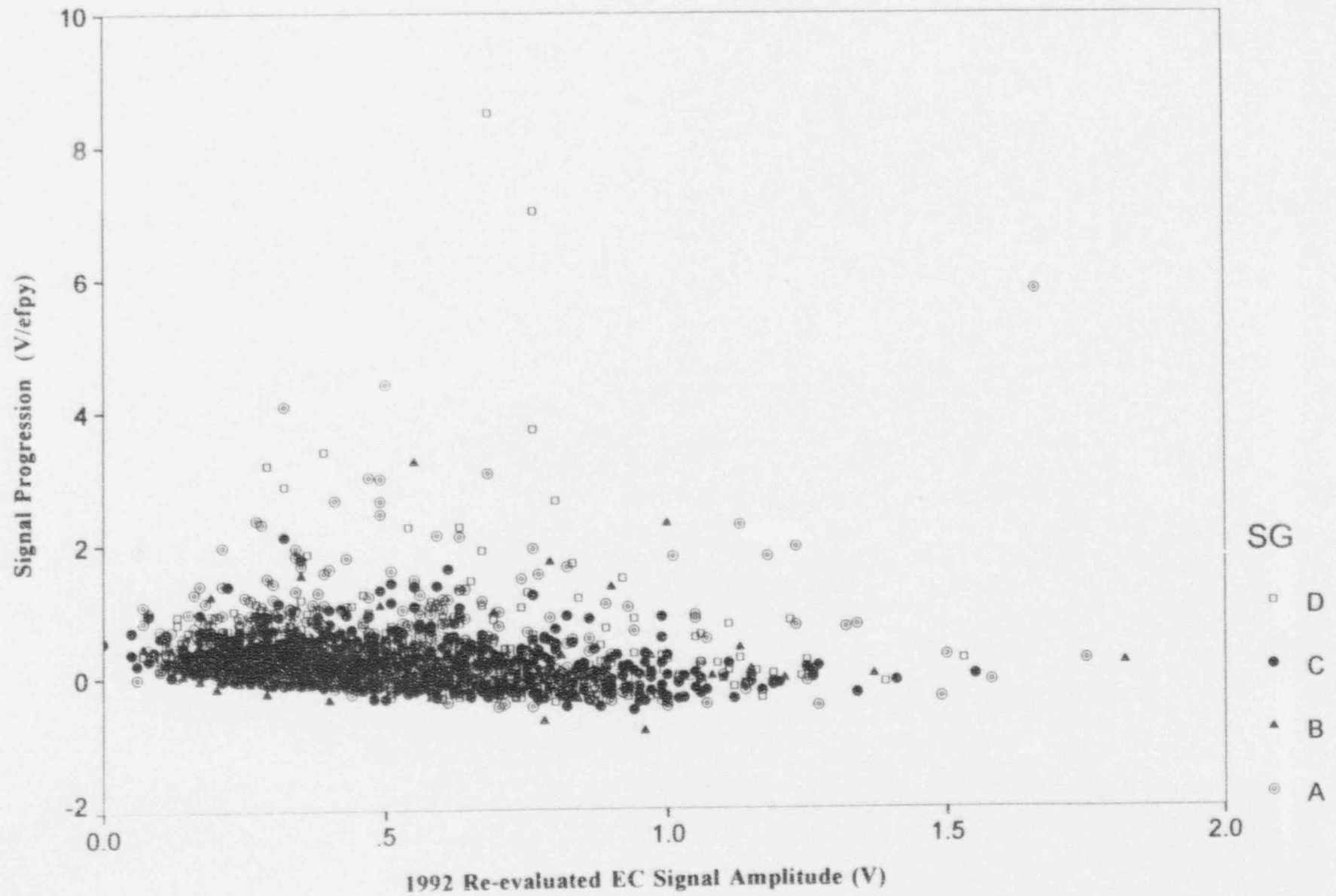
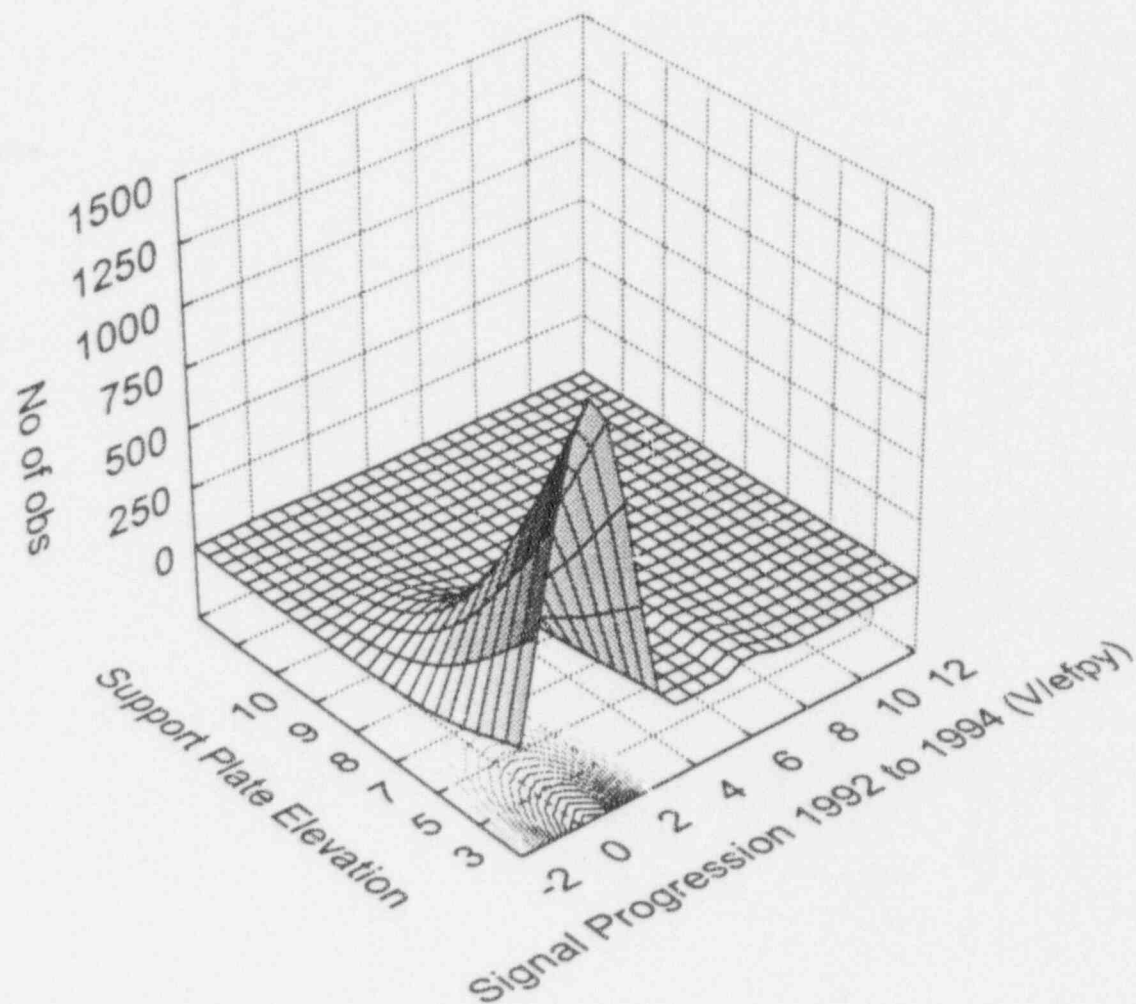


Figure 7-11. Braidwood Unit 1 1994 Inspection, Support Plate ODSCC Signal Progression





**Figure 7-12. Braidwood Unit 1 1994 Inspection Results,
Support Plate ODSCC EC Signal Progression**

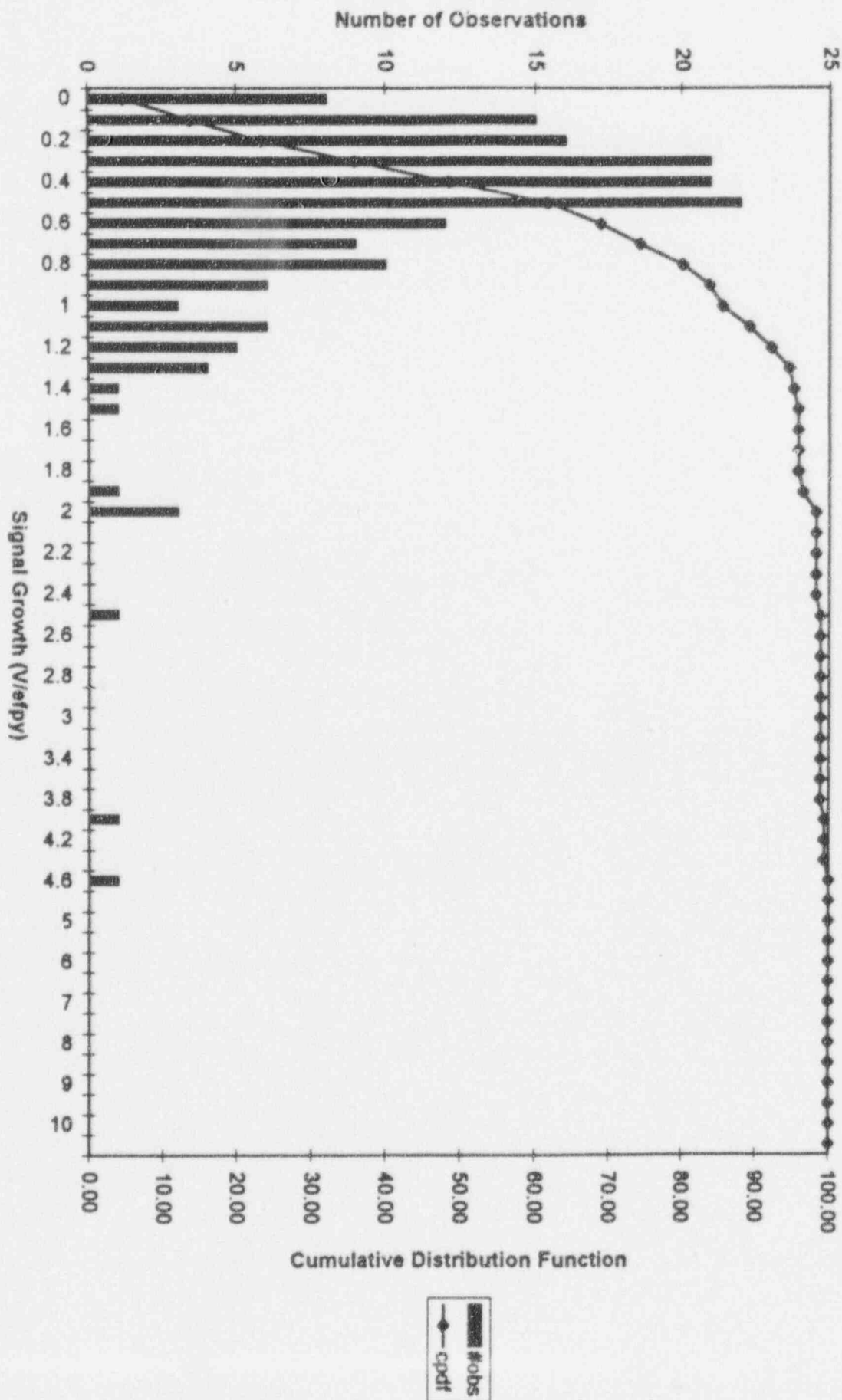


Figure 7-13. Braidwood Unit 1 TSP Bobbin Signal Progression 1991 - 1992, All SGs

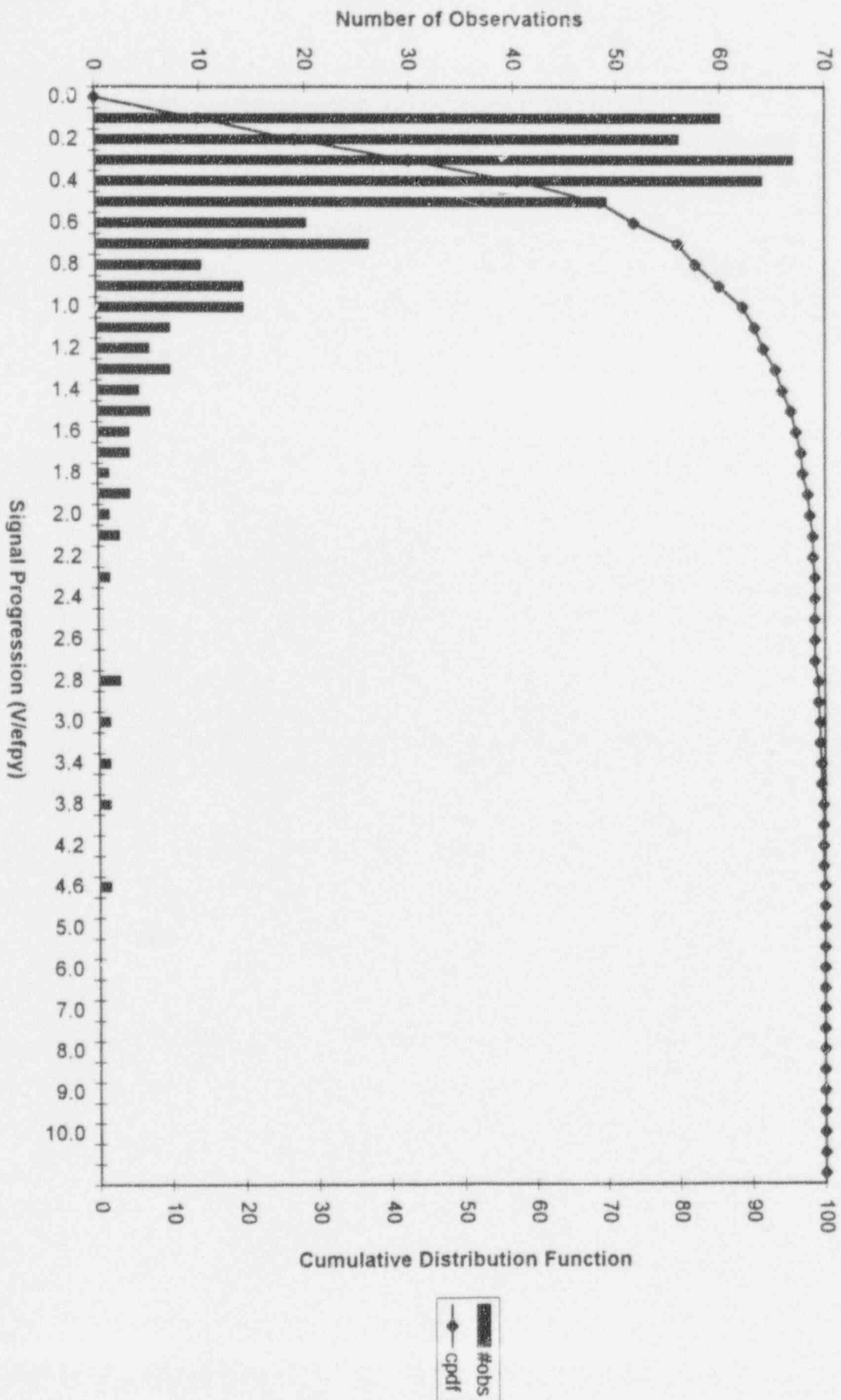


Figure 7-14. Braidwood Unit 1 TSP Robbin Signal Progression 1992 - 1993, SG C

Figure 7-15 Braidwood Unit 1 S/G A TSP Bobbin Progression 92-94

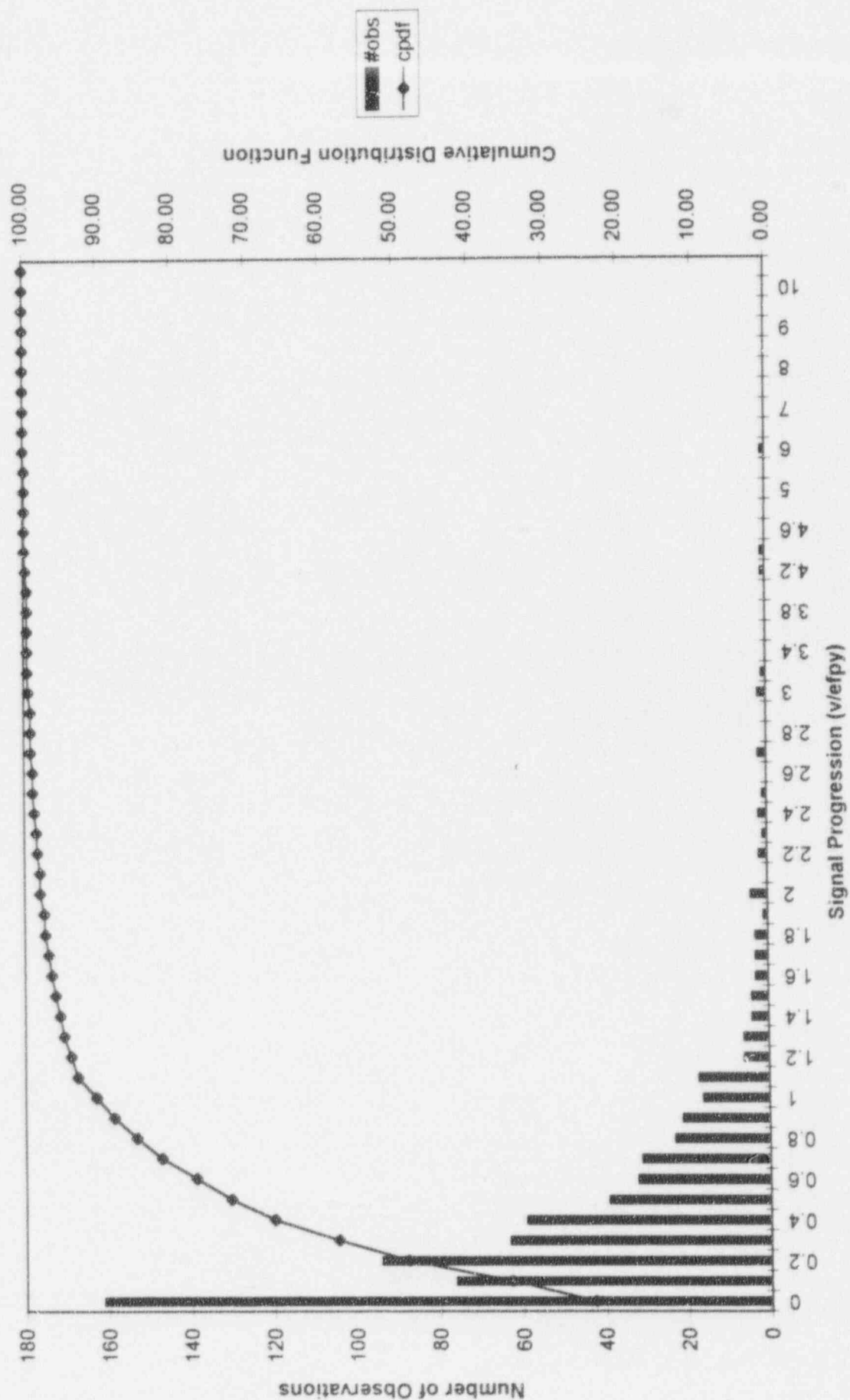


Figure 7-16 Braidwood Unit 1 S/G B TSP Bobbin Progression 92-94

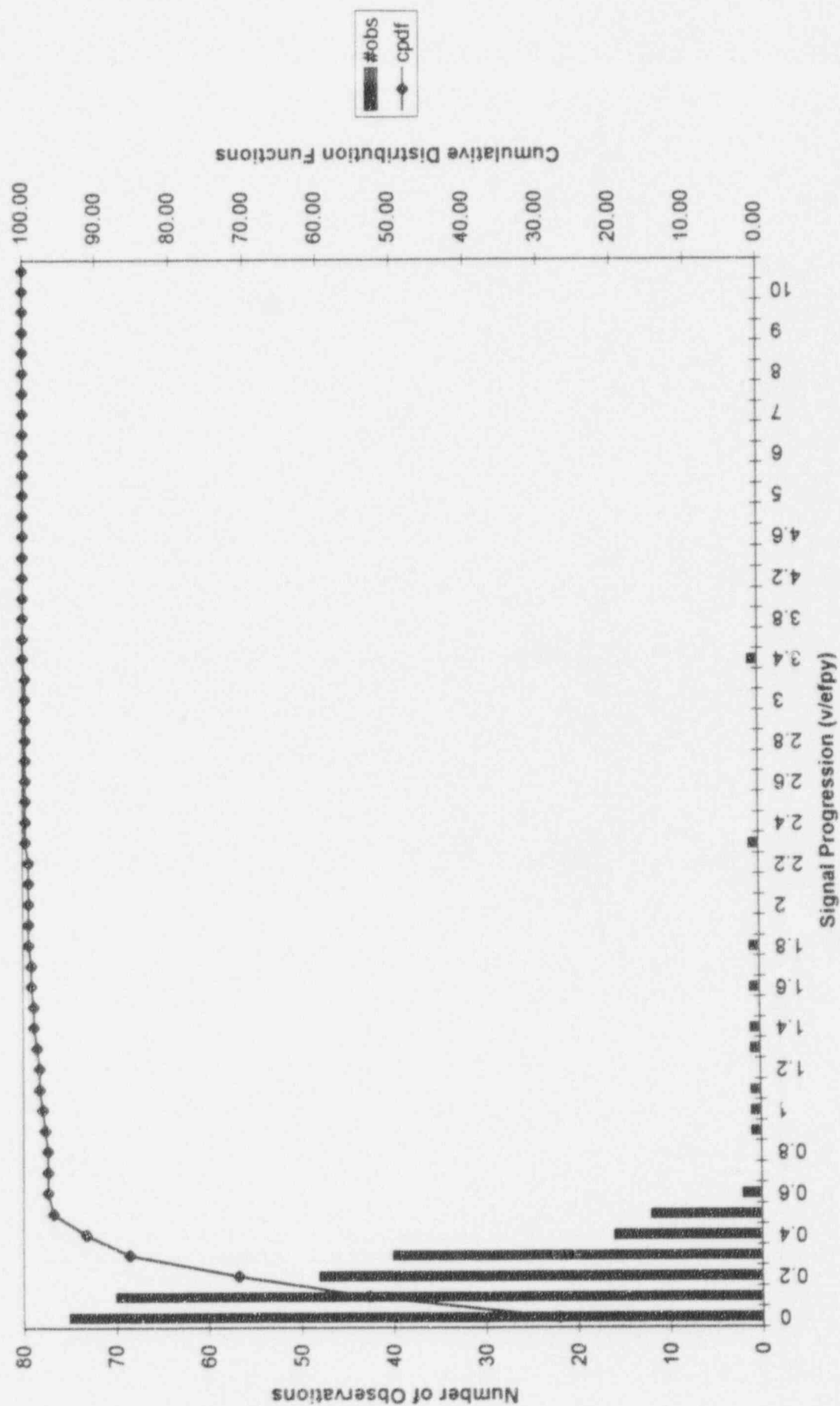
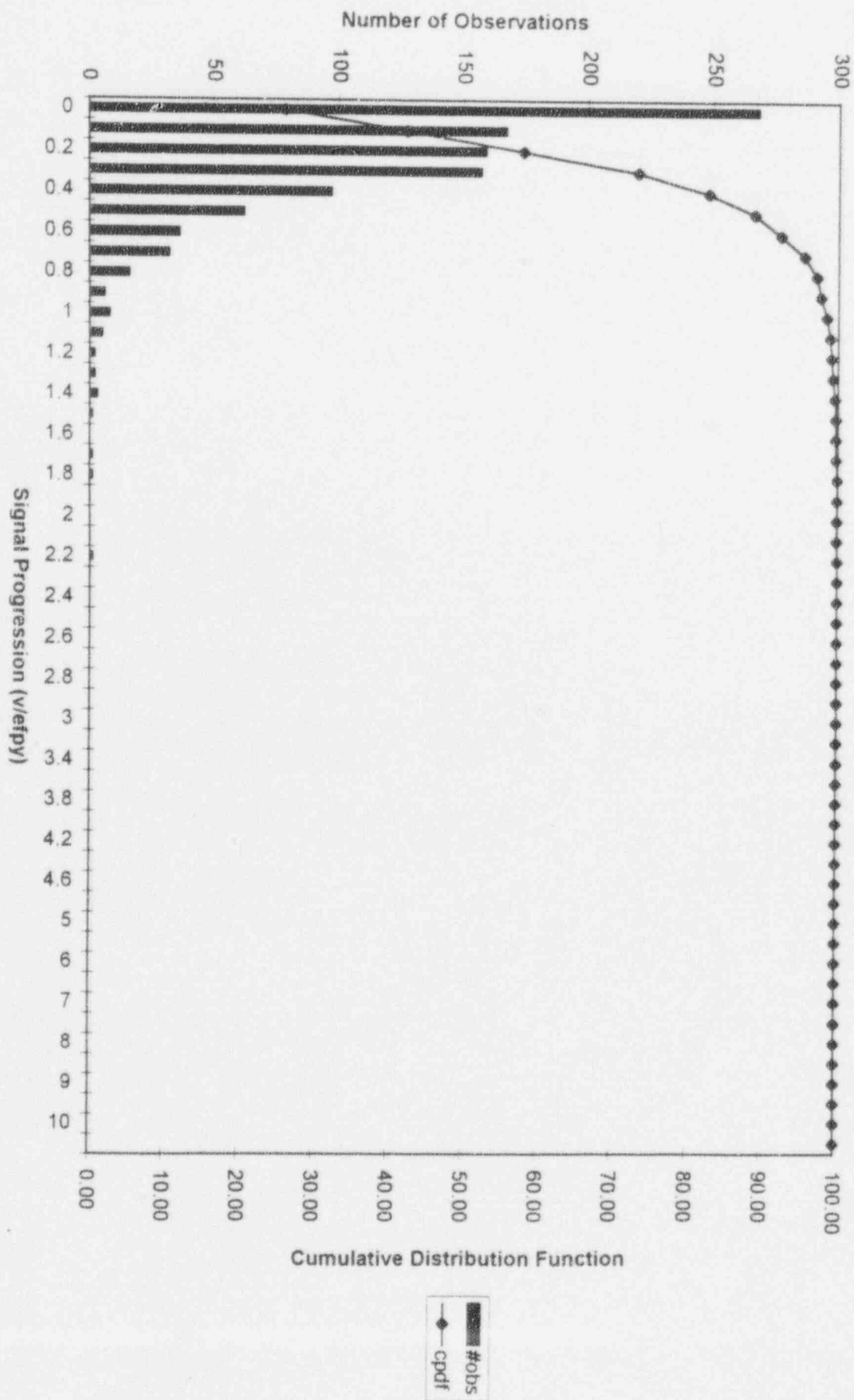


Figure 7-17 Braidwood Unit 1 S/G C TSP Bobbin Progression 92-94



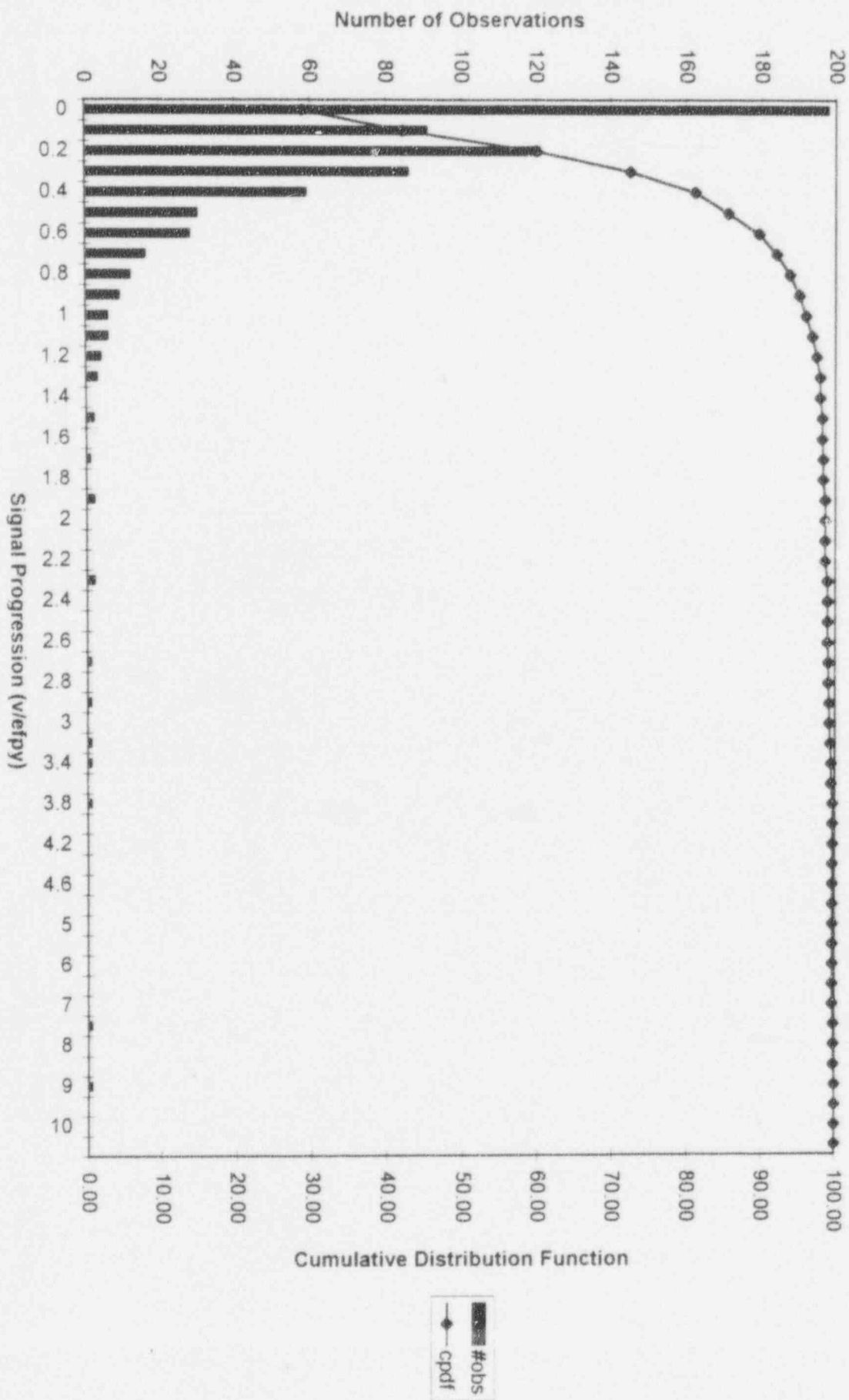


Figure 7-18 Braidwood Unit 1 S/G D TSP Bobbin Progression 92-94

Figure 7-19

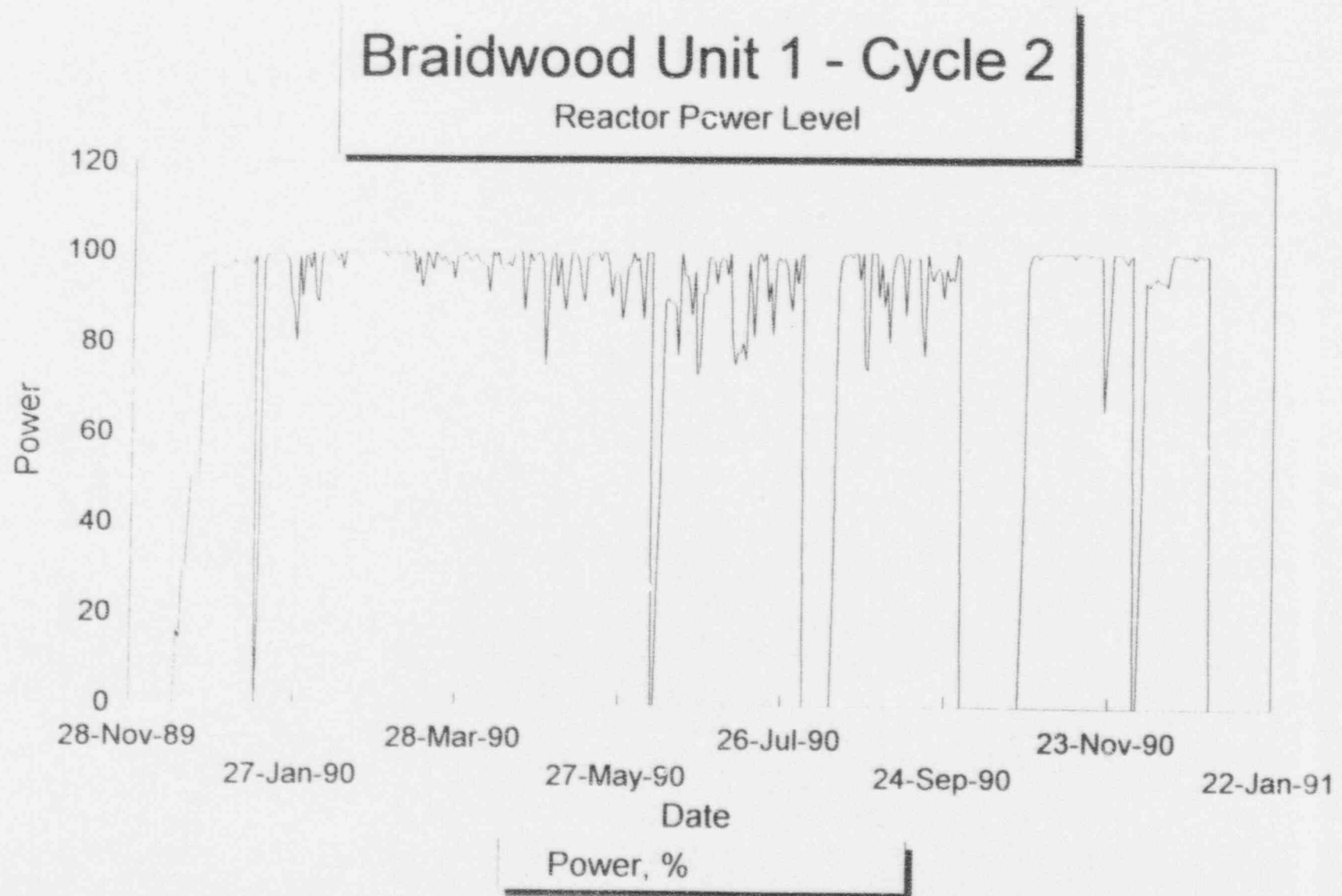


Figure 7-20

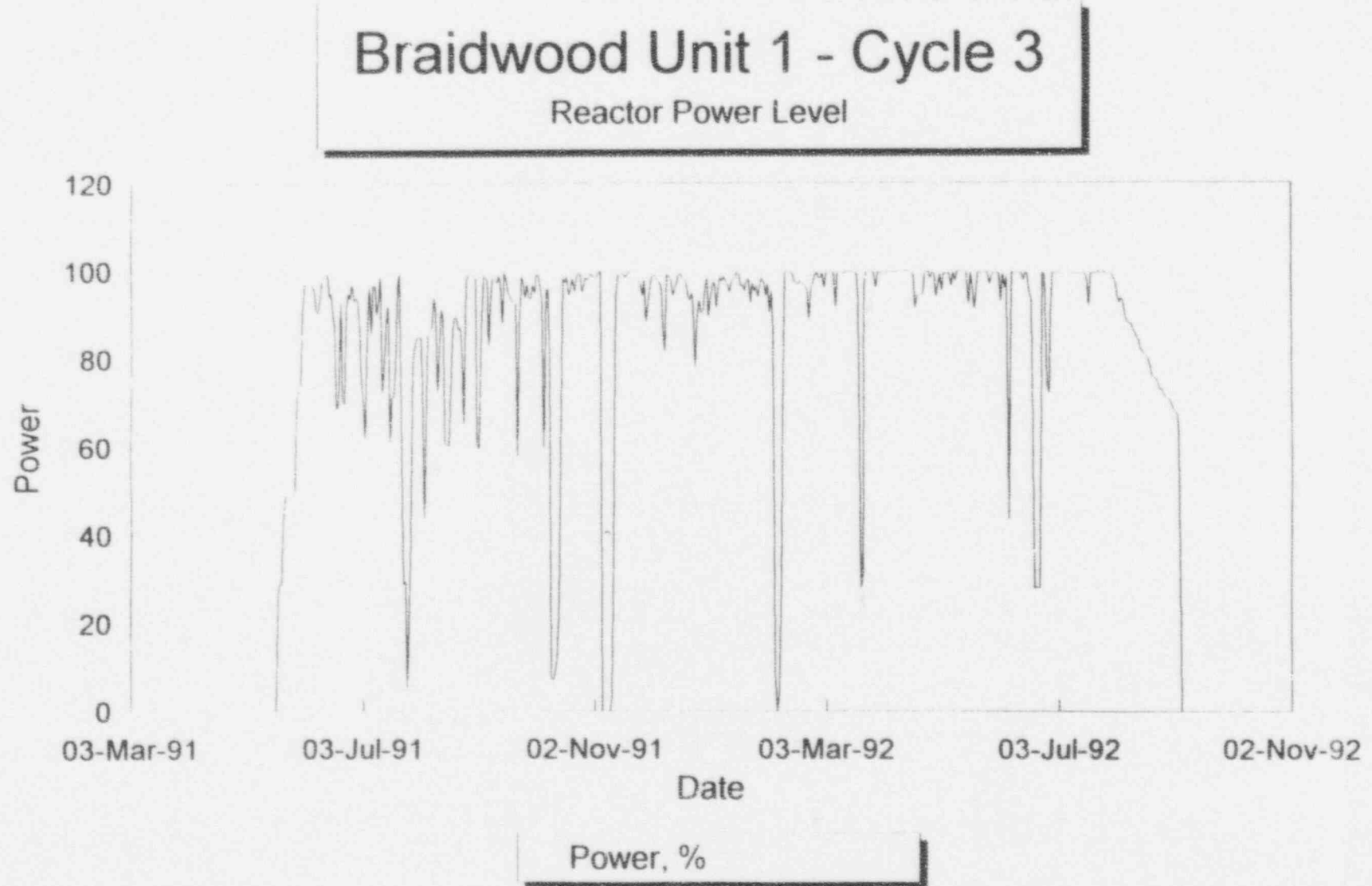


Figure 7-21

Braidwood Unit 1 - Cycle 4

Reactor Power Level

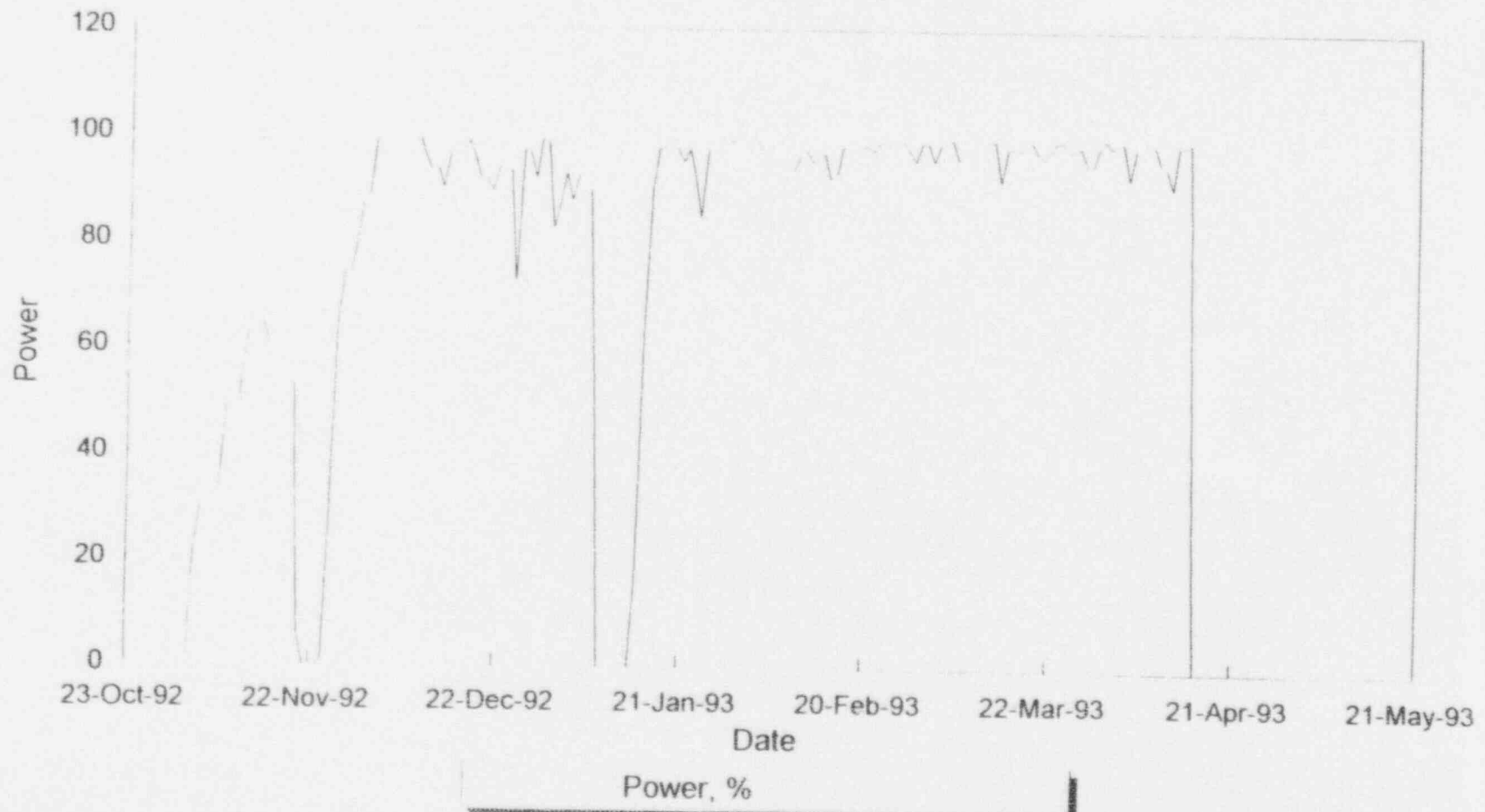


Figure 7-22

Braidwood Unit 1 Cycle 2

Sodium to Chloride Molar Ratio

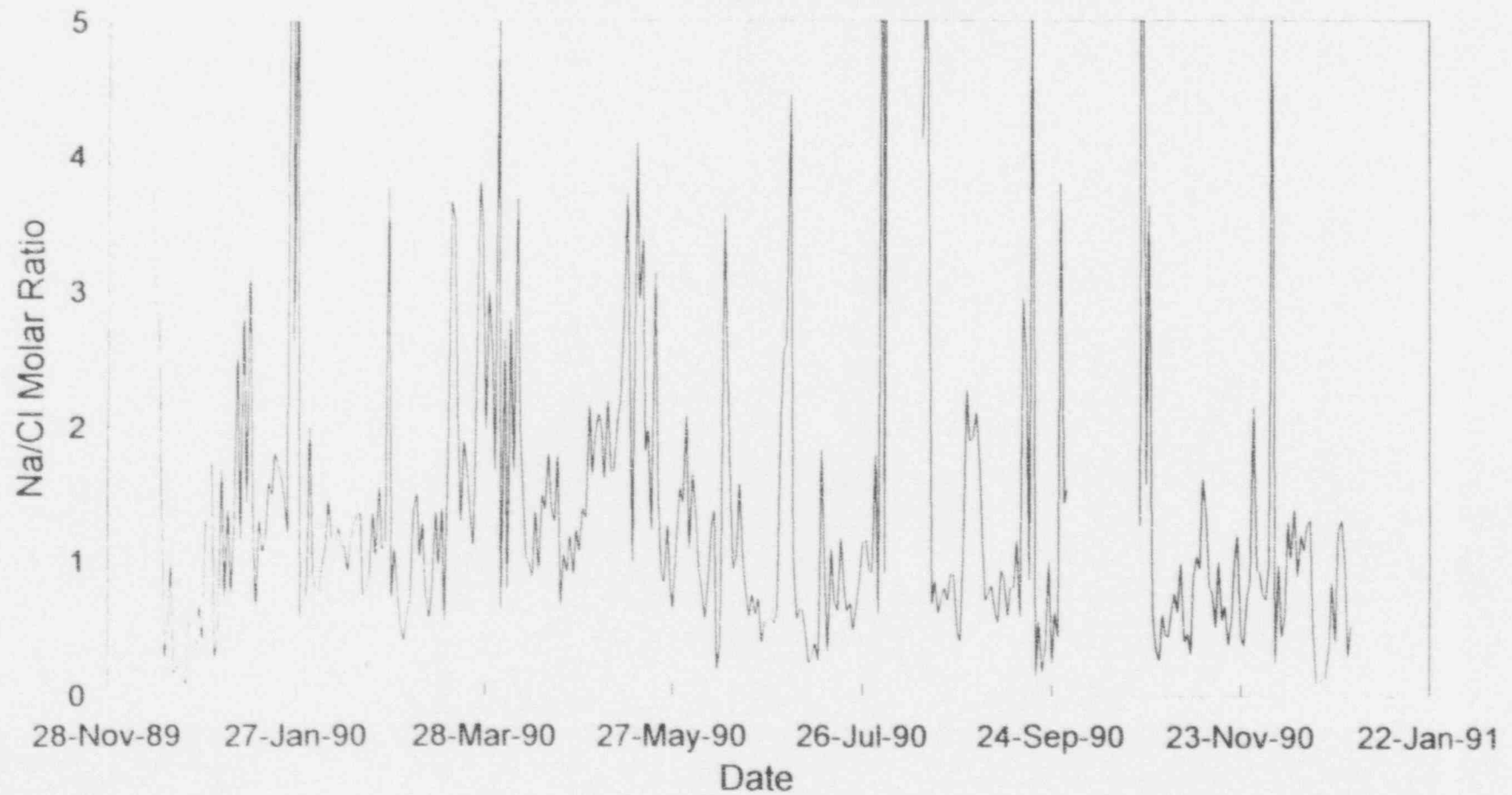


Figure 7-23

Braidwood Unit 1 - Cycle 3

SG Blowdown Sodium to Chloride Molar Ratio

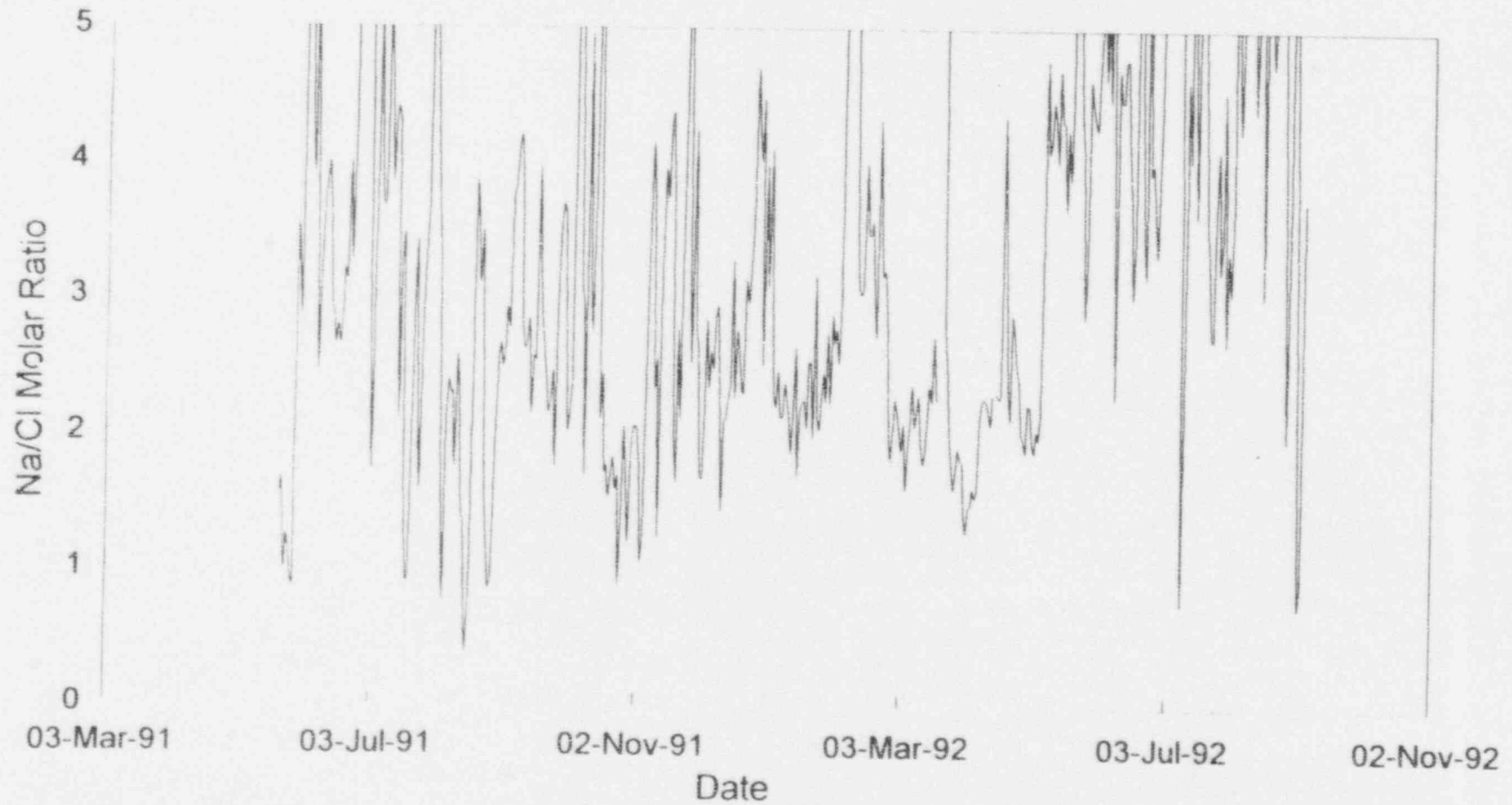


Figure 7-24

Braidwood Unit 1 - Cycle 4

SG Blowdown Sodium to Chloride Molar Ratio

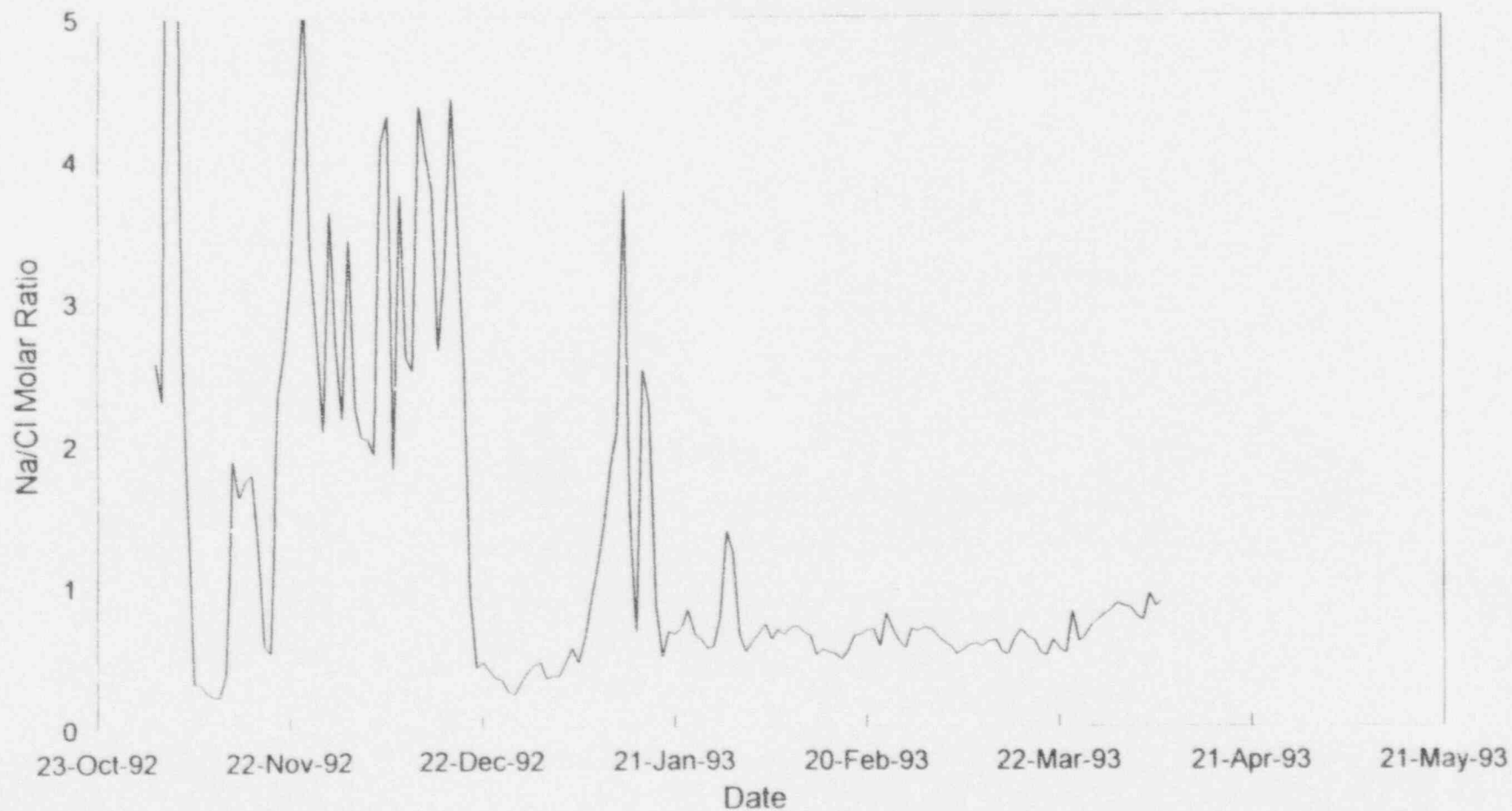


Figure 7-25

Braidwood Unit 1 - Cycle 2

SG Blowdown Sodium & Chloride

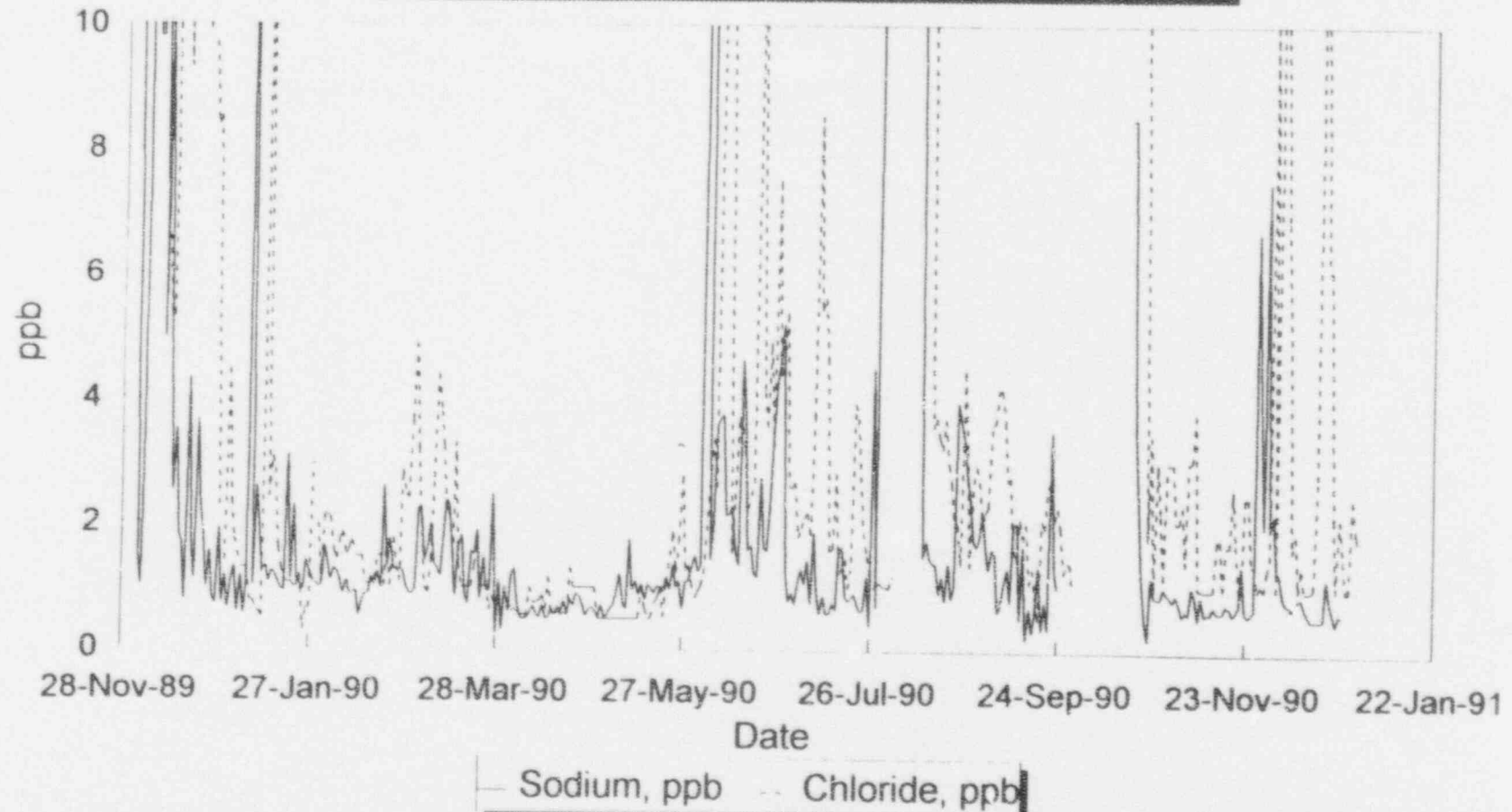


Figure 7-26

Braidwood Unit 1 - Cycle 3

SG Blowdown Sodium & Chloride

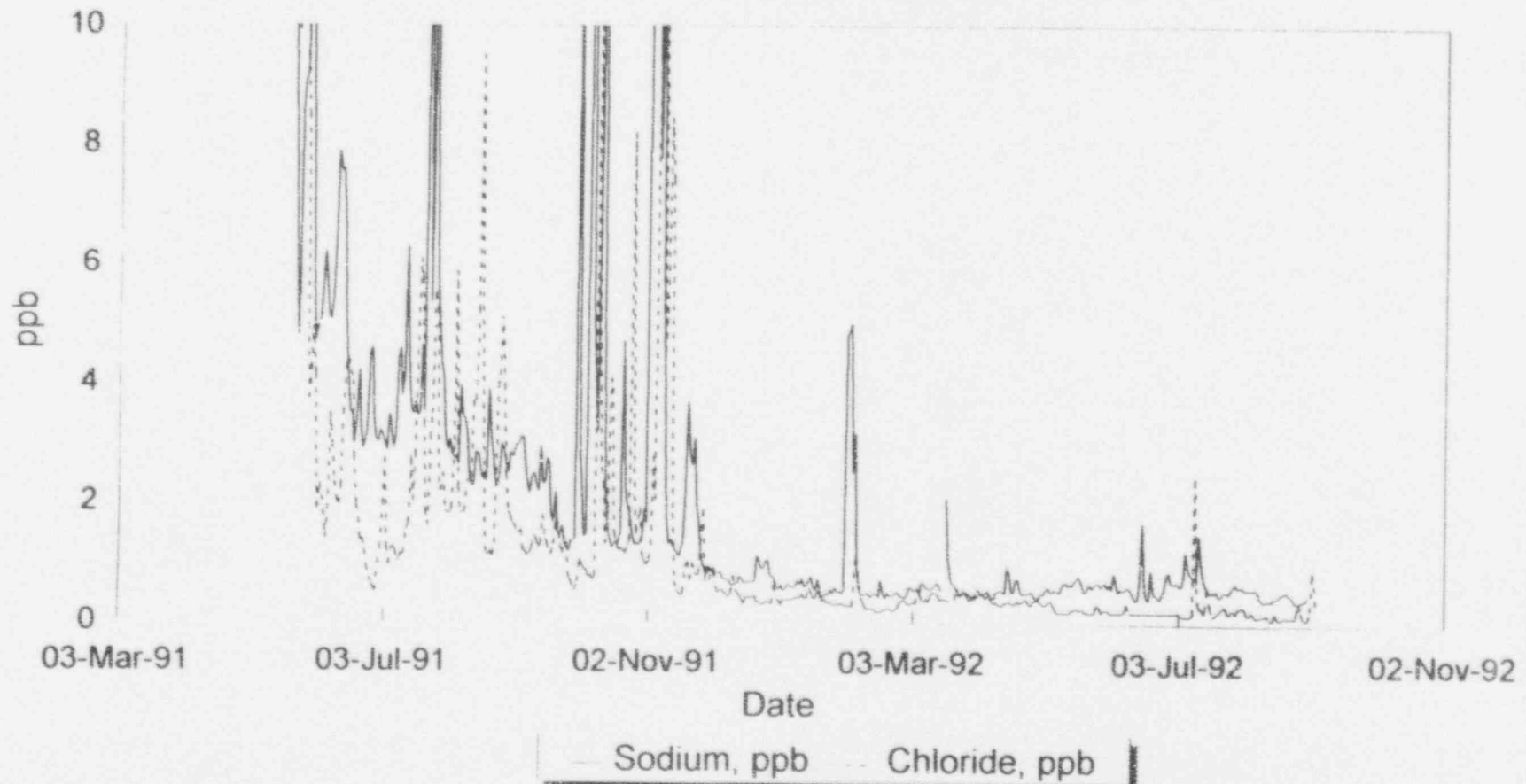


Figure 7-27

Braidwood Unit 1 - Cycle 4

SG Blowdown Sodium & Chloride

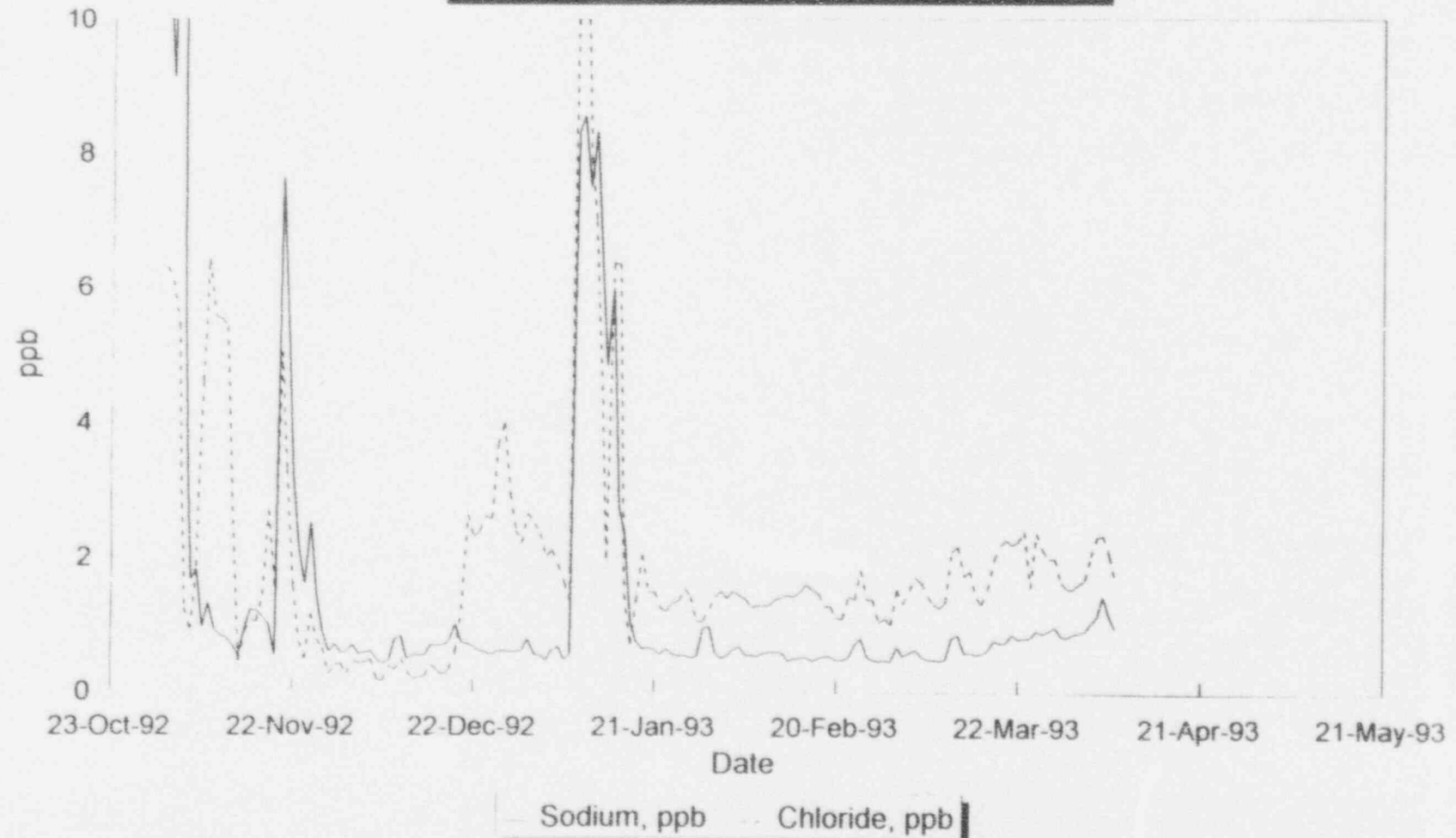
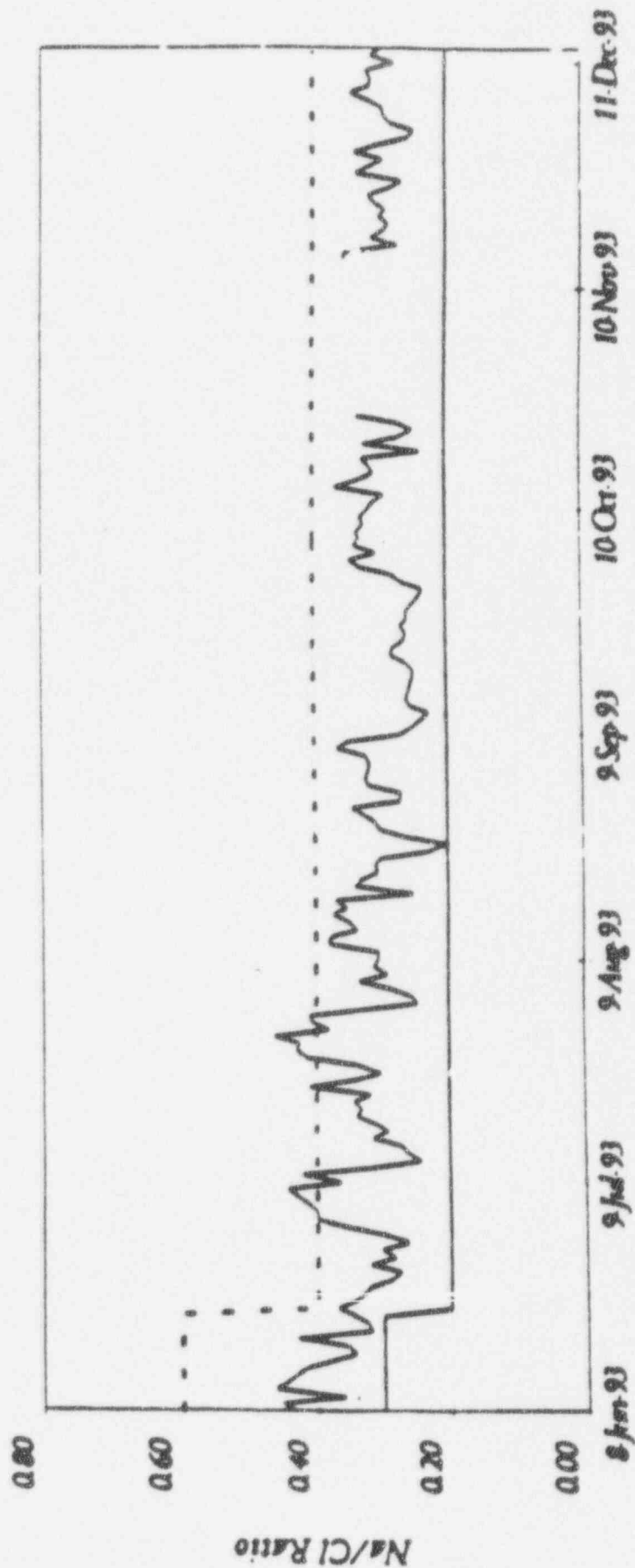


Figure 7-28

Braidwood Unit 1 **SG Na/Cl Ratio**



Sodium to Chloride Ratio Since June Outage

Figure 7-29. Braidwood Unit 1 Hideout Return Molar Ratios

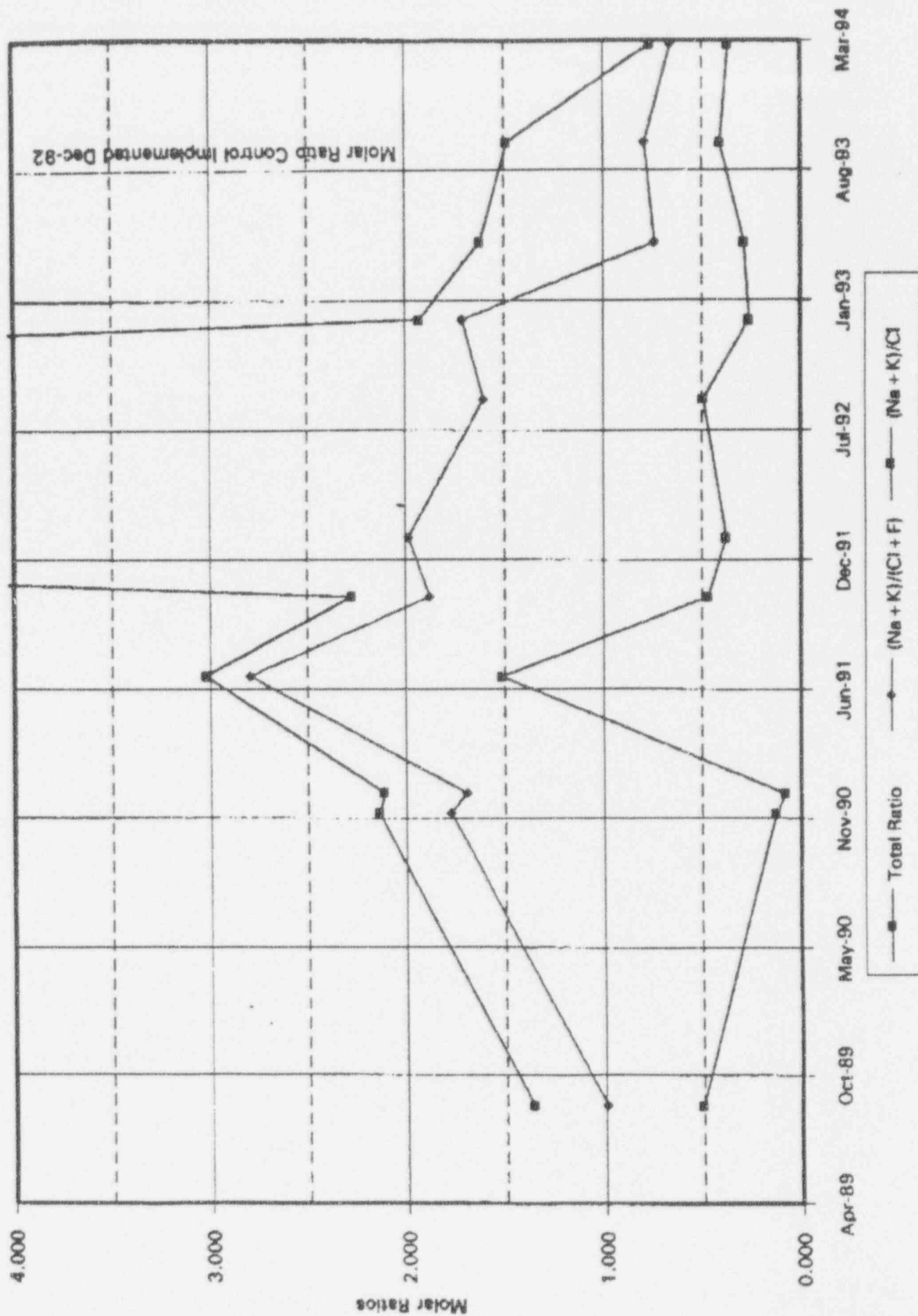


Figure 7-30

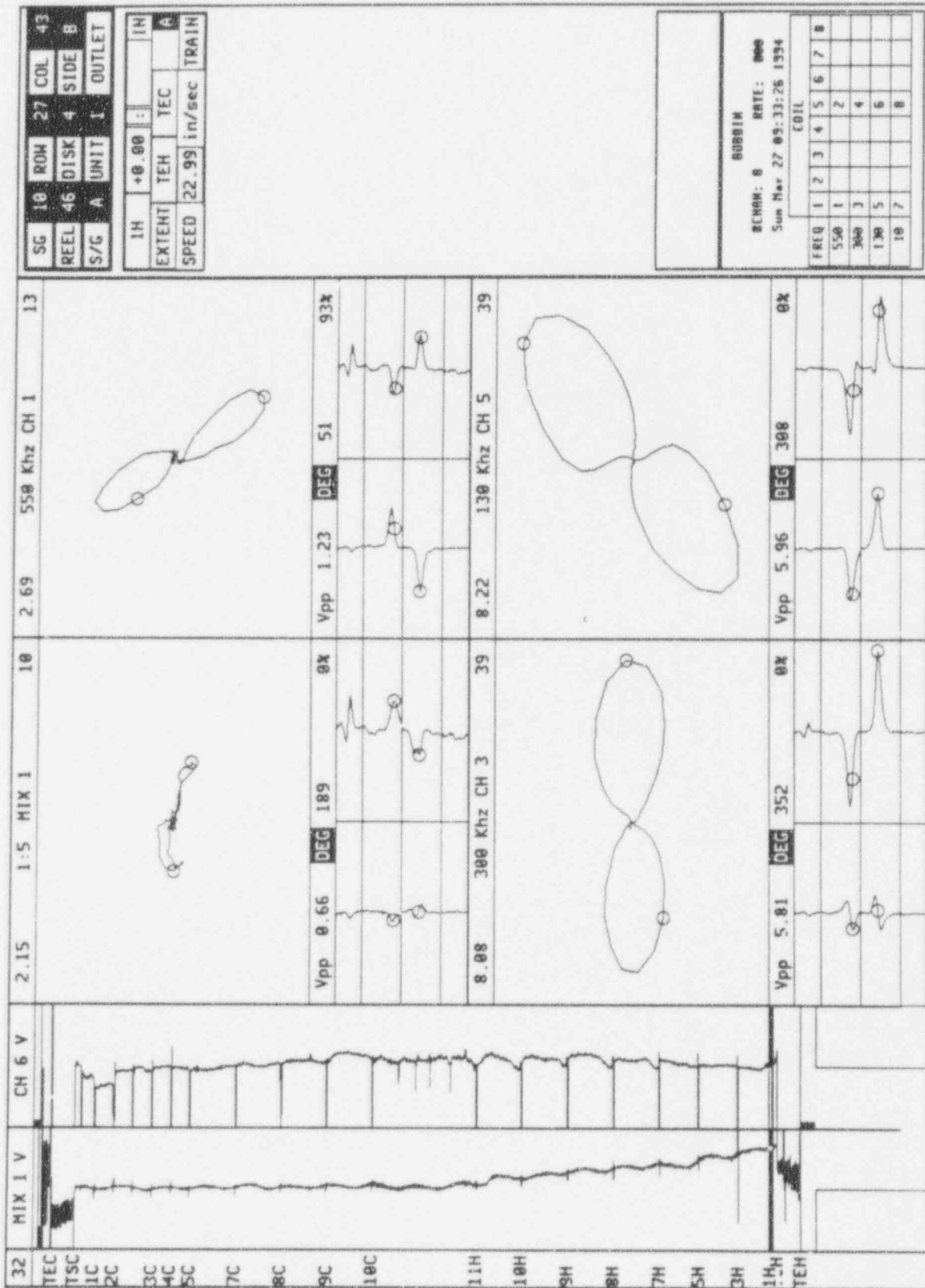


Figure 7-32

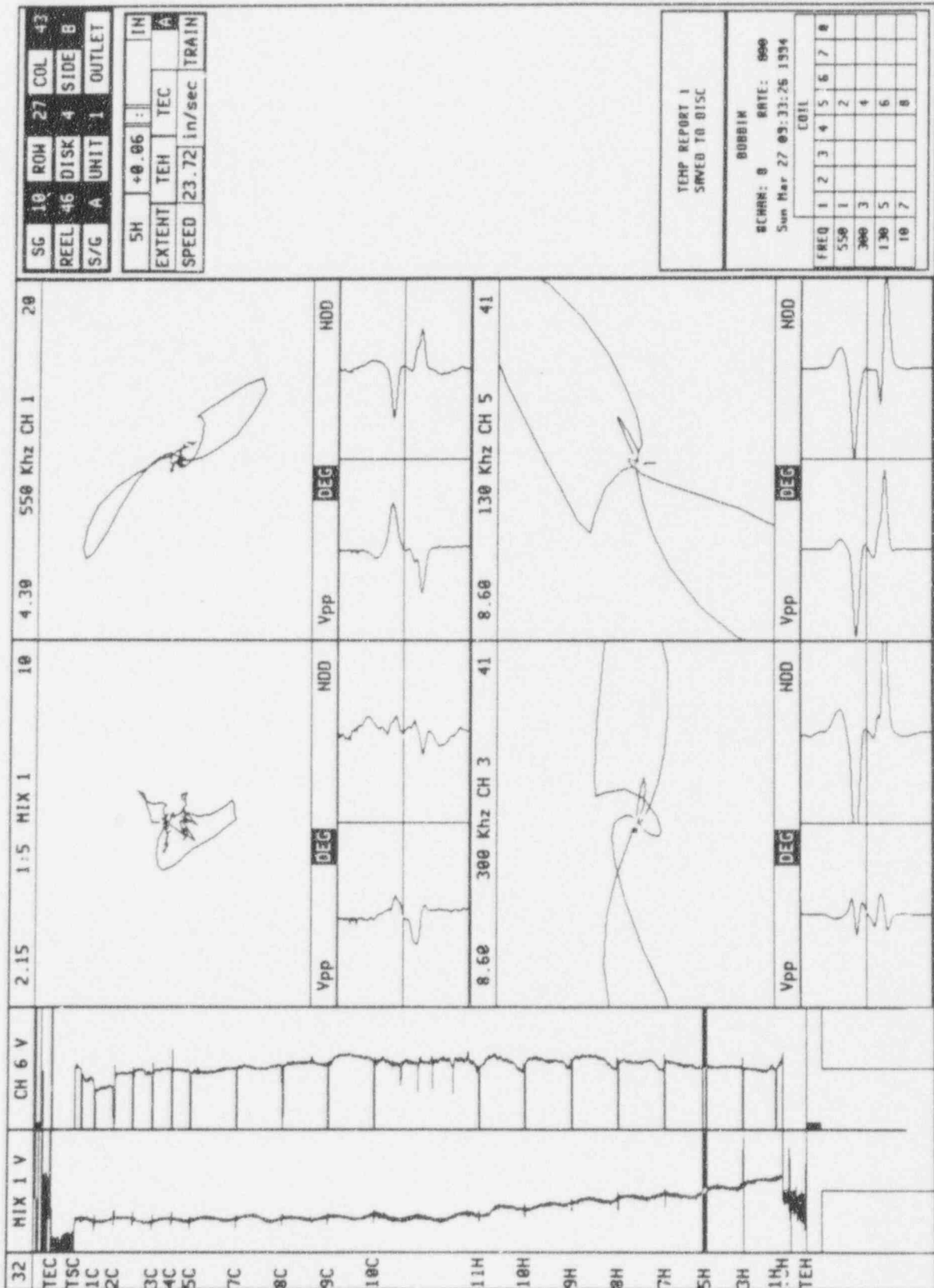


Figure 7-33

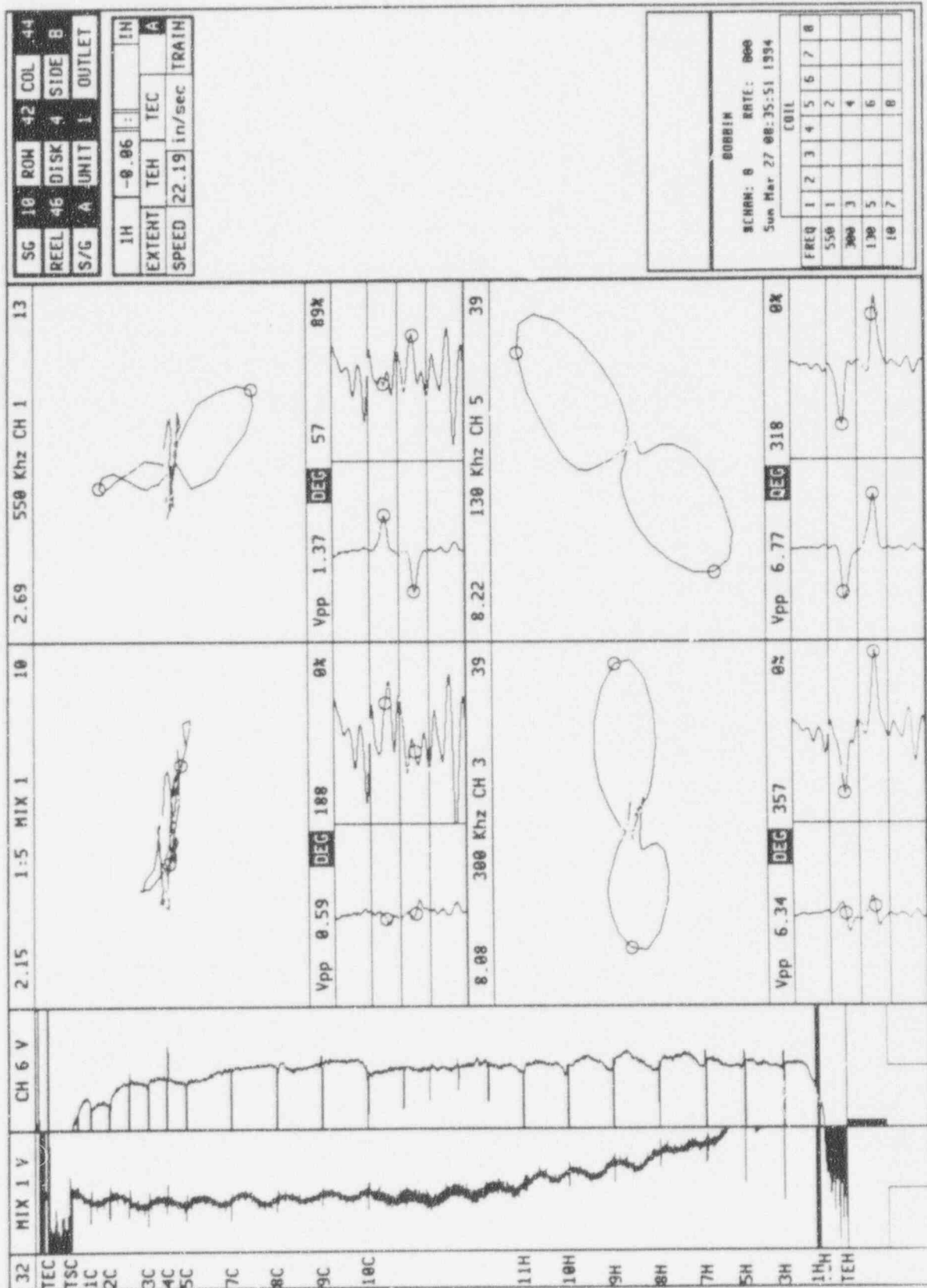


Figure 7-34

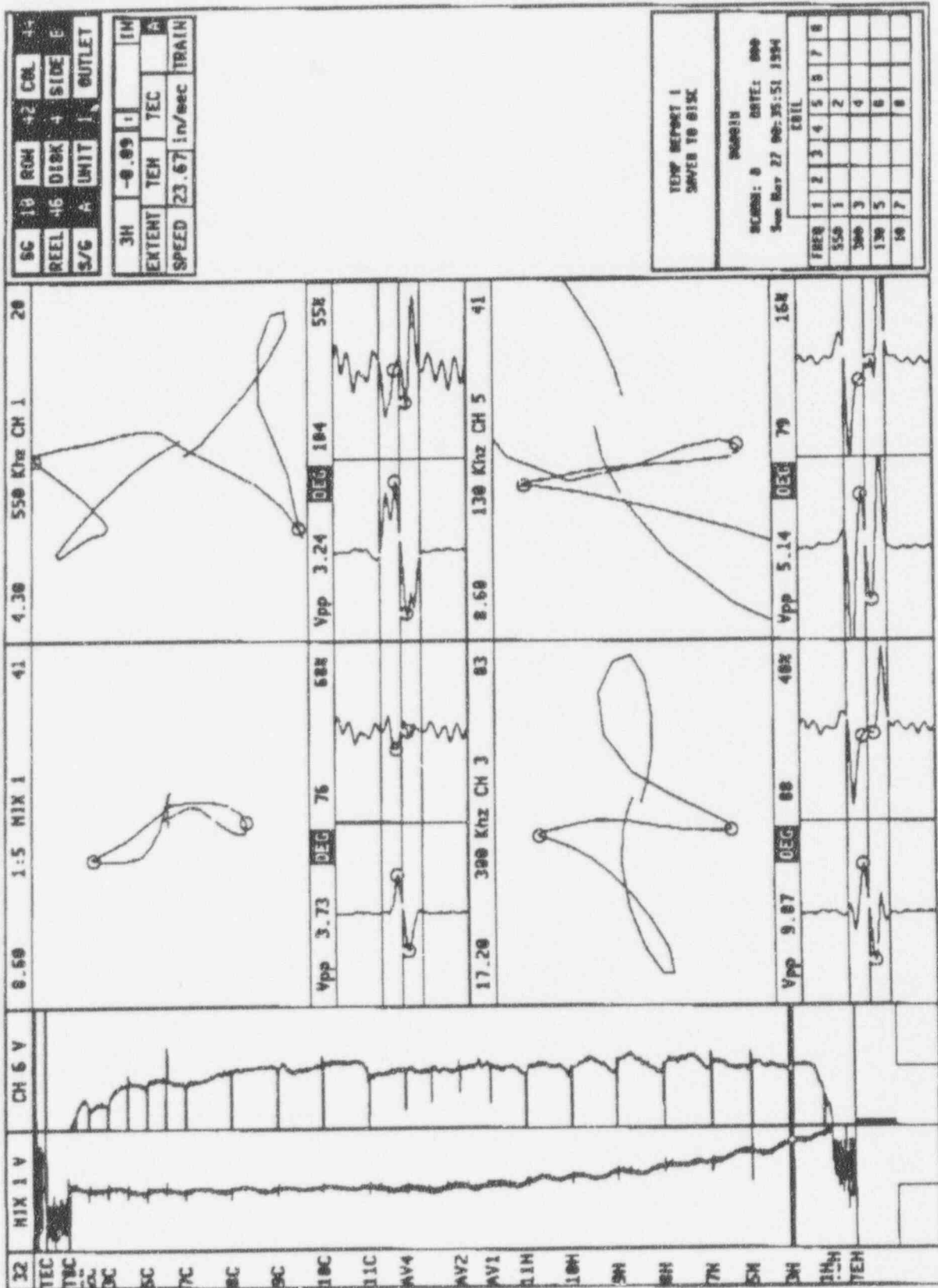


Figure 7-35

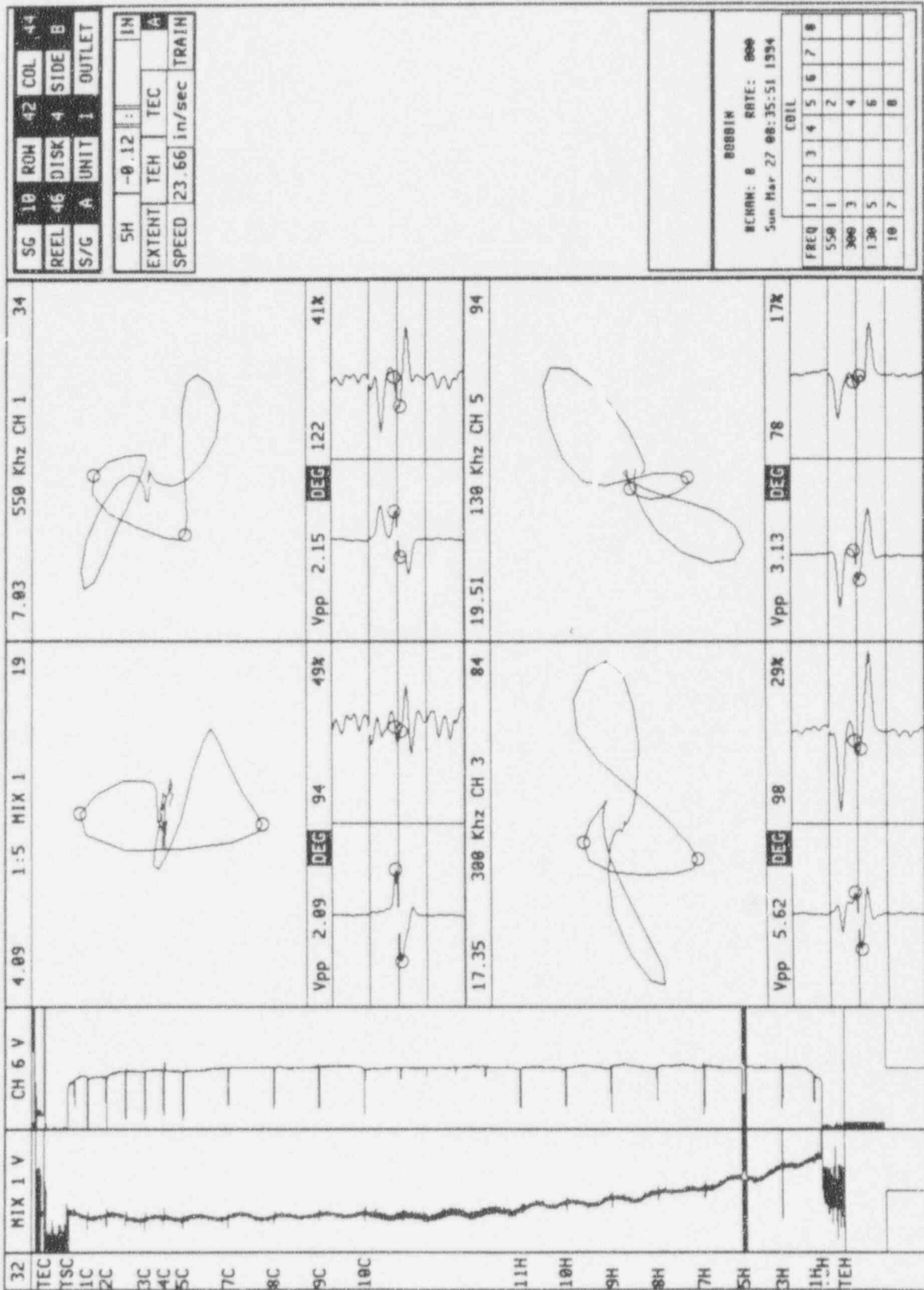


Figure 7-37

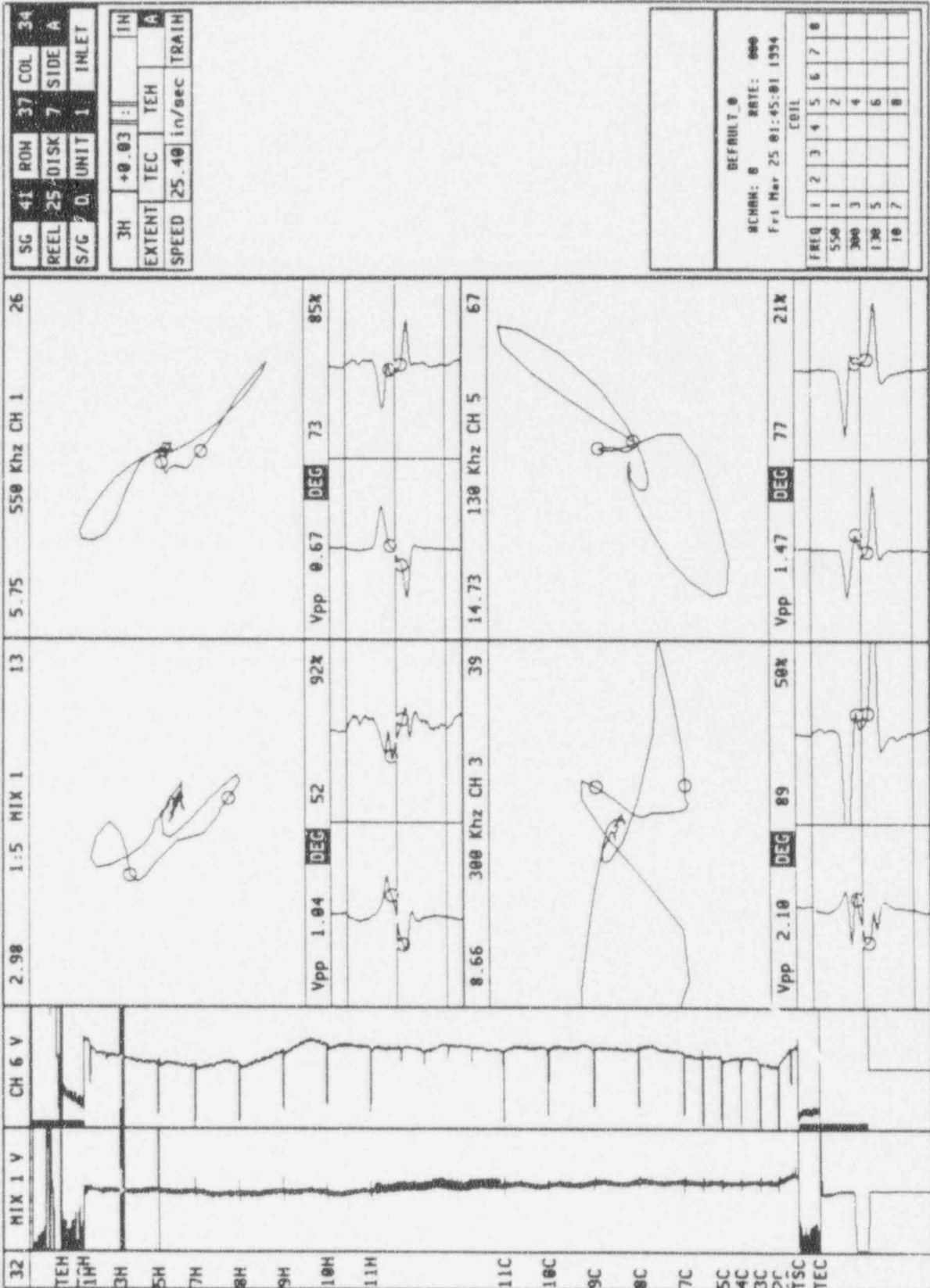


Figure 7-38

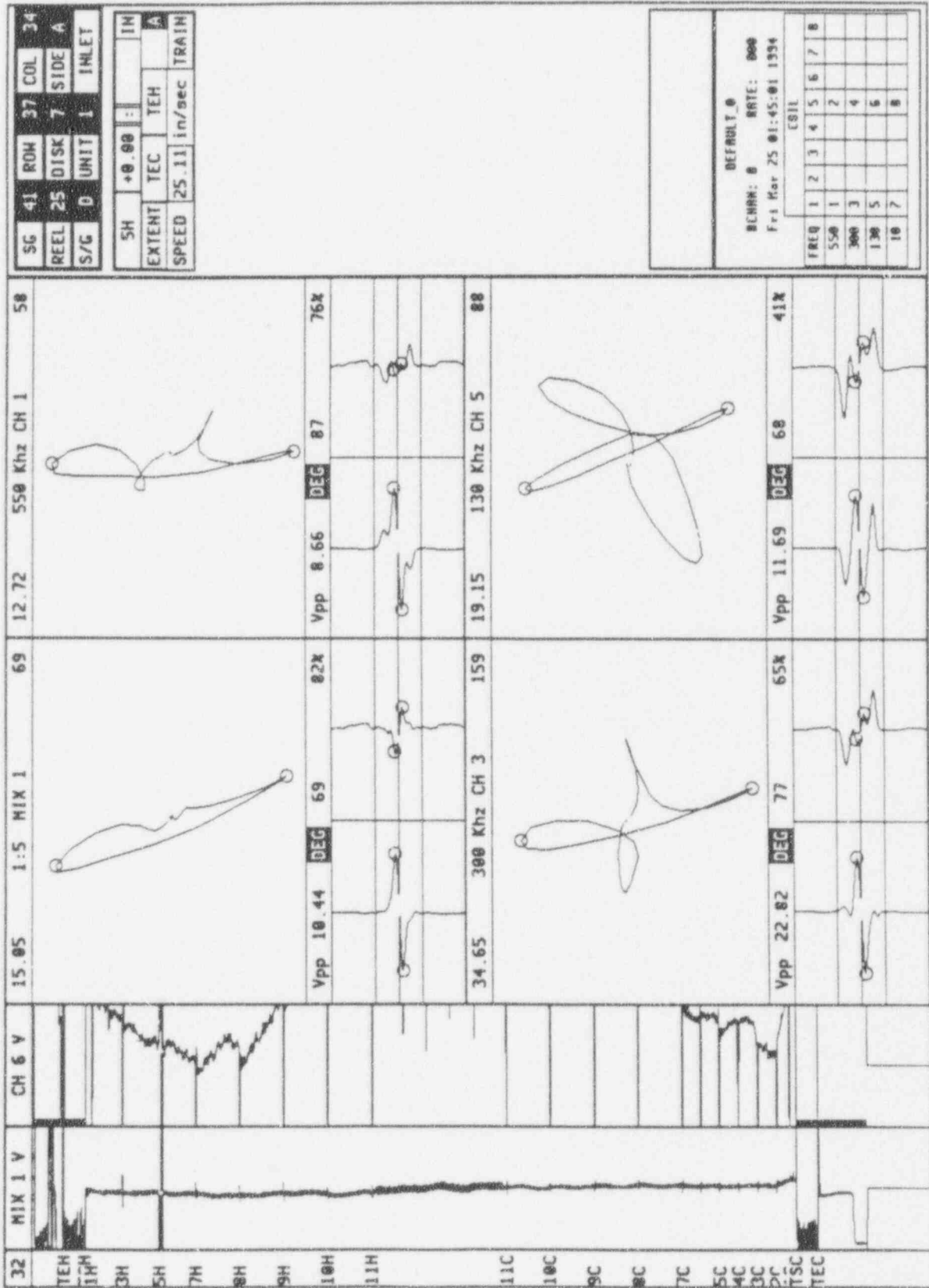


Figure 7-39

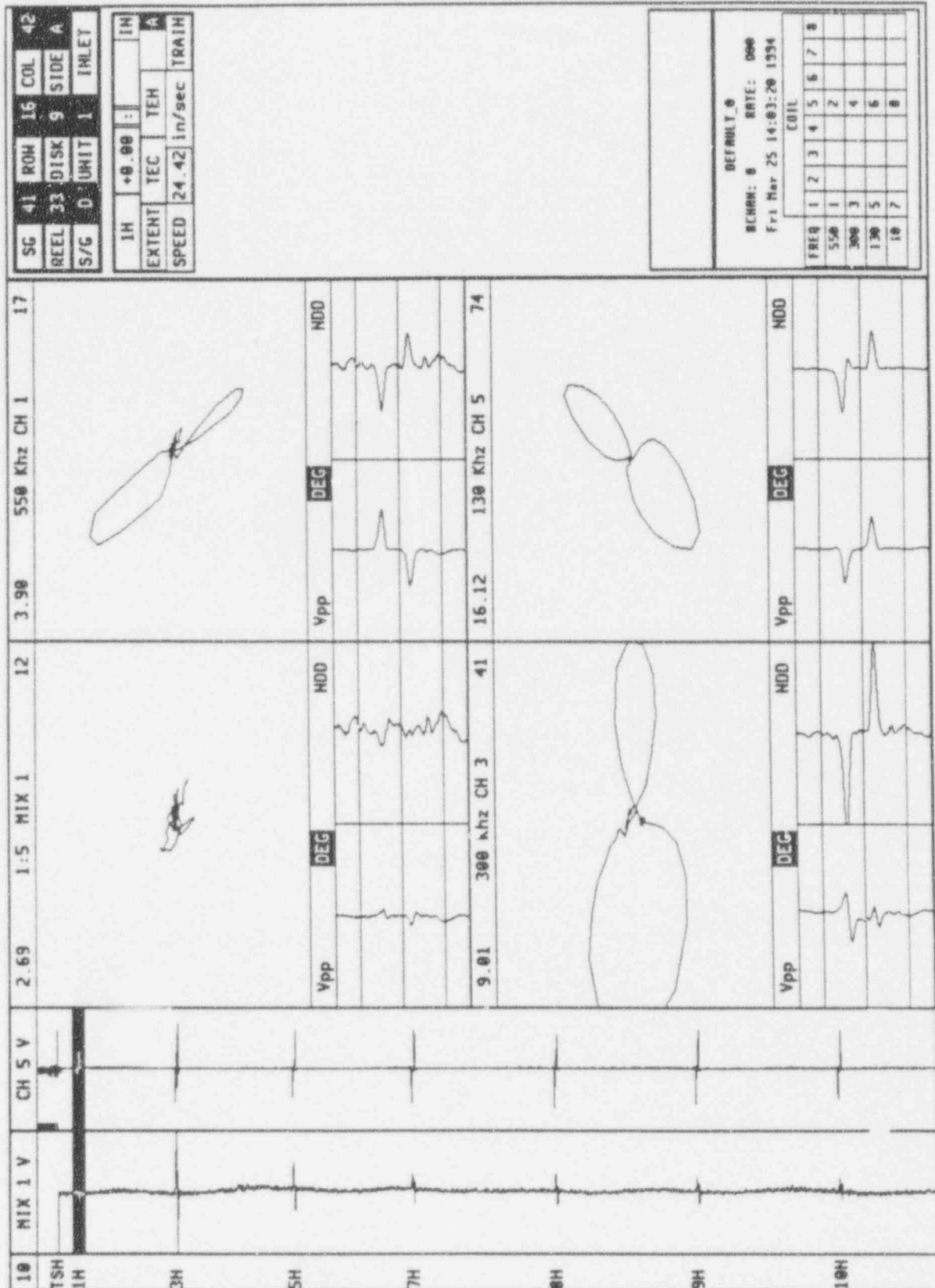


Figure 7-40

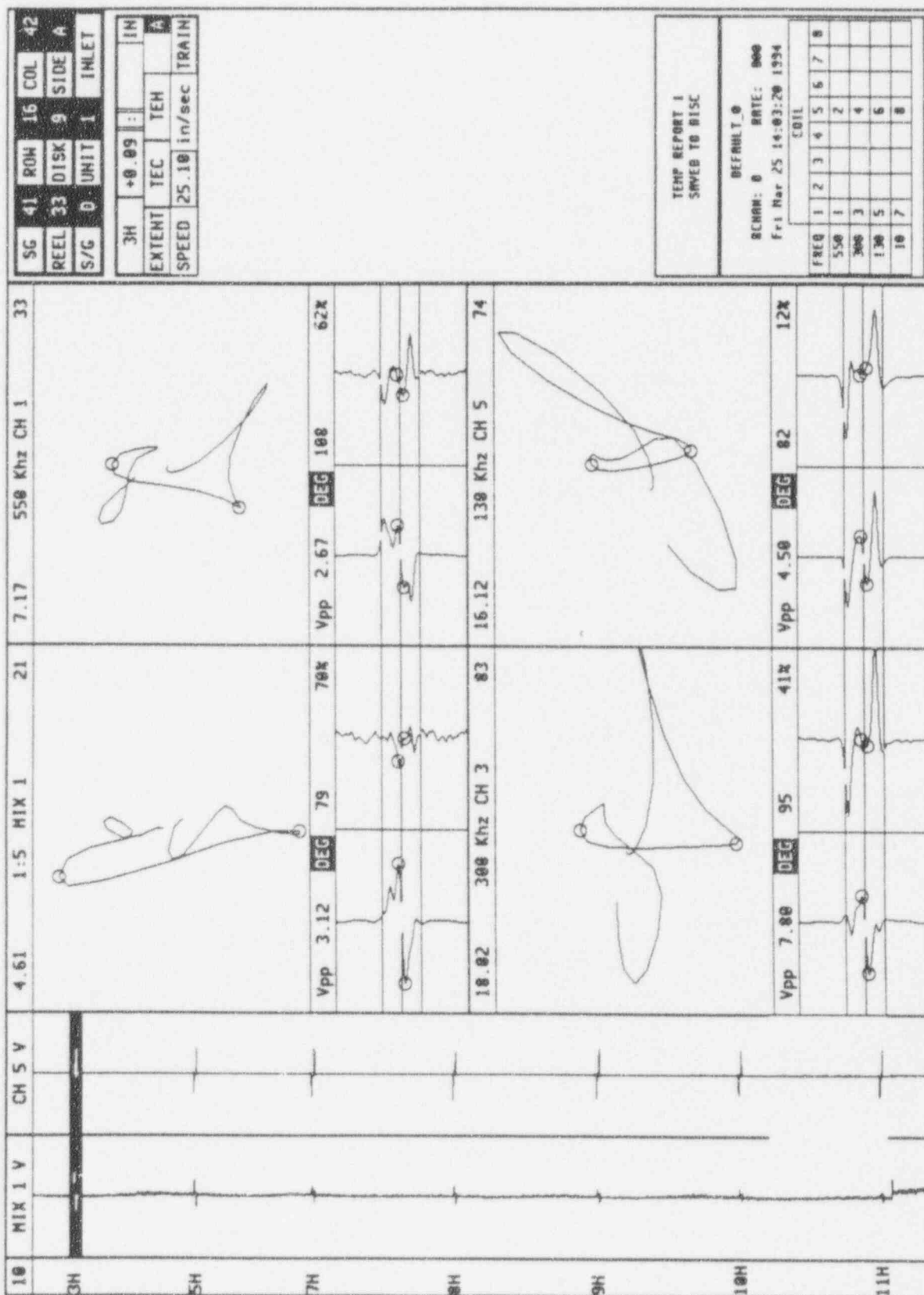
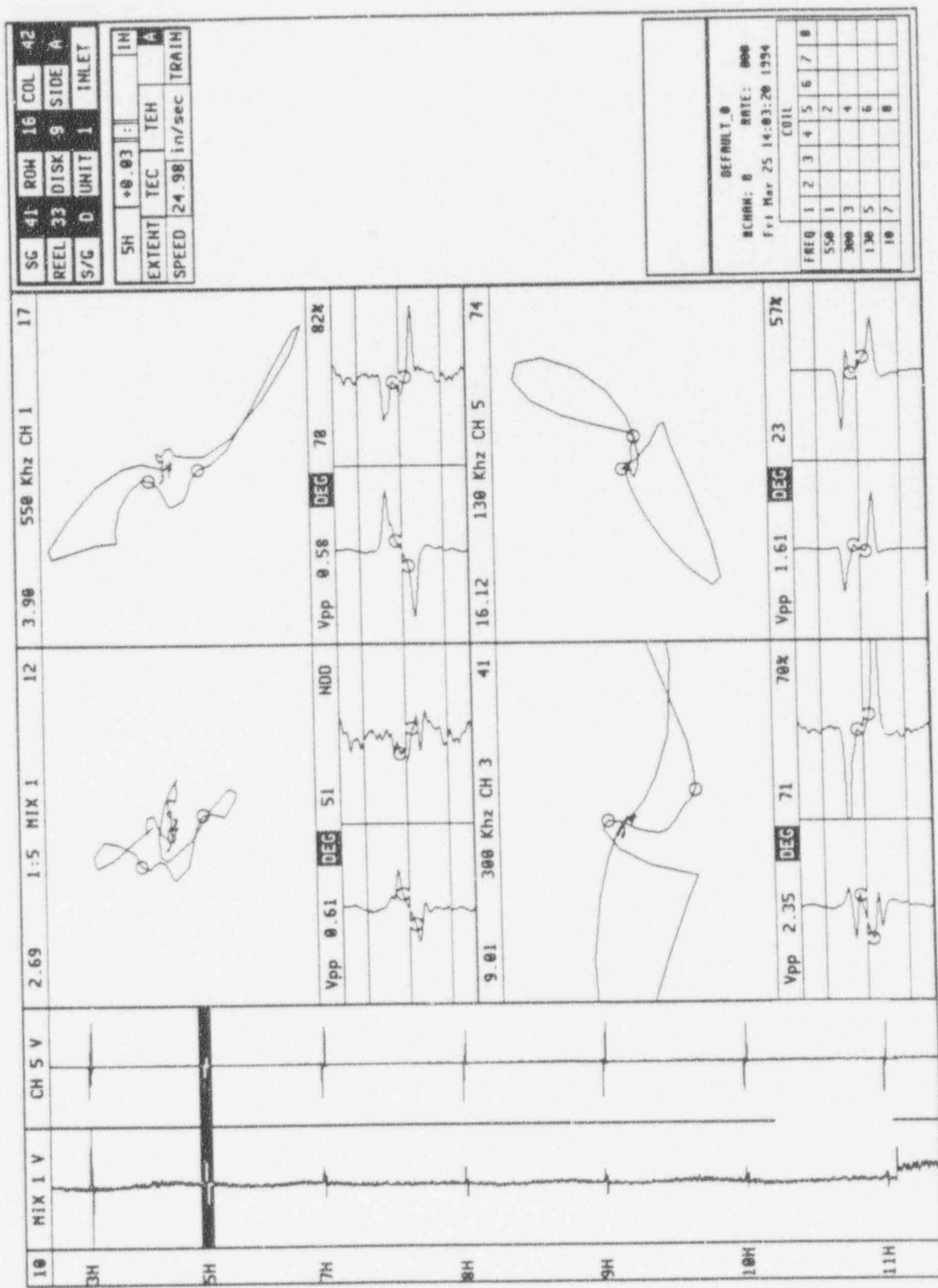


Figure 7-41



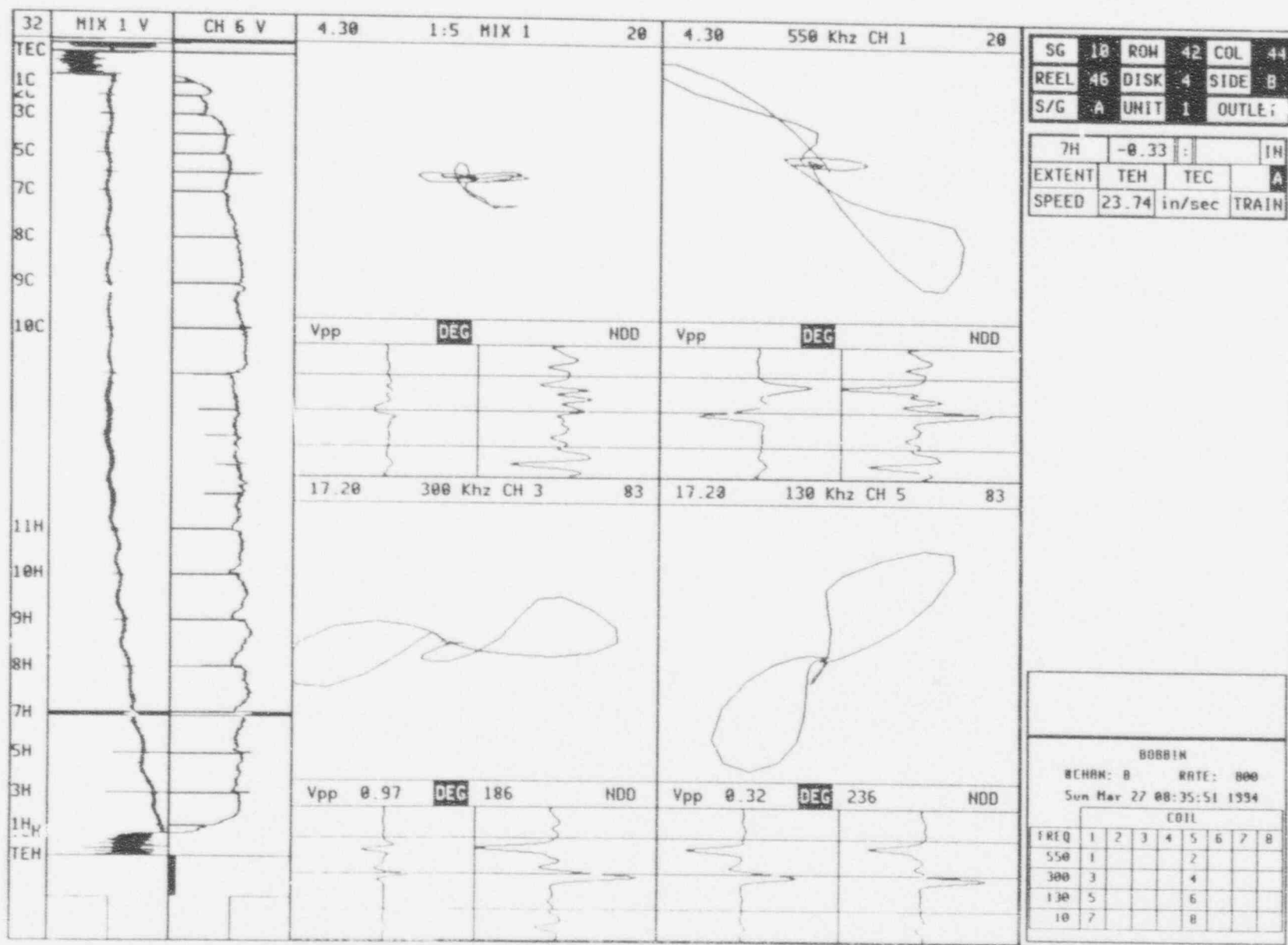


Figure 7-42

Figure 7-43

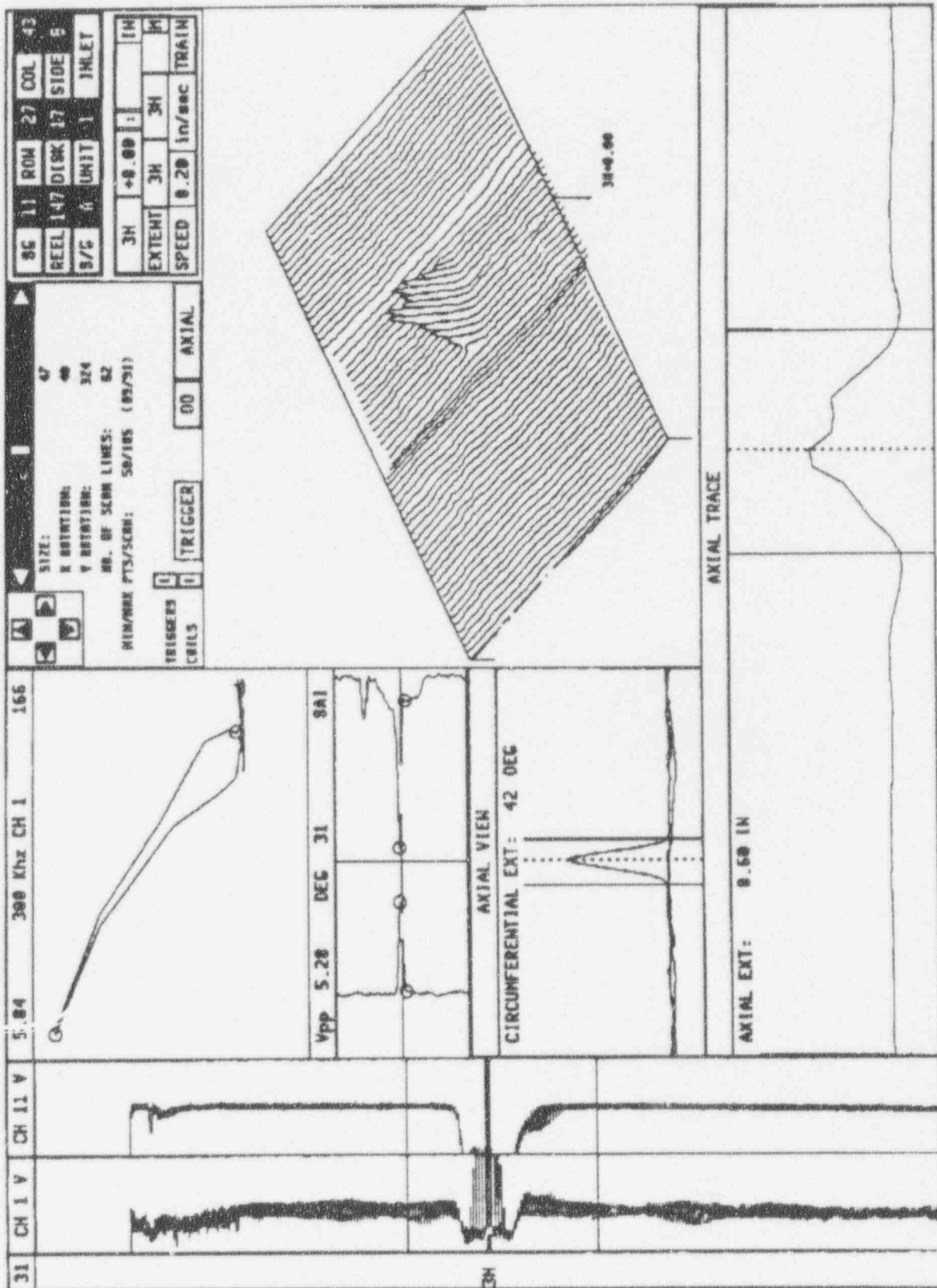


Figure 7-44

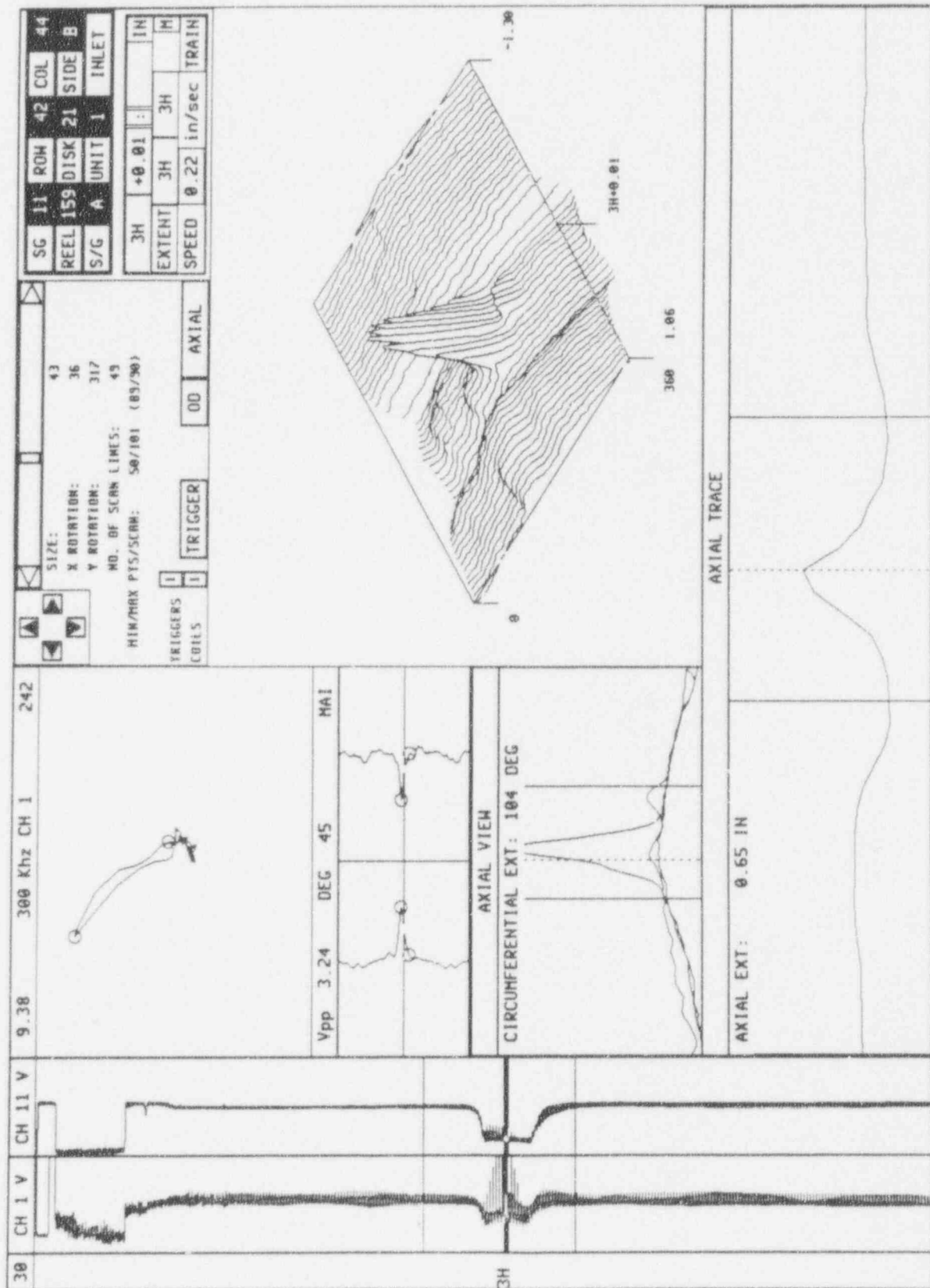


Figure 7-45

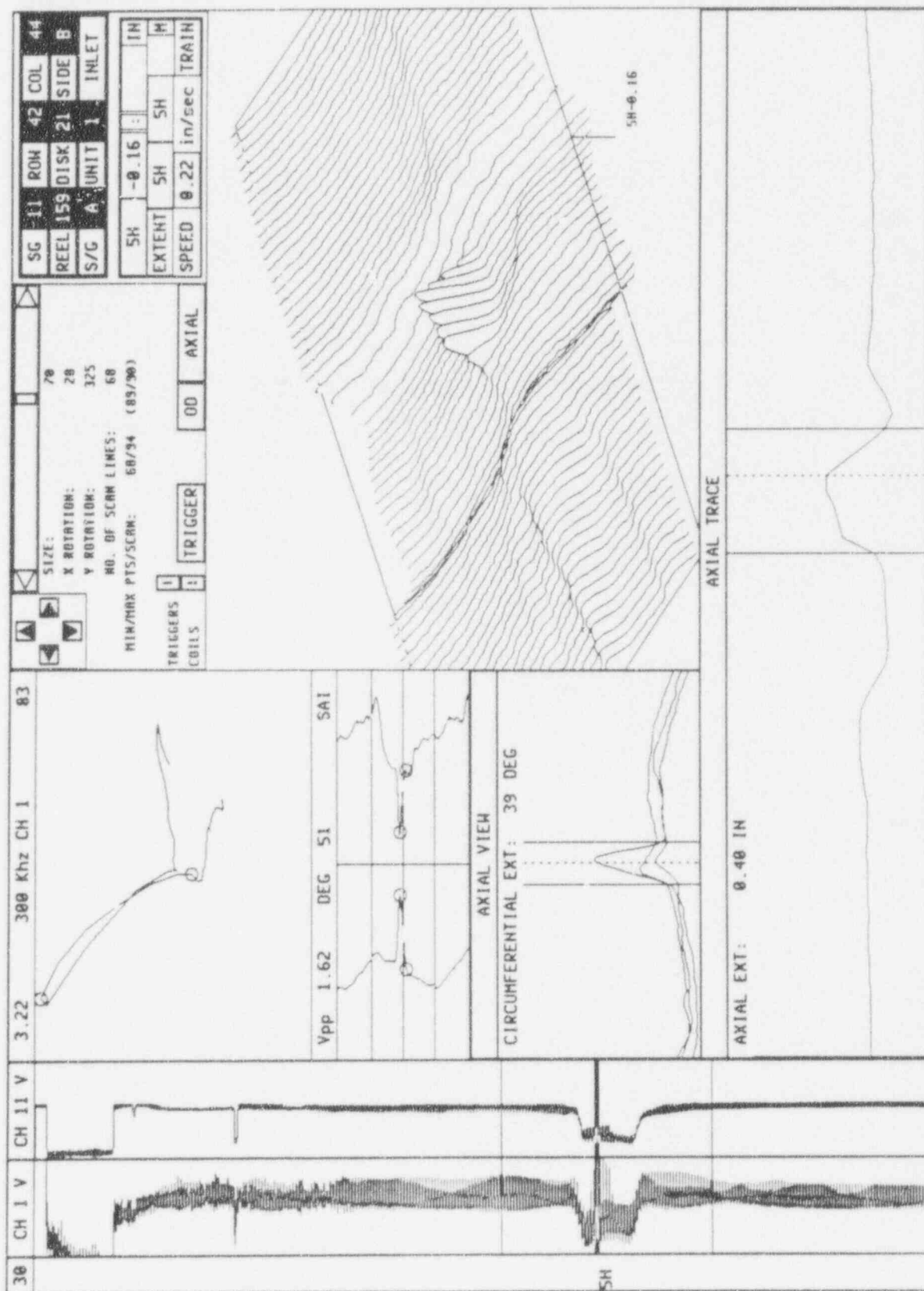


Figure 7-46

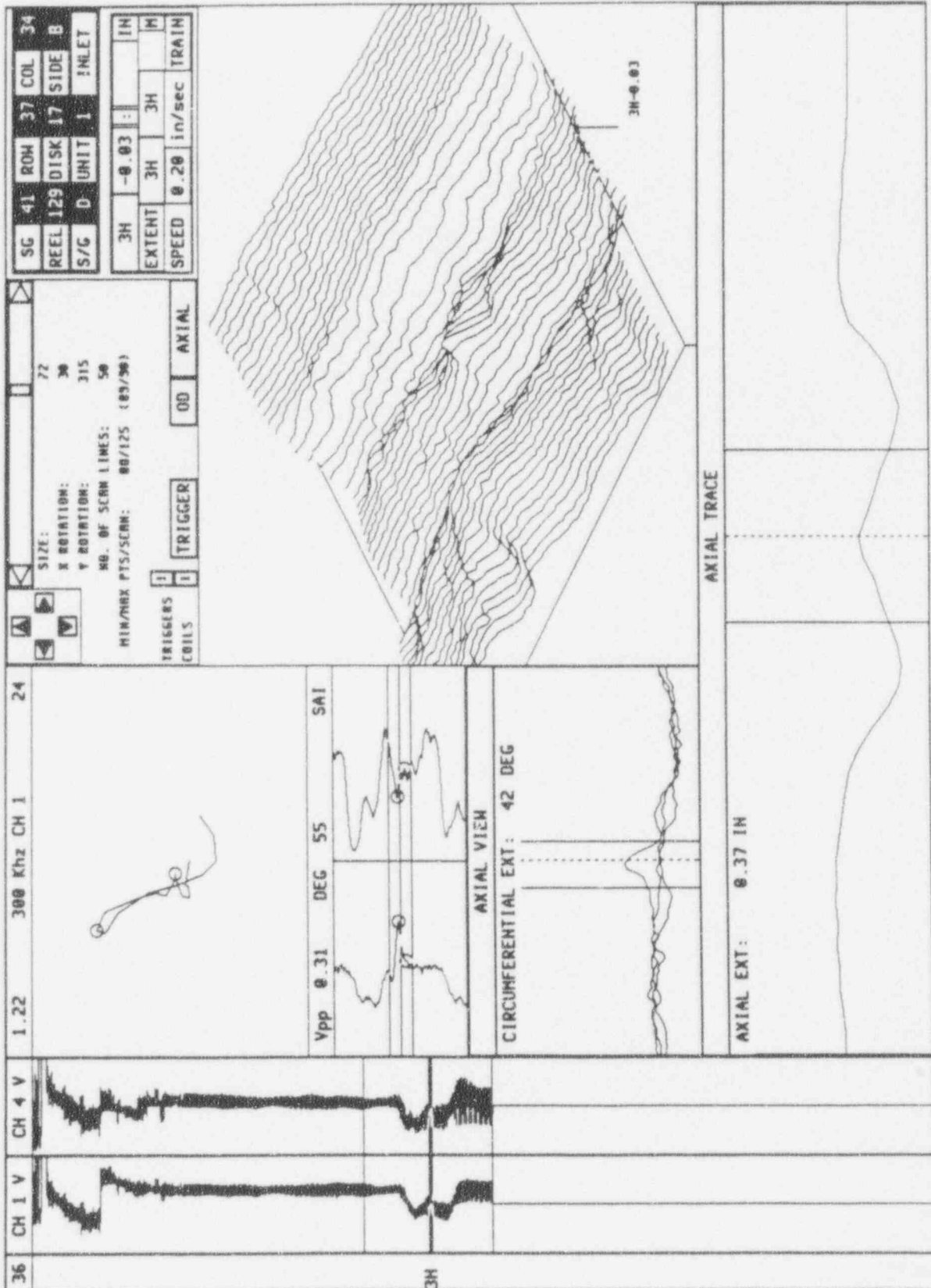


Figure 7-47

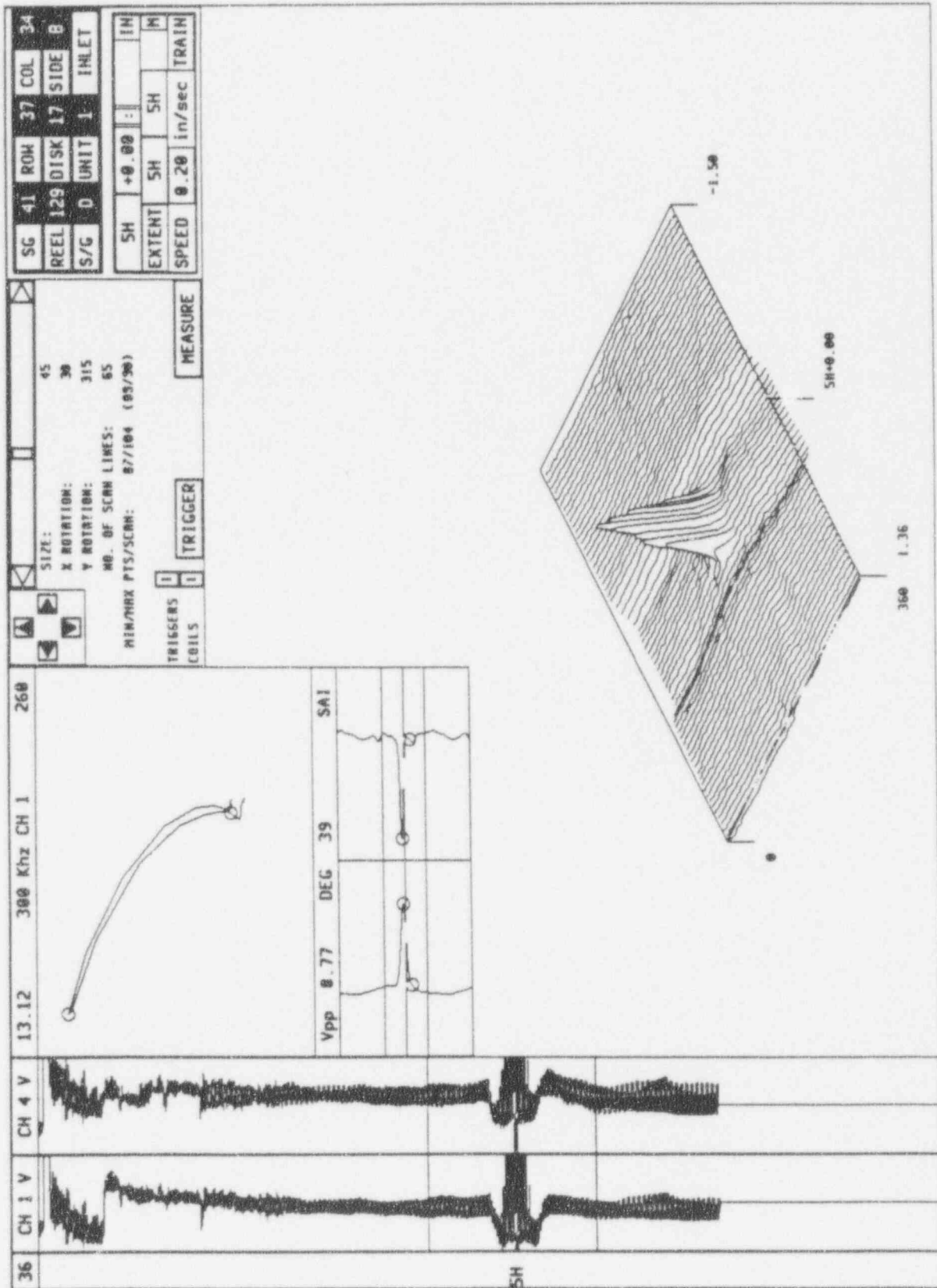
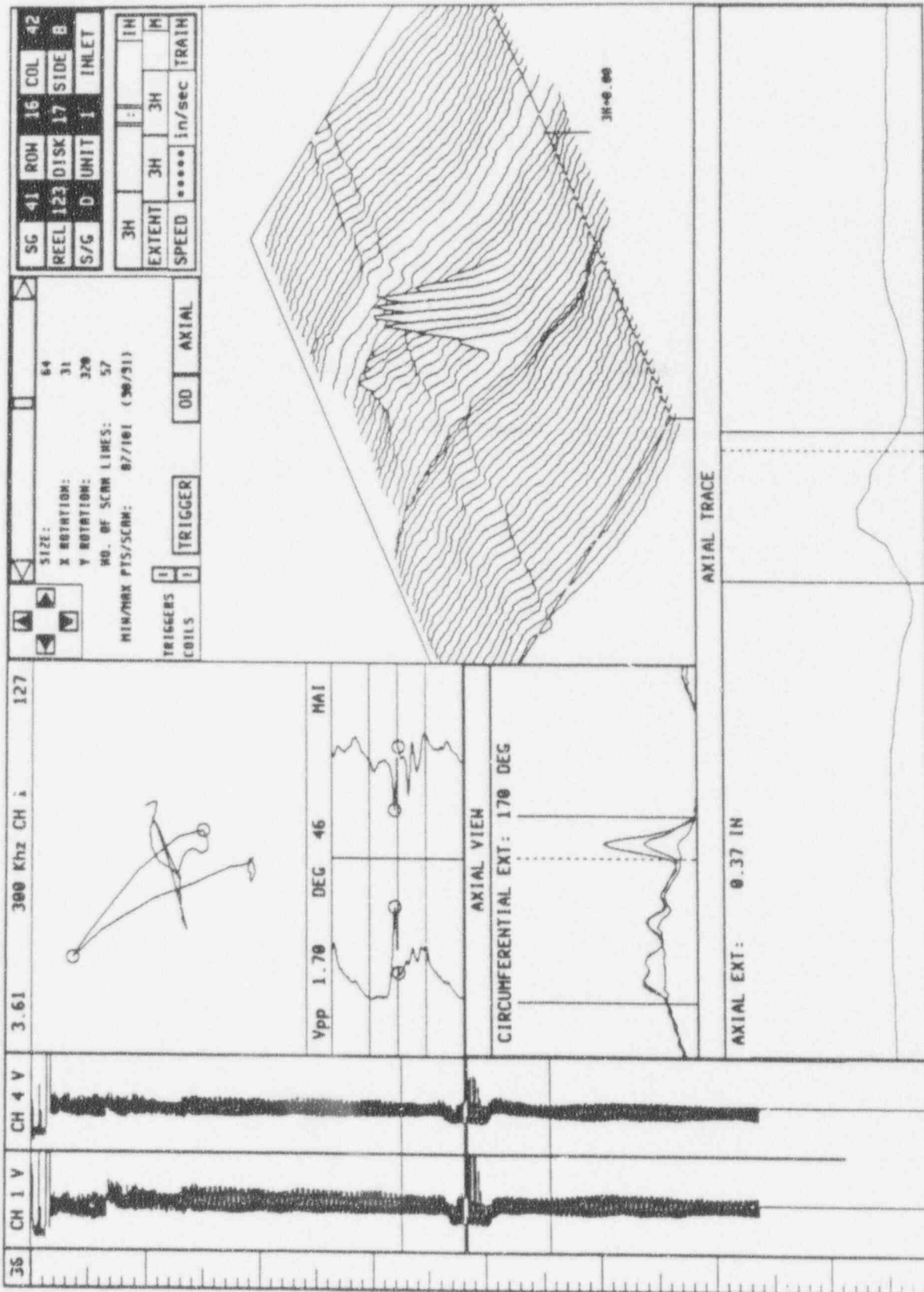


Figure 7-48



8.0 BRAIDWOOD-1 IPC CRITERIA AND EVALUATION

This section summarizes the 1.0 volt IPC implemented for Cycle 5 at Braidwood-1 and the supporting evaluations. The supporting evaluations include projected EOC-5 voltage distributions, SLB leak rates and tube burst assessments. Both deterministic and probabilistic tube burst assessments are given in this section. Revision 1 of this report updates the initial assessment for TSP displacements and associated tube burst probabilities which utilized load analyses available at the time of the report. The updated analyses eliminate unnecessary conservatisms, such as very low water levels, in the prior load analyses and are described in a new Section 8.7. The Braidwood-1 pulled tube examination results given in Section 3 are assessed in Section 8.8 relative to support for tube integrity considerations at EOC-4 and associated implications for Cycle 5.

8.1 General Approach to the IPC Assessment

The tube integrity assessment approach applied to support the Braidwood-1 IPC is based on demonstrating limited TSP displacement in a SLB event to reduce the likelihood of a tube burst to negligible levels and to conservatively calculate SLB leakage as free span leakage even though the limited TSP displacement would reduce leakage compared to free span tube conditions. The structural analyses of Section 4 for obtaining TSP displacements in a SLB event are applied to a conservative assumption that the TSP displacements expose a throughwall crack length equal to the TSP displacement. By applying the burst pressure versus throughwall crack length correlation of Section 6.2, both deterministic and probabilistic burst assessments are made for the assumed exposed throughwall crack length. That is, the burst capability is a function of the exposed throughwall crack length. This analysis is equivalent to assuming that the indication at the TSP has a throughwall crack length approximately equal to the TSP thickness. This is an extremely conservative assumption since the bobbin voltages associated with such long throughwall cracks would be in the many tens of volts and much higher than that found at Braidwood-1 which are bounded by a maximum indication of 10.4 volts at EOC-4. Consequently, the conservatism of the burst assessment bounds any realistic growth rate for Braidwood-1 and the burst margins obtained at EOC-5 based on limited SLB TSP displacements are essentially independent of growth rates.

The limited SLB TSP displacement would result in most of the crack length for indications at TSPs covered by the TSPs and associated crevice deposits. This effect would tend to reduce leakage below that of free span indications which is the basis for data developed to support the EPRI SLB leak rate correlations of Section 6.5 which are used for the leakage analyses of this report. EDF has performed system leak rate measurements on French S/Gs at pressure differentials exceeding SLB conditions. Bobbin voltage levels in the French units at the time

of these tests exceeded that found at Braidwood-1. In addition, the French units included axial free span cracks in the roll transition at the top of the tubesheet which are left in service per repair criteria implemented by EdF. The total system leakage at pressure differentials typical of SLB conditions from these tests was on the order of a few gpm. This leak rate is much lower than would be predicted by the EPRI leak rate correlations considering only the indications at TSPs and ignoring the roll transition indications. Thus the EdF tests demonstrate the conservatism of the EPRI correlations particularly when the indications are within the packed crevice of the TSP.

The BOC-5 bobbin voltage distributions are developed by applying a probability of detection (POD) of 0.6 to all indications found at EOC-4 per the guidance of draft NUREG-1477. This methodology divides the EOC-4 voltage distribution by 0.6 and then subtracts the repaired indications to define the BOC-5 distribution. When voltage indications above a few volts are found in the inspection, for which the POD would be expected to be > 0.6 , this methodology becomes very conservative for the BOC distribution as it leaves 0.7 indication in service for each indication found in the inspection, independent of the voltage level.

8.2 IPC Repair Criteria Implemented at Braidwood-1

This section describes the IPC implemented at the Cycle 4 refuel outage (EOC-4) and the inspection/analysis performed to support the IPC.

Braidwood-1 Interim Plugging Criteria

The implementation of the IPC at Braidwood-1 for ODSCC at TSPs can be summarized as follows:

- Tube Plugging Criteria

Tubes with bobbin flaw indications exceeding the 1.0 volt IPC voltage repair limit and ≤ 2.7 volts are plugged or repaired if confirmed as flaw indications by RPC inspection. Bobbin flaw indications > 2.7 volts attributable to ODSCC are repaired or plugged independent of RPC confirmation.

- Operating Leakage Limits

Plant shutdown will be implemented if normal operating leakage exceeds 150 gpd per SG.

- SLB Leakage Criterion

Predicted end of cycle SLB leak rates from tubes left in service, including a $POD = 0.6$ adjustment and allowances for NDE uncertainties and ODSCC growth rates, must be less than 9.1 gpm for the S/G in the faulted loop.

- Exclusions from Tube Plugging Criteria

Certain tube locations, as identified in Section 4 of this report, are excluded from application of the II^o repair limits. The analyses indicate that these tubes may potentially deform or collapse following a postulated LOCA + SSE event.

Braidwood-1 EOC-4 Inspection

- Eddy current analysis guidelines and voltage normalization consistent with the EPRI ISI guidelines and with prior IPC applications (typical of Appendix A for prior Westinghouse IPC WCAPs such as WCAP-13854).
- Eddy current analysts were trained specifically to voltage sizing per the analysis guidelines and 52% of the analysts were qualified to the industry standard Qualified Data Analysis program.
- Use of ASME calibration standards cross-calibrated to the reference laboratory standard and use of a probe wear standard requiring probe replacement at a voltage change of 15% from that found for the new probe.
- 100% bobbin coil, full length inspection of all active tubes with a 0.610 inch diameter bobbin probe for all straight length tubing.
- RPC inspection of all bobbin indications greater than the 1.0 volt repair limit (actual implemented was all bobbin indications). RPC inspections were performed with a 0.620 inch diameter, 3 coil motorized RPC probe.
- RPC sample inspection of more than 100 TSP intersections with dents (at Braidwood-1, these are typically mechanically induced "dings") or artifact/residual signals that could potentially mask a 1.0 volt bobbin signal. Any RPC flaw indications in this sample will be plugged or repaired.
- The NRC will be informed, prior to plant restart from the refueling outage, of any unexpected inspection findings relative to the assumed characteristics of the flaws at the TSP intersections. This includes any detectable circumferential indications or detectable indications extending outside the thickness of the TSP.

The IPC evaluations given in this report are based on the inspection results implementing the above guidelines and the 1.0 volt IPC repair limit.

8.3 Operating Leakage Limit

Regulatory Guide 1.121 acceptance criteria for establishing operating leakage limits are based on leak-before-break (LBB) considerations such that plant shutdown is initiated if the leakage associated with the longest permissible crack is exceeded. The longest permissible crack length is the length that provides a factor of safety of 1.43 against burst at SLB conditions since a factor of 3 against bursting at normal operating pressure differential is satisfied by the TSP constraint at normal operation. As noted previously, a voltage amplitude of 4.54 volts for typical ODSCC cracks corresponds to meeting this tube burst requirement at the lower 95% prediction interval on the burst correlation. Alternate crack morphologies could correspond to 4.54 volts so that a unique crack length is not defined by the burst pressure-to-voltage correlation. Consequently, typical burst pressure versus throughwall crack length correlations are used below to define the "longest permissible crack" for evaluating operating leakage limits.

The CRACKFLO leakage model has been developed for single axial cracks and compared with leak rate test results from pulled tube and laboratory specimens. Fatigue crack and SCC leakage data have been used to compare predicted and measured leak rates. Generally good agreement is obtained between calculation and measurement with the spread of the data being somewhat greater for SCC cracks than for fatigue cracks. Figure 8-1 shows normal operation leak rates including uncertainties as a function of crack length.

The throughwall crack lengths resulting in tube burst at 1.43 times SLB pressure differentials (3657 psi) and SLB conditions (2560 psi) are about 0.51 and 0.75 inch, respectively, as shown in Figure 6-2. Nominal leakage at normal operating conditions for these crack lengths would range from about 0.24 to ~5 gpm while -95% confidence level leak rates would range from about 0.04 to 0.5 gpm. Leak rate limits at the lower range near 0.04 gpm would cause undue restrictions on plant operation and result in unnecessary plant outages, radiation exposure and costly repair. In addition, it is not feasible to satisfy LBB for all tubes by reducing the leak rate limit. Crevice deposits, the presence of small ligaments and irregular fracture faces can, in some cases, reduce leak rates such that LBB cannot be satisfied for all tubes by lowering leak rate limits.

An operating leak rate of 150 gpd (~0.1 gpm) is implemented in conjunction with application of the tube plugging criteria. As shown in Figure 8-1 this leakage limit provides for detection of 0.4 inch cracks at nominal leak rates and 0.6 inch cracks at the -95% confidence level leak rates. Thus, the 150 gpd limit provides for plant shutdown prior to reaching critical crack

lengths for SLB conditions (2560 psi) at leak rates less than a -95% confidence level and for 1.43 times SLB pressure differentials at less than nominal leak rates.

The tube plugging limits coupled with 100% inspection at affected TSP locations provide the principal protection against tube rupture. Consistent with a defense-in-depth approach, the 150 gpd leakage limit provides further protection against tube rupture. In addition the 150 gpd limit provides the capability for detecting a crack that might grow at greater than expected rates and thus provides additional margin against exceeding SLB leakage limits.

8.4 Projected EOC-5 Voltage Distributions

The BOC-5 voltage distributions are obtained by applying the draft NUREG-1477 $POD = 0.6$ adjustment to all indications found in the EOC-4 inspection and subtracting the repaired indications. Data to develop the BOC-5 bobbin voltage distributions are given in Table 7.3. Monte Carlo analyses are then applied to develop the EOC-5 voltage distributions from the BOC distributions. The BOC voltages are increased by allowances for NDE uncertainties (Section 5.3) and voltage growth (Section 7.3) to obtain the EOC values. In the Monte Carlo analyses, each voltage bin of the BOC distributions (Figure 8-2 for S/G D, for example) is increased by a random sample of the NDE uncertainty and growth distributions to obtain a EOC voltage sample. Each sample is weighted by the number of indications in the voltage bin. The sampling process is repeated 100,000 times for each BOC voltage bin and then repeated for each voltage bin of the voltage distribution. Since the Monte Carlo analyses yield a cumulative probability distribution of EOC voltages, a method must be defined to obtain a discrete maximum EOC voltage value. The method adopted in this report is to integrate the tail of the Monte Carlo distribution over the largest 1/3 of an indication to define a discrete value with an occurrence of 0.33 indication. For N indications in the distribution, this is equivalent to evaluating the cumulative probability of voltages at a probability of $(0.33)/N$. The largest voltages for all distributions developed by Monte Carlo in this report have been obtained with this definition for the maximum EOC discrete voltage. The next largest discrete EOC voltage indication is obtained by integrating the tail of the Monte Carlo distribution to one indication and assigning the occurrence of 0.67 indication. This process for developing the largest EOC voltage indications provides appropriate emphasis to the high voltage tail of the distribution and permits discrete EOC voltages for deterministic tube integrity analyses.

As described in Section 8.5 below, S/G D is the most limiting S/G for SLB leakage analyses and has been evaluated using final Braidwood-1 inspection results and tube plugging data. The Cycle 4 voltage growth distribution of Table 7.6 for S/G D has been used to obtain the EOC voltages by Monte Carlo analyses as described above. The resulting BOC-5 and EOC-5 bobbin voltage distributions are shown in Figure 8-2. Based on applying the POD

adjustment, the largest BOC voltage indication left in service is 0.7 indication at 10.4 volts. At EOC-5, the largest voltage indication is projected to be 11.2 volts. The EOC-5 distribution of Figure 8-1 is used for the S/G D SLB leakage analyses in Section 8.5.

As shown in Table 7.3, the number of indications found at EOC-4 in S/G B was 277 compared to 741 in S/G A, 1062 in S/G C and 696 in S/G D. It is clear that S/G B is not limiting for tube integrity considerations and this S/G was not analyzed to obtain EOC distributions or leak rates. S/Gs A and C were analyzed using preliminary inspection results and growth rate data which have not had large changes in the final data. The voltage growth distribution for S/G A was applied in the Monte Carlo analyses for both S/Gs A and C. The S/G C Cycle 4 growth distribution may have been influenced by tube repairs made in the October, 1993 unplanned outage and thus could be an underestimate of the growth distribution. It is conservative to apply the S/G A growth distribution for S/G C since it has the largest Cycle 4 growth rates. Figures 8-3 and 8-4 show the BOC and EOC-5 voltage distributions obtained from the preliminary data. For S/G A, the largest POD adjusted BOC voltage is 8.33 volts and the largest projected EOC-5 voltage is 9.0 volts. For S/G C, the largest POD adjusted BOC voltage is 2.73 volts and the largest projected EOC-5 voltage is 7.2 volts.

8.5 SLB Leakage Analyses

This section summarizes the results of the projected EOC-5 SLB leak rate analyses applying the EPRI correlations for probability of leakage (POL) and the SLB leak rate versus voltage correlation. The EPRI methodology applies the log logistic form for the POL correlation and the leak rate results are given in Section 8.5.1 as the reference SLB leak rate. The NRC has requested leak rate results to be provided also for the log normal, log Cauchy, logistic, normal and Cauchy POL distributions and the results are also given in Section 8.5.2. The POL and leak rate correlations used for these analyses are described in Sections 6.4 and 6.5, respectively. The SLB leak rate analysis methodology for applying the probability of leakage and leak rate versus voltage correlations is described in Sections 6.6 to 6.8. SLB leak rates are provided at the upper, one-sided confidence of 95% based on the NRC guidance of the February 8, 1994 NRC/industry meeting on resolution of draft NUREG-1477 comments. The EOC-5 voltage distributions have been described above.

SLB leak rate analyses were performed for S/Gs A, C and D using preliminary voltage indication, voltage growth and tube plugging distributions. As noted above, S/G B has fewer indications than the other S/Gs and is not a candidate for the limiting S/G for leakage considerations. The preliminary leak rate analyses showed that S/G D had the highest projected EOC-5 SLB leak rate. The leak rate for S/G A was about half of that for S/G D and S/G C was only about one-third of the S/G D leak rate. Thus S/G D is the limiting S/G

for SLB leakage analyses and the results for this generator are given in Section 8.5.1 for the reference EPRI methodology and in Section 8.5.2 for sensitivity to the alternate POL correlations.

8.5.1 Reference SLB Leakage Analyses (Log Logistic POL)

The projected EOC-5 SLB leak rate for the limiting S/G D, as obtained with the reference EPRI correlations of Section 6, is 3.1 gpm. This leak rate is less than the allowable SLB leak of 9.1 gpm developed in Section 4.8 and thus is acceptable for the Braidwood-1 IPC application. Table 8-1 provides details of the leak rate calculation. The column titled N.i provides the projected EOC-5 voltage distribution including the POD = 0.6 adjustment. The P.i and Q.i columns represent the POL and expected leak rate for each voltage bin. The remaining columns provide data for the upper bound confidence of 95% applied to the leak rate.

Application of the POD adjustment to the EOC-4 voltage distribution leads to large voltage indications postulated to have been missed in the inspection and left in service at BOC-5. With the 1.0 volt repair limit and only RPC NDD indications above 1.0 volt left in service, the expected SLB leakage at BOC-5 would be about zero. The influence of the POD adjustment on predicted leakage values can be estimated by calculating the leak rate for the BOC-5 voltage distribution. The resulting SLB leak rate for S/G D at BOC-5 is 1.7 gpm compared to the expected near zero value. The leak rate thus increases only from 1.7 gpm at BOC to 3.1 gpm at EOC. Thus growth to the EOC only increases the SLB leak rate by about 1.4 gpm which would be near the projected leak rate assuming a POD of about 1.0.

8.5.2 SLB Leak Rate Sensitivity to POL Correlations

The NRC has requested that the projected EOC-5 SLB leak rate be provided for all six POL correlations discussed in draft NUREG-1477. These results provide sensitivity estimates to the form of the POL correlation. As discussed in Section 6.4, the linear and log Cauchy distributions are not consistent with the pulled tube database for low voltage (< 2.0 volt) probability of leakage and are not recommended for consideration as acceptable POL correlations. The estimated BOC-5 and EOC-5 SLB leak rates for all six POL correlations are given in Table 8-2. The results for the reference log logistic POL correlation have been described above and are repeated in Table 8-2.

It is seen from Table 8-2 that the SLB leak rates are essentially independent of the POL correlation applied to obtain the leak rates. The low leak rates for indications below 1 to 2 volts tend to offset the effects of the differences in POL correlations. As seen in

Table 8-1 for the column titled $N_i \cdot P_i \cdot Q_i$, which gives the expected leak rate, the SLB leak rates are dominated by EOC indications above about 3 volts even though only a small fraction of the EOC indications are in this voltage range.

8.6 Assessments of SLB Burst Margins and Probability of Burst

8.6.1 Deterministic Burst Margin Assessments

Although the technical support for the Braidwood-1 IPC is based on tube burst for limited TSP displacement, significant margins exist for free span burst considerations for voltage growth in excess of 95% cumulative probability. Limited TSP displacement considerations are necessary to accommodate only the largest few growth rates. A deterministic assessment of margins against assumed free span burst is given in Table 8-3. For the largest RPC confirmed indications of 1.0 volt left in service, the projected EOC-5 voltage at 95% growth is 2.8 volts compared to the 4.54 volts structural limit for free span burst at $1.43 \times \Delta P_{SLB}$. As shown in Table 8-3, a burst margin in excess of one volt exists even for the largest unconfirmed bobbin indication left in service. Even at 99% cumulative probability, the voltage growth is bounded by 2.7 volts (S/Gs A, D - Table 7.6) and the structural limit is satisfied for the 1.0 volt RPC confirmed indications left in service. Thus the evaluation for tube burst with limited TSP displacement is applied to accommodate only the largest 1% of the voltage growth distribution.

As shown in Section 4, Table 4.5.1, TSP displacements for an SLB at normal operating conditions are small for most plates and bounded by a maximum TSP displacement of 0.45 inch. Only about 40 TSP intersections at the tubelane corners of the 7th TSP are subject to TSP displacements exceeding 0.35". As shown in Section 6, Figure 6-2, a throughwall crack length of about 0.51 inch (lower tolerance limit material properties - LTL) corresponds to a burst capability of $1.43 \times \Delta P_{SLB} = 3660$ psi. Thus, for an SLB at normal operating conditions, the maximum exposed potential throughwall crack length of 0.45 inch is less than the R.G. 1.121 structural limit of 0.51 inch. It is shown in Section 8.6.4 that this corresponds to an extremely low probability of burst. It can also be noted from Figure 6-2, that the free span throughwall crack length for burst at SLB conditions of 2560 psi is about 0.75 inch. Thus a free span throughwall crack the length of the TSP thickness is required for burst at SLB conditions.

The exposed crack lengths associated with the maximum TSP displacements exceed the R.G. 1.121 structural limit of 0.51 inch only for a small number of TSP intersections for the conservative SLB at hot standby conditions. The remainder of this section emphasizes the probability of a SLB tube burst at hot standby conditions resulting from a potentially large indication at the TSP intersections where displacements are large.

8.6.2 Method of Analysis for SLB Tube Burst Probability

Assessment of the tube burst probability at SLB conditions for limited TSP displacement requires an estimate of the probability of a large indication occurring at the corners of the TSP where the TSP displacements are significant. Only plates 3 and 7 have significant TSP displacements such that a burst assessment is appropriate. Although the flow distribution baffle (FDB, plate 1) has a few TSP intersections with significant displacements, no bobbin indications have been found at the FDB. The FDB in the Model D4 S/Gs has large tube to FDB gaps (nominally 100 mils diametral clearance toward the center of the plate and 88 mils with radialized holes for the outer region). Thus there is a significantly lower likelihood of packed crevices with associated tube corrosion at the FDB intersections. Since no Braidwood-1 indications at the FDB have been found, the FDB is not included in the tube burst assessment.

The projected EOC-5 voltage distributions of Section 8.4 above are total indications independent of TSP elevation and tube location. The EOC-4 inspection results can be used to develop the distribution of indications between TSP elevations and the fraction of indications occurring at tube locations where the TSP displacements are significant. TSP displacements as a function of tube location were developed from the analyses described in Section 4 and the number of tube locations as a function of displacement are summarized in Table 4.5.3. Table 8-4 provides the inspection results for S/Gs A, C and D as a function of TSP elevation and TSP displacement. S/G B is not included due to the smaller number of indications found in this S/G. The table includes the fraction, F_D , of indications found as a function of displacement. Also given in the table are the number and fractions of indications for a uniform distribution of all tube intersections. Only 9 indications on plate 7 have been found in all S/Gs at tube locations having displacements large enough (greater than about 0.6 inch) to significantly influence the tube burst probability. The largest bobbin voltage for any of these 9 indications was 1.24 volts and the largest indication found anywhere on plate 7 was 2.74 volts. These indications would have a high burst pressure even as free span indications. Thus, the inspection results indicate a low frequency of indications and low voltages at tube locations subject to significant SLB TSP displacements.

The data of Table 8-4 can be used to define bounding distributions for indications as a function of TSP elevation and displacement. The highest fraction of indications at TSPs 3 and 7 were 67% at TSP 3 in S/G C and 13% at TSP 7 in S/G A. These values are used for the fraction of total indications at these TSP elevations. The bounding distribution for the fraction of indications on the TSP as a function of TSP displacement is obtained as the larger found by inspection or the uniform distribution. The resulting bounding distributions for plates 3 and 7 are given in Table 8-4. Also given is the weighted sum for the fraction of TSP indications as a function of displacement. This is obtained as the sum of the individual plate fractions multiplied by the fraction of indications for the TSP elevation. This weighted sum

of the bounding distributions is applied in the tube burst probability analyses as described below.

The number of indications as a function of TSP displacement can be obtained as the product of the total number of indications times the bounding fractional distribution of Table 8-4. This product can be obtained as a function of bobbin voltage by applying the number of indications in each voltage bin. The voltage bins and the number of EOC-5 indications in each voltage bin are shown in Figure 8-2 and Table 8-1 for S/G D, the most limiting S/G. Conservatively assuming that the TSP displacements expose throughwall cracks, the probability of tube burst as a function of exposed crack length is given by the upper curve in Figure 6-3. The probability of tube burst (PRB) can then be obtained as:

$$PRB = \sum_i PRB_i = \sum_i NV_i \left(0.67 \sum_j F_{D_j}^3 PRB_{D_j} + 0.13 \sum_j F_{D_j}^7 PRB_{D_j} \right) \quad (8.1)$$

$$PRB = \sum_i NV_i \sum_j (0.67 F_{D_j}^3 + 0.13 F_{D_j}^7) PRB_{D_j} \quad (8.2)$$

where

$i = i^{th}$ voltage bin

$j = j^{th}$ TSP displacement bin

NV_i = Number of indications in the i^{th} voltage bin

$F_{D_j}^3, F_{D_j}^7$ = Fraction of indications at plates 3 and 7 having TSP displacement in bin j

PRB_{D_j} = The smaller burst probability of either:

- $PRB(V_i)$ = Probability of burst for a free span indication of voltage V_i
- $PRB(D_j)$ = Prob. of burst for throughwall crack length equal to TSP disp. D_j

PRB_i = Probability of burst for the i^{th} voltage bin

The term in parentheses in Equation 2 is the weighted sum of the bounding distribution given in Table 8-4. Equation 2 is applied in Section 8.6.5 to estimate the burst probability at EOC-5.

8.6.3 SLB Burst Probability for S/G D at EOC-4

The burst probability for S/G D at EOC-4 with limited TSP displacement can be obtained directly from the indications found and the TSP displacement at each specific indication. This application demonstrates the general methodology for the limited TSP displacement, burst probabilities without the need for distributing the indications as described in Section 8.6.2 above. Table 8-5 identifies the indications found in the inspection for the larger voltage indications and for indications at locations having the largest TSP displacements in the hot standby SLB event. The bobbin voltage and free span burst probability at the given voltage level are provided for each indication. Also given in the table are the local TSP displacement and the burst probability for a throughwall crack length equal to the TSP displacement (conservatively assumed exposed throughwall crack length). The applicable SLB burst probability column shows the lower of the free span or throughwall burst probability for each indication. The lower of the two burst probabilities is the appropriate value since the limited TSP displacement can reduce the free span burst probability but the free span probability cannot be exceeded. The throughwall burst probability can exceed the free span value only because it is conservatively calculated for a throughwall crack while the free span value, based on bobbin voltage, is more realistically based on the actual crack morphology as reflected in the voltage amplitude.

For the S/G D indications given in Table 8-5, the total burst probability calculated assuming free span (very large SLB TSP displacements) conditions is 3.7×10^{-2} . Accounting for the limited SLB TSP displacements at the locations of the indications, the total burst probability is 1.7×10^{-5} . Thus the limited TSP displacements reduce the burst probability by three orders of magnitude. It can be noted that none of the high voltage indications occurred at locations of high TSP displacement and the TSP constraint reduces the burst probability for these high voltage indications to approximately zero. Only the small voltage indications found at the corners of plate 7, where SLB displacements are significant, contribute to the burst probability.

The results of Table 8-5 show the effectiveness of limited TSP displacements in reducing the tube burst probability to small values and also show that Braidwood-1 had an acceptably low burst probability at EOC-4.

8.6.4 Conservative Burst Probability for SLB at Normal Operating Conditions

For a SLB at normal operating conditions, it is shown in Section 4, Table 4.5.1 that TSP displacements are small and significantly less than that for an SLB at hot standby conditions.

The maximum TSP displacement occurs for plate J and is limited to 0.438 inch. The maximum displacements for all other plates are < 0.2 inch. An extremely conservative or bounding burst probability for this event can be obtained by assuming that the SLB displacements expose a throughwall crack equal to the displacements at every TSP intersection on all seven hot leg TSPs above the FDB. The FDB is excluded from the analysis as no indications have been found at this plate and the larger tube to TSP gap at the FDB would require supplemental burst tests to determine the influence of the FDB constraint on the burst pressure. The throughwall crack assumption is approximately equivalent to assuming that a throughwall crack equal to the TSP thickness is present at every hot leg TSP intersection.

Table 8-6 summarizes the bounding analysis for the burst probability resulting from an SLB at normal operating conditions. The maximum TSP displacement column represents the maximum displacement at any location on the plate except for plate 7 which is divided into three displacement magnitudes to permit separation of the number of TSP intersections subject to the larger TSP displacements. The number and maximum voltages for EOC-4 indications found at each plate are given in the table for general information. The number of tubes column represents the number of TSP intersections with the maximum displacement of column 2. The exposed length burst probability is that associated with a throughwall crack length equal to the maximum TSP displacement. The last column provides the burst probability obtained by multiplying the exposed length probability by the number of tubes.

The total S/G burst probability for this conservative assumption of throughwall indications at each hot leg TSP intersection is $< 5 \times 10^{-7}$. This very low probability bounds all realistic potential indications at the TSP intersections and demonstrates the effectiveness of modest TSP displacements under the SLB at normal operating conditions. As noted in Section 8.6 below, normal operating conditions dominate the operating time and the highest frequency for an SLB event occurs at power conditions where the SLB loads on the TSPs and associated displacements are lower than for an SLB at hot standby conditions.

8.6.5 Burst Probability for a SLB at Hot Standby Conditions

For Cycle 5 SLB leakage and burst considerations, S/G D is the most limiting and the projected EOC-5 voltage distribution is given in Figure 8-2. The tube burst probability for S/G D at EOC-5, assuming an SLB at hot standby conditions, is evaluated in this section. The methodology of Equation 8.2 given in Section 8.6.2 is applied for this assessment. The total EOC-5 voltage distribution of Figure 8-2 is distributed as a function of TSP displacement using the weighted sum of the bounding distribution of Table 8-4. Free span burst probabilities as a function of voltage are developed from the burst pressure versus bobbin voltage correlation of Section 6.1 and burst probabilities for exposed throughwall cracks are given in Figure 6-3.

The results of the burst probability analysis are summarized in Table 8-7. For each voltage bin of the projected EOC-5 voltage distribution (including $POD = 0.6$ adjustment), the number of indications, free span burst probability, the distribution of indications and throughwall burst probability as a function of the SLB TSP displacement are given in Table 8-7. By applying Equation 2, the net probability of burst for each voltage level is obtained as given in the last column of the table. The total limited TSP displacement burst probability is obtained as 8×10^{-4} . The influence of the limited TSP displacement can be seen by comparison with the estimated free span burst probability (column 3) of 9×10^{-2} . The latter free span result is dominated by the large projected EOC-5 voltage indications up to 11.2 volts which are traceable to applying the POD adjustment to all indications found in the last inspection prior to reducing the population for tubes repaired at EOC-4.

The estimated SLB tube burst probability of 8×10^{-4} is significantly less than the acceptance guideline for IPC applications of 2.5×10^{-2} , which was found acceptable in NUREG-0844. The normal operating and hot standby burst probabilities can be combined by weighting the separate burst probabilities by the fraction of operating time in each operating condition. Applying the Section 4.6 Braidwood 1 fractions of 0.962 for normal operation and 0.038 for hot standby, the combined burst probability is 3.1×10^{-5} .

8.6.6 Braidwood-1 Frequency of SLB Event with a Tube Rupture

In Section 4.6, Braidwood-1 frequencies of occurrence were developed for an SLB at both normal operating and hot standby (Mode 3) conditions. The frequencies are summarized in Figure 8-5. The frequency for an SLB event at hot standby conditions is a factor of 25 lower than at operating conditions and is only about 6.8×10^{-5} per year. Figure 8-5 includes the conditional probability of a tube rupture at normal operating and hot standby conditions as developed in Sections 8.6.4 and 8.6.5, respectively. The SLB event frequencies and conditional tube rupture probabilities are combined in Figure 8-5 to obtain a frequency of about 5.5×10^{-8} per year for a Braidwood-1 SLB event with a subsequent tube rupture. This very low frequency has negligible influence on the core damage frequency and supports full cycle operation at Braidwood-1 following implementation of the IPC for Cycle 5.

8.7 Updated SLB TSP Loads, Displacements and Burst Probability Assessment

The assessment described in Section 8.6 above was developed from the preliminary, bounding SLB hydraulic loads on the TSPs available at the time of Revision 0 of this report as described in Section 4.2. The TSP hydraulic loads in a SLB were updated by TRANFLO reanalyses using the latest code version and input data as described in Section 4.10. The TSP displacements associated with the updated loads are described in Section 4.11. This section provides an assessment of the updated SLB TSP loads and displacements to also update the burst probability resulting from the new TSP displacements. The prior analyses provided a

bounding set of SLB loads for the SLB at hot standby conditions in that an available analysis was utilized that had a guillotine break of the steamline at the exit of the S/G with the S/G water level at the elevation of the uppermost TSP and the transient included an excess feedwater flow condition simultaneously with the SLB. The updated analyses assume the same guillotine break location with the water level at the controlled water level of 487 inches above the top of the tubesheet. Updated analyses were performed for an SLB at both hot standby and full power operating conditions. With water level at the controlled elevation, the TSP loads and displacements are slightly larger for the SLB at full power than for the SLB at hot standby and the full power displacements are further evaluated in this section. Two analyses at full power conditions were performed. Case 5, called the reference case for comparisons with other cases, was setup to have low TSP pressure drops at steady state, time = 0, conditions in the TRANFLO analysis. Case 6 was setup to match the expected pressure drops as determined from performance analyses for the Braidwood-1 S/Gs. Case 5 was found to result in somewhat higher maximum SLB TSP displacements than Case 6 and is applied for the tube burst probability estimates given below.

8.7.1 TSP Displacements as a Function of Tube Location

For TSP 3, which has the maximum displacement for the limiting full power SLB (Case 5) TSP displacements were developed as a function of tube location. Summary total tubes at varying displacements are given in Table 4-38. Figure 8-6 shows a map of the TSP 3 displacements for the SLB at normal operating conditions. The largest displacements, maximum of 0.472 inch, occur only at the corners of the plate near the tubelane as shown in Figure 8-6. The notes to the figure also provide the tube burst probability per indication (See Section 6.3) evaluated at the maximum displacement for each displacement bin of the figure. It is seen that the TSP displacements at most (4468 out of 4578 locations) have TSP displacements < 0.1 inch. For the 4 tube locations with displacements in the range of 0.45 to 0.48 inch, the burst probability, very conservatively assuming an exposed throughwall crack equal to the displacement of the TSP, remains < 7×10^{-7} per indication. Only 50 tube locations have TSP displacements in the range of 0.35 to 0.45 inch with burst probabilities < 10^{-7} per indication. It is readily seen that the TSP displacements are sufficiently small to limit the tube burst probability to very small levels. A more quantitative demonstration of the associated low tube burst probability is given in Section 8.7.2.

Figure 8-7 shows the location of indications on TSP 3 for each S/G from the EOC-4, March 1994 inspection. S/Gs A and D have the most indications near the edges of the plate with maximum SLB displacements. Only 8 out of 1590 indications at TSP 3, as summed over all four S/Gs, are located at tubes with TSP displacements between 0.35 and 0.45 inch. All other indications at TSP 3 have displacements < 0.35 inch and burst probabilities < 7.4×10^{-12} per indication.

8.7.2 Bounding Tube Burst Probability for Updated Analyses

The very conservative tube burst probability analysis of Section 8.6.5 and Table 8-6 is updated in Table 8-8 for the latest SLB at full power (Case 5). As noted previously, the maximum SLB TSP displacements, with water level at the controlled value of 487 inches, occurs for an SLB at full power conditions. The prior, bounding SLB analyses were obtained at hot standby conditions with the water level at the uppermost TSP elevation of 280 inches. With the hot standby SLB water level at the controlled value of 487 inches, the hot standby SLB TSP displacements are slightly less than the case for the SLB at full power.

The conservative analysis of Table 8-8 assumes that every hot leg TSP has an exposed (uncovered from TSP constraint against burst) throughwall crack length equal to the length of the maximum TSP displacement shown in the Table for each plate. Even under this assumption, it is seen that the tube burst probability would be $\leq 5.4 \times 10^{-6}$. This burst probability, which envelopes that for SLBs at both hot standby and full power conditions, can be compared to the prior bounding analysis result of 8×10^{-4} for an SLB at hot standby (Table 8-7) and 5×10^{-7} for an SLB at full power. The updated analyses based on SLBs at the controlled water level thus lower the burst probability by about a factor of 70 compared to the prior bounding analyses. The updated analyses for an SLB at full power result in a factor of 10 increase in the burst probability compared to that of Table 8-6. However, the net (weighted by fraction of time at each operating condition from Figure 8-5) conditional probability of a tube rupture, given a SLB event, was 3.1×10^{-5} by the prior analyses and is bounded by the 5.4×10^{-6} value for the updated analyses.

The results of the updated analyses with revised Model D4 hydraulic loads confirm the expected result that the prior analyses bound the Braidwood-1 tube burst probability projected at EOC-5. Both the prior and updated analyses for the conditional burst probability result in values much less than the acceptance guideline of 2.5×10^{-2} . Thus the burst probability for Braidwood-1 at EOC-5, based on limited SLB TSP displacements, is acceptable for full cycle operation.

8.7.3 Margin Factors on Loads for Prior Bounding TSP Displacement Analyses

Comparison of the TSP hydraulic loads from the prior and updated analyses permit an assessment of margins on the loads that result in acceptable tube burst probabilities. Peak pressure drops minus the steady state pressure drop at time = 0 are used for this comparison as this quantity represents the peak change in pressure drop resulting from the SLB event and the TSP displacements from the SLB are calculated relative to the time = 0 positions. For hot standby analyses with no steady state flow, the time = 0 pressure drops and displacements are zero and the peak pressure drops are used for this comparison. Table 8-9 provides a summary of the peak hydraulic load at each TSP for each of the six TRANFLO analyses

performed and described in Section 4. The last column of the table provides the ratio of the peak load for the prior bounding hot standby SLB to the updated peak load for the full power SLB of Case 5 which envelopes (larger maximum TSP displacement) the updated hot standby SLB load and the Case 6 full power TRANFLO analysis. This ratio in Table 8-9 shows that acceptable burst probabilities are obtained for peak pressure drop ratios ranging from 1.24 to 4.22 relative to the updated reference analysis which represents the more probable SLB TSP displacements. Plate 7(J) had the maximum TSP displacements in the prior hot standby analyses. It is seen that the prior analyses provide a margin ratio of 2.15 on the load for Plate 7 even though the TSP displacements resulting from the prior analyses resulted in an acceptable tube burst probability. Thus large margins on the TSP loads are acceptable for the Model D4 S/G while maintaining low tube burst probabilities due to the limited TSP displacements.

Acceptable burst probabilities are obtained for Plates 3 and 5 with load ratios of 1.24 and 1.55, respectively, and loads in the downward direction (negative loads in Table 8-9). Loads in the upward direction (positive loads in Table 8-9) up to about 1 psi were also found acceptable for Case 2. Plate 7 has also been analyzed for loads in both directions with load margin factors up to 2.15 since the loads on this plate have been found in some analyses (Figure 4-10 for Case 2, for example) to reverse in direction during the event. Plates 8 to 11 are acceptable even with the highest loads and margin ratios of 1.99 to 4.22 relative to the updated analyses. Overall, the summary of Table 8-9 shows that large margins on the TRANFLO hydraulic loads can be applied to the reference, updated analyses and continue to result in acceptable burst probabilities. Since the SLB of Case 3 still results in a factor of 30 margin on burst probability (8×10^{-4} versus 2.5×10^{-2} guideline) compared to the acceptance guideline based on NUREG-0844, larger load margin factors than those of Table 8-9 would be expected to also result in acceptable burst probabilities.

8.8 Tube Integrity Assessment Based on Braidwood-1 Pulled Tube Results

The Braidwood-1 pulled tube examination results (See Section 3) show burst pressures and SLB leak rates in very good agreement with the EPRI correlations used in the initial release of this report. There is no need to update the EPRI correlations based on the Braidwood-1 results and the prior analyses given above for SLB leak rates and free span burst probabilities remain applicable. Eleven indications were burst tested and all indications burst, as expected, in the axial direction. The crack morphology of dominantly axial indications is consistent with the EPRI database and the EPRI correlations are applicable to Braidwood-1.

All burst test results exceeded R.G 1.121 burst requirements with the lowest measured burst pressure of 4,730 psi obtained for the 10.3 volt indication, which was the largest indication found in the 1994 inspection. The burst pressures lie above and below the best fit regression

correlation for burst pressures and all data are within the 95% confidence bands on the burst correlation. Inclusion of the Braidwood-1 data in the correlation has a negligible influence on the correlation. SLB leak rates measured for the Braidwood-1 pulled tubes are below the regression fit to the EPRI database and inclusion of the Braidwood-1 data in the correlation would lower the estimated SLB leak rates given above by about 14% (not included in current analyses). Bobbin indications at 2.05, 5.00 and 10.3 volts had measured SLB leakage while indications at 0.21, 0.28, 0.91, 3.35 and 3.73 volts had no SLB leakage. The largest SLB leak rate of 12.8 liter/hr (0.056 gpm) was obtained for the 10.3 volt indication which is less than the nominal SLB leak rate correlation value of about 60 liter/hr at 10.3 volts. Thus, the Braidwood-1 pulled tube results support probable SLB leak rates significantly less than obtained from the analyses in this section based on the upper 95% confidence on the predicted leak rate.

The Braidwood-1 pulled tube results indicate that all tube integrity requirements were satisfied at EOC-4 in that burst pressures for all indications including the largest 10.3 volt indication met R.G. 1.121 requirements and that SLB leak rates would have been well below 10CFR100 limits. The tube burst probability calculated from the actual EOC-4 voltage distribution, without any adjustment for the pulled tube results, is 4.4×10^{-2} . Eliminating only the 10.3 volt indication, which was burst tested, from the EOC-4 analysis results in a burst probability of 2.1×10^{-2} . The general trend of the Braidwood-1 burst data to be near the mean of the burst correlation would indicate that the burst probability would likely be significantly lower than the 2.1×10^{-2} value which satisfies the acceptance guideline of 2.5×10^{-2} . The SLB leak rate calculated from the actual S/G D voltage distribution at EOC-4 is 2.1 gpm at 95% confidence which is lower than the allowable leak rate of 9.1 gpm that provides a factor of 10 margin against 10CFR100 dose limits. Based on the pulled tube results, the potential SLB leakage at EOC-4 would very likely have been lower than the calculated, acceptable value. Thus, structural and leakage integrity requirements were met at EOC-4.

Since tube integrity requirements were satisfied at EOC-4 and the limiting indications at EOC-5 are expected to be smaller than or, as a minimum, insignificantly larger than found for Cycle 4, it can be expected that all tube integrity requirements will be satisfied at EOC-5. The Braidwood-1 pulled tube results strongly support full cycle operation for Cycle 5.

8.9 Summary of Results

An IPC with a 1.0 bobbin voltage repair limit has been implemented for Braidwood-1 Cycle 5 operation. Inspection requirements typical of IPC practice, such as the guidelines of the Catawba-1 NRC SER, were applied at the Cycle 4 refueling outage to support implementation of the IPC. An operating leakage limit of 150 gpd is being applied for Cycle 5 operation. The results of the Braidwood-1 IPC assessment can be summarized as follows:

- The Braidwood-1 pulled tube results indicate that tube integrity structural and leakage requirements were satisfied at EOC-4. Burst pressures for all indications including the largest indication (10.3 volts) found in the inspection exceeded R.G. 1.121 requirements. Measured SLB leak rates for the 3 indications that leaked were below the best fit regression fit to the EPRI database which would indicate expected Braidwood-1 leak rates significantly less than the plus 95% confidence level applied for the leakage analyses. Since the EOC-4 tube integrity requirements were satisfied and the EOC-5 maximum voltage indications are expected to be smaller or no worse than found for Cycle 4, the Braidwood-1 pulled tube results strongly indicate that tube integrity requirements would be satisfied at EOC-5.
- The projected EOC-5 SLB leakage is 3.1 gpm which is less than the allowable limit of 9.1 gpm for Braidwood-1. The SLB leak rate was evaluated for the six alternate formulations of the probability of leak versus voltage correlation identified in draft NUREG-1477 and found to be essentially independent of the correlation applied in the analysis. The SLB leak rates were obtained by applying the leak rate versus voltage correlation based on the EPRI database and outlier evaluation consistent with the NRC guidance of the February 8, 1994 NRC/industry meeting on resolution of draft NUREG-1477 comments.
- Updated hydraulic analyses for SLB loads on the TSPs were performed to eliminate conservatism in the prior analyses. The prior analyses for a SLB at hot standby conditions assumed a water level at the uppermost TSP elevation while the updated analyses apply the controlled water level of 487 inches above the tubesheet. The prior analyses utilized existing TRANFLO loads and were intended to bound more realistic estimates. The updated analyses confirm that the prior analyses were bounding in that peak pressure drops across the TSPs are factors of 1.24 to 4.22 higher than obtained for the updated, more realistic analyses for the loads.
- The conditional SLB tube burst probability for the updated analyses is 5.4×10^{-6} , which bounds SLBs at hot standby and full power conditions, compared to the prior analysis result of 8×10^{-4} for a SLB at hot standby conditions. For the prior analyses, the probability of burst during a postulated SLB, obtained by combining the hot standby and full power results based on operating times at each plant condition, was 3.1×10^{-5} . Thus the updated, more realistic SLB hydraulic loads result in tube burst probabilities significantly lower than the prior analyses which were intended to bound the updated results. Both the prior and updated burst probabilities are significantly lower than the IPC acceptance guideline of 2.5×10^{-2} . The tube burst analyses are developed based on limited TSP displacements predicted during an SLB event for the Braidwood-1 S/Gs even when applying very conservative load conditions for the hot standby SLB.

- Deterministic tube burst analyses show that the projected EOC voltage, with voltage growth rates up to 99% cumulative probability on the Cycle 4 measured growth distribution, is less than the R.G. 1.121 structural limit of 4.54 volts for a $1.43 \times \Delta P_{SLB}$ burst margin.
- The modest EOC-5 SLB leakage and low tube burst probabilities strongly support full cycle operation for Cycle 5 at Braidwood-1 following implementation of the 1.0 volt IPC.

Table 8-1: Braidwood 1, SG "D", PoD = 0.6, EOC 5 Volts								Cauchy
EOC Volts	Cum Prob	Tubes with ≥ Volts	N.i	P.i	Expected Q.i @2560 psi	Variance Q.i	N.i*P.i*Q.i	Variance P.i * Q.i
0.2	0.000984	1016.00	1.0	3.11E-02	5.17E-04	6.15E-05	1.61E-05	1.92E-06
0.3	0.010827	1015.33	10.0	3.19E-02	1.78E-03	3.49E-04	5.67E-04	1.12E-05
0.4	0.049213	1005.09	39.0	3.26E-02	4.12E-03	1.22E-03	5.24E-03	4.02E-05
0.5	0.123031	966.28	75.0	3.34E-02	7.83E-03	3.26E-03	1.96E-02	1.11E-04
0.6	0.222441	891.35	101.0	3.42E-02	1.32E-02	7.40E-03	4.55E-02	2.59E-04
0.7	0.334646	790.25	114.0	3.51E-02	2.04E-02	1.50E-02	8.17E-02	5.40E-04
0.8	0.447835	675.79	115.0	3.60E-02	2.99E-02	2.78E-02	1.24E-01	1.03E-03
0.9	0.550197	561.22	104.0	3.70E-02	4.18E-02	4.84E-02	1.61E-01	1.85E-03
1.0	0.639764	456.55	91.0	3.80E-02	5.64E-02	8.00E-02	1.95E-01	3.16E-03
1.1	0.712598	366.30	74.0	3.91E-02	7.41E-02	1.27E-01	2.14E-01	5.16E-03
1.2	0.771654	291.82	60.0	4.02E-02	9.51E-02	1.94E-01	2.29E-01	8.13E-03
1.3	0.817913	231.92	47.0	4.14E-02	1.20E-01	2.87E-01	2.33E-01	1.25E-02
1.4	0.853346	184.96	36.0	4.27E-02	1.48E-01	4.15E-01	2.27E-01	1.86E-02
1.5	0.880906	148.63	28.0	4.40E-02	1.81E-01	5.86E-01	2.23E-01	2.72E-02
1.6	0.902559	120.69	22.0	4.55E-02	2.18E-01	8.12E-01	2.18E-01	3.90E-02
1.7	0.919291	99.09	17.0	4.70E-02	2.60E-01	1.11E+00	2.07E-01	5.50E-02
1.8	0.932087	82.01	13.0	4.86E-02	3.06E-01	1.48E+00	1.94E-01	7.65E-02
1.9	0.942913	69.04	11.0	5.04E-02	3.59E-01	1.96E+00	1.99E-01	1.05E-01
2.0	0.950787	58.50	8.0	5.23E-02	4.16E-01	2.56E+00	1.74E-01	1.42E-01
2.1	0.956693	50.34	6.0	5.43E-02	4.80E-01	3.30E+00	1.57E-01	1.91E-01
2.2	0.961614	43.86	5.0	5.66E-02	5.50E-01	4.22E+00	1.56E-01	2.55E-01
2.3	0.965551	38.83	4.0	5.89E-02	6.27E-01	5.34E+00	1.48E-01	3.36E-01
2.4	0.968504	34.97	3.0	6.15E-02	7.11E-01	6.69E+00	1.31E-01	4.41E-01
2.5	0.971457	31.96	3.0	6.44E-02	8.01E-01	8.33E+00	1.55E-01	5.75E-01
2.6	0.973425	29.39	2.0	6.75E-02	9.00E-01	1.03E+01	1.21E-01	7.45E-01
2.7	0.975394	27.19	2.0	7.09E-02	1.01E+00	1.26E+01	1.43E-01	9.60E-01
2.8	0.976378	25.24	1.0	7.47E-02	1.12E+00	1.54E+01	8.36E-02	1.23E+00
2.9	0.978346	23.55	2.0	7.89E-02	1.24E+00	1.86E+01	1.96E-01	1.58E+00
3.0	0.979331	21.99	1.0	8.35E-02	1.37E+00	2.24E+01	1.15E-01	2.01E+00
3.1	0.981299	20.58	2.0	8.88E-02	1.52E+00	2.68E+01	2.69E-01	2.57E+00
3.2	0.982283	19.34	1.0	9.47E-02	1.67E+00	3.19E+01	1.58E-01	3.26E+00
3.3	0.983268	18.25	1.0	1.01E-01	1.83E+00	3.79E+01	1.85E-01	4.15E+00
3.4	0.984252	17.35	1.0	1.09E-01	2.00E+00	4.47E+01	2.18E-01	5.27E+00
3.6	0.985236	15.74	1.0	1.29E-01	2.37E+00	6.15E+01	3.05E-01	8.55E+00
3.7	0.986220	15.01	1.0	1.41E-01	2.57E+00	7.18E+01	3.63E-01	1.09E+01
3.9	0.987205	13.56	1.0	1.74E-01	3.01E+00	9.67E+01	5.24E-01	1.81E+01
4.0	0.988189	12.83	1.0	1.96E-01	3.25E+00	1.12E+02	6.37E-01	2.35E+01
4.1	0.989173	12.08	1.0	2.23E-01	3.50E+00	1.28E+02	7.83E-01	3.08E+01
4.3	0.990157	10.55	1.0	3.01E-01	4.05E+00	1.69E+02	1.22E+00	5.42E+01
4.4	0.991142	9.71	1.0	3.55E-01	4.34E+00	1.93E+02	1.54E+00	7.26E+01
4.5	0.992126	8.94	1.0	4.19E-01	4.64E+00	2.19E+02	1.95E+00	9.71E+01
4.7	0.993110	7.51	1.0	5.63E-01	5.30E+00	2.82E+02	2.99E+00	1.66E+02
4.8	0.994094	6.90	1.0	6.30E-01	5.65E+00	3.19E+02	3.56E+00	2.08E+02
5.1	0.995079	5.62	1.0	7.89E-01	6.80E+00	4.54E+02	5.22E+00	3.57E+02
5.7	0.996063	4.60	1.0	8.79E-01	9.55E+00	8.75E+02	8.40E+00	7.80E+02
7.4	0.997047	3.52	1.0	9.51E-01	2.14E+01	4.24E+03	2.04E+01	4.05E+03
8.9	0.998031	2.52	1.0	9.68E-01	3.81E+01	1.33E+04	3.69E+01	1.29E+04
9.7	0.999016	1.58	1.0	9.73E-01	5.00E+01	2.29E+04	4.87E+01	2.24E+04
10.5	0.999705	0.65	0.7	9.77E-01	6.43E+01	3.80E+04	4.40E+01	3.72E+04
11.2	1.000000	0.33	0.3	9.79E-01	7.89E+01	5.76E+04	2.32E+01	5.65E+04
Regression Equations Analysis								
Sum[Ni * E(Qi) * Pi] =								205.592
Sum[Var + Cov] =								9.17E+04
Effective Standard Deviation =								3.03E+02
Confidence =								95.0%
Z - Deviate =								1.645
Q.total (LPH) =								703.6
Q.total (GPM) =								3.098

Table 8-2. Summary of Cycle 5 SLB Leak Rate Analyses for S/G D		
Method of Analysis	BOC	EOC
EPRI SLB Leak Rate versus Voltage Correlation		
<ul style="list-style-type: none"> • POD = 0.6 • Leak rates based on EPRI voltage correlation • POL Correlation 		
Reference SLB Leak Rate		
- Log logistic POL	1.71	3.1
SLB Leak Rate Sensitivity to POL Correlation		
- Log normal POL	1.71	3.1
- Log Cauchy POL	1.69	3.1
- Logistic POL	1.73	3.1
- Normal POL	1.73	3.2
- Cauchy POL	1.70	3.1

Table 8-3. Summary of Deterministic Margins Against Burst at SLB Conditions
(95% Confidence)

Parameter	S/G A	S/G B	S/G C	S/G D
RPC Confirmed Indications Left in Service				
Largest bobbin voltage	1.00	1.00	1.00	1.00
NDE uncertainty at 95% confidence • 20% of bobbin voltage	0.20	0.20	0.20	0.20
Voltage growth at 95% cumulative probability	1.40	0.50	1.40 ⁽¹⁾	1.00
Projected EOC-5 Voltage	2.60	1.7	2.60	2.20
Allowable EOC Voltage at $1.43 \times \Delta P_{SLB}$	4.54 volt			
Largest Bobbin Voltage, RPC NDD Left in Service				
Largest bobbin voltage	1.48	2.03	1.55	1.8
NDE uncertainty at 95% confidence • 20% of bobbin voltage	0.30	0.41	0.31	0.36
Voltage growth at 95% cumulative probability	1.40	0.50	1.40 ⁽¹⁾	1.00
Projected EOC-5 Voltage	3.18	2.49	3.26	3.16
Allowable EOC Voltage at $1.43 \times \Delta P_{SLB}$	4.54			
Notes: 1. Growth rate for S/G A conservatively applied to S/G C				

Table 8-4

Distribution of Indications as a Function of Hot Standby TSP Displacement and Elevation

SG	TSP	Cycle 4		Number and Fraction of Indications as a Function of TSP Displacement															
		Indications		< 0.45"		0.45" - 0.50"		0.50" - 0.55"		0.55" - 0.60"		0.60" - 0.65"		0.65" - 0.70"		0.70" - 0.75"		> 0.75"	
		No.	%	No.	F _D	No.	F _D	No.	F _D	No.	F _D	No.	F _D	No.	F _D	No.	F _D	No.	F _D
A	3	368	50%	368	1.0	0		0		0		0							
	5	248	33%	248	1.0														
	7	93	13%	86	0.924	2	0.0215	0		2	0.0215	1	0.0108	1	0.0108	1	0.0108	0	
	≥8	33	4%	33	1.0														
C	3	713	67%	712	0.999	1	0.0014	0		0		0							
	5	237	22%	237	1.0														
	7	94	9%	88	0.936	2	0.0213	3	0.0319	0		0		0		1	0.0106	0	
	≥8	22	2%	22	1.0														
D	3	404	58%	403	0.998	0		1	0.0025	0		0							
	5	181	26%	181	1.0														
	7	77	11%	66	0.857	3	0.0390	3	0.0390	0		1	0.0130	2	0.0260	1	0.0130	1	0.0130
	≥8	34	5%	34	1.0														
Uniform TSP Dist. (4578 tubes)	3			4548	0.993	18	0.0039	10	0.0022	2	0.00044	0							
	7			4366	0.954	48	0.0105	42	0.0092	34	0.0074	30	0.0066	22	0.0048	14	0.0031	22	0.0048
Bounding Distribution • Weighted Sum	3		67%		0.993		0.0039		0.0025		0.0004		0						
	7		13%		0.834		0.0390		0.0390		0.0215		0.0130		0.0260		0.0130		0.0130
	3+7				0.774		0.0077		0.0067		0.0031		0.0017		0.0034		0.0017		0.0017

Table 8-5
Braidwood-1, SG D - Estimated Hot Standby SLB Burst Probability at EOC-4

Tube/Location			Free Span Burst		Limited TSP Disp Burst (1)		Applicable SLB Burst Prob. (2)
Row	Col	TSP	Volts	Burst Prob.	Local TSP Disp.	TW Burst Prob.	
37	34	5	10.44	2.0E-02	< 0.12	< 1.0E-12	~ 0.0
23	12	3	8.82	1.2E-02	< 0.35	< 1.0E-11	~ 0.0
12	9	3	5.02	1.5E-03	< 0.35	< 1.0E-11	~ 0.0
11	9	3	4.28	8.0E-04	< 0.35	< 1.0E-11	~ 0.0
19	7	3	3.95	5.7E-04	< 0.35	< 1.0E-11	~ 0.0
33	20	3	3.83	5.0E-04	< 0.35	< 1.0E-11	~ 0.0
35	29	3	3.62	3.9E-04	< 0.35	< 1.0E-11	~ 0.0
11	12	3	3.21	2.3E-04	< 0.35	< 1.0E-11	~ 0.0
16	42	3	3.12	2.0E-04	< 0.35	< 1.0E-11	~ 0.0
2	105	3	2.84	1.3E-04	< 0.35	< 1.0E-11	~ 0.0
8	20	3	2.77	1.2E-04	< 0.35	< 1.0E-11	~ 0.0
43	56	3	2.60	8.8E-05	< 0.35	< 1.0E-11	~ 0.0
32	27	5	2.48	7.1E-05	< 0.12	< 1.0E-12	~ 0.0
45	53	3	2.30	4.9E-05	< 0.35	< 1.0E-11	~ 0.0
31	20	3	2.20	4.0E-05	< 0.35	< 1.0E-11	~ 0.0
27	35	3	2.18	3.8E-05	< 0.35	< 1.0E-11	~ 0.0
41	55	3	2.16	3.7E-05	< 0.35	< 1.0E-11	~ 0.0
43	53	3	2.11	3.3E-05	< 0.35	< 1.0E-11	~ 0.0
2	113	3	0.59	2.2E-07	0.514	1.9E-05	2.2E-07
3	110	3	0.58	2.1E-07	0.406	3.5E-09	3.5E-09
2	113	7	0.56	1.9E-07	0.804	4.5E-01	1.9E-07
2	108	7	1.10	3.5E-06	0.631	9.0E-03	3.5E-06
2	105	7	0.64	3.5E-07	0.530	5.3E-05	3.5E-07
2	11	7	0.72	5.6E-07	0.498	4.9E-06	5.6E-07
4	106	7	0.52	1.4E-07	0.532	6.3E-05	1.4E-07
4	112	7	1.24	6.0E-06	0.718	1.2E-01	6.0E-06
5	112	7	1.24	6.0E-06	0.692	6.4E-02	6.0E-06

(continued on next page)

Table 8-5
Braidwood-1, SG D - Estimated Hot Standby SLB Burst Probability at EOC-4

Tube/Location			Free Span Burst		Limited TSP Disp. Burst (1)		Applicable SLB Burst Prob. (2)
Row	Col.	TSP	Volts	Burst Prob.	Local TSP Disp.	TW Burst Prob.	
7	105	7	0.59	2.2E-07	0.456	2.7E-07	2.2E-07
13	110	7	0.88	1.3E-06	0.417	8.0E-09	8.0E-09
Total Burst Probability				3.7E-02			1.7E-05

Notes:

1. Analysis conservatively assumes the TSP displacement exposes a throughwall crack length equal to the displacement.
2. The applicable burst probability is the lower of the free span or TW burst probabilities.

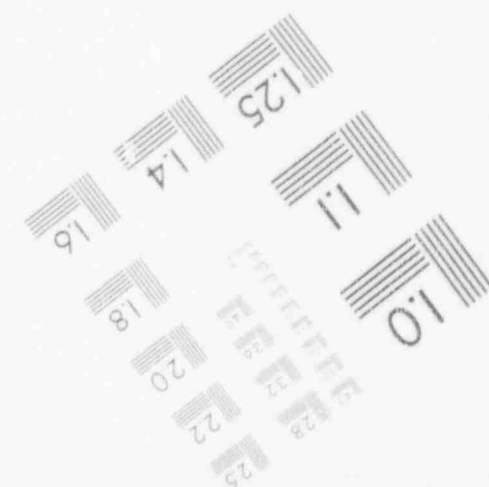
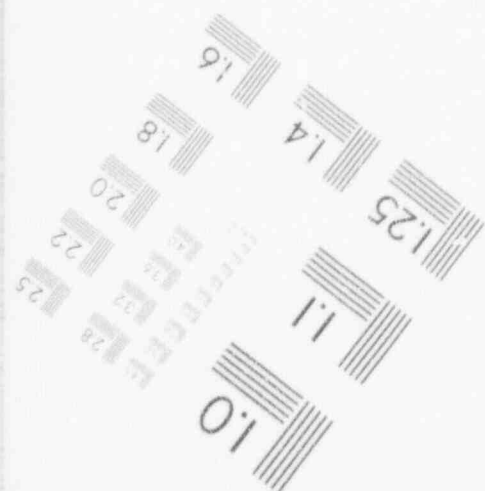
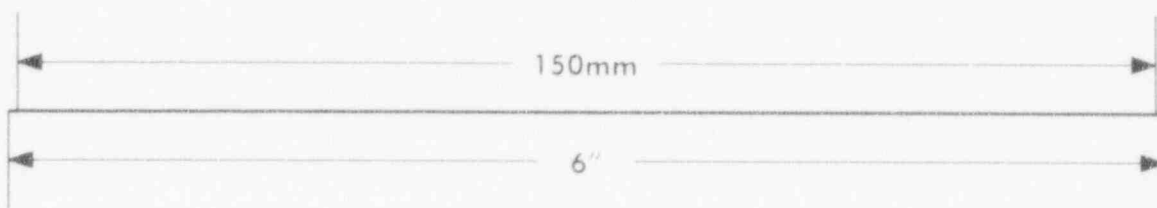
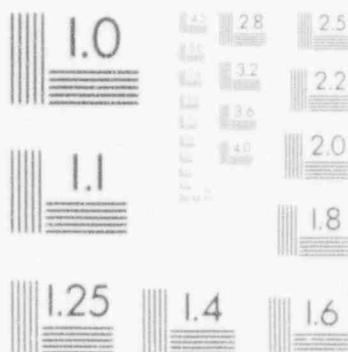
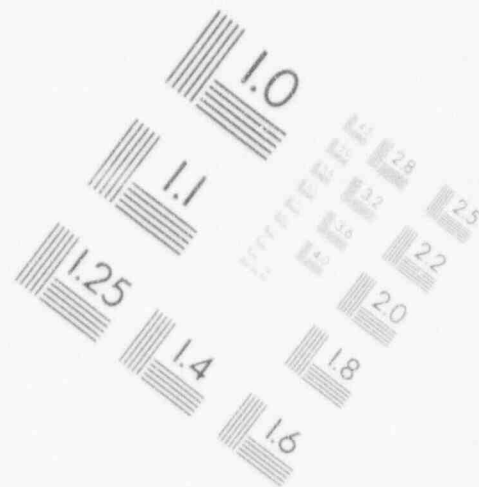
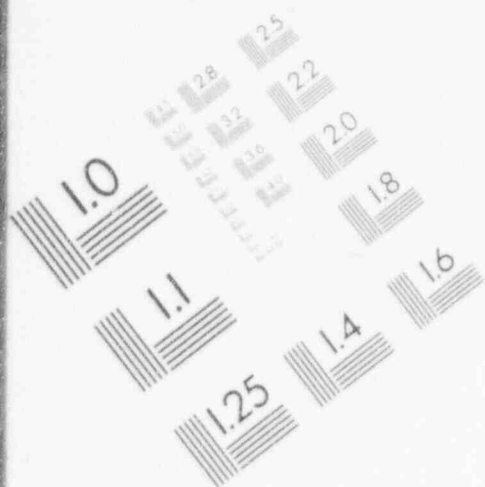
Table 8-6. Bounding SLB Burst Probability at Normal Operating Conditions

TSP	Maximum TSP Displacement (inch)	EOC-4 Indications		Bounding SLB Burst Probability		
		Max. No. Ind. at TSP	Max. Volts at TSP	Number Tubes	Exposed Length Burst Prob. ⁽²⁾	Burst Prob. for Ind. at All H.L. Int. ⁽³⁾
1/A						
3/C						
5/F						
7/J						
8/L						
9/M						
10/N						
11/P						
				Total Burst Probability	<5 x 10 ⁻⁷	

- Notes:
1. Maximum number of indications in any S/G at the noted TSP.
 2. Burst probability for a throughwall crack length equal to the maximum TSP displacement of column 2.
 3. Burst probability assuming all hot leg TSP intersections have a throughwall crack length at maximum TSP displacement.

2

IMAGE EVALUATION TEST TARGET (MT-3)



PHOTOGRAPHIC SCIENCES CORPORATION
770 BASKET ROAD
P.O. BOX 338
WEBSTER, NEW YORK 14580
(716) 265-1600

Table 8-7
Braidwood-1 SG D: EOC-5 Burst Probability for Hot Standby SLB with Limited TSP Displacement

Voltage Bin	EOC-5 No. of Ind. NV _i	Free Span Burst Prob. PRB(V _i)	Plate 3 and 7 Contribution: F _D and PRB _D as a Function of TSP Displacement													Net Prob. of Burst PRB _i
			< 0.45"		0.45" - 0.50"		0.50" - 0.55"		0.55" - 0.60"		0.60" - 0.65"		≥ 0.65" (2)			
			F _D	PRB _D	F _D	PRB _D	F _D	PRB _D ⁽¹⁾	F _D	PRB _D ⁽¹⁾	F _D	PRB _D ⁽¹⁾	F _D	PRB _D ⁽¹⁾		
1.0			0.774	1.1E-8	0.0077	7.9E-7	0.0067	3.0E-5	0.0031	6.1E-4	0.0017	6.5E-3	0.0068	≤3.8E-2		
1.1	74.0	3.5E-6	0.774	1.1E-8	0.0077	7.9E-7	0.0067	3.5E-6	0.0031	3.5E-6	0.0017	3.5E-3	0.0068	≤3.5E-2	5.8E-6	
1.2	60.0	5.1E-6	8.5E-9 (Note 3)		6.1E-9 (Note 3)		0.0067	5.1E-6	0.0031	5.1E-6	0.0017	5.1E-6	0.0068	5.1E-6	6.5E-6	
1.3	47.0	7.3E-6	8.5E-9		6.1E-9		0.0067	7.3E-6	0.0031	7.3E-6	0.0017	7.3E-6	0.0068	7.3E-6	7.0E-6	
1.4	36.0	1.0E-5	8.5E-9		6.1E-9		0.0067	1.0E-5	0.0031	1.0E-5	0.0017	1.0E-5	0.0068	1.0E-5	7.1E-6	
1.5	28.0	1.4E-5	8.5E-9		6.1E-9		0.0067	1.4E-5	0.0031	1.4E-5	0.0017	1.4E-5	0.0068	1.4E-5	7.6E-6	
1.6	22.0	1.8E-5	8.5E-9		6.1E-9		0.0067	1.8E-5	0.0031	1.8E-5	0.0017	1.8E-5	0.0068	1.8E-5	7.6E-6	
1.7	17.0	2.3E-5	8.5E-9		6.1E-9		0.0067	2.3E-5	0.0031	2.3E-5	0.0017	2.3E-5	0.0068	2.3E-5	7.4E-6	
1.8	13.0	3.0E-5	8.5E-9		6.1E-9		0.0067	3.0E-5	0.0031	3.0E-5	0.0017	3.0E-5	0.0068	3.0E-5	7.3E-6	
1.9	11.0	3.8E-5	8.5E-9		6.1E-9		2.0E-7 (Note 3)		0.0031	3.8E-5	0.0017	3.8E-5	0.0068	3.8E-5	7.2E-6	
2.0	8.0	4.7E-5	8.5E-9		6.1E-9		2.0E-7		0.0031	4.7E-5	0.0017	4.7E-5	0.0068	4.7E-5	6.1E-6	
2.1	6.0	5.8E-5	8.5E-9		6.1E-9		2.0E-7		0.0031	5.8E-5	0.0017	5.8E-5	0.0068	5.8E-5	5.3E-6	
2.2	5.0	7.1E-5	8.5E-9		6.1E-9		2.0E-7		0.0031	7.1E-5	0.0017	7.1E-5	0.0068	7.1E-5	5.2E-6	
2.3	4.0	8.5E-5	8.5E-9		6.1E-9		2.0E-7		0.0031	8.5E-5	0.0017	8.5E-5	0.0068	8.5E-5	4.8E-6	
2.4	3.0	1.0E-4	8.5E-9		6.1E-9		2.0E-7		0.0031	1.0E-4	0.0017	1.0E-4	0.0068	1.0E-4	4.1E-6	
2.5	3.0	1.2E-4	8.5E-9		6.1E-9		2.0E-7		0.0031	1.2E-4	0.0017	1.2E-4	0.0068	1.2E-4	4.8E-6	
2.6	2.0	1.4E-4	8.5E-9		6.1E-9		2.0E-7		0.0031	1.4E-4	0.0017	1.4E-4	0.0068	1.4E-4	3.7E-6	

Table 8-7
Braidwood-1 SG D: EOC-5 Burst Probability for Hot Standby SLB with Limited TSP Displacement

Voltage Bin	EOC-5 No. of Ind NV _i	Free Span Burst Prob. PRB(V _i)	Plate 3 and 7 Contribution: F _D and PRB _D as a Function of TSP Displacement												Net Prob. of Burst PRB _i
			< 0.45"		0.45" - 0.50"		0.50" - 0.55"		0.55" - 0.60"		0.60" - 0.65"		≥ 0.65" (2)		
			F _D	PRB _D	F _D	PRB _D	F _D	PRB _D ⁽¹⁾	F _D	PRB _D ⁽¹⁾	F _D	PRB _D ⁽¹⁾	F _D	PRB _D ⁽¹⁾	
2.7	2.0	1.7E-4	8.5E-9 (Note 3)		6.1E-9 (Note 3)		2.0E-7 (Note 3)		0.0031	1.7E-4	0.0017	1.7E-4	0.0068	1.7E-4	4.4E-6
2.8	1.0	2.0E-4	8.5E-9		6.1E-9		2.0E-7		0.0031	2.0E-4	0.0017	2.0E-4	0.0068	2.0E-4	2.5E-6
2.9	2.0	2.3E-4	8.5E-9		6.1E-9		2.0E-7		0.0031	2.3E-4	0.0017	2.3E-4	0.0068	2.3E-4	5.8E-6
3.0	1.0	2.6E-4	8.5E-9		6.1E-9		2.0E-7		0.0031	2.6E-4	0.0017	2.6E-4	0.0068	2.6E-4	3.2E-6
3.1	2.0	3.0E-4	8.5E-9		6.1E-9		2.0E-7		0.0031	3.0E-4	0.0017	3.0E-4	0.0068	3.0E-4	7.4E-6
3.2	1.0	3.4E-4	8.5E-9		6.1E-9		2.0E-7		0.0031	3.4E-4	0.0017	3.4E-4	0.0068	3.4E-4	4.2E-6
3.3	1.0	3.8E-4	8.5E-9		6.1E-9		2.0E-7		0.0031	3.8E-4	0.0017	3.8E-4	0.0068	3.8E-4	4.4E-6
3.4	1.0	4.3E-4	8.5E-9		6.1E-9		2.0E-7		0.0031	4.3E-4	0.0017	4.3E-4	0.0068	4.3E-4	5.2E-6
3.5	1.0	5.4E-4	8.5E-9		6.1E-9		2.0E-7		0.0031	5.4E-4	0.0017	5.4E-4	0.0068	5.4E-4	6.5E-6
3.7	1.0	6.0E-4	8.5E-9		6.1E-9		2.0E-7		0.0031	6.0E-4	0.0017	6.0E-4	0.0068	6.0E-4	7.2E-6
3.9	1.0	7.4E-4	8.5E-9		6.1E-9		2.0E-7		0.0031	6.1E-4	0.0017	7.4E-4	0.0068	7.4E-4	8.4E-6
4.0	1.0	8.2E-4	8.5E-9		6.1E-9		2.0E-7		1.9E-6 (Note 3)		0.0017	8.2E-4	0.0068	8.2E-4	9.1E-6
4.1	1.0	9.0E-4	8.5E-9		6.1E-9		2.0E-7		1.9E-6		0.0017	9.0E-4	0.0068	9.0E-4	9.8E-6
4.3	1.0	1.1E-3	8.5E-9		6.1E-9		2.0E-7		1.9E-6		0.0017	1.1E-3	0.0068	1.1E-3	1.1E-5
4.4	1.0	1.2E-3	8.5E-9		6.1E-9		2.0E-7		1.9E-6		0.0017	1.2E-3	0.0068	1.2E-3	1.2E-5
4.5	1.0	1.3E-3	8.5E-9		6.1E-9		2.0E-7		1.9E-6		0.0017	1.3E-3	0.0068	1.3E-3	1.3E-5
4.7	1.0	1.5E-3	8.5E-9		6.1E-9		2.0E-7		1.9E-6		0.0017	1.5E-3	0.0068	1.5E-3	1.5E-5

Table 8-7
Braidwood-1 SG D: EOC-5 Burst Probability for Hot Standby SLB with Limited TSP Displacement

Voltage Bin	EOC-5 No of Ind. NV _i	Free Span Burst Prob PRB(V _i)	Plate 3 and 7 Contribution: F _D and PRB _D as a Function of TSP Displacement												
			< 0.45"		0.45" - 0.50"		0.50" - 0.55"		0.55" - 0.60"		0.60" - 0.65"		≥ 0.65" (2)		Net Prob. of Burst PRB _i
			F _D	PRB _D	F _D	PRB _D	F _D	PRB _D ⁽¹⁾	F _D	PRB _D ⁽¹⁾	F _D	PRB _D ⁽¹⁾	F _D	PRB _D ⁽¹⁾	
4.8	1.0	1.7E-3	8.5E-9 (Note 3)		6.1E-9 (Note 3)		2.0E-7 (Note 3)		1.9E-6 (Note 3)		0.0017	1.7E-3	0.0068	1.7E-3	1.7E-5
5.1	1.0	2.1E-3	8.5E-9		6.1E-9		2.0E-7		1.9E-6		0.0017	2.1E-3	0.0068	2.1E-3	2.0E-5
5.7	1.0	3.1E-3	8.5E-9		6.1E-9		2.0E-7		1.9E-6		0.0017	3.1E-3	0.0068	3.1E-3	2.8E-5
7.4	1.0	7.8E-3	8.5E-9		6.1E-9		2.0E-7		1.9E-6		0.0017	6.5E-3	0.0068	7.8E-3	6.6E-5
8.9	1.0	1.4E-2	8.5E-9		6.1E-9		2.0E-7		1.9E-6		1.1E-5 (Note 3)		0.0068	1.4E-2	1.1E-4
9.7	1.0	1.9E-2	8.5E-9		6.1E-9		2.0E-7		1.9E-6		1.1E-5		0.0068	1.9E-2	1.4E-4
10.5	0.7	2.4E-2	8.5E-9		6.1E-9		2.0E-7		1.9E-6		1.1E-5		0.0068	2.4E-2	1.2E-4
11.2	0.3	2.9E-2	8.5E-9		6.1E-9		2.0E-7		1.9E-6		1.1E-5		0.0068	2.9E-2	6.3E-5
Net Free Span Burst Probability Σ NV _i *PRB(V _i)		9x10 ⁻²											Net Limited TSP Displacement Burst Probability, Σ PRB _i		8x10 ⁻⁴

- Notes: 1) Initial column entry shows the burst probability for an exposed throughwall crack equal to the TSP displacement. The remaining column entries show the lower burst probability for either free span based on the bobbin voltage or a throughwall crack at the length exposed by the TSP displacement.
- 2) For TSP displacements >0.65 inch, the free span burst probability for the EOC-5 voltages are always lower than for an assumed throughwall crack greater than the 0.65 inch TSP displacement.
- 3) Numerical value represents F_D*PRB_D for the TSP displacement bin. Below this entry, the burst probability for an assumed throughwall crack at the given TSP displacement is always less than that for free span based on the voltage level.

Table 8-8. Bounding SLB Burst Probability at Normal Operating Conditions for Updated TRANFLO Analyses

TSP	Maximum TSP Displacement (inch)	EOC-4 Indications		Bounding SLB Burst Probability		
		Max. No. Ind. at TSP	Max. Volts at TSP	Number Tubes	Exposed Length Burst Prob. ⁽²⁾	Burst Prob. for Ind. at All H.L. Int. ⁽³⁾
1/A	< 0.30	0	-		N/A	N/A
3/C	0.45 to 0.48	0	-	4	$\leq 7.0 \times 10^{-7}$	$\leq 2.8 \times 10^{-6}$
	0.40 to 0.45	1	0.80	26	$\leq 1.0 \times 10^{-7}$	$\leq 2.6 \times 10^{-6}$
	0.35 to 0.40	4	1.25	30	$\leq 1.1 \times 10^{-8}$	$\leq 3.3 \times 10^{-8}$
	0.30 to 0.35	10	1.39	50	$\leq 7.4 \times 10^{-12}$	$\leq 3.7 \times 10^{-10}$
	< 0.30	704	8.82	4468	$\leq 3.5 \times 10^{-14}$	$\leq 1.6 \times 10^{-10}$
5/F	< 0.086	248	10.4	4578	$< 10^{-16}$	~ 0
7/J	< 0.147	97	2.74	4578	$< 10^{-16}$	~ 0
8/L	< 0.152	28	3.46	4578	$< 10^{-16}$	~ 0
9/M	< 0.082	9	1.02	4578	$< 10^{-16}$	~ 0
10/N	< 0.090	2	0.76	4578	$< 10^{-16}$	~ 0
11/P	< 0.132	1	0.52	4578	$< 10^{-16}$	~ 0
				Total Burst Probability		$\leq 5.4 \times 10^{-6}$

Notes:

1. Maximum number of indications in any S/G at the noted TSP.
2. Burst probability for a throughwall crack length equal to the maximum TSP displacement of column 2.
3. Burst probability assuming all hot leg TSP intersections have a throughwall crack length at maximum TSP displacement.

WESTINGHOUSE PROPRIETARY CLASS 2

Table 8-9

SLB Peak TSP Pressure Drops and Ratio of Prior Bounding to Updated Reference Analysis

Case No.	Case 3 Model D4 Bounding Analysis Condition	Case 1 Model D3 Reference Analysis Condition	Case 2 Model D4 Prior Analysis Condition	Case 4 Model D4 Updated Analysis Condition	Case 5 Model D4 Updated Reference Analysis Condition	Case 6 Model D4 Updated Analysis Condition	Ratio Bounding Case 3 to Reference Case 5
Operating Condition	Hot Standby with Excessive Feedwater	Hot Standby	Full Power	Hot Standby	Full Power (Note 3)	Full Power (Note 3)	

a

Notes:

1. For Case 1, the TSP identification numbers for the Model D3 S/G are different than given for Model D4 S/G.
2. The peak pressure drop minus the steady state pressure drop at time = 0 represents the change in pressure drop from the SLB event and is judged to be the most appropriate quantity for comparing the analysis cases. For an SLB at hot standby conditions, the steady state pressure drop is zero.
3. Cases 5 and 6 differ in the input establishing the steady state pressure drops across the TSPs at time = 0. Case 5 has lower than expected pressure drops while Case 6 has the expected pressure drops based on performance analyses for the Braidwood-1 S/Gs.

Figure 8-1. Leak Rate Under Normal Operating Conditions
versus Crack Length for 3/4 Inch Tubing

Figure 8-2: Braidwood 1, SG "D" BOC & EOC 5 Indications
 BOC Indications Adjusted for PoD = 0.6

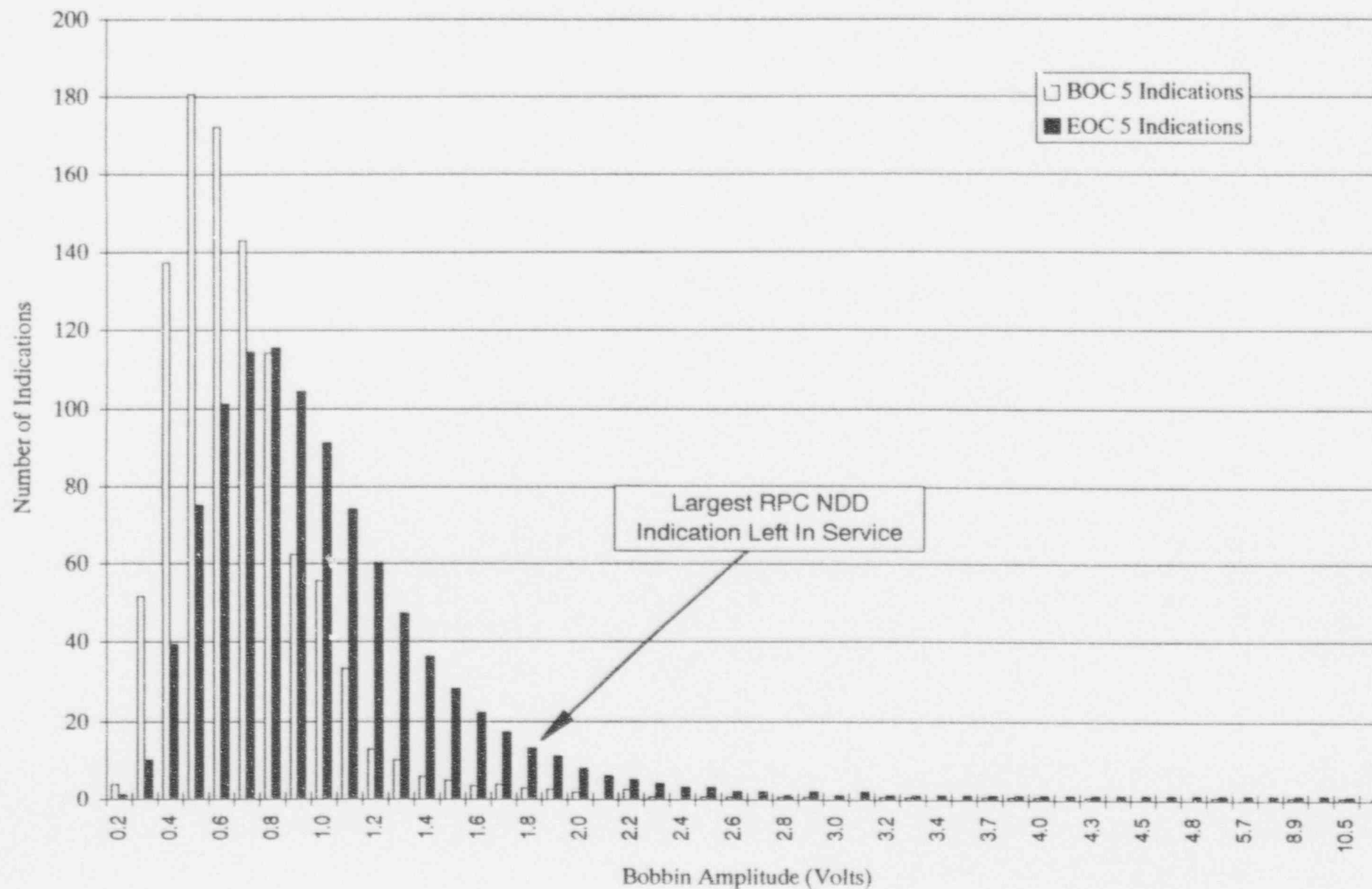


Figure 8-3: Braidwood 1, SG "A" BOC & EOC 5 Indications
 BOC Indications (Preliminary) Adjusted for PoD = 0.6

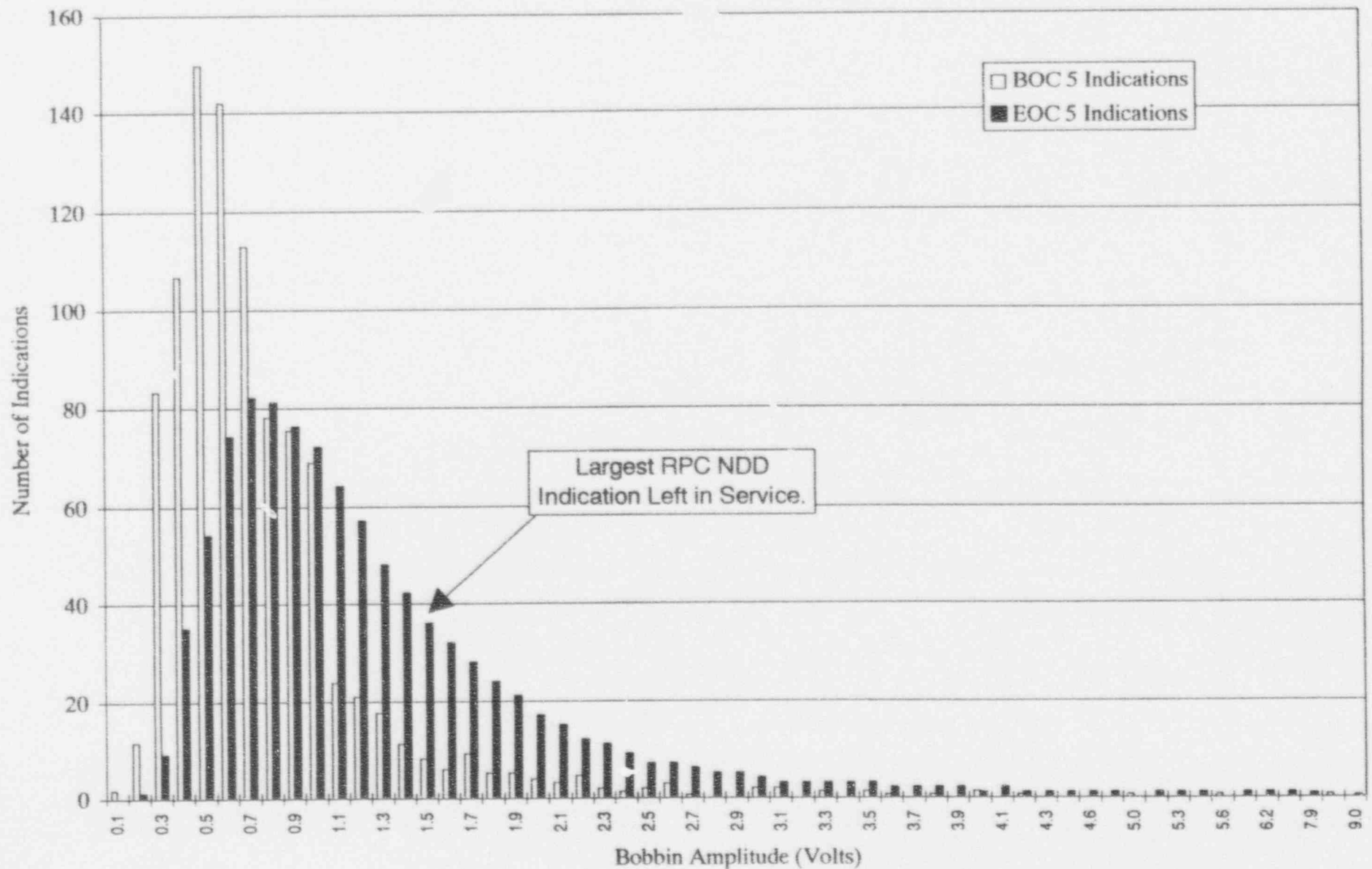


Figure 8-4: Braidwood 1, SG "C" BOC & EOC 5 Indications
 BOC Indications (Preliminary) Adjusted for PoD = 0.6

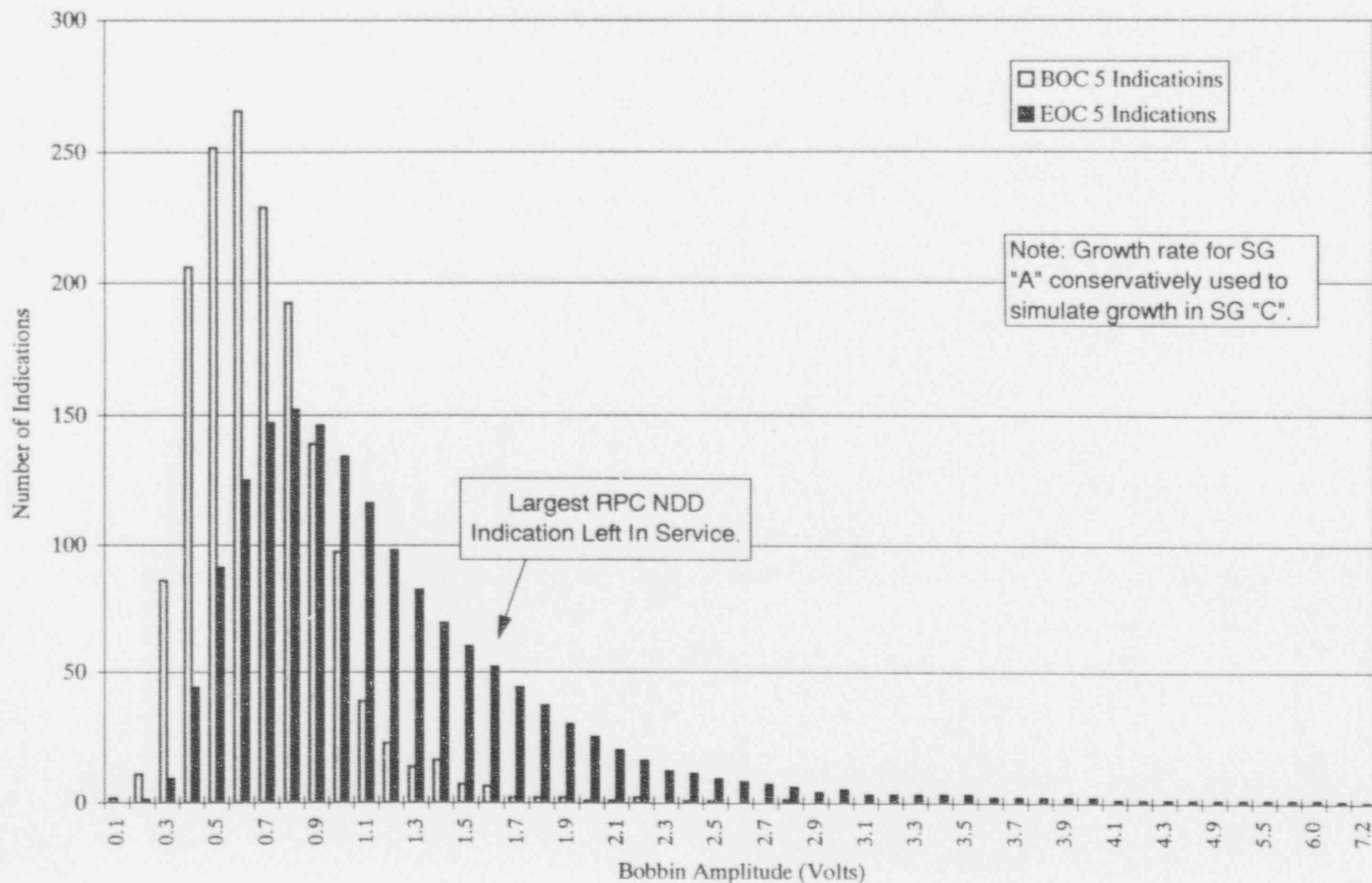
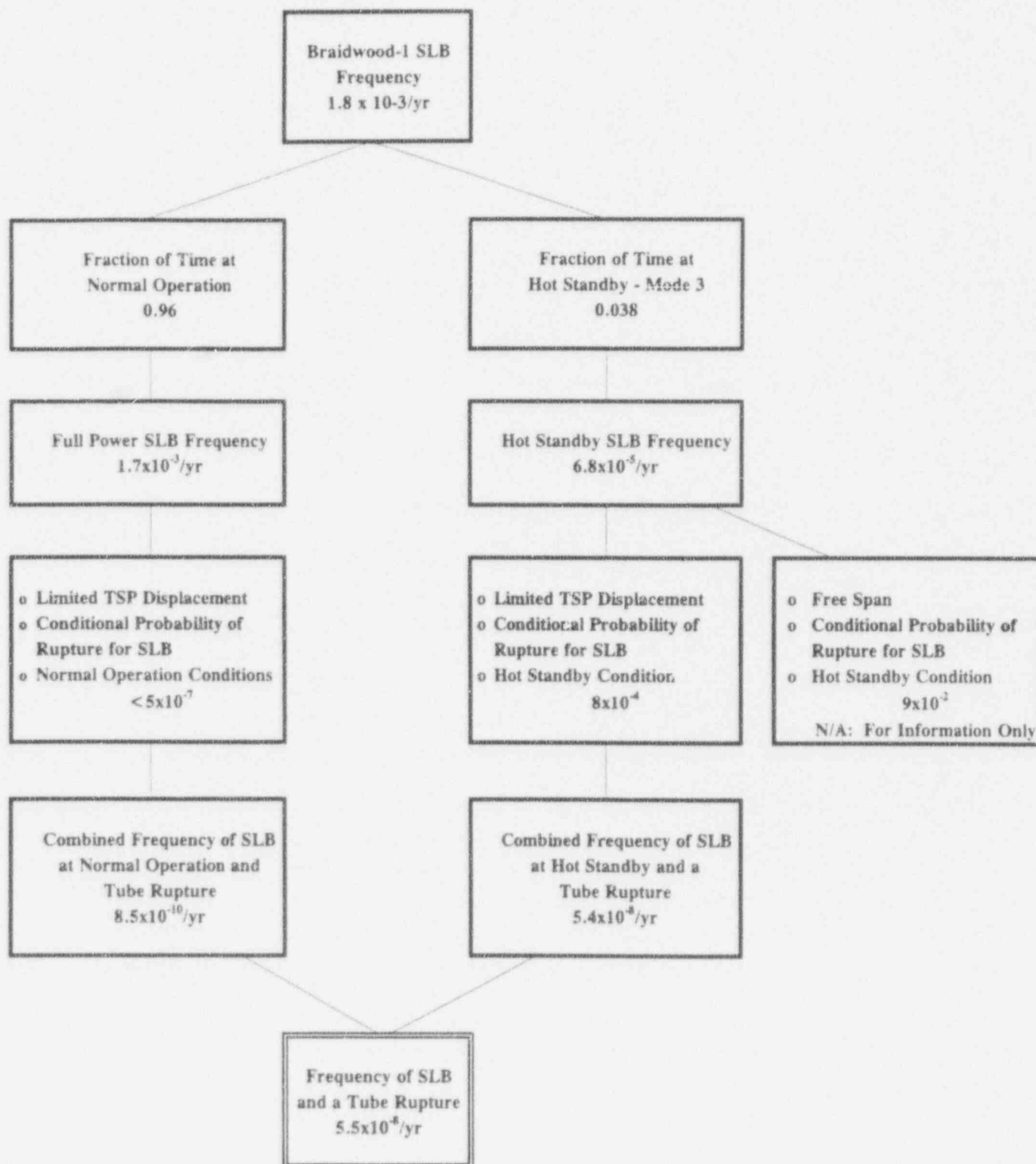


Figure 8-5. Estimated Braidwood-1 EOC-5 Frequency of SLB Event with a Tube Repair



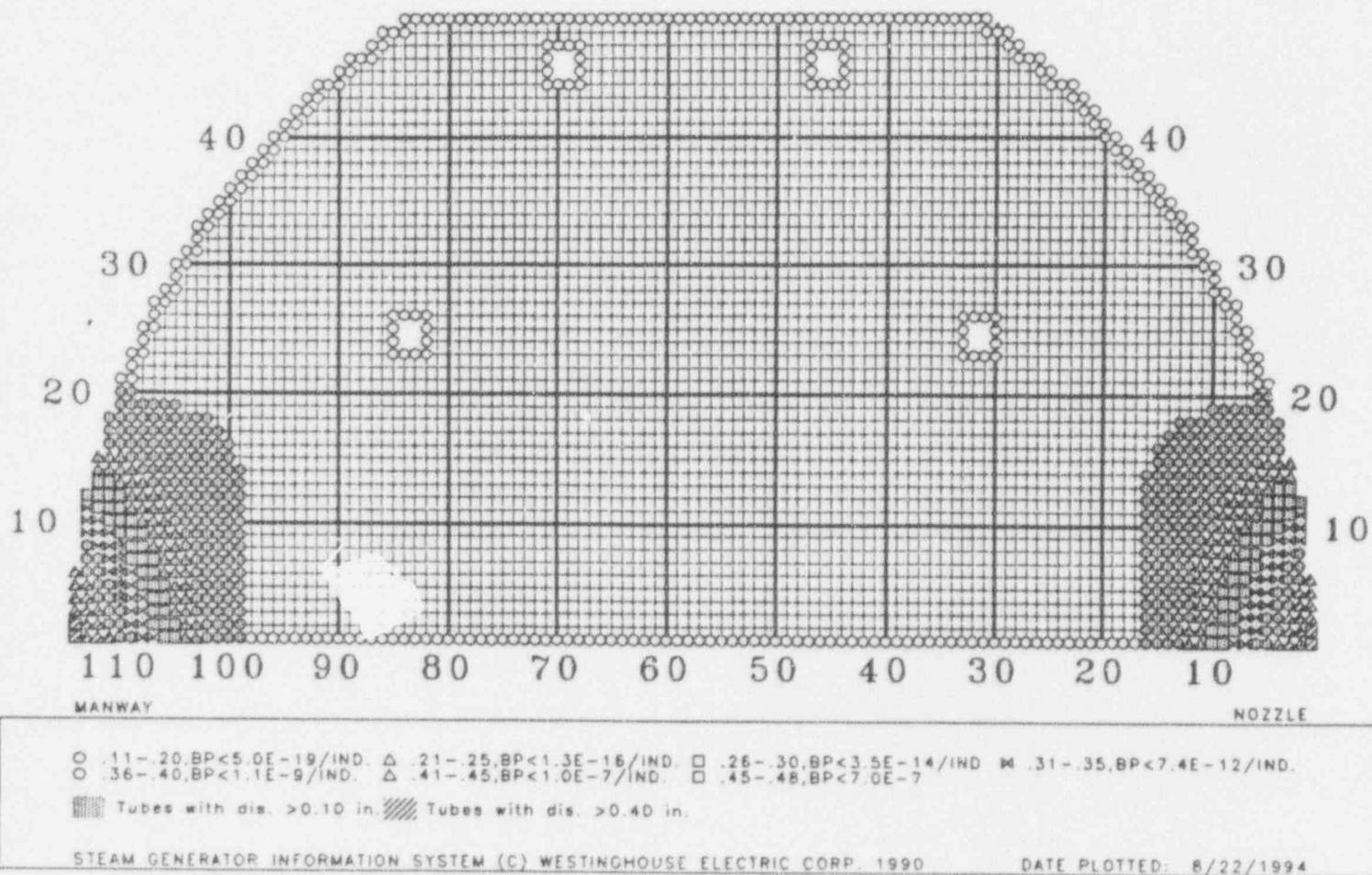


Figure 8-6. Model D4 Normal Operating SLB TSP3 Displacement and Burst Probability

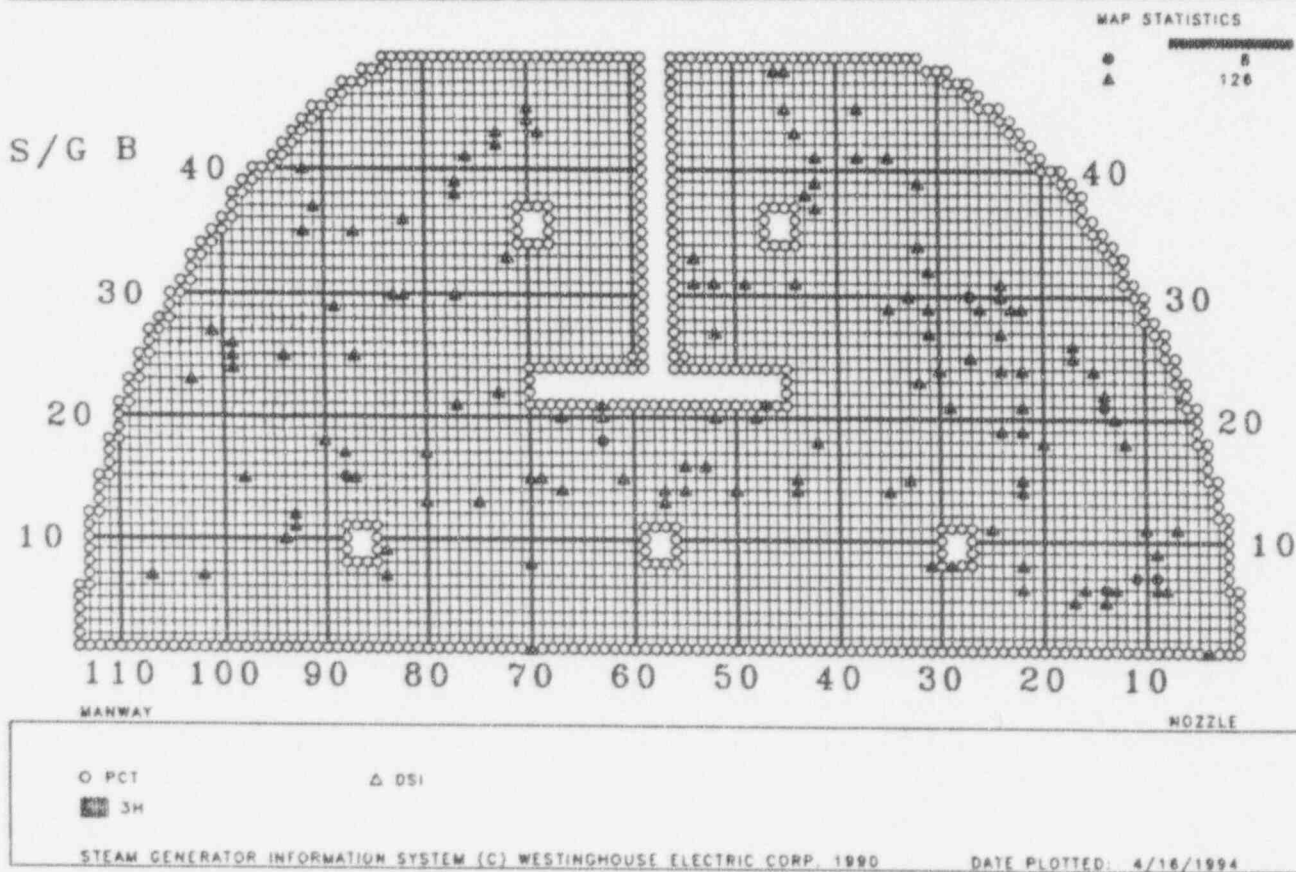
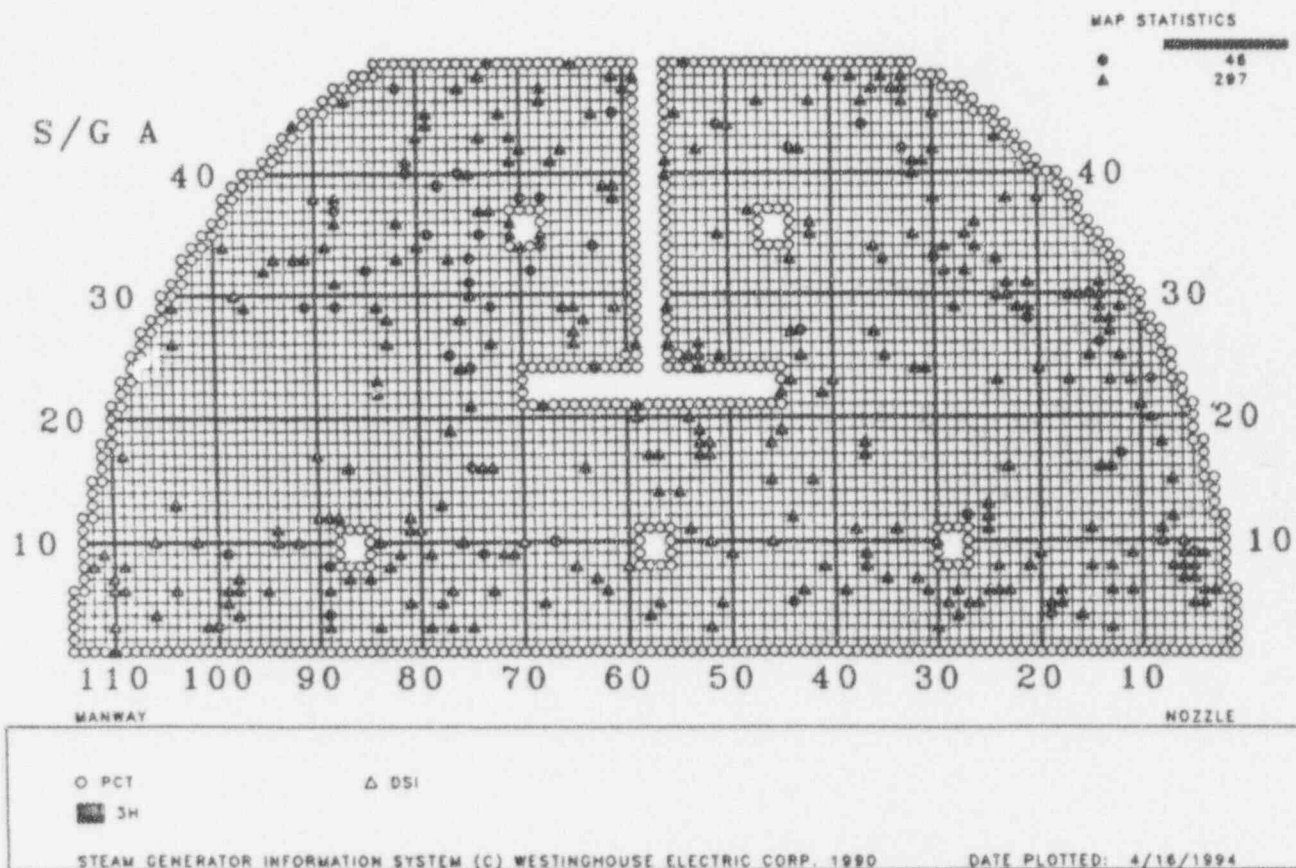


Figure 8-7(a). Locations of 4/94 Bobbin Indications at TSP3 for S/Gs A and B

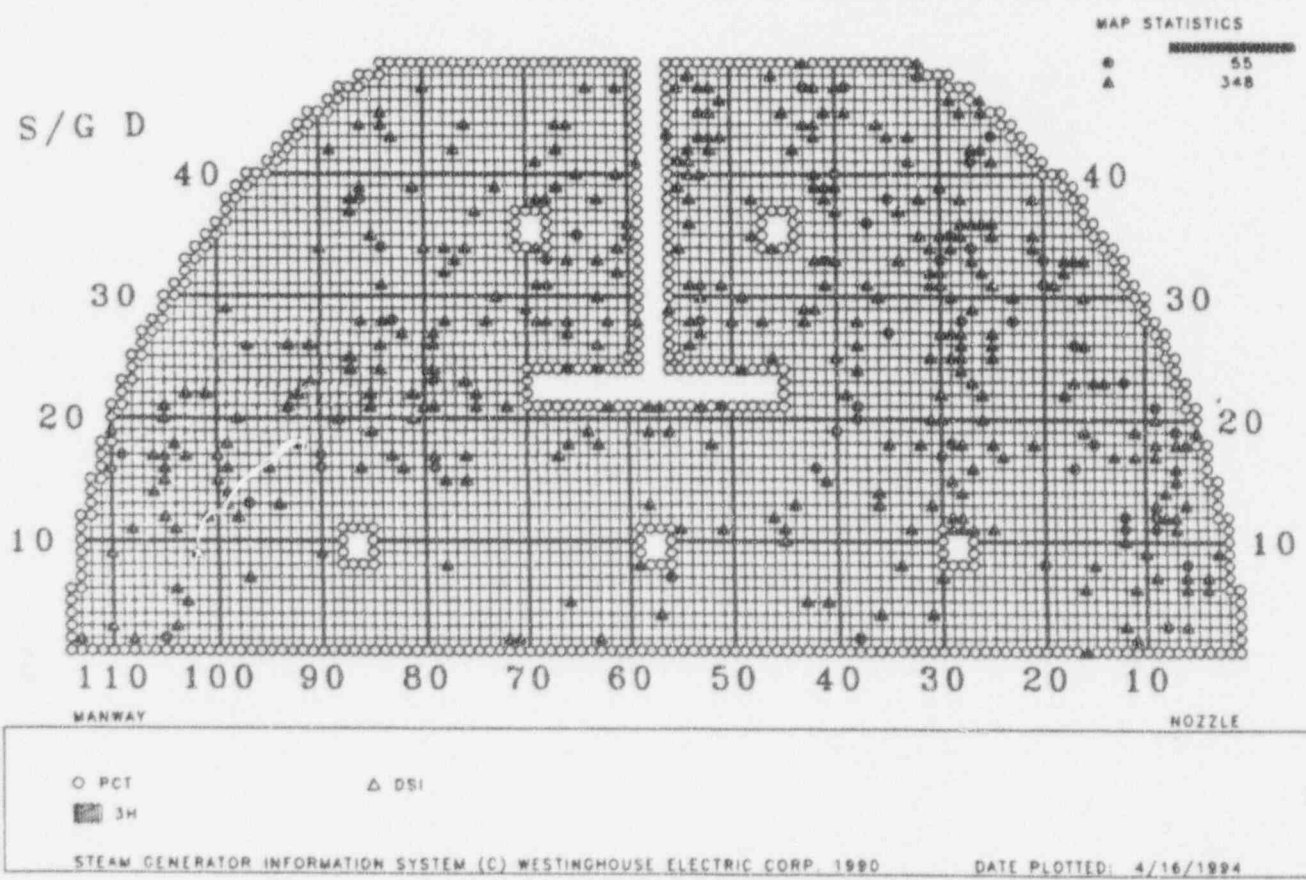
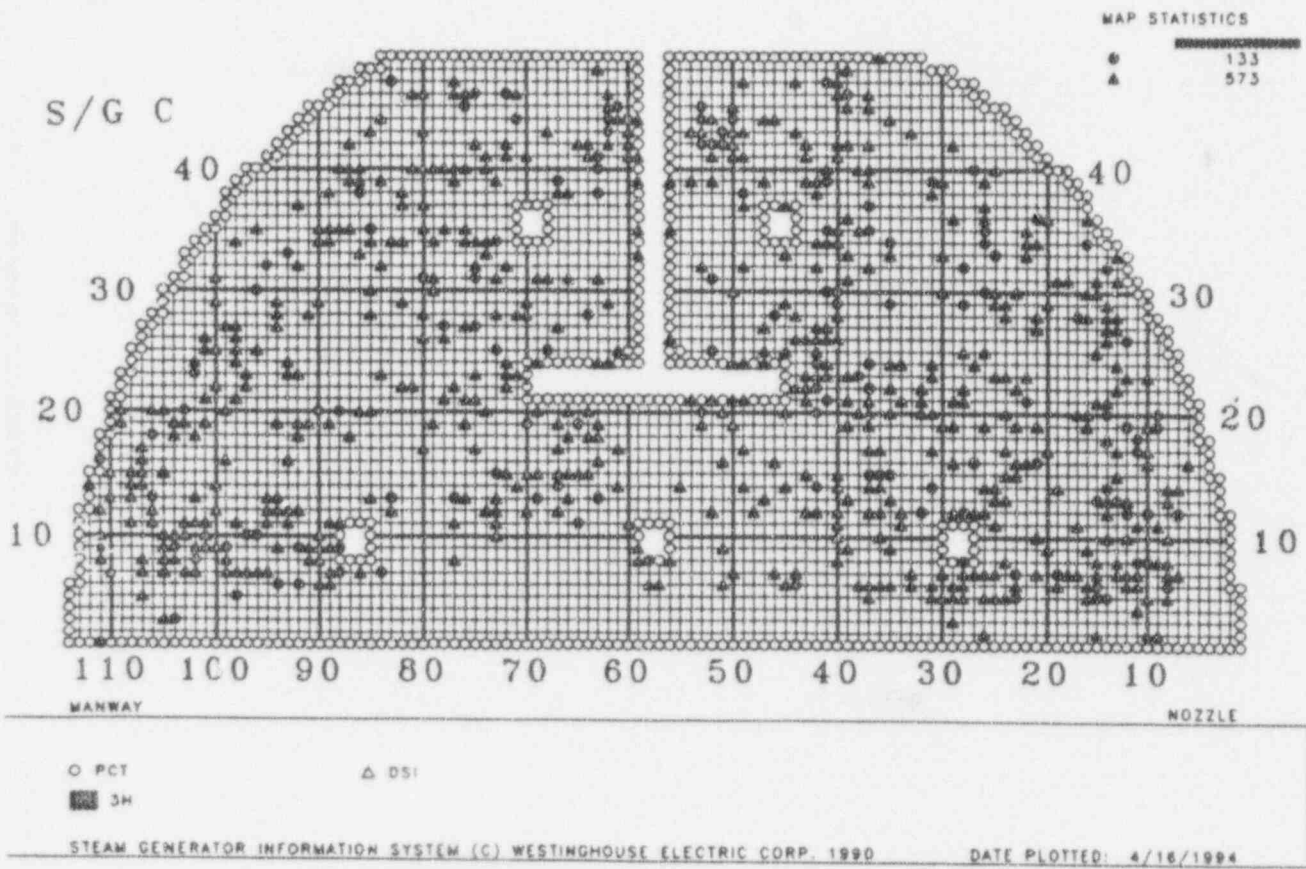


Figure 8-7(b). Locations of 4/94 Bobbin Indications at TSP3 for S/Gs C and D

